~~SECRET~~
~~RESTRICTED DATA~~
~~Atomic Energy Act - 1954~~

CCN

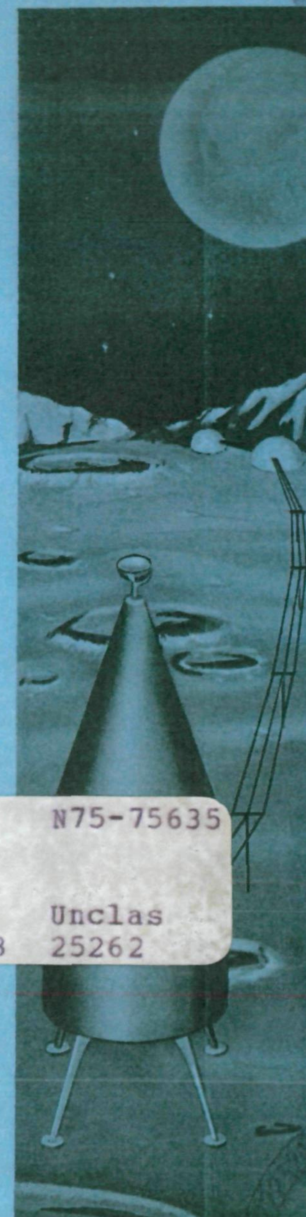

NATIONAL AERONAUTICS
AND SPACE ADMINISTRATION

SUBMITTED BY
OFFICE OF THE CHIEF OF ENGINEERS

CLASSIFICATION CHANGE
To UNCLASSIFIED
By authority of NASA Hqs TD 75-370
Changed by [signature] Date 7/30/75
Classified Document Master Control Station, NASA
Scientific and Technical Information Facility

X66 50855

(NASA-CR-71681) NUCLEAR POWER PLANT, LUNAR EXPLORATION SYSTEMS FOR APOLLO. VOLUME 2: CONCEPT SELECTION. PART 3: STATE-OF-THE-ART (Westinghouse Astronuclear Lab., Pittsburgh) 247 p N75-75635 Unclas 00/98 25262

VOLUME II - CONCEPT SELECTION
PART 3 - State-of-the-Art

[U]

NUCLEAR POWER PLANT

LUNAR EXPLORATION SYSTEMS FOR APOLLO

(TITLE UNCLASSIFIED)

WESTINGHOUSE ASTRONUCLEAR LABORATORY
WANL-PR(S)-004-A

~~SECRET~~
~~RESTRICTED DATA~~
~~Atomic Energy Act - 1954~~

565-1772

FOREWARD

This volume presents, in abridged form, basic information on the state-of-the-art of the various systems and technologies considered in the selection of a plant concept. Section I is concerned solely with a discussion of materials, and Section II with a discussion of the various reactor and power conversion system technologies which were reviewed and used as reference information during the course of the study.

Page Intentionally Left Blank

TABLE OF CONTENTS

VOLUME II CONCEPT SELECTION

PART 3 STATE-OF-THE-ART

Page Intentionally Left Blank

LIST OF ILLUSTRATIONS

LIST OF TABLES

I. MATERIALS

A. REACTOR MATERIALS (FUEL-CLAD-COOLANT COMBINATIONS)

FUEL ELEMENT REQUIREMENTS

The design of a reactor for a lunar based nuclear-electric power plant which is to be launched by 1972, must be based on a reliable fuel element technology which is presently available. The fuel element technology should be developed to the point where the principal material and fuel element design problems have not only been determined, but have been largely resolved. The operating limits of time, temperature and power density must have been established by means of irradiation testing, compatibility testing, and corrosion testing at conditions comparable to the requirements of the application. These requirements are essential to an accelerated reactor development program.

Generally, the simultaneous development of reactor design and fuel element technology has been attempted in current space reactor programs. Fuel element development has become the pace setter, and in many cases, the reactor programs are chronologically unbalanced. The reliability of these systems can be improved, using the presently developed fuel materials, if the fuel element design is made stronger; or if there is a reduction in the design requirements for operating time, temperature and power density. There has been a trend in these directions since the results of short-term irradiation tests have become available. Long-term irradiations are in progress, but few have been completed at this time. In this section of the report, the available data on space reactor fuels technology will be reviewed for the selection of a fuel for a lunar based power plant.

In the gas-cooled reactor technology, emphasis has been placed on long reactor life for production of power using fuel elements operating at high fuel cladding surface temperatures and moderate or low fuel power densities. Satisfactory performance for fuels and fuel elements has been indicated for operating times of 10,000 hours in irradiation experiments. The status of these fuel development programs will also be evaluated, and consideration will be given to the possibility of using liquid metal coolants with these fuels.

Reliability must be regarded as the major consideration in the selection of the fuel element concept for a lunar based power plant. The choice of the fuel element for the reactor is recognized to be one of the most important factors in determining the reliability of all nuclear power plant systems. A conservative choice of fuel element materials, design, and operating conditions will permit an earlier attainment of a reliable 10,000 hr reactor system and still provide the potential of developing a plant with 20,000 or 30,000 hr reliability.

The method of evaluation of the current status of fuel element technologies for the purpose of fuel element concept selection will be as follows:

1. The approximate range of fuel element requirements will be determined in order to limit the evaluation to applicable fuel element technologies. Careful consideration will be given to the relative importance of the fuel element requirements, and to those changes in an operating fuel element which might constitute an operational failure of the reactor.
2. The existing fuel element technologies must be searched and evaluated to find the fuel element concepts which are most likely to meet the above requirements. The comparison will be made on the basis of the quantity and quality of data from in-reactor testing of fuel samples and fuel element prototypes; from compatibility testing with the fuel, clad, and coolant materials; and, from basic property measurements. This type of information must be used in lieu of prolonged actual operating experience with reactors having bulk outlet temperatures above 1000°F.

Before attempting to select a reactor fuel element concept for this application, it must be pointed out that a lunar reactor power plant must be compact. The upper limit on the core size is strongly influenced by the effect of core size on radiation shielding weight. The lower limit is determined by criticality requirement and control problems in a compact reactor. Another requirement for the lunar based reactor is set by the necessity for radiation cooling as a heat sink for the power conversion system. A lower limit for reactor temperature is determined by the rapid increase in radiator size with decreasing heat rejection temperatures. Fuel surface temperatures then must be well above 1000°F. The upper limit on the fuel surface temperature is probably 2000°F as indicated by the state-of-the-art of fuel development as described below. Liquid metal coolants are particularly desirable for a compact reactor because of their high thermal conductivities and heat capacities compared to gas coolants. However, fuel element technologies from gas-cooled reactor programs can be considered applicable when it is demonstrated that there is no clad-coolant or fuel-coolant incompatability with liquid metals.

The power density requirements for the initial needs of the lunar based power plant are equivalent to the power-densities used in the gas-cooled reactor programs. With an approximate core size of 12 to 14 in. and a thermal power of 0.8 to 1.5 Mwt, the required fuel power density ranged from 0.1 to 0.4 kw/cm^3. Extensive, non-accelerated irradiation testing in the gas-cooled reactor programs at high surface temperatures and at times up to 10,000 hrs are appropriate for evaluation for this application.

In view of the fact that the proposed power plant will operate on a remote and essentially isolated site, the most stringent requirement of the reactor core design is for 10,000 hrs of maintenance-free operation. This requirement places very rigid demands on the fuel materials system selected for the reactor core. The most important condition that must be satisfied is that the system of fuel, cladding, and coolant be mutually compatible in the operating environment even in the event of a cladding defect. The problems associated with incompatability are complex functions of thermodynamic and kinetic properties which are best evaluated by means of engineering tests. The second major requirement is that the fuel elements be capable of extreme dimensional stability. This is particularly important for compact reactors, since fuel element swelling may restrict coolant flow or affect core reactivity.

The principal factors to be considered in selecting a fuel material are:

1. Only limited swelling has been previously demonstrated to occur at the thermal operating conditions of the reactor in irradiation tests.

2. The thermal expansion of the fuel up to the operating temperature does not cause excessive stressing of the cladding.
3. The uranium loading is sufficient to permit criticality of the reactor in a compact size.
4. The technology of fuel material fabrication is soundly based requiring little or no development effort.
5. The fuel material must be compatible with both the coolant and the clad.

The principal factors to be considered in selection of a fuel cladding are: its mechanical strength and ductility at the operating temperatures; its compatability with the fuel and coolant materials; and production, fabrication, welding, and annealing characteristics must be well defined in order to minimize fuel development problems.

Although the behavior of the fuel and cladding at operating conditions is important, it is equally vital that certain features be incorporated into the fuel element design. One such feature is that provision be made for accomodation of gases such as fission products generated and released during irradiation. Several design principles have proven valuable, such as thick walled or "pressure vessel" cladding design; large internal void volume; and external pressure on the cladding. These same principles have been found effective in limiting the diametral swelling of fuel elements as measured on the cladding. The successful operation of many of the high temperature fuel element irradiations has been related in most cases to the application of one or more of the above three design principles. Instances of their application will be noted in the succeeding paragraphs.

DEVELOPMENT STATUS OF PRESENT FUEL ELEMENT TECHNOLOGIES

The purpose of this paragraph is to describe and report on fuel element technologies for high temperature reactor systems, with fuel cladding temperatures in excess of 1000°F, which show potential for application to the lunar based power plant. It is also a status report of six fuel material technologies. The fuel materials which are considered are UO_2-BeO, UO_2, UC, U-ZrH, UN, and UO_2-cermets. Twelve high temperature reactor concepts have been based on these fuels with various combinations of cladding, coolants, and operating temperatures, as shown in Table 1.1.

Irradiation Stability Studies of UO_2-BeO Fuels

Studies in the last several years have indicated that dispersion type UO_2-BeO fuels possess favorable properties for high-temperature, long-duration irradiation utilization. Preliminary studies have indicated that under irradiation at elevated temperatures, the UO_2-BeO fuels appear to have excellent dimensional stability and retention of fission products. Other advantages associated with dispersion fuels of this composition, are better neutron economy, improved heat transfer characteristics, increased thermal capacity, and higher strength. Since it was realized that the behavior of the fuel would be governed by the fuel particle size, structure, density, and temperature of operation, irradiation experiments have been performed to analyze these factors. In the following discussion, irradiation experiments of UO_2-BeO fuel will be reviewed in the order of demonstrated reliability, (i.e., the longest duration successful irradiations):

1. At General Atomics an irradiation capsule (MGCR-4) containing eight specimens of 30 v/o UO_2 - 70 v/o BeO fuel pellets was prepared and irradiated to study the effects of fuel particle size on the performance of this fuel. This capsule accumulated 11,700 hours of irradiation during 30 MTR cycles at full power. A peak burnup of 55 percent of the U^{235} (approximately 3.7×10^{20} fissions per cm^3; 43,000 Mwd/ton) was achieved in an integrated fast neutron flux of 1.6×10^{20} nvt (E > 1 Mev). During irradiation the capsule was subjected to 170 thermal cycles and maximum fuel surface temperatures reached 2000°F. The power density of this experiment was in the range of 0.2 kw/cm^3.

   Each specimen of this capsule was designed to contain an approximate 2.0 in. column of fuel pellets clad with 0.015 in. thick Monel. A dense sintered BeO pellet was incorporated in one end of each specimen to facilitate post-irradiation disassembly. Each clad fuel specimen was approximately 2.5 in. long by 0.420 in. in diameter with a fuel-clad radial gap of 0.0005 in. to 0.001 in. as assembled.

TABLE 1-1 - A LIST OF MATERIALS FOR REACTORS INCLUDED IN THE SURVEY

Reactor Designation	Fuel	Cladding	Coolant	Surface Hot-Spot Temp (°F)	Power Density (kw/cm^3)
PWR	UO_2	316 S.S.	Pressurized Water	~ 500	
EGCR	UO_2	316 S.S.	Helium gas	~ 1700	0.15
ML-1	UO_2	Hastelloy X	Nitrogen gas	1750	0.35
MCR	UO_2 (or UO_2- Cb)	Cb-1 Zr	Liquid potassium	~ 1650	0.4
MPRE	UO_2	316 S.S.	Boiling potassium	1540	0.15
STAR-C	UO_2	W (or Mo)	Liquid sodium	3600	
ML-1	*.35 UO_2-BeO	Hastelloy X	Nitrogen gas	1750	0.35
EBOR	.3 UO_2-BeO	Hastelloy X	Helium gas	1750	0.34
LCRE	.5 UO_2-BeO	Cb-1 Zr	Liquid lithium	(2300)	0.7
SNAP-8	U-ZrH(C)	Hastelloy N glass-lined	Liquid NaK	1480	0.05
SNAP-2	U-ZrH(C)	Hastelloy N glass-lined	Liquid NaK	--	
SNAP-10A	U-ZrH(C)	Hastelloy N glass-lined	Liquid NaK	--	
SNAP-50	UC (or UO_2-BeO) (or UN) (or UN-W)	Cb-1 Zr (W or Ta liner)	Liquid lithium	~ 2300	1.5
STAR-R	.8 UO_2-W (or UC)	Tungsten	Radiation cooled	> 3000	
HTGR	.2 UC_2-Graphite	Impregnated graphite	Helium gas	(1600)	

* by volume.

The fuel pellets of the specimens were fabricated by dry-pressing in a steel die and subsequently sintering in an atmosphere of 25 percent hydrogen and 75 percent nitrogen. Following the sintering process the pellets were ground to required dimensions; approximately 0.4 in. in diameter and 0.5 in. long. The required uranium enrichment of 12 a/o U^{235} was obtained by blending natural enrichment UO_2 powder and fully enriched UO_2 powder.

Fuel pellets of both fine and coarse homogeneously dispersed UO_2 in a matrix of BeO were fabricated. The fine UO_2 particles were found to be irregularly shaped with maximum dimensions of about 25μ whereas the coarse particles possessed maximum dimensions of about 150μ. The coarse particles were made by agglomerating very fine particles.

During irradiation of this capsule, temperatures were controlled by varying the coolant gas composition and thus thermal conductivity. Helium or nitrogen or a mixture of the two were continually introduced into a temperature controlling annulus in the capsule.

During post-irradiation examinations, the Monel cladding in seven of the eight specimens was found to be badly cracked. Examination of the Monel cladding revealed that a substantial grain growth occurred during irradiation and that the metal reacted with a graphite sleeve in the capsule. It was believed that under the thermal cycling conditions, the carbon supersaturated in the Monel and precipitated as graphite modules in grain boundaries resulting in embrittlement of the cladding.

Visual examinations of the sixteen coarse particle UO_2 dispersion pellets revealed no gross cracking or deformation. The sixteen fine particle UO_2 dispersion pellets were all broken into several pieces. Measured dimensional changes of the coarse particle pellets indicated length increases from 0.2 percent to 0.5 percent with diameter increases of from 0.4 percent to 0.9 percent. These correspond to a density decrease of 1.5 percent to 3 percent.

Fission gas release measurements were conducted only on the one specimen on which the cladding had remained intact. This specimen contained fine particle UO_2 dispersion pellets from which the Kr^{85} release was measured to be only about 0.1 percent of that generated during irradiation. Metallographically the coarse UO_2 particles were found to have remained relatively dense and uniform while the fine UO_2 particle pellets had large grained, severely cracked, and porous structure in the dispersed UO_2 fuel particles.

2. At Aerojet General Nucleonics an in-pile test fuel element sub-assembly (1B-8T-2) was successfully irradiated in the AGN-GETR loop for 10,150 hours. The purpose of this irradiation was to study the behavior of an ML-1 fuel element prototype. The power density of this experiment was in the range of 0.35 kw/cm^3. This assembly contained 19 fuel pins arranged in a hexagonal array in which the central pin was unfueled, the inner ring of six pins contained fully enriched UO_2 clad with Hastelloy-X, and the outer ring of twelve pins contained 70 w/o UO_2 - 30 w/o BeO clad with Hastelloy-X. The fuel pellets of each pin were 0.176 in. in diameter and were clad with 0.030 in. of Hastelloy-X. Pure BeO pellets were incorporated at the ends of each fuel pin to act as reflectors. Spacing in the fuel element assembly was maintained by helically wound wires wrapped around each fuel pin.

During the first 6415 hours of irradiation, a coolant gas of 99.5 v/o N_2 + 0.5 v/o O_2 was utilized after which air was used for the final 3735 irradiation hours. During the entire irradiation, no fission products were detected in the coolant stream. Cladding hot spot temperatures of 1750°F were experienced with average operating temperatures being in the range of 1500°F.

Preliminary results of post-irradiation examinations have revealed that the cladding of three pins cracked during irradiation and that spiral twisting in six pins had occurred. Negligible swelling was observed. Fission gas sampling of all pins showed that they contained He, Xe, and Kr with small amounts of O_2 and H_2. The final results of the post-irradiation examinations of this assembly have not yet been fully reported.

3. At Battelle Memorial Institute a program of capsule irradiation experiments was conducted jointly with General Atomics to evaluate fuel materials for EBOR application. One such experiment (Capsule MGCR-BRR-9) included the irradiation of eight speciments of 70 v/o BeO-30 v/o UO_2 clad with Hastelloy X. The fuel pellets were about 0.388 in. in diameter and were positioned in two separate 1.0 in. long columns in each specimen. The Hastelloy X cladding of each speciment was 0.045 in. thick by 3.50 in. long.

The fuel pellets in half of the speciments contained fine UO_2 particles (about 10 micron diameters) in a matrix of BeO, while those in the remaining specimens contained coarse UO_2 particles (about 150 micron diameters). As previously discussed for the General Atomics MGCR-4 capsule, the coarse UO_2 particles were made by agglomerating very fine particles. All pellets were fabricated by dry-pressing followed by subsequent sintering in a controlled atmosphere furnace. Sizing of the pellets was achieved by grinding operations. The required uranium enrichment of these specimens was 12 a/o of uranium-235.

This capsule was irradiated in the MTR for a total of about 7400 hours. A peak burnup of about 35 percent of the U-235 (about 28,800 Mwd/ton) was achieved with fuel surface temperatures near 1600 $\pm$ 5 F. The power density of this experiment was near 0.25 kw/cc.

During post-irradiation examinations, the fission gases released from specimens containing pellets with fine UO_2 particles was found to be less than 0.3 percent of the total generated, while the pellets containing coarse UO_2 particles released between 17 and 24 percent of the Kr-85. All specimens were generally broken, however this condition has been attributed to high thermal stresses within the Hastelloy cladding during irradiation and to difficulties encountered during post-irradiation disassembly. Density decreases of the specimens ranged from 2.3 to 4.5 percent.

4. At Aerojet General Nucleonics an in-pile test element (1B-8T-1) was successfully irradiated in the GETR for 6415 hours. The design of this fuel element assembly was identical to that previously described above for the 1B-8T-2 experiment. The coolant gas throughout the entire irradiation was 99.5 v/o N_2 + 0.5 v/o O_2. The estimated maximum fuel burnup of this element was about 24,300 Mwd/ton and the peak clad surface temperatures were in the range of 1600°F. The power density of this experiment was in the range of 0.35 kw/cm^3.

   Post-irradiation examinations revealed that some twisting in fuel pins had occurred. The fission gas sampling of each pin indicated that only 1 percent or less of the gases formed in the element had been released. Examinations of the UO_2-BeO pellets disclosed that no swelling had occurred with only a slight degree of cracking. Microstructural studies of the Hastelloy-X cladding revealed that severe changes had occurred during irradiation resulting in embrittlement. This embrittlement appeared to be the result of an unidentified grain boundary precipitate.

5. At the CANEL facility of Pratt and Whitney Aircraft an extensive irradiation test of 50 v/o UO_2-BeO has been conducted in support of the Lithium Cooled Reactor Experiment Program. In this experiment, the fuel was prepared by cold-pressing and sintering to final dimensions with no grinding required. Densities of 95 percent theoretical or greater were obtained. The fuel was clad with Cb-1 Zr alloy and was exposed to 6500 hours of neutron irradiation at cladding temperatures as high as 2000°F. The nominal power density of this experiment was in the range of 0.6 to 0.7 kw/cm^3.

   Post-irradiation studies of this test revealed that only about 1 to 2 percent of the fission gases produced had been released and that swelling was limited to less than 1 percent of the diameter. One deterrent observation in this test was that a high release of helium (approximately 25 percent of that produced) had occurred.

   Other irradiations tests of 50 v/o UO_2-BeO conducted at CANEL for shorter durations have generally shown that:

a. Acceptable performance of the fuel clad with Cb-1 Zr might be expected for 2000 hours at maximum cladding temperatures of 2200°F.

b. Irradiation testing for 2000 hours at clad surfaces temperatures of 2300°F resulted in swelling of greater than 1 percent of the diameter.

c. UO_2-BeO is not compatible with Cb-1 Zr cladding at higher temperatures and would require diffusion barriers or cladding liners.

6. Another experiment of UO_2-BeO fuel which is of some value is an accelerated irradiation of both 70 and 80 w/o UO_2 in BeO. This experiment was a capsule irradiation conducted jointly by Battelle Memorial Institute and Aerojet General Nucleonics in support of the ML-1 reactor fuel evaluation program. The fuel of each specimen in this capsule was fabricated by cold pressing and sintering into 0.176 in. diameter by 0.211 in. long high-density pellets. Five pellets of either 70 or 80 w/o UO_2-BeO were enclosed in a 0.240 in. OD by 0.030 in. thick Hastelloy-X tubing under a helium atmosphere. Specimen ends were closed with press-fit and heli-arc welded Hastelloy-X plugs. Thin-sectioned stainless steel spacers at each specimen end prevented the pellets from touching the end plugs. A 0.002 to 0.003 in. radial gap existed between the pellets and cladding in the as-assembled condition. Four specimens were made containing 70 w/o UO_2-BeO pellets and two specimens were made containing 80 w/o UO_2-BeO pellets. The six specimens were aligned vertically in NaK and sealed in the capsule.

The irradiation of this capsule (BMI 38-1) was performed in the MTR in an effective neutron flux of 1.2×10^{13} nvt. A burnup of 8.5 percent of the U^{235} was achieved during about 4000 hours at full power (equivalent to 8750 hours of ML-1 reactor operation) with maximum surface temperatures ranging near 1710°F. Average surface temperatures ranged from 1300 to 1520°F.

Post-irradiation examination of the test specimens revealed that one of the 80 w/o UO_2-BeO specimens had failed through cladding rupture due to a swelling of 16 percent of the diameter. No swelling was detected on any of the other specimens.

Fission gas released from the fuel varied between 0.59 and 2.7 percent except for the failed specimen which released about 69 percent. Considerable change was observed in the microstructure of the irradiated specimens, although subsequent x-ray diffraction studies did not indicate serious damage to the crystal structure of either the BeO or UO_2.

Irradiation Stability Studies of UO_2 Fuels

There is extensive irradiation testing experience and reactor operating experience using 316 SS clad UO_2 in a pressurized water reactor. The essential question as to the applicability of the fuel materials technology developed for the PWRs to an application with higher coolant and cladding temperatures has not been completely answered. However, the extensive materials properties and mechanical testing data, as well as the fuel fabrication experience, are definitely applicable. There is a broad agreement throughout the reactor technology field as to the advantages and the limitations peculiar to this fuel. It has good dimensional stability under PWR operating conditions where the pressure external to the cladding may be 1,000 to 2,000 psi. It exhibits a high fission gas release, but the effect of the resulting internal pressurization of the cladding on the dimensional stability is probably offset by the high external pressure. It has the lowest thermal conductivity of the six fuels which results in the fuel centerline temperature having a strong dependance on fuel geometry and power density.

After 10,000 hrs of irradiation at ML-1 (Mobile Low Power Reactor) operating conditions, a fuel element sub-assembly containing six UO_2 fueled rods with 0.030 in. thick Hastelloy-X cladding of 0.244 in. diameter showed negligible swelling. The maximum surface temperature was 1750°F and the power density was 0.35 kw/cm^3. Fission gas release was high, but the cladding thickness and void volume were chosen to accomodate 100 percent release of the fission gases. The UO_2 fuel cracked radially but no operational failure occurred. The coolant was 99.5 a/o nitrogen gas at 330 psi pressure.

The AGN group who performed the experiment estimates the fuel element life is 20,000 hrs, based on the results of this test and several tests of shorter duration. However, an increase of the cladding temperature to 1850°F is estimated as the upper limit of temperature of operation with the present fuel element design at 10,000 hrs operating time. The Hastelloy-X was chosen for the cladding on the basis of its high stress rupture strength and it corrosion resistance to the coolant gas. Other alloys tested were Inconel, Inconel-X, Inconel-702, and Hastelloy-N. A corrosion penetration of 3.5 mils was observed in the above nitrogen loop irradiation. The Hastelloy-X and UO_2 were found to be compatible to 2900°F. No liner is recommended. The loss of 50 percent ductility in the Hastelloy-X was found in irradiation tests.

The UO_2 fuel pellets were prepared at AGN by cold pressing and sintering to final dimensions with a 70 percent acceptance level. A one mil tolerance is acceptable on both the diameter and length. No machining or grinding is required. A three mil radial cold gap exists between the fuel and clad in the fabricated fuel element.

Over 600 UO_2 fuel pellets were irradiated at surface temperatures to 1650°F in support of the EGCR (Experimental Gas Cooled Reactor) fuel development program at ORNL. The reactor design power density is 0.35 kw/cm^3. The UO_2 was clad in 316 SS of 20 mil thickness and the clad fuel was immersed in NaK liquid metal alloy at 310 psi external pressure during the irradiations. Irradiation times up to 4000 hrs have indicated no fuel diameter swelling. The high fission gas release is accomodated in a large central void in the hollow, cylindrical UO_2 fuel pellets. In-reactor creep rupture tests with 316 SS shows a sharp drop in strain to rupture. No incompatibility between NaK and UO_2 was observed.

The MPRE (Medium Power Reactor Experiment) reactor program has selected UO_2 clad in 316 SS for the fuel element, using boiling potassium for coolant. No corrosion problem is found between UO_2 and potassium although UO_2 is not compatible with lithium. No catastrophic fuel element failure is expected if the 316 SS clad is defective and potassium contacts the UO_2. The maximum and average fuel surface temperature in the boiling potassium is designed for 1540°F, with a fuel centerline temperature of 2670°F. The fuel elements are expected to have a three year life of operation at a 1 Mwt reactor power to a three a/o burnup of the uranium. The average power density for the design is 0.15 kw/cm^3. The MPRE program does not have a fuel irradiation test program at this time.

The MCR (Military Compact Reactor) has selected UO_2 clad in Cb-1 Zr as the primary candidate for its liquid potassium cooled reactor at a power density of 0.4 kw/cm^3. The alternate fuel is a 80 v/o UO_2-Cb cermet.

The STAR-C (Space Thermionic Advanced Reactor, Convection Cooled) considers UO_2 fuel clad in W as the fuel materials for the sodium cooled reactor. The fuel surface temperature is very high (3600°F). In-reactor testing is limited. A thermionic converter was operated successfully in-pile to 240 hr. There is evidence of compatability between stoichiometric UO_2 and W at a temperature of 3900°F for 2600 hrs. However, if the UO_2 is hyper-stoichiometric, the compatability is not certain. With sub-stoichiometric UO_2 there is a formation of metallic uranium which has apparently resulted in no compatability problem.

Radiation Stability Studies of UC Fuels

Initial studies of the uranium carbide fuel system in the past several years have indicated that this ceramic fuel possess favorable properties for high-temperature utilization. Preliminary studies have indicated that under irradiation at temperatures up to 1800°F, high density uranium carbide appears to have excellent dimensional stability and reasonable fission gas retention properties. The principal advantages of UC are relatively high thermal conductivity, high uranium loading, and compatability with liquid metals. Some conditions that must be factored into the evaluation of uranium carbides are: (1) the composition, (2) the method of fabrication (i.e. arc casting or powder metallurgical techniques), and (3) the density of the fuel. Although uranium carbide has not yet demonstrated 10,000 hr irradiation stability, it must be pointed out that most of the irradiation testing of this material has been conducted at accelerated rates (generally greater than 1.0 kw/cm^3) as compared to lunar based reactor applications. Basically, most of the irradiation testing has been conducted by Pratt & Whitney Aircraft and Battelle Memorial Institute. Other testing has also been conducted by the United Nuclear Corporation. Following is a review of these studies:

1. At Pratt & Whittney Aircraft the longest term irradiation of UC has been reported. In this experiment UC produced by powder metallurgical techniques was clad with Cb-1 Zr alloy and was irradiated for 6000 hours with maximum clad temperatures near 2000°F.

Pratt & Whittney has generally utilized pin-type specimens with Cb-1 Zr cladding and end caps 0.296 in. OD with 0.025 in. thick walls. The UC matrix has generally been 0.244 in. OD by 0.65 in. long fabricated from 10 percent enriched uranium. The design power densities are 1.5 kw/cm^3.

The post-irradiation studies of the 6000 hr irradiation showed no measurable swelling of the fuel pin diameter with a tolerable fission gas release.

In another experiment, $UC_{1.08}$ clad with Cb-1 Zr with a fuel-clad liner of tantalum was irradiated for 2600 hrs at maximum surface temperatures of 2100°F. The measured increase of the fuel pin diameter was less than 1 percent and the fission gas release was approximately four atom percent.

Additional short duration irradiations of UC have been conducted by Pratt & Whittney in the temperature range of 2000°F to 2200°F at power densities near 1.5 kw/cm^3. Studies of these experiments have generally lead to the following conclusions:

a. The extent of densification has a profound influence on the irradiation behavior of uranium carbides.
b. Density effects overshadow and are probably much more important than carbon composition effects with UC containing 4.8 to 5.2 percent carbon.
c. Low fission gas releases (less than one percent) are attainable from sintered high-density UC even above 2000°F, although swelling is observed.
d. Fission gas release varies inversely with density in the range 90 to 97 percent of theoretical density.
e. Swelling increases with density in the same density range.

2. At Battelle Memorial Institute the irradiation testing of uranium carbides has generally been of a research and development nature. Early irradiations of uranium carbides were conducted for the AEC as a fuels development program.

Two capsules (BRR-5 and BRR-6) contained specimens of uranium with 5 w/o, 6.7 w/o and 8.5 w/o carbon fabricated by arc casting techniques. The specimens contained 10 percent enriched uranium and no claddings were utilized. The bare fuel was immersed in NaK and irradiated in the Battelle Test Reactor to uranium burnups ranging from 0.5 to 0.7 a/o. The fuel surface temperatures varied from 800°F to 1500°F during irradiation. It was generally found that dimensional changes after irradiation were less than one percent of the diameter with density decreases of less than 1.2 percent. The fission gas release was measured to be only about 0.3 percent of that produced.

In another experiment, 12 percent enriched UC clad with 0.030 in. thick Cb-1 Zr was irradiated to a uranium burnup of 3 a/o. The clad surface temperature during this irradiation was about 1200°F with centerline temperatures near 2300°F. Post-irradiation studies of this fuel showed diametral swelling of only one to two percent.

Higher temperature irradiations of $UC_{1.08}$ and $UC_{1.45}$ clad with Cb-1 Zr have also been conducted. These fuel specimens have been irradiated at surface temperatures ranging above 1900°F with centerline temperatures as high as 2650°F. Fuel swelling with excessive fission gas release was observed. In general the following observations resulted:

a. $UC_{1.08}$ reacts with Cb-1 Zr to form free uranium, causing melting.
b. $UC_{1.45}$ reacts erratically at two a/o burnup with Cb-1 Zr, sometimes producing free uranium.
c. $UC_{1.45}$ in Cb-1 Zr releases about ten percent of its fission gases after two a/o burnup at 2000°F to 2200°F. (There is a sharp increase in fission gas release near 2300°F.)
d. Decarburization of the fuel by lithium sharply increases fission gas release.

Radiation Stability Studies of U-ZrH

The U-ZrH fuel is being developed for a set of similar space power reactor cores, the SNAP 8, 2, and 10A (Space Nuclear Auxiliary Power). Its principal advantages are: (1) the fuel is essentially metallic in thermal conductivity and creep strength, (2) the fission gas release rate is low, and (3) it has a built-in moderator for thermalizing neutron energies and for high prompt negative reactor temperature coefficients.

Its principal problems are: (1) it is thermodynamically unstable and tends to lose hydrogen at high temperature, and (2) it tends to be dimensionally unstable during irradiation.

The fuel is a single-phase ternary or quaternary composition of H, Zr, U and C. On the basis of atomic fractions, it is mostly hydrogen. The hydrogen to zirconium ratio is 1.7 H to 1.0 Zr. It has as many hydrogen atoms/cm^3 as H_2O at 450°F. The zirconium to uranium ratio is 24.2 zirconium atoms to each uranium atom. The zirconium to carbon atomic ratio is 23.7 to 1.0 for the 0.5 w/o carbon quaternary composition (carbon-modified SNAP fuel).

The process of the fuel material fabrication is well developed. The extruded billets of ten w/o U-Zr alloy are prepared for the hydriding step. Early billets containing approximately 0.5 w/o C were found to be better for the hydriding process since they did not tend to crack and they yielded both grain refinement and more equiaxed grains. Subsequent fabrication development has made it possible to prepare the fuel with as little as 0.15 percent carbon, but the 0.4 w/o carbon composition was found to be desirable as a result of mechanical testing and has been selected as the composition for the SNAP 8 fuel.

The SNAP 8 fuel material (unclad) is known to be unstable at high temperatures unless kept in a gas atmosphere with a hydrogen partial pressure equal to the dissociation pressure of the fuel. At a temperature of 1500°F, the hydrogen pressure over the fuel with the 0.4 w/o carbon composition must be 117 psia or the hydrogen content will change. At the SNAP 8 peak cladding temperature of 1480°F, a strong, hermetically sealed cladding is necessary to maintain the core reactivity. The fabrication of a fuel element for the SNAP 8 reactor is under development at this time. Several high temperature, high strength, super-alloys have been considered, but all must be used in moderate thicknesses since they have high thermal neutron absorption cross-sections, and the SNAP 8 is a thermal neutron flux reactor. Present cladding is only 10 mils thick on a 0.56 in. diameter fuel. The cladding alloy is of Hastelloy-N. Increases in the clad thickness will reduce the core reactivity in a thermal reactor. The metal claddings are generally poor barriers for hydrogen permeation, particularly when thin-walled, because of inclusions in the metal. A glass coating method is being developed for the internal surface of the cladding which shows great improvement in the ability of the cladding to retain hydrogen. However, it depends upon structural integrity and continuity of the glass coating, which in turn depends on the strength of the metal cladding. Hydrogen permeability tests in a hot-cell facility are being terminated because of mechanical damage during remote handling operations, and this effect of irradiation on hydrogen permeability is better tested in-reactor.

In addition to the problem of retaining the hydrogen in the fuel element the fuel exhibits swelling or dimensional instability. The volume increases with the 3/2 power of the burnup, according to the equation:

$$\frac{\Delta V}{V} = 2300\, b^{3/2} \exp(-12,000/T)$$

where T is the surface temperature in $^{\circ}R$, and b is the metal atom percent burnup. At a burnup of 0.4 a/o of the total U plus Zr atoms (approximately 10.0 a/o burnup of the uranium atoms) at 1300° to 1500°F temperature the diameter was found to increase 4 to 5.8 percent. At 0.9 a/o burnup of total metal atoms (22.5 a/o burnup of uranium atoms) the diameter swelling was measured to be 11.9 to 12.5 percent. Since the irradiation tests were at accelerated burn-ups, the fuel was held at temperature for a shorter time than if the irradiation were performed at a designed power density of 0.05 to 0.11 kw/cm^3. It is possible that the swelling may be greater at the design power density because of longer time at the high temperature of operation. An extensive irradiation testing program is planned.

One of the basic requirements of a fuel element is that it have a stable nuclear reactivity. The effect of hydrogen loss on the reactivity of the fuel element was mentioned above. Another effect that is important in this particular fuel is the uranium burnup. For example, at 10,000 hours of operation at the same fuel power density, the fraction of the uranium loading which is burned up or fissioned is eight times greater than in the case of UO_2 fuel. This is a direct result of the low uranium loading in the U-$ZrH_{1.70}$ fuel. It has one-eighth the uranium per unit volume of straight UO_2 and one-fourth that of 50 v/o UO_2-BeO.

Another consideration that will be studied is the possible relocation of the hydrogen within an element as a result of axial or radial temperature gradients. This may have effects on reactivity, coefficients of expansion, phase transformation, etc. The hydrogen will tend to distribute itself in the temperature gradient so that it will have a uniform dissociation pressure and hydrogen thermodynamic activity.

Radiation Stability Studies of UN

The development and testing of uranium mononitride has progressed somewhat slower than for other fuels. Pratt and Whitney has doen some development work on the fuel since it is under consideration as the backup fuel for SNAP 50. Battelle Memorial Institute has also performed fabrication and irradiation studies of this fuel as a joint effort of the United States and European Atomic Energy Community. UN has a higher uranium density and a higher themal conductivity than UO_2. Thermodynamic considerations and preliminary tests lead to the assumption that UN should exhibit fewer compatability problems with some cladding materials (i.e. stainless steel) than UC. A discussion of the irradiation testing to date is as follows:

1. At Pratt and Whitney Aircraft five irradiation experiments of pin-type UN specimens have been completed. In these experiments 0.237 in. diameter by 0.65 in. long pellets of sintered UN were clad in 0.035 in. thick Cb-1 Zr. The uranium enrichments of these specimens varied from 10 percent to 93 percent. The specimens in each capsule were immersed in liquid lithium during irradiation. It was generally found that after 1690 hrs of irradiation (to a uranium burnup of 1.1 percent with surface and centerline temperatures of about 2150°F and 2490°F respectively), a maximum diametral increase of only 0.75 percent was experienced with 13 percent of the fission gases being released (see Table 1-2). However it is noted that only five percent fission gas release was experienced at slightly lower temperatures. As with other fuels,the density of UN appears to affect the fission gas retention properties.

2. At the Battelle Memorial Institute, six capsules, containing two or three specimens each of isostatically hot-pressed uranium mononitride pellets, were irradiated in the MTR. The fuel specimens were generally 0.300 in. in diameter, varied in length up to 1.03 in. had densities from 96 to 99 percent. Some of the specimens were clad with Type 304 stainless steel and others remained bare. All the specimens were immersed in NaK in the six capsules. The irradiation parameters were selected to permit an evaluation of the effect of both fuel burnup and hydrogen formation (from the $N^{14}(n, P)C^{14}$ reaction) in the stability of UN. The irradiation conditions of the six capsules ranged from uranium burnups of 0.13 percent to 3.8 percent and specimen surface temperatures up to 1150°F with centerline temperatures up to 2300°F. The results of the irradiations generally showed that UN exhibited good dimensional stability (less than 1.7 percent diametral increase) and low fission gas release (less than 0.6 percent). An increase in hardness of about 25 percent was also detected. Only the most stringent temperatures and burnup conditions produced definite microstructural changes in the UN. Some grain growth occurred and a white second phase precipitated near the UN cladding interface. There was no attack of the UN by NaK during irradiation.

TABLE 1-2 -UN IRRADIATION RESULTS

SINTERED UN ENCAPSULATED IN 35-MIL WALL Cb-1 Zr ALLOY TUBING

Spec.	Fuel Density, Percent	Surf. Temp, C	CL Temp. C	Time hr	U^{235} Percent	Burnup, a/o U	Power Density, kw/cc	Percent Gas Release	Pellet Percent Diameter Change
42 T	90	830	880	391	93	0.07	0.04	0.09	0.042
43 M	91	940	975	391	93	0.06	0.41	0.1	0.042
44 B	90	850	885	391	93	0.06	0.37	-	0.17
39 T	90	965	1055	1595	93	0.5	0.93	-	-
40 M	91	1075	1160	1595	93	0.5	0.95	3.5	-
41 B	91	1040	1160	1595	93	0.5	1.23	5.1	-
108 T	96	1100	1220	1092	32	1.1	1.11	3.0	0.38
109 T	96	1160	1280	1092	32	1.1	1.12	3.6	0.72
110 B	96	1155	1270	1092	32	1.1	1.05	2.6	0.25
123 T[a]	96	1140	1410	855	11	0.71	1.94	1	0.3
124 M[a]	96	1215	1480	855	11	0.72	1.93	1	0.2
125 B[a]	96	1115	1410	855	11	0.71	1.94	1	0.0
118 T	94	1020	1205	1690	12	1.1	1.54	5	0.45[b]
119 M	94	1175	1365	1690	12	1.1	1.53	13	0.75[b]
121 B	94	1030	1215	1690	12	1.2	1.55	5	0.35[b]

[a] 1-mil W barrier

[b] based on Cb-1 Zr alloy clad dimensions

Radiation Stability Studies of UO_2 Cermet

A cermet fuel is defined as containing more than 50 v/o fuel phase, and a dispersion fuel as containing less than 50 v/o fuel. The cermet fuels at Battelle are formed by hot isostatic pressing using gas pressure. They have experience in forming 80-20 v/o cermets of UO_2-tungsten, UO_2-molybdenum, UO_2-chromium and UO_2- stainless steel. Spherical metal-coated particles of UO_2 are the raw material. The metal is coated on the particles by vapor deposition. They have also prepared UC-molybdenum in 80-20 volume ratio and a cermet of UN-molybdenum in 80-20 volume ratio. They have formed a 50-50 v/o UO_2-tungsten cermet which has a thermal conductivity at 800°C that is 14 to 15 times better than the thermal conductivity of UO_2. The thermal conductivity of the 80-20 volume ratio cermet is slightly less. The density of the UO_2-tungsten cermet can be made close to 98 percent of the theoretical density. The fuel is stronger than a UO_2 pellet. It cannot be easily cold-rolled. By means of hot isostatic pressing, it is possible to clad a cermet fuel; for example, they have clad UO_2-Cb with columbium in a single operation with hot isostatic pressing of the Cb coated particles.

The coefficient of thermal expansion of the UO_2 cermet fuels shows a strong reduction from the thermal coefficient of expansion of UO_2. This is generally true when the metal phase has a low coefficient of thermal expansion. The coefficient of the cermet is not predictable but it is reproducible.

The isostatic pressing temperatures have been to 2800 or 2900°F in order to get 96 to 98 percent of theoretical density.

They have had irradiation experience with UO_2- columbium to about 3 a/o burnup.

DISCUSSION

A representation of the quantity of irradiation testing of the six fuels in Table 1-1 is given in bar graph form in Figure 1-1. It can be seen that the largest amount of irradiation testing experience at high temperatures and long duration is with UO_2-BeO. Satisfactory performance was reported at times exceeding 7000 hrs by three laboratories; GA, AGN and BMI. Fabrication experience with the six fuels is indicated in Figure 1-2. The UO_2 fuel has been fabricated in large quantities. The second fuel in order of fabrication experience is UO_2-BeO. It is presently produced at CANEL (over 8 LCRE core loadings), at GA (over one EBOR core loading), and at GE-NMPO. Fuel element fabrication with the UO_2 and the UO_2-BeO fuel is fully developed, as indicated in Table 1-3, whereas fuel fabrication is under development for the U_2-ZrH with the glass-lined clads, and for the UC with the W or Ta lined clad.

It is concluded, as a result of the information available on fuel-clad-coolant combinations, that the most conservative choice of fuel material for the lunar base reactor is either UO_2-BeO or UO_2, if reactor outlet temperatures are from 1200°F to 1680°F. These fuels are compatible with liquid K or NaK. The UO_2 choice permits a smaller reactor diameter for the same power level. It is not recommended that a maximum clad temperature of 1800°F be exceeded in the design of a first generation lunar reactor plant because of lack of long-term irradiation test data at the higher temperatures.

If a reactor outlet temperature above 1300°F is required, a Cb-1Zr alloy cladding should be selected rather than stainless steels or super-alloys. The strength of the stainless steels is considered minimal at the maximum cladding temperature of 1500°F required for this outlet temperature. The super-alloys, although stronger, have shown mass transport problems with liquid metals which are associated with the nickel and cobalt in the alloys. The Cb-1Zr alloy is compatible with all the liquid metals at high temperatures, and is considered a conservative choice for use with liquid K at a 1600°F reactor outlet temperature.

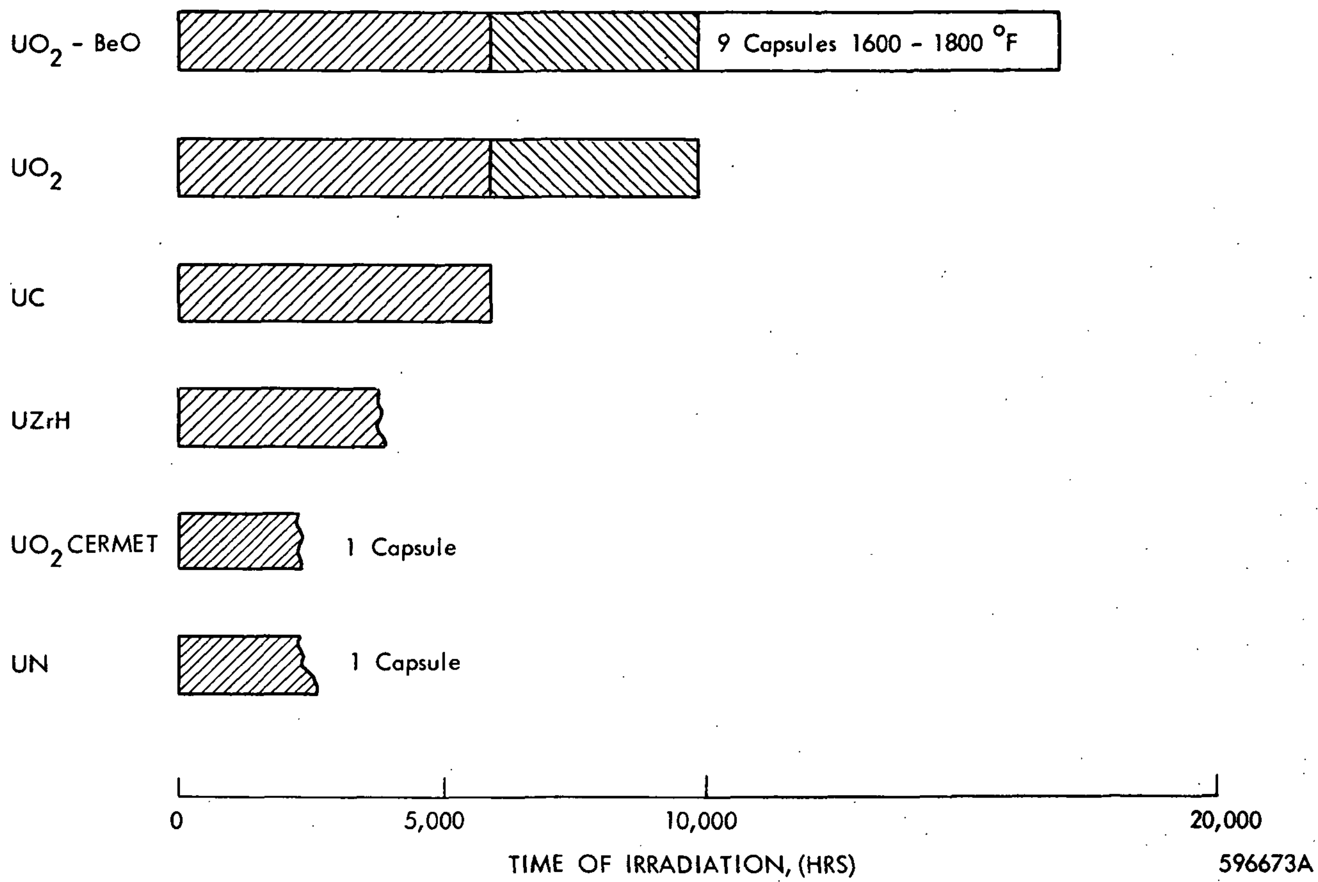

Figure 1-1 - Completed Irradiation Tests of High-Temperature Fuels

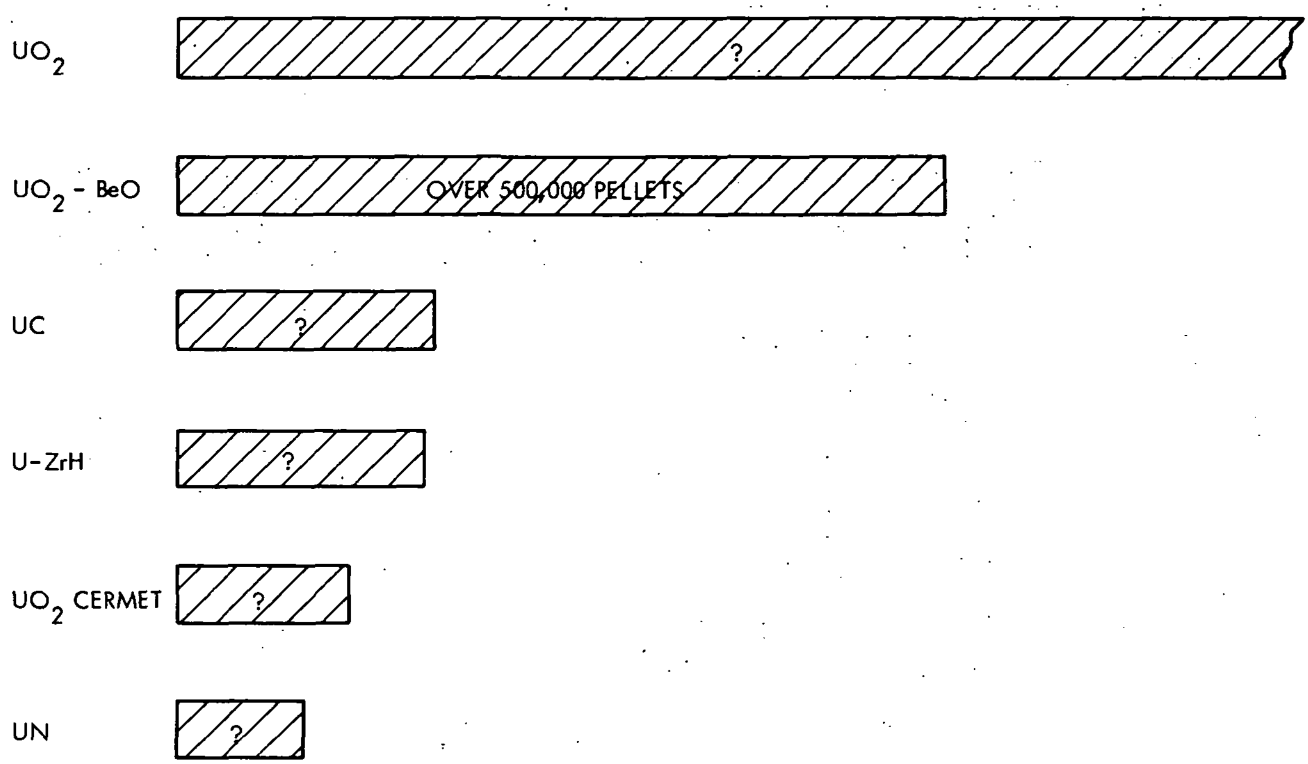

FUEL ELEMENTS

IN-PRODUCTION:

UO_2 in 304SS for EGCR

UO_2 - BeO in Hastelloy-X for EBOR

UO_2 in Hastelloy-X for ML-1

UO_2 - BeO in Hastelloy-X for ML-1

FABRICATION DEVELOPED:

UO_2 - BeO in Cb-1Zr (no liner)

UC in Cb-1Zr (no liner)

FABRICATION UNDER DEVELOPMENT:

U-ZrH in glass-lined Hastelloy-N

UC in W or Ta lined Cb-1Zr

UO_2 - Cermet in Cb or W

UN in Cb-1Zr

Figure 1-2 - Fabrication Experience with High-Temperature Fuels and Fuel Elements

The mutual compatibility of the UO_2 fuel clad in Cb-1Zr and cooled by liquid K gives reasonable assurance of continuing reactor operation in the event of a cladding defect and will not result in an operational fuel element failure at 1600°F bulk reactor outlet temperature. Table 1-3 summarizes the recommended fuel element materials and suggested design parameters for the lunar base reactor application.

TABLE 1-3. SELECTED FUEL - CLAD - COOLANT MATERIALS AND LIMITING CONDITIONS OF OPERATION FOR LUNAR BASE REACTOR

Fuel: UO_2-BeO; or UO_2

Liner: none

Clad: Cb-1Zr of 0.030 to 0.040 in. thickness (depending on diameter)

Coolant: Liquid potassium

Bulk coolant outlet temperature: approximately 1600°F

Fuel diameter: Less than 0.5 in., greater than 0.25 in.

Fuel to clad, radial cold gap: 3 to 4 mils.

Fuel power density: 0.1 to 0.5 kilowatts/cm^3

Clad maximum surface temperature: 1800°F

Fuel element and core life: 10,000 hrs.

B. STRUCTURAL MATERIALS
(COOLANTS—STRUCTURAL MATERIALS—WORKING FLUID COMBINATIONS)

STRUCTURAL MATERIAL REQUIREMENTS

The design of a lunar nuclear-electric power plant must be based upon advanced structural materials technology, as well as an available and reliable fuel element technology. A detailed review of materials activities associated with plant systems and related technologies was carried out in conjunction with analysis of current materials research and development programs. While materials requirements associated with Rankine cycle, Brayton cycle, thermionic, thermoelectric, and MHD systems were explored, it became apparent from the plant system studies that major emphasis should be directed to the alkali metal-Rankine, mercury-Rankine, and Brayton systems. Consequently, the state-of-the-art structural materials survey is essentially confined to these systems. This survey is aimed at delineating the major constraints imposed by current structural materials technology on plant design and identifying major development areas.

Potential structural materials are analyzed in terms of their compatibility with the primary coolants and working fluids of interest, as well as other environmental factors. Strength, ductility, and fabricating characteristics comprise the other major criteria for evaluation.

COOLANT—STRUCTURAL MATERIALS COMBINATIONS: REACTOR SYSTEM

As noted previously, liquid metal coolants are particularly desirable for compact reactors because of their high thermal conductivities and heat capacities as compared to gas coolants.

In alkali metal cooled reactors, structural materials for reactor pressure vessels and piping present a lesser problem than fuel claddings, since the latter must be compatible with the fuel as well as the coolant. NaK, Li, and more recently K are being evaluated for reactor coolants. Lithium is the most corrosive of the alkali metals. However, extensive work at CANEL has shown that when columbium containing an internal getter such as zirconium is exposed to purified lithium no significant corrosive attack occurs at temperatures up to at least 2200°F (Reference 1). A pumped Li loop constructed of Cb-1Zr operated successfully at a 2000°F hot leg temperature for 10,000 hours (Reference 2). No metallic mass transfer deposits were observed anywhere in the loop. Successful utilization of refractory metals for Li containment is predicted upon prevention of oxygen contamination during fabrication and welding, and prevention of contamination from the environment during loop operation. However, the techniques required for handling refractory metals have been developed and are now well established. While Li may be successfully contained in Cb-1Zr and other refractory metal alloys, use of Fe, Ni, and Co base alloy is limited to temperatures below 1100°F because of serious solution corrosion and mass transport problems (Reference 1).

While there is considerable less corrosion data in potassium than lithium, data have indicated good resistance of gettered refractory metals to potassium at temperatures up to at least 2200°F. Tests at ORNL with boiling K natural circulation loops have shown essentially no attack of Cb-1Zr at 2000°F for times up to 3000 hours. Similar tests at 1600°F with 316 stainless steel, Haynes 25, and Inconel have also shown good results. A pumped boiling potassium Cb-1Zr loop is also in operation at 2000°F at Oak Ridge. Extensive studies of potassium corrosion are in progress at GE - Evandale, NASA-Lewis, CANEL, and many other laboratories, and much additional data will be available in the near future.

Extensive corrosion data for Na and NaK are available for a large number of high temperature materials, including stainless steel, nickel and cobalt base alloys, and refractory metals. While these data will not be reviewed here, a summary of the data may be found in Reference 3. Generally, NaK is compatible with most high temperature structural materials, provided oxygen levels are maintained below 100 ppm.

For the reactor system, structural materials are available with sufficient corrosion resistance to be utilized at temperatures up to at least 2000°F. Based upon demonstrated corrosion resistance the refractory metals are most attractive for this application. The Cb-1Zr alloy has had extensive development and is available in all mill shapes. It is easily fabricable and processing techniques are well defined. Long time creep data for Cb-1Zr in a potassium environment are not available; however, data for Li have been obtained by CANEL (Reference 4) and these data should be valid for K. However, one area in which data are required is in irradiation effects on reactor pressure vessel and piping material and in particular the effect of simultaneous irradiation and creep. To reduce reactor size and weight, and particularly to permit reactor control by an external reflector, the pressure vessel of a fast spectrum power reactor must be thin, and is, therefore, highly stressed. Because it must operate at reactor inlet temperature or higher, it is in the temperature range where creep effects limit the design. Long term testing will be necessary to give assurances that secondary creep rates and time-temperature stress correlations determined in the absence of radiation are still valid for the design of these fast reactor vessels.

From the standpoint of compatibility of the coolant with the structural and fuel cladding materials, the Brayton cycle presents a less serious problem. However, to be competitive on a weight basis with Rankine cycle systems, Brayton cycle requires relatively high reactor operating temperatures. This in turn requires the use of a refractory metal fuel cladding because of fuel compatibility problems. While the use of argon, helium, xenon or, other inert gases in the Brayton cycle presents a much less serious corrosion problem, it should be pointed out that in the use of refractory metals in a Brayton cycle system the impurity level of the inert working fluid must be kept low, particularly with respect to O_2, N_2, CO and CO_2. Contamination of the structural materials by oxygen, nitrogen, and carbon can have a serious embrittling effect. Thus, in any analysis of a Brayton cycle system the problems encountered in achieving and maintaining low impurity levels in the inert working fluid must be analyzed in some detail. The permissible tolerance for impurities in the working fluid must be determined by experimental evaluations.

WORKING FLUID—STRUCTURAL MATERIALS COMBINATIONS: POWER CONVERSION SYSTEM

The corrosion and mass transport problems involved in a Rankine system may be expected to be more severe in the power conversion area. This arises from the fact that larger ΔT's are encountered in this area, and more basically, because of the use of a two-phase system rather than a single-phase liquid system in the power conversion loop. In a two-phase system the working fluid is being distilled in the boiler so that there is a continuous supply of unsaturated vapor (that is, unsaturated with respect to the containment materials) available in the condensing areas of the system to accelerate corrosive attack. The erosion of nozzles and blades in the turbine area also presents an additional problem in the power conversion loop which is not encountered in the reactor coolant system. Despite these problems the corrosion data noted previously on potassium have included refluxing capsule tests, and natural circulation loops. The ORNL studies have shown no evidence of mass transport in a 2000°F Cb-1Zr potassium loop. While a similar pumped loop is in operation at Oak Ridge, testing has not been completed so that information on mass transport in this system is not available.

Another problem encountered in the power conversion system involves the use of dissimilar metals and the resultant interaction effects on corrosion and mass transport. It is inevitable that dissimilar metals will be required in this system because of the necessity for highly stressed turbine components and bearing materials. In the SNAP 50 SPUR System, for example, Cb-1Zr will be used as the container material, but molybdenum TZM is planned for the turbine. However, under this program, capsule compatibility tests of Cb-1Zr and Mo-TZM have been conducted with no evidence of any significant corrosion effects or transport problems. More detailed studies are required of transport phenomena in dissimilar metals systems to explore the effect of such things as interstitial migration from one material to another, and its resultant effect upon properties. The data available at the present time indicates, however, that the use of a potassium Cb-1Zr system appears to be quite promising. More detailed data on erosion effects and transport phenomena are to be expected in near future from the SNAP 50 SPUR Program and the General Electric turbine program being conducted under contract NAS 5-1143.

A detailed investigation of materials for mercury containment in the temperature range of 1000 to 1300°F has been conducted at NASA-Lewis. The materials examined included austenitic stainless steels, semi-austenitic stainless steels, martensitic chromium steels including 400 series stainless steels, cobalt base alloys, refractory metals alloys, and nickel base alloys. Tantalum and the columbium 1 percent zirconium alloy showed no measurable penetration for times up to 2000 hours, the limit of the test run to date. The martensitic and low alloy steels were the next best in corrosion behavior for test times up to 5000 hours. However, these materials showed several mils penatration after test. The remaining materials tested showed considerable more corrosive attack than the martensitic and low alloy steels. The results indicated that the corrosion by mercury was directly related to the total percentage of mercury soluble elements present in the alloy. These reflex capsule tests cannot, of course, simulate behavior in an actual system for the effects of the corrosion products on systems components. However, these data indicate some likelihood of corrosion problems in two phase mercury systems constructed from materials other than refractory metals.

In the power conversion system the mechanical properties of construction materials impose a major constraint on the designer particularly in the turbine area where creep and fatigue are extremely important parameters. Mechanical property data in the working fluid environment are important for design purposes, but in general, data in this area are quite limited. However, some preliminary creep and fatigue data have been conducted by BMI for their research under the SPUR program. The effect of potassium vapor on the properties of the Mo-0.5 percent Ti alloy was determined at 1800 and 2000°F for stress levels ranging from 25,000 to 60,000 psi. These tests conducted for time periods somewhat less than 1000 hours indicated no difference between tests conducted in potassium vapor versus those conducted in vacuum.

Axial fatigue tests of this alloy were also conducted in potassium vapor in temperatures of 1500 and 2000°F. Peak stress ranged from 31,500 psi to 100,000 psi with a load ratio of 0.95. These data, while preliminary in nature, indicated a very substantial reduction in the endurance limit of this alloy in potassium vapor versus data obtained in vacuum or an inert atmosphere.

Flexure fatigue tests were also conducted on Cb-1Zr sheet in liquid potassium and lithium. Testing was done at 800°F for potassium and 1600°F for lithium with peak stresses of 27,000 psi to 49,000 psi for potassium and 20,000 to 30,000 psi for lithium under reverse bending conditions. Endurance limits of 27,000 psi at 800°F for potassium and 20,000 psi for 1600°F lithium were established on the basis of limited data.

Much more detailed testing is required to adequately establish the fatigue characteristics of materials intended for rotating components in the power conversion system. Because of the known dependence of surface characteristics and surface effects on endurance properties and materials, environmental effects on fatigue characteristics may be expected. For most of the components of the power conversion system including the boiler, primary piping, condenser areas, materials (such as Cb-1Zr), appear to have satisfactory strength and corrosion properties. Data available at present also indicate that austenitic stainless steels and cobalt base alloys may also serve satisfactorily in these areas at relatively low system temperatures, that is temperatures under 1600°F.

In the turbine area the molybdenum base alloys appear to be very attractive from a strength standpoint, however, available creep data on these alloys are limited to times on the order of 1000 hours. Much more extensive creep testing is required to assess the design properties of these alloys for longtime use in rotating components. Long time vacuum creep tests of potential refractory metal containment materials are currently in progress at NASA-Lewis.

A parallel creep program on potential turbine materials is being conducted under NASA sponsorship at TRW, contract number NAS 3-2545. These programs will provide detailed creep information on advanced refractory metal alloys under carefully controlled environmental conditions.

Materials for liquid metal lubricated bearings present a major development area. A number of active development programs are in progress on bearing materials and in bearing test programs. A successful bearing test of 710 hours duration was reported by Rocketdyne. The bearing was tested in potassium with lubricant temperatures as high as 950°F at a speed of 28,000 rpm. An endurance test was made with a titanium carbide journal bearing and a shaft of Mo-0.5 percent Ti flame-plated with tungsten carbide. An extensive bearing material survey is also in progress at General Electric Evandale under NASA-Lewis sponsorship. Under this program a large number of potential bearing materials are being tested in potassium. Bearing studies are also in progress at AiResearch under the SPUR program. An initial test of the Mo-TZM-tungsten carbide combination at 250 hour duration has appeared very promising. Several potassium lubricated bearing rigs are currently in operation at AiResearch and materials compatibility data are being developed. Hydrodynamic bearing tests have also been conducted at Pratt and Whitney CANEL in lithium using titanium carbide and tungsten carbide combinations.

Friction and wear tests in potassium are also in progress at CANEL. These tests involve solid discs and shoes which are deadweight loaded at loads of at least 300 psi at temperatures of 700 and 1000°F. The materials being investigated include Cb-1Zr, Mo-0.5 percent Ti_2 and Ta-8W-1Zr, Tantalum 8 Tungsten 1 zirconium. A number of cemented carbides and plasma spray carbide coatings have provided good results in initial tests. The bearing area still remains one which requires more detailed materials evaluation.

REFERENCES

1. PWAC-355, Corrosion of Columbium Base and Other Structural Alloys in High Temperature Lithium.

2. PWAC-381, Lithium Corrosion Investigation of a High Power Columbium Alloy System.

3. DMIC Report 169, May, 1962.

4. CNLM-4267, Creep Rupture Data for Cb-1Zr Alloy.

II. PLANT SYSTEMS AND TECHNOLOGIES

A. LITERATURE SURVEYS AND PROGRAM BRIEFINGS

To assure that data utilized on the state-of-the-art of applicable systems and technologies was as up-to-date and accurate as possible, the project undertook a literature survey of the latest documents available on government funded nuclear power system and technology programs. Emphasis was placed on those nuclear power systems and technologies being developed for space application. These compact system technologies most nearly neet the general requirements demanded in a lunar nuclear power plant.

To develop a detailed compilation of data in those areas of major importance, a series of meetings were held with government agencies and major contractors involved in various phases of the development of reactor systems. This phase of the program involved some twenty-five to thirty individual meetings and discussions. The major review sessions are listed in Table 2-1, to provide a general indication of the areas of technology considered in detail during Phase I of the study program.

Table 2-1

1. Lewis Laboratories, Cleveland, Ohio—Review of NASA space power system programs
2. Atomics International, Canoga Park, Calif.—Review of SNAP 2, SNAP 8 and SNAP 10A systems and technology
3. Aerojet General, Azusa, Calif.—Review of SNAP 8 power conversion equipment
4. Atomics International—Meeting at NASA, Washington, D. C.—Atomics International briefing on SNAP 8 adapted to the lunar environment
5. AEC, Germantown, Md.—Review of development programs for SNAP reactor systems
6. Pratt & Whitney (CANEL)—Meeting at OCE, Washington, D.C.—Review of SPUR/SNAP 50 adapted to the lunar environment
7. Pratt & Whitney (CANEL)—Review of SPUR/SNAP 50 technology (AiResearch personnel present)
8. Aerojet General, San Ramon, Calif.—Review of ML-1 and advanced gas cooled reactor - Brayton cycle systems

9. Aerojet General (San Ramon) and AiResearch (Phoenix)—Meeting at OCE, Washington, D. C.—Review of 100 kwe direct cycle gas cooled reactor - Brayton cycle study
10. AEC, Germantown, Md.—Review of MCR program
11. General Motors, Allison Div., Indianapolis, Indiana—Review of MCR reactor plant program
12. Thompson-Ramo-Wooldridge, Cleveland, Ohio—Review of SUNFLOWER, SNAP 2 mercury turbine technology
13. General Electric, Evandale, Ohio—Review of potassium turbine and liquid metals work
14. Oak Ridge National Laboratory—Review of direct cycle boiling potassium reactor program
15. General Electric, Vallecitos, Calif.—Review of thermionics systems (STAR-R, STAR-C, etc.)
16. Los Alamos Scientific Laboratory—Review of thermionic system technology
17. RCA (Lancaster, Pa. - with Harrison, N. J. personnel)—Review of thermionic system technology
18. Martin Co., Baltimore, Md.—Review of thermionics and thermoelectric systems
19. Battelle Memorial Institute, Columbus, Ohio—Review of reactor fuels technologies
20. Westinghouse, Atomic Power Division, Pgh., Pa.—Superheat water reactor systems
21. Boeing Co., Seattle, Wash.—Meeting at OCE, Washington, D. C.—Boeing mid-term and final report briefings

Obviously it is not possible to discuss in a summary document all or even a major portion of the information gathered during the course of an extensive state-of-the-art review. Each area of technology or major system under development would in itself require many volumes to describe, and such detailed information is best provided by the individual government agencies and contractors involved. The intent of the following summary is to provide very basic state-of-the-art information covering three general areas listed in Table 2-2:

Table 2-2

1. Objectives of each program
2. Current technical status of work
3. Current development program and schedule (where applicable)

The salient points concerning each approach to plant design which were fundamental to concept selection are evaluated in Section 11-B, Part 2 of Volume II. The information contained in the following pages is solely the framework of factual background information on which this evaluation is based.

The discussion of the systems and technologies considered is presented on the basis of the type of power conversion cycle utilized. Within this framework, major system development programs are discussed first and then specific programs in related areas of technology.

It will be noted that data presented in some areas of technology are far more detailed than in others. Where certain areas could be eliminated quickly for the lunar application, because it was apparent that major points (such as developability by 1972) made further consideration unnecessary, no further time was devoted to detailed information gathering. For Phase II it may be necessary to develop more detailed information in certain specific areas as a part of the basic problem of detailed evaluation of system growth. This is, however, not currently anticipated.

B. THERMOELECTRIC POWER SYSTEMS STATE OF THE ART

The use of semiconductor thermoelectric materials in electrical power generation devices is established and useful proven thermoelectric materials are available to cover a temperature range from normal room temperature to 1600°F. Such thermoelectric devices can expect 10,000 or more hours of use without maintenance—with less than 10 percent degradation. At nuclear heat source temperatures of 1200°F, the specific power output of thermoelectric conversion systems can be expected to be of the order of 3 watts/lb. This number does not include the weight of the nuclear heat source and its shielding.

INTRODUCTION

Understanding and use of the emf (thermoelectricity) generated in two dissimilar electrical conductors in contact in the presence of a temperature gradient along the conductors dates from the early 19th century (Reference 1). In the late 1950's in the U.S.A. (Reference 2), and somewhat earlier in the USSR (Reference 1), a substantial research effort was expended in an effort to discover and develop improved thermoelectric materials. A sampling of U. S. Government contracts in the area of thermoelectrics are listed in the References and List of Government Contracts.

In general, the government-sponsored thermoelectric materials research program took the form of an investigation of many combinations of materials from the periodic table of elements. The evaluation of these combinations was primarily in terms of the thermoelectric parameter ZT, as well as of other properties such as stability and strength which make a material ultimately useful. The parameter $ZT_1 = \alpha^2/k\rho \quad T_1$ is the fundamental one by which thermoelectric materials are evaluated, where:

- α is the Seebeck emf coefficient of the materials
- k is the thermal conductivity of the material

ρ is the electrical resistivity of the material

T_1 is the thermocouple hot side temperature

The importance and singular value of this parameter as a criterion of thermoelectric materials is illustrated by the well known approximate equation for maximum efficiency in thermoelectric power generation (Reference 1).

$$\eta_{max} = \eta_{carnot} \left[\frac{\frac{m}{m+1}}{1 + \frac{1}{ZT_1} - \frac{\eta_{carnot}}{2(m+1)}} \right] \qquad (1)$$

where

η_{max} is the maximum power generation efficiency

η_{carnot} is the efficiency of a Carnot (ideal heat) engine operating between the same hot and cold temperatures as the thermoelectric device

m is the ratio of external load resistance to the thermoelectric device internal resistance (user's choice in general)

Present theory of thermoelectric materials does not allow an upper limit to be set on the value of ZT. By the middle of 1961, however, after literally hundreds of materials had been investigated, a semi-emperical upper limit of ZT 1.0 was postulated by Dykstra (Reference 3) making use of the work of others (References 4 to 12). Some present day materials yield a $ZT > 1.0$ near the material liquidus temperature. This is not a practical condition for use, however.

STATE-OF-THE-ART

Useful Materials

Thermodynamic Performance

Although literally hundreds of materials have been investigated, only a few have been widely used. Useful materials are available to cover an operating temperature range from about room temperature to 1600 °F. No single material can best cover the entire range. For best results, materials must be selected with reference to the temperature range of operation.

Figures 2-1 and 2-2 give values of the differential efficiency, ϵ (T), as a function of temperature for the most widely used materials (Reference 13). The quantity of ϵ (T) comes from using the thermoelectric efficiency equation in the form

$$\eta_{max} = \left[\epsilon \, (T) \right] \eta_{carnot} \tag{2}$$

where

$$\epsilon \, (T) = \frac{\sqrt{1 + ZT} \quad -1}{\sqrt{1 + ZT} \quad -1} \tag{3}$$

As can be seen from Figures 2-1 and 2-2, to obtain ideal maximum thermodynamic performance with a large hot to cold temperature ratio, several materials must be used in series in a single thermocouple leg, or several thermocouples staged in series thermally. Experimental units incorporating these ideas have had modest success.

In the case of several materials in a single couple leg, the contact resistances and/or structural problems with materials of differing thermal coefficients of expansion usually cancel any improvement. In the case of thermally staged or cascaded thermocouples, the thermal interface temperature drops usually cancel out the performance improvement that would be expected on the basis of material parameters alone (Reference 14). The end

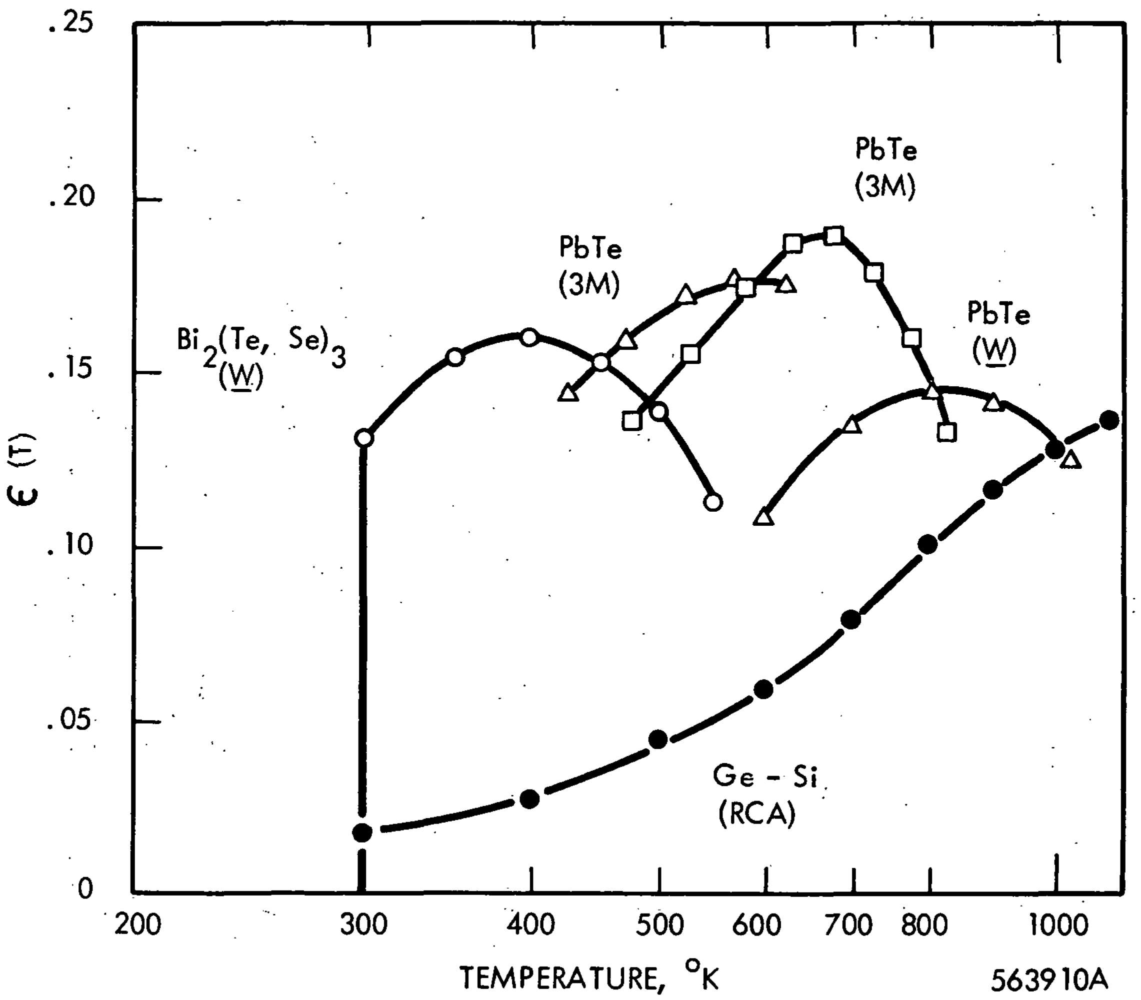

Figure 2-1 - Differential Efficiency of N-Type Thermoelectric Materials

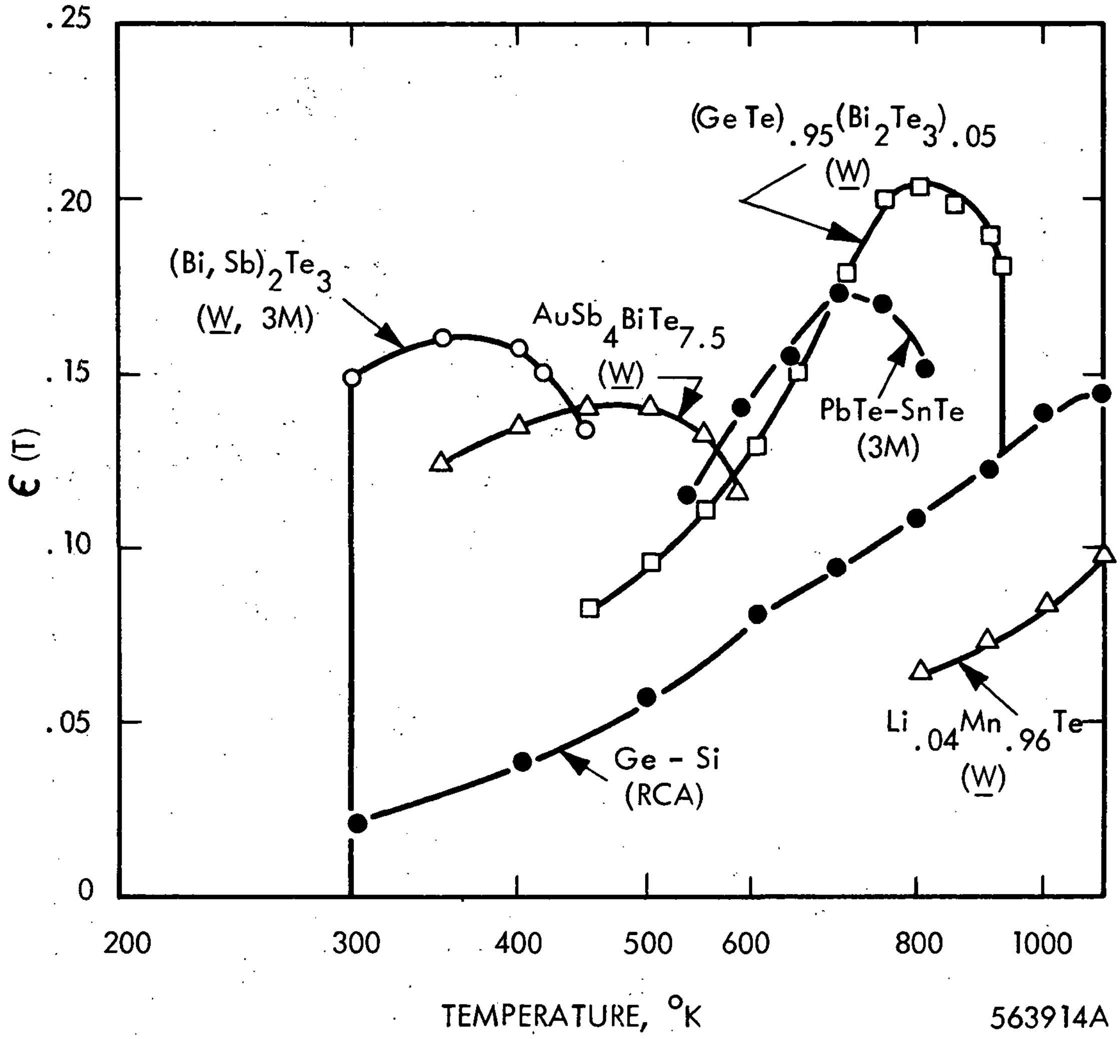

Figure 2-2 - Differential Efficiency of P-Type Thermoelectric Materials result of these difficulties is that, while over-all thermal efficiencies of thermoelectric devices can approach 20 percent as an ideal, actual efficiencies seldom exceed 10 percent and 5 percent or lower is more common. For example, the over-all thermal efficiency of a lead telluride, in-leg, germanium bismuth telluride, p-leg, thermocouple operating between a hot side temperature of 723°K and a cold side temperature of 307°K was measured as 7.8 percent (Reference 20). A representative efficiency of germanium-silicon thermocouples operating at the same hot and cold temperature is 4.1 percent (Reference 15). It should be pointed out, as a thermodynamic consideration, that the proper temperatures of use for germanium-silicon are higher than those selected for this example.

Limitations in Use of Thermoelectric Materials

Aside from the limitations on the use of the various thermoelectric materials from thermodynamic considerations, limitations of other kinds exist.

The bismuth telluride materials, $(Bi, Sb)_2 Te_3$ and $Bi_2 (Te, Se)_3$ are generally useful (aside from thermodynamic considerations) only at temperatures below those most attractive for use in space, because they have a tendency to vaporize and/or soften badly above 600°F. Gold antimony bismuth telluride $(Au Sb_4Bi Te_{7.5})$ can be used to slightly higher temperatures (800°F) before difficulties with electrical contacts become prohibitive, but this is still too low a limit on device top temperature to make full use of nuclear capability even today.

The lead tellurides, both n and p types, are attacked by atmospheric oxygen, as is germanium bismuth telluride. These materials must be enclosed in an inert atmosphere. Germanium-silicon is insensitive to oxygen attack (Reference 15), as are the bismuth tellurides in their proper operating temperature regimes.

The maximum useful temperature — set by vaporization and metallic conductor materials compatibility difficulties — is about 950°F for germanium bismuth telluride and perhaps

1050°F for the lead tellurides. Germanium-silicon also is reported to have compatibility and/or contacting problems with metallic conductors above the 1050°F level (Reference 16). Vaporization of germanium-silicon is not a problem at such a low temperature, so it can be used at higher than 1050°F hot side temperatures by using a germanium-silicon material as the hot side conductor (Reference 16). Since germanium-silicon is a semiconductor, its high electrical and thermal resistance prevents obtaining full germanium-silicon potential from a couple constructed in this way.

Good metallurgical bonds can be obtained between selected electrical conductors and n type lead telluride, the bismuth tellurides, germanium bismuth telluride, and germanium-silicon. The p type lead tellurides appear to be limited to pressure type electrical contacts. The n type lead tellurides and germanium bismuth tellurides function better if the metallurgical bond is kept in compression.

The lead tellurides and germanium bismuth tellurides have very low ultimate tensile strengths of a few hundred to perhaps several thousand psi, depending upon temperature and material. These materials are brittle and exhibit little (if any) reduction before fracture (Reference 17). Because of their low strengths and brittleness, these materials must be well protected against stress or mechanical shock when used.

The tensile strength of germanium-silicon is reported to be in excess of 5000 psi (Reference 16). This allows the use of the material as a part of device structure.

None of these thermoelectric materials suffer important damage from nuclear radiation at levels likely to be encountered in use (References 18 and 19).

Life Expectancy of Thermoelectric Materials

Properly applied, all of the thermoelectric materials commonly used give long mean times to failure and low degradation with operating life.

Germanium-silicon materials operated at a hot side temperature of 900°F to a cold side temperatue of 615°F show less than 10 percent degradation in 10,000 hrs life (Reference 21). In addition, the failure rate on acceptance testing is less than 1 per 1000. Germanium-silicon materials have also been operated at hot side temperatures of 1500-1600°F and cold side temperatures near room temperature for upwards of 5000 hours with a moderate number (about 45) of thermal cycles with less than 5 percent degradation (Reference 15).

Thermocouples of p type germanium bismuth telluride and n type lead telluride can be operated between 932°F and 302°F hot to cold side temperature with 100 thermal cycles, with 5 percent degradation in 5000 hours. At the same operating temperatures and 250 thermal cycles, degradation approaches 20 percent (Reference 22). With these materials, at least, degradation tends to be more a function of thermal operating cycles than total operating time. At 850°F hot side and 120°F cold side, degradation is less than 10 percent in 10,000 hours and 100 thermal cycles (Reference 20).

Present Day Devices

General

Almost all thermoelectric conversion devices have been built for small electrical power output. The maximum size device reported is one of 5 kw electrical output (Reference 23). Most devices developed have been under 100 watts electrical output. Current operational space thermoelectric devices are radioisotope-fueled, such as the 2.7 watt generator in the Transit IVA satellite and the 25-watt SNAP 9-A (Reference 2). Specific output of these isotope generators is about 1 watt per pound including the isotope and nuclear radiation shielding.

The most prominent reason why larger thermoelectric conversion systems have not been built is that competitive generation systems become lighter and more efficient than thermoelectric in the larger sizes.

Two thermoelectric systems characteristic of the present state of the art, the SNAP 10A and a 27.6 watt portable heating and ventilating unit built for the U.S. Army Natick Laboratories are described below. These are existing devices in which the thermocouples are distributed along the cold side heat transfer surface. The SNAP 10A is included because it could be the forerunner of other germanium-silicon thermoelectric nuclear conversion systems. The portable heating and ventilating unit developed by Pouchot (Reference 25) is included because it illustrates the technology of lead-telluride n leg, germanium bismuth telluride p leg thermocouples.

Another possible type is one in which the thermocouples are closely packed together and heat is conveyed from the thermocouple cold side to the ultimate cold side heat transfer surface by some fluid medium. This type is also used to illustrate lead-telluride p and n leg technology. A brief parametric study was done on this type in lunar plant size, using data from an actual module of the kind as a base.

SNAP 10A

Most of the information on the SNAP 10A power conversion system is taken from Reference 24. The SNAP 10A is scheduled for orbital flight-test demonstration in 1964 and its development status is well along. Nearly all components have been flight-qualified and reliability tests are in progress or completed. Integration with the Agena D flight vehicle is progressing.

A summary of some of the more important conversion system parameters is presented in Table 2-3.

A brief schematic of the SNAP 10A conversion system is given by Figure 2-3 and an artist's conception of the physical assembly in Figure 2-4.

TABLE 2-3

SNAP 10A CONVERSION SYSTEM PARAMETERS

Electrical Power, minimum	500 watts
Conversion System Weight (without reactor, shield, etc.)	506 lbs
Design Life	1 year
Radiator Area	62.5 ft^2
Over-all Length (including reactor)	130 inches
Mounting Base Diameter	50 inches
Hot Side Heat Transfer Fluid	NaK-78
Hot Side Heat Transfer Fluid Flow Rate	4920 lb/hr
Conversion System Inlet Temperature	985°F
Conversion System Outlet Temperature	885°F
Average Radiator Temperature	604°F
Thermoelectric Material	Germanium-silicon
Design Load Voltage	28.5
Over-all Thermal Efficiency	1.96%
Average Hot Side Thermocouple Temperature	900°F
Average Cold Side Thermocouple Temperature	615°F

ELECTRICAL POWER	-	500 WATTS
EFFICIENCY	-	1.96%
VOLTAGE	-	28.5

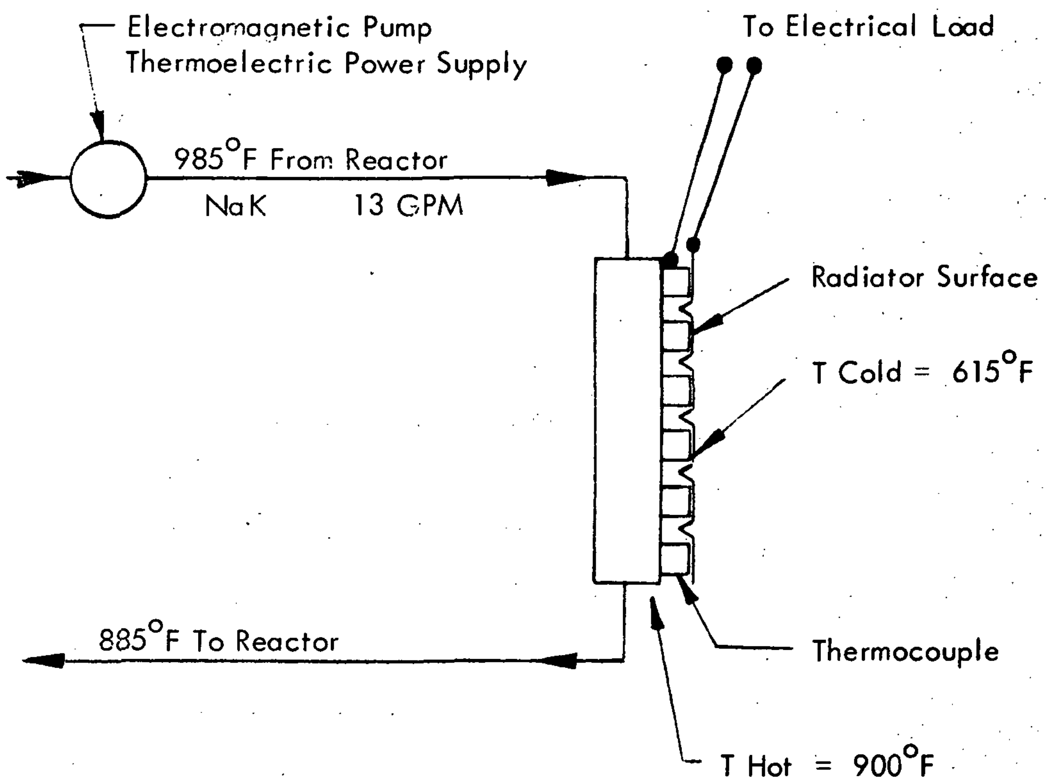

Figure 2-3 - System Schematic for SNAP 10A Power Conversion System

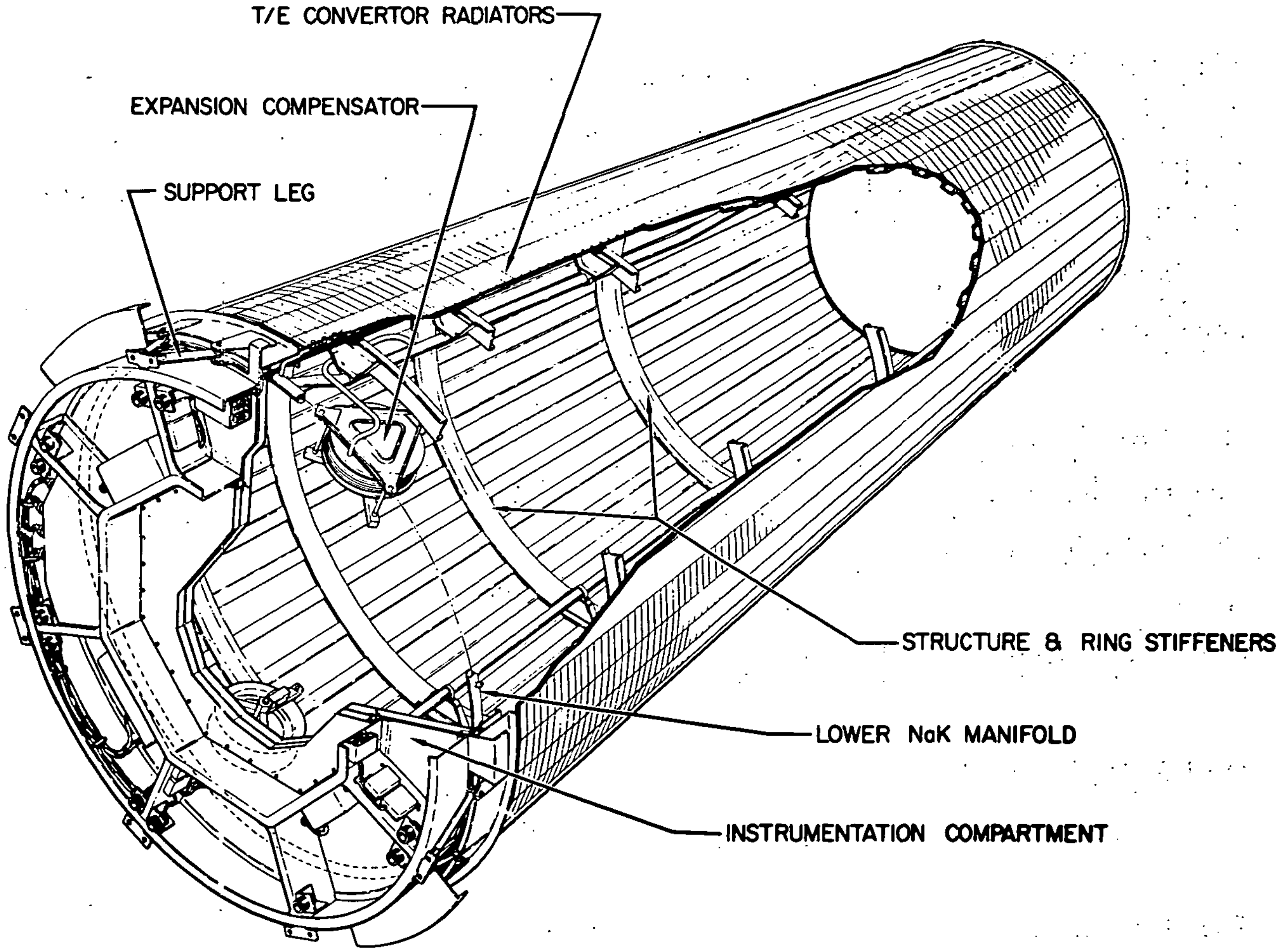

Figure 2-4 - SNAP 10A Flight System

Heat is supplied to the thermoelectric elements by NaK-78 heat transfer fluid. Heated NaK enters the power conversion system at $985^{\circ}F$ and is circulated at a rate of approximately 13 gpm by means of a liquid metal electromagnetic pump composed of a permanent magnet and an integral thermoelectric power supply.

The power conversion system consists of n and p germanium-silicon thermoelectric pellets, thermally coupled but electrically isolated from the NaK heat transfer system. These pellets are bonded to 40 parallel stainless steel tubes arranged vertically around a conical structure (see Figure 2-4). The NaK flows through these 40 tubes. Distributed along any one tube are 36 thermocouples (72 pellets). There are 1440 thermocouples in the entire assembly. The pellets are isolated electrically from the NaK tubes by thin alumina discs.

Heat flows from the NaK tube through the thermoelectric pellet to an individual aluminum radiator. Insulation of the hot from the cold sides between pellets is the vacuum of space. The total effective radiator area is $62-1/2\ ft^2$, and it has an average thermal power dissipation capacity of $1/2\ kw/ft^2$ at a mean temperature of $604^{\circ}F$. This is sufficient capacity to maintain an average ΔT of $298^{\circ}F$ over the thermocouples.

All materials which comprise the pellet subassemblies are brazed or otherwise metallurgically bonded to each other to give a sound structure and good thermal conduction.

The electrical circuit is through the p and n pellets connected alternately on the hot side to a copper strap and on the cold side through the aluminum radiator. Provision for relative expansion between hot and cold sides is in the cold side radiator. The 72 pellets on a tube are connected electrically in series. The series string on each NaK tube has been cross-coupled to an adjacent string at four discrete points along the tubes. To further increase the reliability of the converter, electrical jumpers are placed at each adjacent radiator in a leg pair. Twenty pairs of adjacent series parallel connected tubes connected in series make up the complete converter network.

At the outlet of the power conversion system, the NaK heat transfer fluid is collected for return to the reactor. In the two return lines are bellows type expansion compensators which pressurize the system in orbit to about 5 psi and can accommodate twice the thermal expansion of the NaK during heatup. For meteoroid protection, the NaK piping is arranged to take advantage of structure and components.

In addition to the power conversion sytem proper, suitable instrumentation and controls are provided for orbital startup, shutdown and monitoring.

U.S. Army Natick Labs Portable Heating and Ventilating Unit (References 24 and 25)

The purpose of the portable heating and ventilating unit is to provide hot or ambient air to a "climate suit" or CBR warfare uniform. It is an engineering demonstration unit to be worn on a man's back. While the interest here is in the thermoelectric generator (converter), a brief description of the unit as a whole is appropriate.

A plan view layout of the unit is shown in Figure 2-5 and the actual physical appearance of the unit is shown in Figure 2-6. Looking at the layout (Figure 2-5) combustion air and cooling air for the generator enters the generator blower (about 24 cfm). From this blower the air flows into a plenum at the left hand end of the generator. All but 1 cfm of this air flows through the heat exchanger on the cold side of the thermocouples to the right hand side of the generator, where it either is exhausted to ambient or is partially deflected by a grid valve into a duct leading to the filter case and thence into the inlet of the suit blower. The mix of heated and ambient air is controlled by a flipper valve acting in unison with a grid valve. In the figure ambient air is called ventilating air. The heated and ambient air mix in the filter case and are drawn into and through the suit blower conditioned for entrance into a suit.

One cfm of generator air is used as combustion air. This air is directed around the unit from left to right and enters at a hollow bullet mounted on the center line of the unit. The fuel

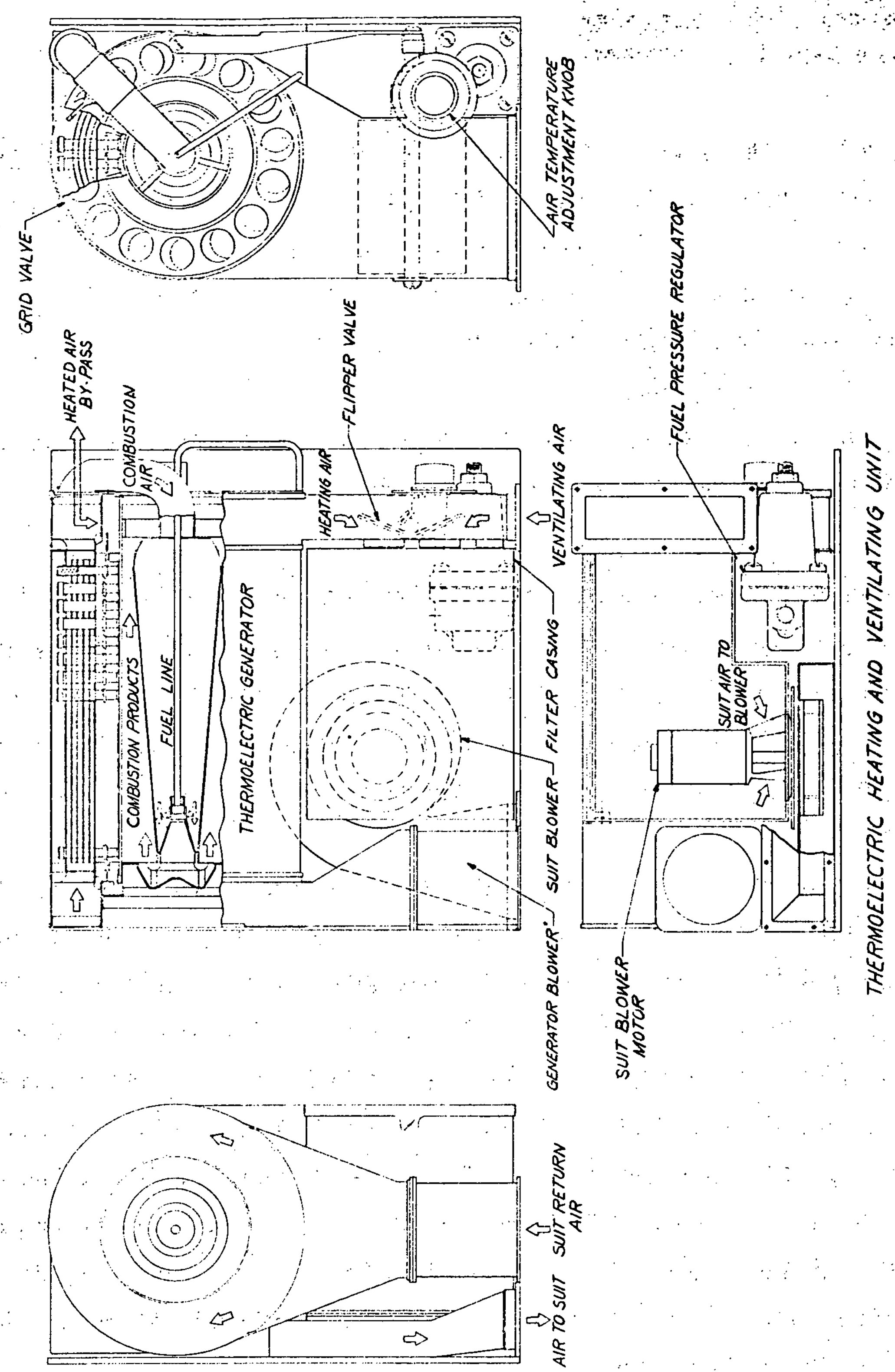

Figure 2-5 - Thermoelectric Heating and Ventilating Unit

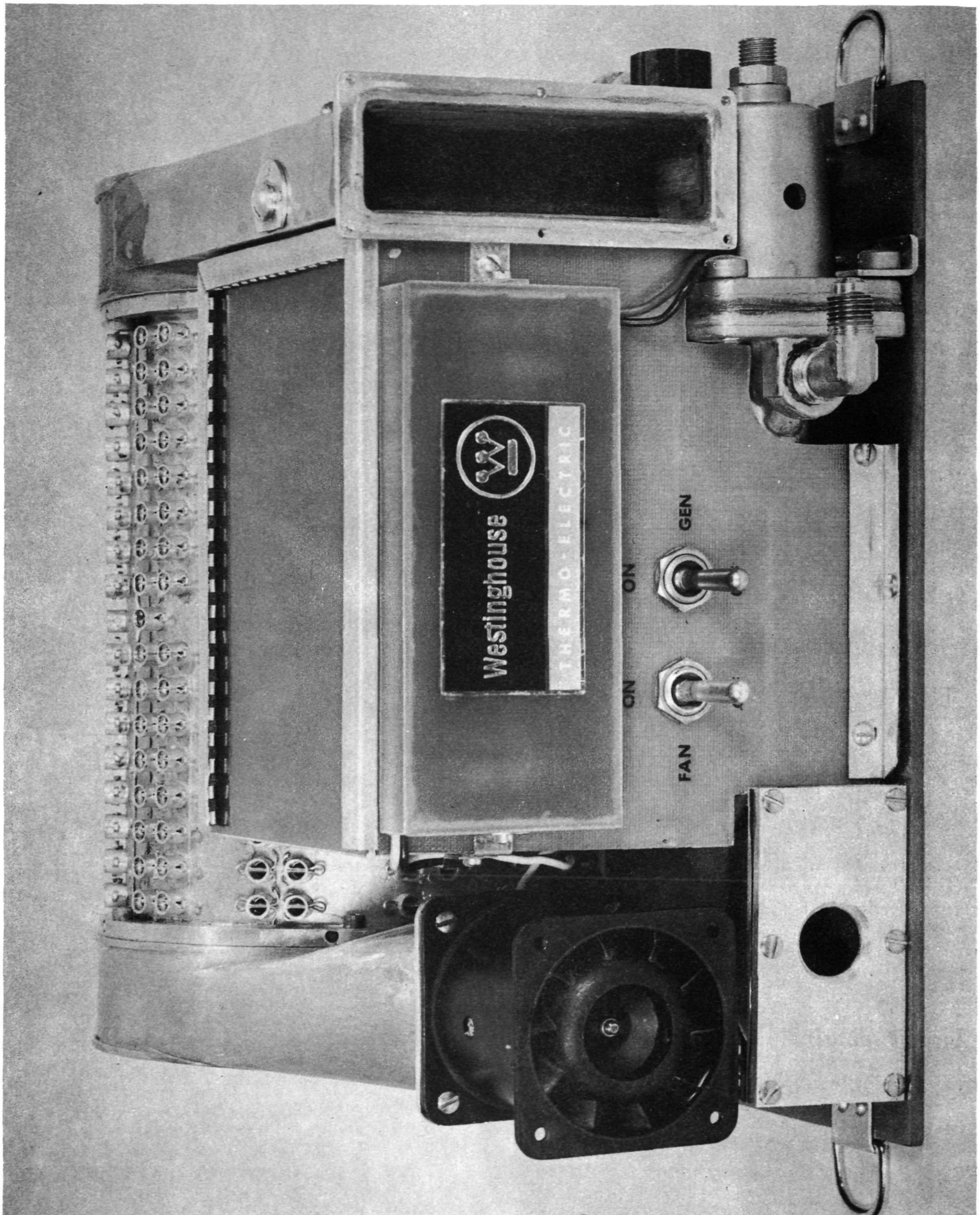

Figure 2-6 - Bottom View, Heating and Ventilating Unit also enters at this location. The fuel used is propane from hand torch bottles (Burnzomatic). The fuel and combustion air flow to the left hand end of the unit, where they mix in a bunsen type aspirator and then burn in the annular space between bullet and core. The fuel flow is controlled by the fuel pressure regulator at the lower right hand side of the unit.

The photo (Figure 2- 6) corresponds to the bottom elevation view of Figure 2-5 and is the bottom of the unit as mounted on the man's back. Visible here are the fuel regulator, generator blower, generator and suit blower electrical switches, electrical junction box (above switches) with two auxiliary power taps and suit blower exit covered by an orifice to simulate a suit.

Some of the pertinent parameters of this unit are given in Table 2-4.

The unit was operated for 200 hours in approximately 40 startup and shutdown cycles prior to final delivery to the U. S. Army and had not degraded in this time.

The generator contains 160 thermocouples (320 legs) connected electrically in series. The thermocouples are grouped in 20 modules of 8 thermocouples each. Electrical connection between thermocouple legs (in series) was by brazing to Armco iron straps on the hot side, and by braided wire soldered to the cold-side caps of Armco iron. The thermocouple legs are of n type PbTe pellets, 3/16 in. dia. x 1/4 in. long, and p type GeBiTe pellets of the same dimensions. The pellets are on 3/8 in. centers. Insulation around the pellets between the hot and cold sides was Johns-Mansville Cerafelt. The thermocouples were not sealed from the outside atmosphere.

The actual assembly arrangement can be seen in Figure 2- 5 . The burner is mounted inside the central core, and the individual thermocouple legs are pressed against this core by

TABLE 2-4

HEATING AND VENTILATING UNIT PARAMETERS

Total System (24°C ambient temperature)

Output Flow	11.7 cfm
Output Pressure Rise	4.62 in. H_2O
Weight	10.35 lbs
Size	10-1/2" x 10-1/2" x 5"
Expected Overhaul Period	500 hrs (burner and motor limits)

Generator Alone (24°C ambient temperature)

Output (Matched to heating and ventilating unit)	27.6 watts
EMF (Matched to heating and ventilating unit)	10.85 volts
Current (Matched to heating and ventilating unit)	2.55 amps
Output (To matched Load)	30.0 watts
Fuel Flow Rate	0.26 lb/hr
Weight	6.5 lbs (including fuel pressure regulator)
Size	5" dia. x 10" long
Over-all Thermal Efficiency (To heating and ventilating unit)	1.8% (fuel in-elec. power out)
Over-all Thermal Efficiency (To matched load)	1.96% (fuel in-elec. power out)
Average Hot Side Thermocouple Temperature	440°C
Average Cold Side Thermocouple Temperature	139°C
Thermocouples - PbTe-n leg, $(GeTe)_{.95}(Bi_2Te_3)_{.05}$-p leg	
Thermoelectric Degradation Expected	10%-1600 hrs, 200 - 8 hr operating cycles

individual followers protruding into hollow pins in the cold side heat exchanger. These followers are under spring compression.

The heat flow path is from the burner core to the thermocouple strap, through the legs and followers to the cold side heat exchanger pins and cylindrical fins, and then to the generator cooling air. The heat exchanger is positioned relative to the core by means of 5 radial pins inserted into pads on the core through 5 of the hollow pins. Electrical insulation along this path is provided on the hot side by an aluminum oxide layer plus a 2 mil mica layer. On the cold side of the thermocouple, electrical insulation is provided by a "hard coat" on the aluminum followers plus silicone grease over the followers. The grease also reduces sliding friction on the followers.

The main effort on this design is to provide minimum restraint between the couples and related parts during relative thermal expansion of these pieces under transient operation with isolation of the thermocouples from external loads and shocks.

Except for the burner (Inconel) and the thermocouples, all the materials in the generator were aluminums of some appropriate type.

The generator blower is a Dean and Benson Vaneaxial Model HF 3-1. This blower delivers approximately 27 cfm at 0.25 in. H_2O static pressure when operated at 9000 rpm. The fuel pressure regulator is of an Underwriter's Laboratories approved type and is set (nominally) for 19 psi gage pressure.

Analytical Substitution of Germanium-Silicon in Portable Heating and Ventilating Unit

The SNAP 10-A does not fully utilize the high temperature capabilities of germanium-silicon material. To evaluate these capabilities better, a paper substitution has been made of germanium-silicon into the generator of the previously discussed portable heating and ventilating unit. This substitution is based on information released by RCA on their "Improved 50 Watt Generator" (Reference 26). This substitution is approximate only and is not a redesign in depth.

Some of the pertinent parameters of this revised unit are given in the following Table 2-5. It was assumed that the fuel flow to the revised unit would remain the same as for the actual unit.

TABLE 2-5

REVISED HEATING AND VENTILATING UNIT GENERATOR

Output (To a matched load)	36.8 watts
EMF	9.9 volts
Current	3.72 amps
Fuel Flow Rate	0.26 lb/hr
Weight	8.0 lbs (including fuel pressure regulator)
Over-all Thermal Efficiency	2.4% (fuel in-elec. power out)
Average Hot Side Thermocouple Temperature	850°C
Average Cold Side Thermocouple Temperature	200°C
Thermocouples	p and n germanium-silicon

As can be seen by comparing the foregoing figures with those of Table 2-4, a performance advantage would result from the germanium-silicon substitution. There would be a weight increase, because the 850°C hot side thermocouple temperature assumes a stainless steel core to be substituted for the aluminum core (440°C), and this increase in weight over-balances savings in weight in the cold side heat exchanger and thermocouples. Even so, the specific output in watts/lb is not unfavorable to the germanium-silicon substitution.

It is of interest to note that the next generation of these portable heating and ventilating units is actually being constructed using even lower hot side temperatures and modified bismuth-telluride thermoelectric materials. The reason for this is economic — the thermocouple cost is reduced by a factor of 10.

Close Packed Thermoelectric Generator — Parameterized "Conceptual Design"

In order to evaluate a conceptual design of a liquid metal heated and cooled thermoelectric power generating system using current close packed PbTe modules, the system of Figure 2-7 was assumed. The system consists of heat source (not shown) supplying energy to the heat transfer fluid, which is electromagnetically pumped through the thermoelectric array (Figure 2-8) and back through the heat source. The fluid temperature out of the heat source is assumed constant at 1660°R. A portion of the heat energy delivered to the thermoelectric bundle is converted into electrical energy; the rest is dumped, via another liquid metal loop, to the main radiator. The electrical output from the thermoelectric array is put through the power conditioning package, where a portion is extracted to power the loop pumps. The remainder is then available as electrical power to the load. Heat generated in the power conditioning package is ejected through fin radiators attached directly to the package housing.

The total system weight is given by:

$$W_t = W_p + W_{rad} + W_{T/E} + W_{pc} + W_{rad'} + W_{fl} + W_{st}$$

where:

W_t = total system weight excluding weight of heat source.

W_p = weight of hot side loop pump.

W_p was taken from Figure 2-9 where the flow rate is given by:

$$\dot{M} = \frac{\Delta Q_{hs}}{C_{p_k} \times \Delta T_{he}}$$

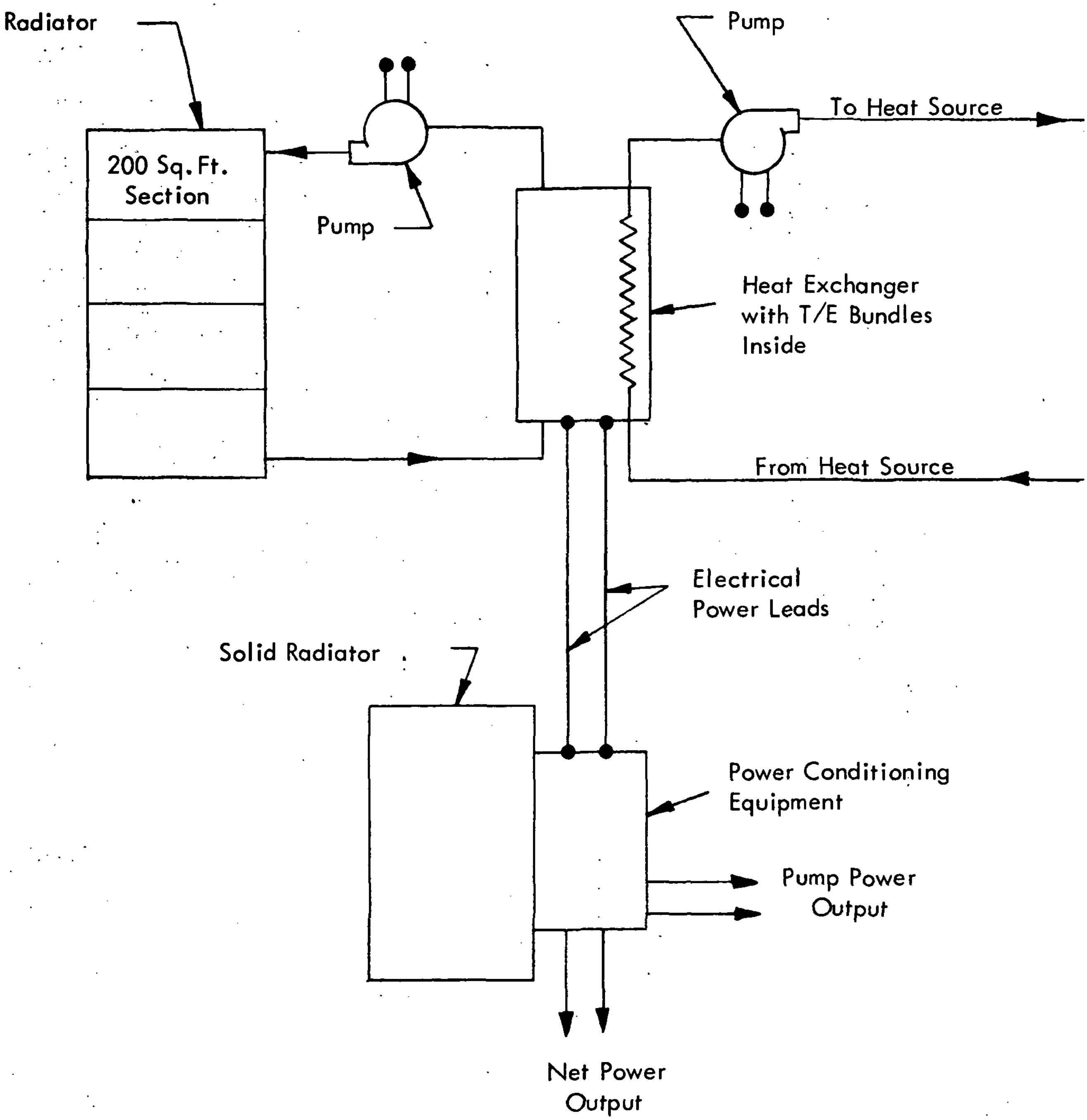

Figure 2-7 - Conceptional Design of T/E Power Generator

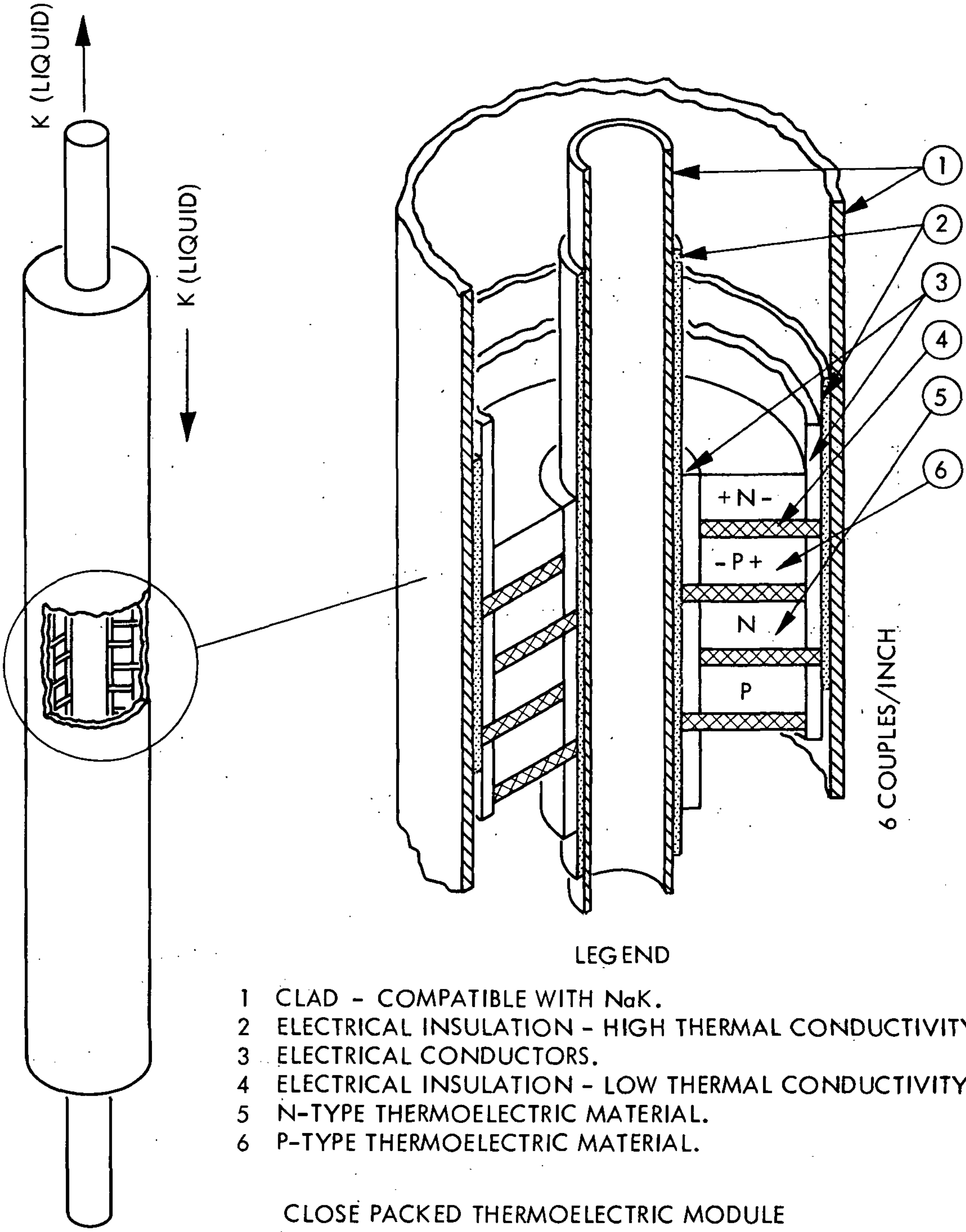

LEGEND

1 CLAD - COMPATIBLE WITH NaK.
2 ELECTRICAL INSULATION - HIGH THERMAL CONDUCTIVITY.
3 ELECTRICAL CONDUCTORS.
4 ELECTRICAL INSULATION - LOW THERMAL CONDUCTIVITY.
5 N-TYPE THERMOELECTRIC MATERIAL.
6 P-TYPE THERMOELECTRIC MATERIAL.

CLOSE PACKED THERMOELECTRIC MODULE
(OUTER LIQUID METAL JACKET NOT SHOWN)

563908A

Figure 2-8 - Close Packed Thermoelectric Module (Outer Liquid Metal Jacket Not Shown)

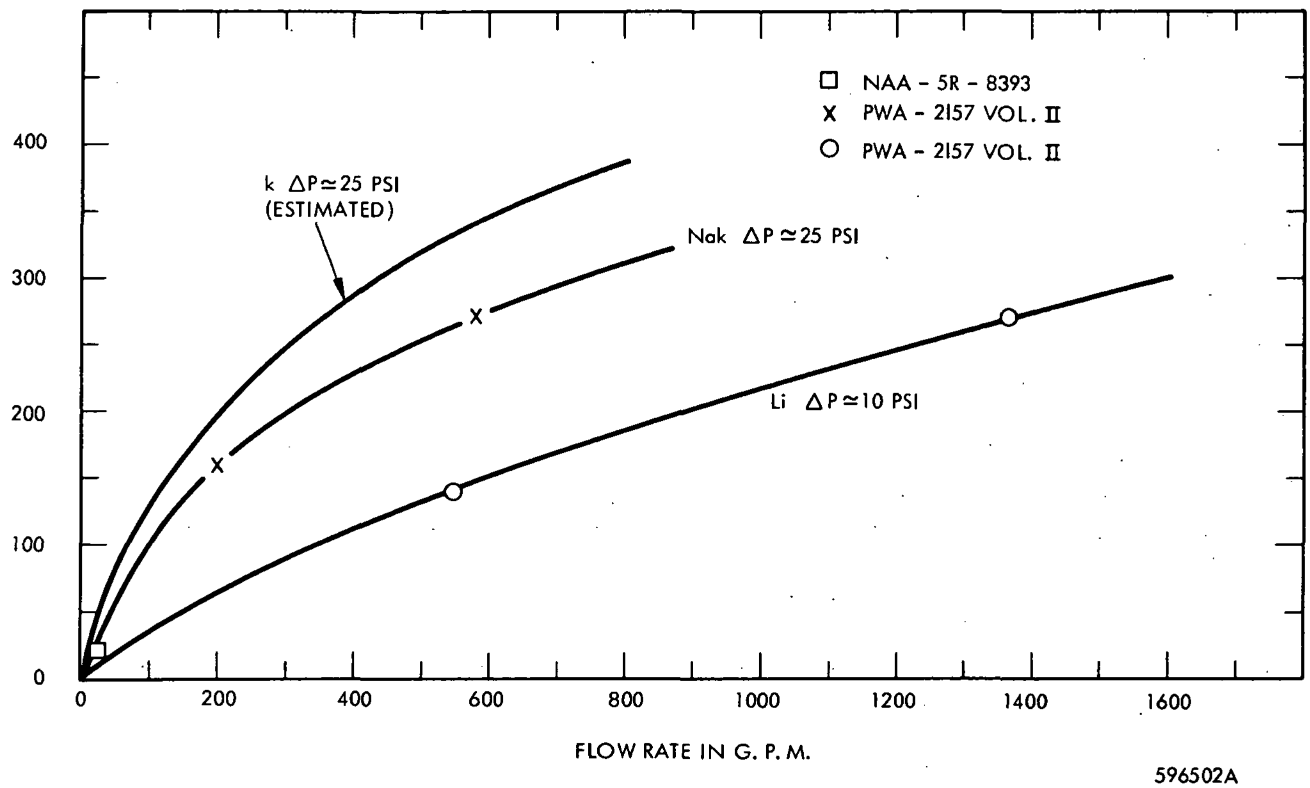

Figure 2-9 - Pump Weight

ΔQ_{hs} = rate of heat delivery to the hot side of the T/E elements.

C_{p_k} = specific heat of potassium.

ΔT_{he} = temperature drop across the heat exchanger ($\sim 135^{\circ}R$)

W_{rad} = weight of main radiator.

The total radiator area is given by:

$$A = \frac{\Delta Q_{hs} - 1/2 P_p - Pnet/\eta_{pc}}{\eta_{rad} \; \epsilon \; \sigma \; T_{eff}^4}$$

where

$$T_{eff}^4 = T_{rad}^4 - T_{sink}^4 \quad ; \quad T_{sink} \simeq 650^{\circ}R$$

$1/2 P_p$ = power consumed by the pumping system, taken as 50% efficient.

η_{rad} = radiator effectiveness, assumed to be 0.7

ϵ = emissivity of the radiating surface, taken as 0.8

σ = radiation constant

P_{net}/η_{pc} is electrical power delivered to the power conditioning package and is calculated from:

$$P_{net} = \eta_{pc} \left(\eta_c \; \eta_d \; \Delta \; Q_{hs} - P_p \right)$$

where

η_{pc} = efficiency of power conditioning equipment*

η_c = carnot efficiency defined as

$$\eta_c = \Delta \; T_{T/E} / T_h$$

* From data in reference 2, η_{pc} was taken as 90%.

$\Delta T_{T/E}$ is the temperature drop across the T/E modules, and T_h is the module hot-side temperature.

η_d = device efficiency of the modules, which was approximated by the expression

$$\eta_d = \frac{\epsilon_{T/E}}{\eta_c} Kd$$

with $\epsilon_{T/E}$ taken from Figures 2-1 and 2-2 and the device constant K_d estimated at 0.55 from data taken on close packed type elements now running in our laboratories.

P_p = power consumed by the E.M. pump and is calculated from

$$P_p = \frac{1}{\eta_p} \quad \frac{Fxd}{t}$$

η_p = pump efficiency, taken as 50%.

$\frac{Fxd}{t}$ = $g_m \times \dot{m} \times d$

where

g_m is the gravitational acceleration at moon surface = $g_o/6$ where g_o = earth gravitational acceleration.

$\dot{m}$ is the mass flow rate of the fluid as defined previously.

d is the pressure head rise over the loop pump - estimated at 28 ft.

Once the total area is known, Figure 2-10 can then be used to estimate the radiator weight. Aluminum was selected as the principal radiator material with columbium tube liners.

$W_{T/E}$ = weight of T/E elements and heat exchanger in which they are supported.

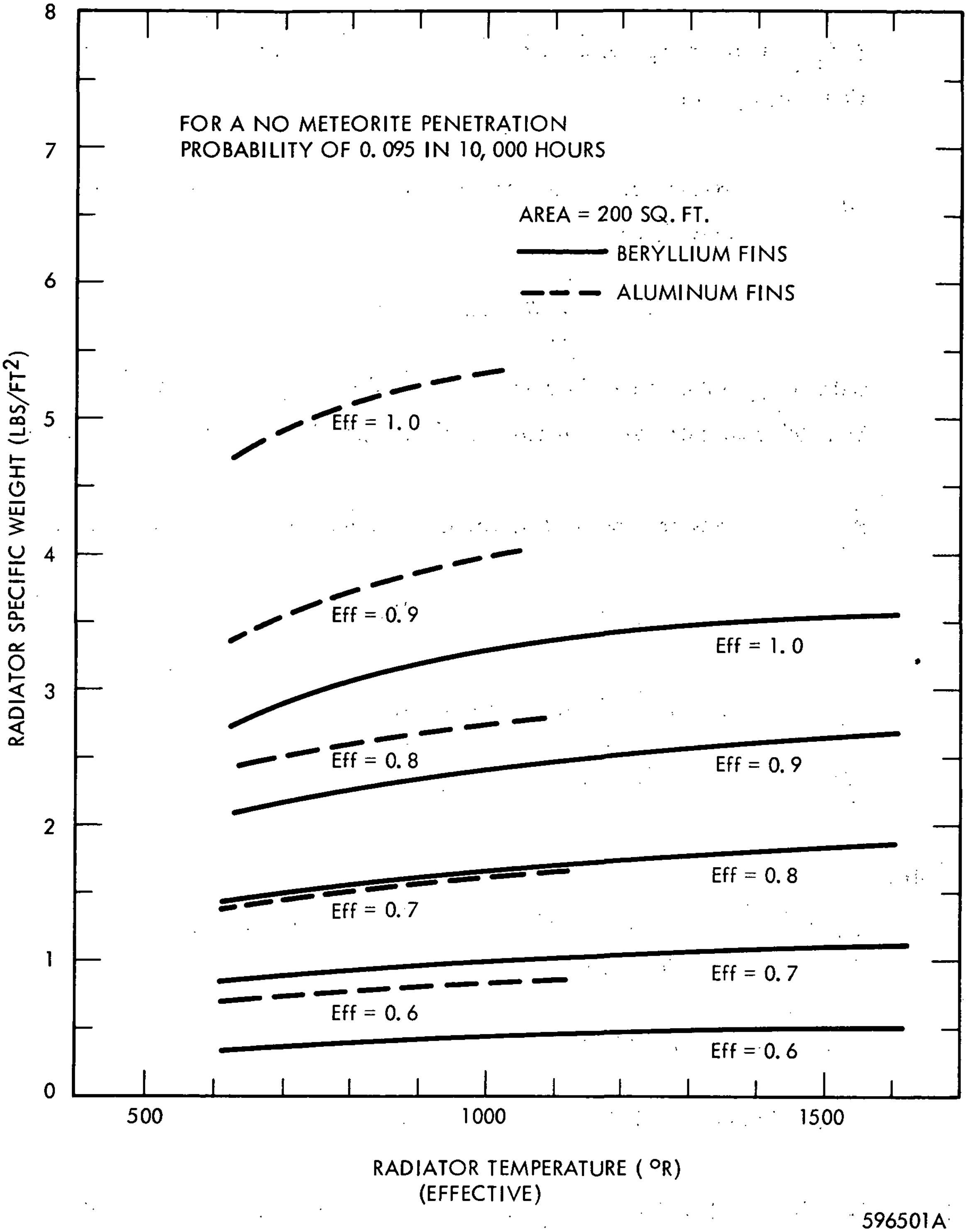

Figure 2-10 - Radiator Specific Weight

From data on actual close-packed modules, and assuming a reasonable geometry for the heat exchanger, the weight per module has been estimated as approximately 3.8 lbs/module.

Then:

$$W_{T/E} = 3.8 \times \text{no. of modules}$$

Since the type of modules under consideration have a thermal through put of 5.4 watts/module ^{o}R,

$$W_{T/E} \simeq 0.666 \quad \Delta Q_{hs} \; / \; \Delta T_{T/E} \quad \text{(lbs)}$$

where ΔQ_{hs} and $\Delta T_{T/E}$ are as previously defined.

W_{pc} = power conditioning package weight

This weight was obtained from Figure 2-11.

$$W_{pc} = \text{Specific weight} \times P_{pc}$$

where

P_{pc} = *Pnet/* η_{pc} *is the input to the power conditioning package.*

$W_{rad'}$ - Radiator for power conditioning package

$$W_{rad'} = \text{Specific weight } (\text{lbs/ft}^2) \times \text{area required (sq ft)}$$

where specific weight was again estimated from Figure 2-10, and the area is given by

$$A = \frac{Pec - Pnet}{\eta_{rad'} \; \epsilon \; \sigma \; T_{eff}^4}$$

$\eta_{rad'}$ = effectiveness of power condition package radiator, taken as 0.6

ϵ, σ, T_{eff}^4 are as previously defined

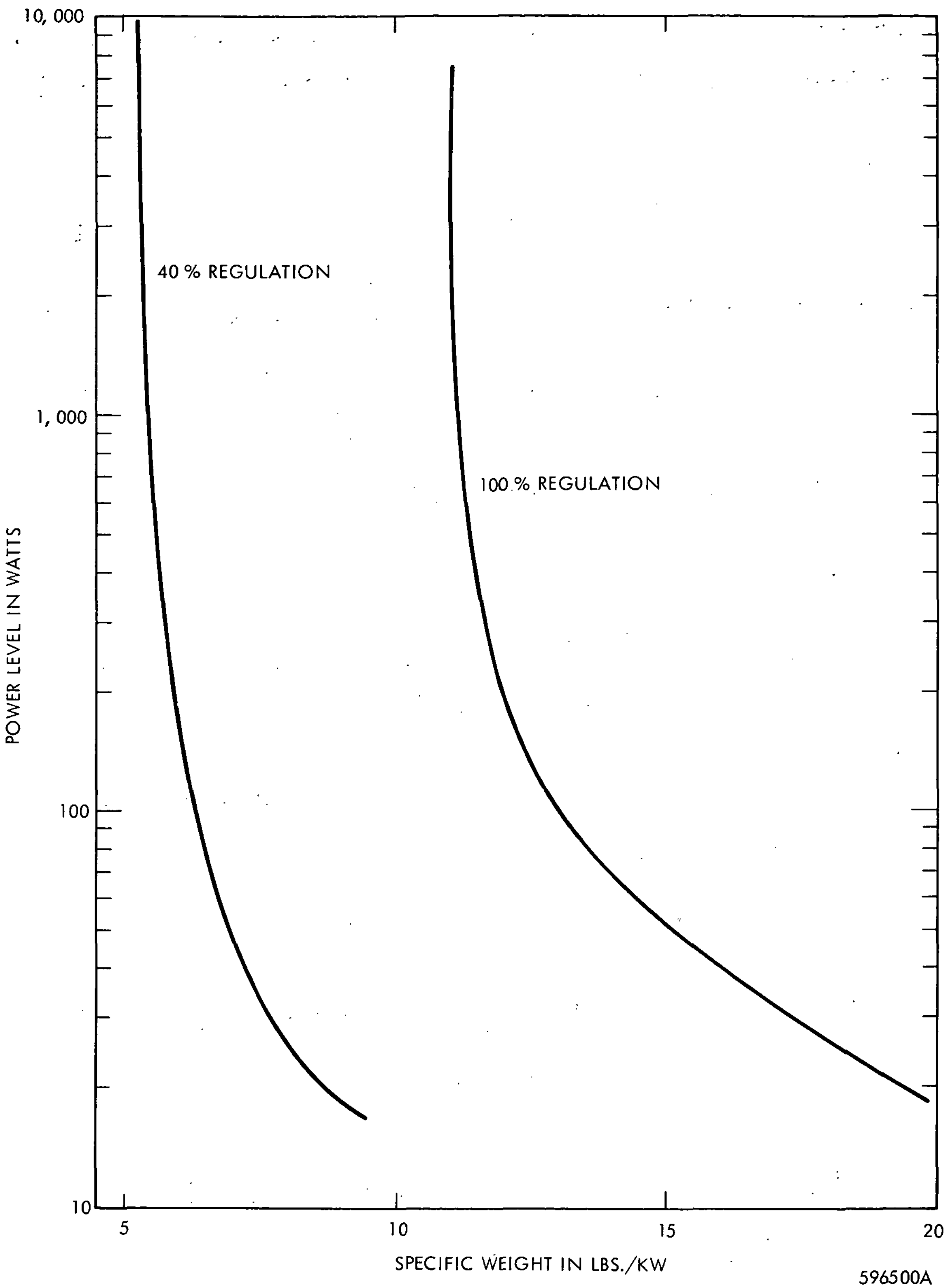

Figure 2-11 - Power Conditioning Package Specific Weight

W_{fl} = total weight of heat transfer fluid in the hot-side loop (cold-side fluid weight accounted for in Figure 2-10).

= C (no. of T/E elements x wt. of fluid/element)

where

Number of T/E elements as given previously

weight of fluid/element = vol. of fluid tube x density at 1480°F

C was estimated at 5x to account for fluid in the rest of the system.

W_{st} = Structure weight and was taken as 10% of total system weight.

The results of examining this assumed system parametrically are shown in Figure 2-12. This is a plot of partial system weight (heat source weight excluded) as a function of actual radiator area with parameters of system net electrical power output, heat input, and radiator temperature. System maximum temperature was held constant at 1660°R, and effective ambient temperature was held constant at 650°R. The minimum weights for given net electrical outputs taken from Figure 2-12 are replotted in Figure 2-13. For example, the minimum partial system weight is 11,000 lb for a net electrical output of 30 kw. Maximum partial system specific outputs are at the 3 watts/lb level.

CONCLUSIONS

Useful proven thermoelectric materials are available to cover a temperature range from room temperature to 1600°F. When properly applied in devices, 10,000 or more hours of use without maintenance with less than 10 percent degradation can be expected.

Thermoelectric thermal conversion efficiencies normally run about 5 percent but can go as high as 8 percent or 9 percent, or as low as the 2 percent of SNAP 10A. Efficiency is somewhat a function of designer and the constraints of the total system concept.

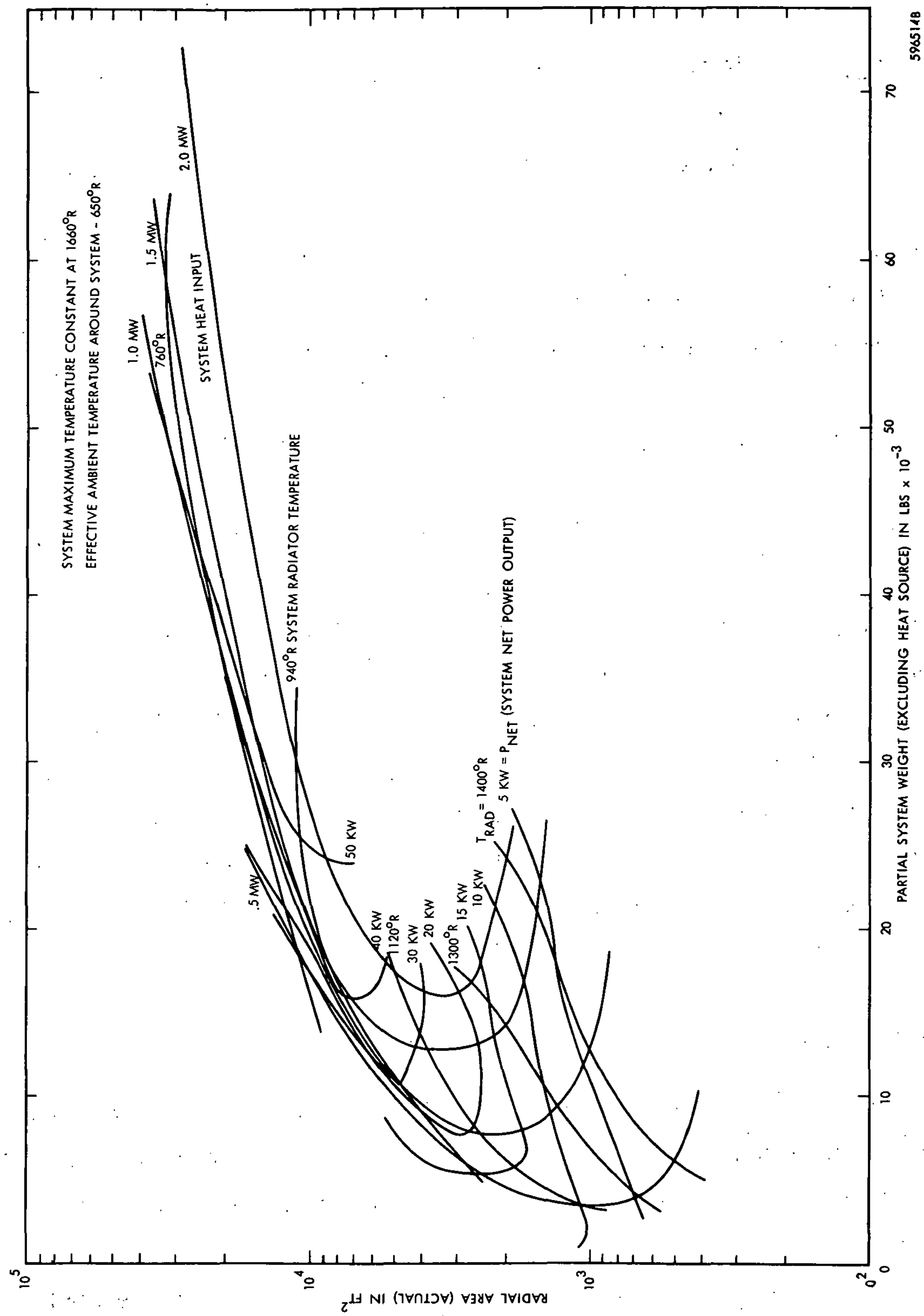

Figure 2-12 - Partial System Weight (Excluding Heat Source) in lbs x 10^{-3}

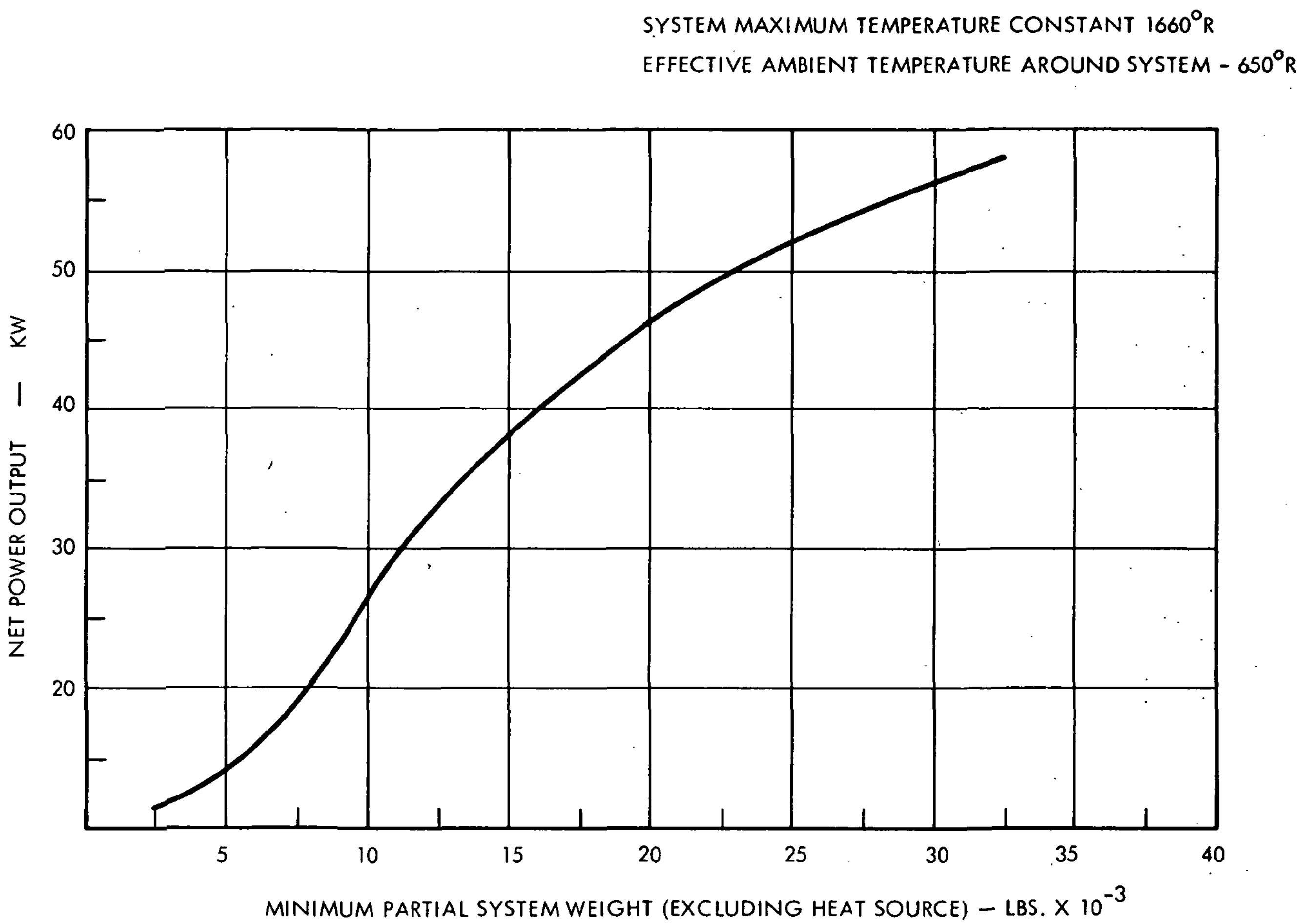

Figure 2-13 - Minimum Partial System Weight (Excluding Heat Source) — lbs x 10^{-3}

Specific output per unit weight for the converters, plus necessary heat exchangers and attendant equipment but without heat source, run from about 1 watt/lb on the SNAP 10A to above 5 watts/lb for long-lived, ground-based, air-cooled generators. This is somewhat a function of application, size, and designer. It would appear from our examination that specific power outputs of about 3 watts/lb at 1050°F top thermocouple temperatures are quite in order.

For available nuclear heat source temperatures of 1200°F or lower, the lead tellurides, germanium bismuth telluride, and germanium silicons are candidates for use. It is our opinion that the lead telluride n leg, germanium bismuth telluride p leg combination is the best choice because of its high figure of merit.

For available nuclear heat source temperatures substantially above 1200°F, germanium-silicon materials have the field to themselves at the present time.

REFERENCES AND LIST OF GOVERNMENT CONTRACTS — THERMOELECTRIC ENERGY CONVERSION SYSTEMS

1. Semiconductor Thermoelements and Thermoelectric Cooling. IOFFE, A.F., Infosearch Limited.

2. Teem, J. M. and Szego, G. C. Electric Propulsion and Power Astronautics and Aerospace Engineering. Nov. 1963.

3. Dykstra, L. J. Westinghouse Research Report 929-8904-R1, 1961.

4. Chasmar, P. P., and Stratton, R. J. Electronics and Control 7, 52, (1959). (See also Goldsmid, H. J., J. Electronics and Control 1, 218 (1955), and Proc. Phys. Soc. London 71, 633 (1958).)

5. Battelle Summary Report on Materials and Techniques for Thermoelectric Cooling, October 12, 1960.

6. Maximum Figure of Merit of Thermoelectric Materials. Simon, R. Battelle Memorial Inst.

7. Westinghouse Thermoelectricity Quarterly Progress Reports No. 3 and No. 4.

8. Weiss, H. Ann. der Physik 4 121, (1959).

9. Abrahams, M. S., Braunstein, R., Rosi, F. D. Jour. Phy. Chem. Solids 10, 204 (1959).

10. Chasmar, R. P. and Stratton, R. Phys. Rev. 102, 1686, (1956).

11. Keyes, R. J. Appl. Phys. 30, 454 (1959).

12. Ure, R., and Heikes, R. R. Thermoelectricity-Science and Engineering (Interscience, New York, 1961), Chapter 11.

13. Heikes, R. R. Private Communication, Sept. 9, 1963.

14. Evans, W. G., Characteristics of Thermoelectric Materials. Semiconductor Products, April 1963.

15. Silicon-Germanium Thermocouple Development. Raag, Valvo, 17th Annual Power Sources Conference, May, 1963.

16. RCA Trip Report WANL-TR-2469.

17. Westinghouse Module Improvement Program. Progress Report No. 3, March 15, 1963.

18. Radiation Resistance of RCA Germanium-Silicon Alloy. RCA Data Sheet.

19. Westinghouse - In-Pile Tests of PbTe.

20. Westinghouse, Module Improvement Program, Final Report, August 31, 1962.

21. Nuclear Reactor Systems, Anderson, G. M., Astronautics and Aerospace Engineering, May 1963.

22. Thermoelectric Power-Generating Couples Utilizing Diffusion Bonded Tin Contacts, C. S. Duncan, et al, Westinghouse Research Report 63-929-242-R1.

23. 5 KW Thermoelectric Generator. Westinghouse Report No. 9160-01102-903(1). U. S. Navy Contract No. NOBS-77093.

24. Sedgley, D. B., Progress Report SNAP 10A Nuclear Compact Reactor Development, NAA-SR-8393.

25. Pouchot, W. D., Westinghouse Electric Corp. Report, Engineering of Thermoelectric Heating and Ventilating System, Contract DA19-129-QM-1981 (OI 6069) Project No. 7X80-01-001, Dec. 7, 1962.

26. RCA Silicon-Germanium Thermoelectrics, June 1963. RCA Data Sheet.

Contractor	Report Dist.	Contract No.	Current Starting Date	P.I.C. No.	Funding	Subject (End Item)
Ⓦ Elec. Corp.		NObs-77093	Mar. 1959 Completed	226 Completed	FY59-342, 500	(Disc.) Design & construct a 5000 watt self-contained thermo-electric power generator fueled by diesel oil or kerosene. A water cooler will be used. Power to pump fuel and cooling provided by generator.
Internal Program			Init. Rec. by PIC Oct. 1960 Issued PIC Jan. 1961	275 Partly Completed		Thermal Characteristics of Energy Conversion Devices
Princeton Univ.	No. 53D Apr. 59 54A-5/59 & more	DA-31-124-ARO(D)21	Rec. by PIC Dec. 1960 Issued PIC Jan. 1961	291 Completed	FY63-35, 000	Reports
European Res. Assoc.		AF61(052)-568	Oct 5, 1961 completed	309 Completed	FY61-44, 550	Knowledge (Title: Fundam. Studies on Therm. Materials)
Gen. Elec. Co.		DA-44-177-R-639	Rec PIC Feb. 1961 Issued PIC Mar. 61	352 Completed		(Title) Ther. Conversion of Elec.
Ⓦ Elec. Corp.	ASTIA	NObs-84329	Mar. 1, 1963	373 Completed	FY61-336, 990	Improved Generator Module
Mass. Inst. of Tech.		NONR-1841(78)	Rec. by PIC Mar. 1961 Issued PIC Mar. 1961	376 Continuing		Knowledge (Title) (Energy Conversion Research)
General Instruments Corp.	Div. of Tech. Inf. Ext. USAEC	AT(30-1)-2605	Mar. 31, 1961	442 Phase I Completed	FY62-180, 000	3-5 watt thermoelectric generator fueled with mixed fission product radioisotopes
General Instruments Corp.		DA36-0395C-87364	Sept. 6, 1960	453 Continuing	FY62-130, 000	Development model of 45 watt Generator

Contractor	Report Dist.	Contract No.	Current Starting Date	P.I.C. No.	Funding	Subject (End Item)
General Instruments Corp.		NObs-84299	April 1961 Completed	506 Completed	FY62-15,000	5 watt thermo power unit
TYCO Lab., Inc.	ASTIA	NObs-86015	Contract Period July 1961	509 Continuing	FY62-61,157	Technical Reports
RCA		NObs-85531	Jan 1961 Completed	510 Completed	FY62-8,995	One 25 watt Thermo. Generator
(W) Elec.Corp. Aerospace	ASTIA	AF33(657)-8089	Rec PIC May 1961 Issued PIC June 1961	552 Continuing	$94,000	10 watt Solar Thermo. Generator Tech. Reports
Monsanto Dayton Labs	DDC	AF33(657)-7387	Oct. 1961	681 Pt. Completed	FY63-173,297	High temp. T/E Modules (800°C-1200°C) - 50 watt generator
Atomics International		AT(11-1)-GEN-8	Mar.15, 1962	687 Continuing	FY63-227,000	Application of RCA materials to higher than SNAP-10A cond.
Servomechanisms, Inc.	ASTIA	NObs 86367	Completed July 1962	B32		Cylindrical elements, end constrained, 16% degradation in 1600 hr must in first 300 hr, initial specific power was 0.75 watts per gram active material. P&N PbTe Washer diam.-.5" OD, .315" ID overall diam. 1" dia. Final dated July 1962.
RCA, Princeton Lab.		NObs-86651	April 1962 Jan 1963	864 Continuing	FY62-208,000	Fabrication of GeSi T/E's application studies 250 watt Propane Fuel Burner
US Naval Research Labs	DDC	None	Nov 1958 Continuing	227	FY63-60,000	New theoretical developments, materials evaluation
Union Carbide	DDC	NObs-77066	Jan 1959 Completed	232		Research info, Tech. reports, prototype gear
RCA	DDC	NObs-77057	Feb. 1959 Completed	233	FY59-278,000	Tech. Reports

Contractor	Report Dist.	Contract No.	Current Starting Date	P.I.C. No.	Funding	Subject (End Item)
Battelle Mem. Inst.		NObs-77034	Sept. 1957 Completed	234	FY60-137,800	Tech. Reports
Internal Program	ASTIA	5B-51-02-004	1958 Continuing	251		Feasibility Determinations & Experimental Devices
Ⓦ Elec. Corp.	ASTIA	NObs-78197	Feb. 28, 1961 1960 comp.	258 Completed	FY61-44,329	500 watt Portable Thermoelectric Generator
Minnesota Mining & Mfg. Co.		NObs-78198	Feb. 28, 1961 Completed	260	FY-61-94,000	500 watt Portable Thermoelectric Generator
Carrier Corp.		NObs-77093	Completed	265	FT59-194,000	To design, construct, test & furnish on 5-W thermoelectric generator, in accordance with Bureau of Ships "Specifications for a 5 kw T/E Generator" date 27 Aug. 1958 (description)
Stanford Univ.		AF-49(638)1123	Rec PIC July 1961 Issued PIC July 1961	591	FY62-500,000	Knowledge (Title: Gen. Res. in Energy Conv.)
Gen. Elec. Corp		AF33(616)-8256	Rec PIC Sept. 1961 Issued PIC Sept. 1961	614	FY61-75,000 62-106,000	Lab. Samples & final report Rev. No. 2 - Power supply feasibility model to be evaluated at Contractor's Lab. & Final Report
Battelle Mem. Inst.		DA36-039-5690838	Feb. 1962	705	FY62-95,000	Tech. Reports-Breadboard Model
Martin-Marietta Corp (NASA)		AT-(30-1)2952	Jan 11, 1962	711	FY63-530,000	Curium-242 fueled thermoelectric generator for use on the NASA's surveyor soft lunar landing missions
Gen. Inst. Corp		AT(30-1)-2783	Rec & Issued PIC Nov. 1962	769	47,000	Feasibility Report
Gen. Atomic	ASTIA	AF33(657)-9203	Rec & Issued PIC Oct. 1962	758	FY62-39,925	ASD Tech. Reports

Contractor	Report Dist.	Contract No.	Starting Date	P.I.C. No.	Funding	Subject (End Item)
RCA		DA36-039-AMC-00110 (E)	July 1962	776	FY63-99,000	Study Report and Sample of T/E Power Module
Internal		None	PIC (Rec)Dec.'62 Issued PIC Jan 1963	782	FY63-1/4 man-year	Investigate feasibility of a cryogenic fueled thermoelectric generator & establish design parameters for specific application
Mat. Res. Corp.	ASTIA	NObs-86216	Cont. Period Oct. 1961	834	FY62-72,722	Technical Reports
Atomics International		AT(11-1)-GEN-8	April 22, 1963			Technical Report

C. THERMIONIC POWER SYSTEMS STATE-OF-THE-ART

A survey of the State-of-the-Art of thermionic energy conversion systems is presented in the following pages. Because this essentially simple and attractive static system bears the burden of operating effectively only in the present-day fringe area of materials' capability, it has no demonstrated present-day ability to meet the operating lifetime requirements of the lunar base power supply. Its projected ability, based on successful operation, out of nuclear pile, of diode strings, is good, but the timing of such an event is most uncertain.

INTRODUCTION

Historically, the thermionic phenomenon was first noticed and mentioned by Edison. It was investigated and treated theoretically in depth by Langmuir as early as 1915. In comparison to thermoelectric energy conversion systems which operate at lower temperature levels, thermionic converters provide high amperage current flows at a voltage higher than thermocouple output.

In thermionic energy conversion, heat from any suitable source is applied to one member, the emitter, of a dipole system. The space between the emitter member and the second, collector member is maintained at a very low pressure. When the emitter temperature has been raised to the ionization temperature characteristic of the emitter material, the "free-gas electrons" in the interior of the emitter material have acquired enough energy to cross the surface potential barrier, escape as free electrons and travel to the collector. Thus, the heat energy applied to the emitter flows from the emitter to the collector, and although the major part of the total energy flow is heat, an attractively large proportion - 10 percent or more - is electrical. The collector is electrically connected externally through a useful load to the emitter.

The above description is, however, too simple. As the electrons are "boiled out" of the emitter an electron cloud is formed adjacent to the emitters' external surface, the dense electron charge reinforces the surface potential barrier and inhibits passage of the individual electrons to the collector. A common means of reducing this "space charge" effect is cesium vapor, at very low pressure, maintained between the emitter and collector. The cesium atoms when ionized by contact with the hot emitter surface or by electron bombardment become positively charged ions and to a large degree neutralize the space charge without blocking passage of electrons from emitter to collector.

Nuclear technology now provides compact thermal energy packages which can maintain heat energy output in very large quantity over long periods of time. Thermionic energy conversion of this available heat appears to offer a good "fit", in the sense that the temperature levels of heat output from the nuclear reactors are approaching the neighborhood of acceptable temperature levels for the input to the thermionic converter, and the sizes, areas, and geometries are compatible. In addition, the high temperature levels of thermionic devices are advantageous where system waste heat must be rejected by thermal radiation.

Work in various phases of nuclear pile-thermionic conversion systems, suitable for space and extra-terrestial operation, is being carried out by a substantial number of groups. Refer to the Thermionic References and List of Government Contracts on Thermionics which lists a sampling of contracts and programs. Some of these programs involve complete system concepts, others are restricted to some particular area of thermionic interest. In general, the system concepts involve one of three different physical locations of the thermionic converter — in the nuclear pile, in a heat exchanger on an external portion of a liquid metal cooling loop, or on the radiator surface of a liquid metal coolant loop.

In our survey of the Thermionic State of the Art we draw upon these contractors' program reports, our trip reports of visits to contractor installations and discussions with their personnel, and a review of their conclusions, to form our conclusions and summary.

STATE-OF-THE-ART

Power Converters

Investigation of thermionic conversion is being carried out in many places. Basic research or development is proceeding on variants of the initial diode system, such as triode configurations (Reference 1), liquid diode collectors (References 2 and 3), barium diodes (Reference 4), auxiliary discharge (Reference 5), capillary emitter (Reference 6), and many others. The time frame of reference of the present program does not permit value judgments of this work.

The main line of successful development has been on the cessiated diode.

A necessary part of the effort on thermionic power converters is materials investigation and evaluation. For use as emitters, because of the high temperatures involved, effort has been directed principally at the refractory metals or metal carbides such as tungsten, tantalum, columbium, molybdenum, and uranium carbide/zirconium carbide. Of particular interest is the compatibility of these materials with nuclear fuels for converters to be used in pile. Other areas of interest are electrical insulators and collector materials.

Of the possible electrical insulators only high purity alumina or sapphire seems to have the proper resistance to metal vapor attack, chemical and physical stability, and insulator to conductor sealing ability required for thermionic power converters.

Present choice of emitter materials when considering system design is either tungsten or molybdenum. Tungsten apparently could be used to 2000°C in contact with UO_2 nuclear fuel (Reference 7) and to 1800°C in contact with UC/ZrC nuclear (References 7 and 8) fuel. Best tungsten for use is formed by a vapor deposit process (Reference 9). Molybdenum may possibly be used to 1600°C in contact with UC/ZrC fuels although testing time has been short (Reference 8). Molybdenum is also compatible with UO_2-Mo-Cermet nuclear fuel to temperatures of at least 1600°C (Reference 10). Columbium (Reference 10) and nickel (Reference 11) are used as collector materials.

Out-of-Pile Cessiated Diode Results

As has been stated previously, the main line of successful development has been on the cessiated diode. An example of a successful (out of pile) cessiated diode is the RCA diode 1197-A, Figure 2-14. This figure shows an in-pile test configuration. The emitter material is molydbenum, the collector is nickel, the insulation is alumina ceramic. The nominal operating conditions for this diode are an emitter temperature of 1350°C (2372°F), collector temperature at 570°C (1058°F), power density of 2.5 watts/cm^2, efficiency 11 percent. The converter operated in the "ball-of-fire" or arc discharge mode, as do all presently useful thermionic converters. The converter automatically enters this mode above 1300°C. Below this temperature arc discharge can be initiated electrically.

The optimized performance of the RCA diode for other than nominal operating conditions is given by Figure 2-15. It will be noted that the volt-ampere characteristic of the converter is linear at constant heat input. As a consequence, series arrangements of diodes can be used to give directly additive outputs, neglecting the minor lead losses. The RCA (Reference 11) diodes have been operated in triple series strings without trouble. To date about 1500 hours of running on a series string has been accumulated.

The Martin Company (Reference 10) have constructed similar diodes and have run parallel out-of-pile tests. Their thermionic diodes have run for over 2000 hours successfully. Two diode elements in series actuated hundreds of times without difficulty. The particular style converter was run at a power output density of 19 watts/cm^2 without evidence of degradation or failure.

The longest endurance running of thermionic diodes is reported by General Electric (References 8 and 10). Six different cylindrical diodes were placed on test. Three ran a substantial period of time. Failures of the three long lived diodes were connected with attempts to replace burned out heater elements in the test equipment. Table 2-6, following, gives the reported results.

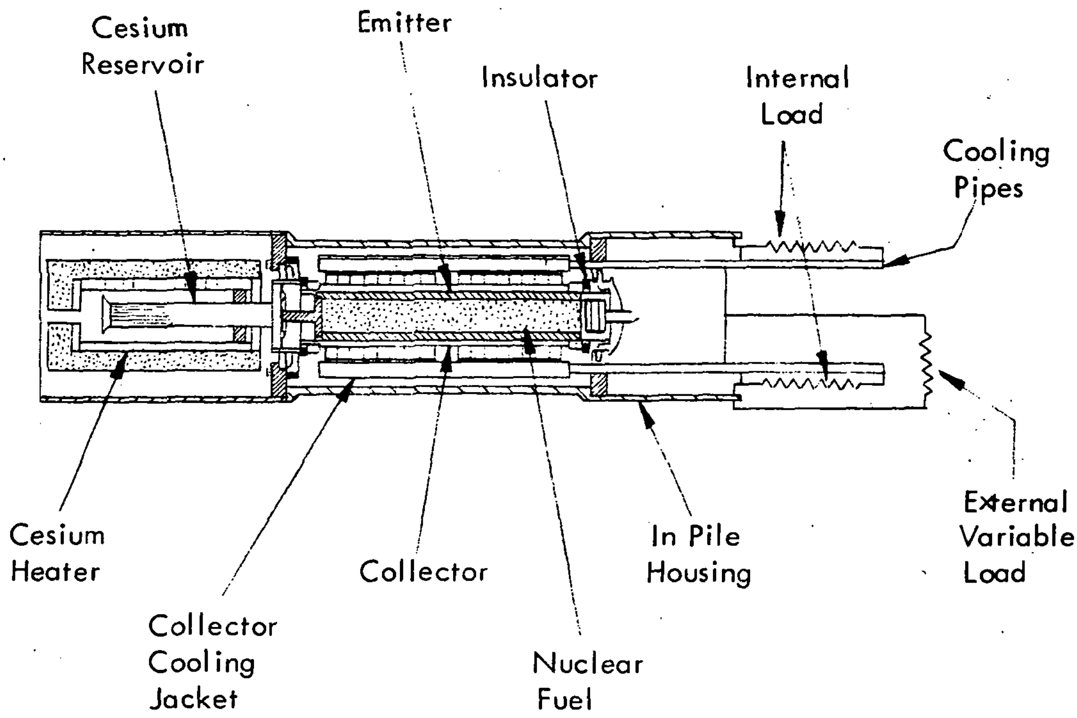

Figure 2-14 - RCA Converter Type 1197-A In Pile Configuration

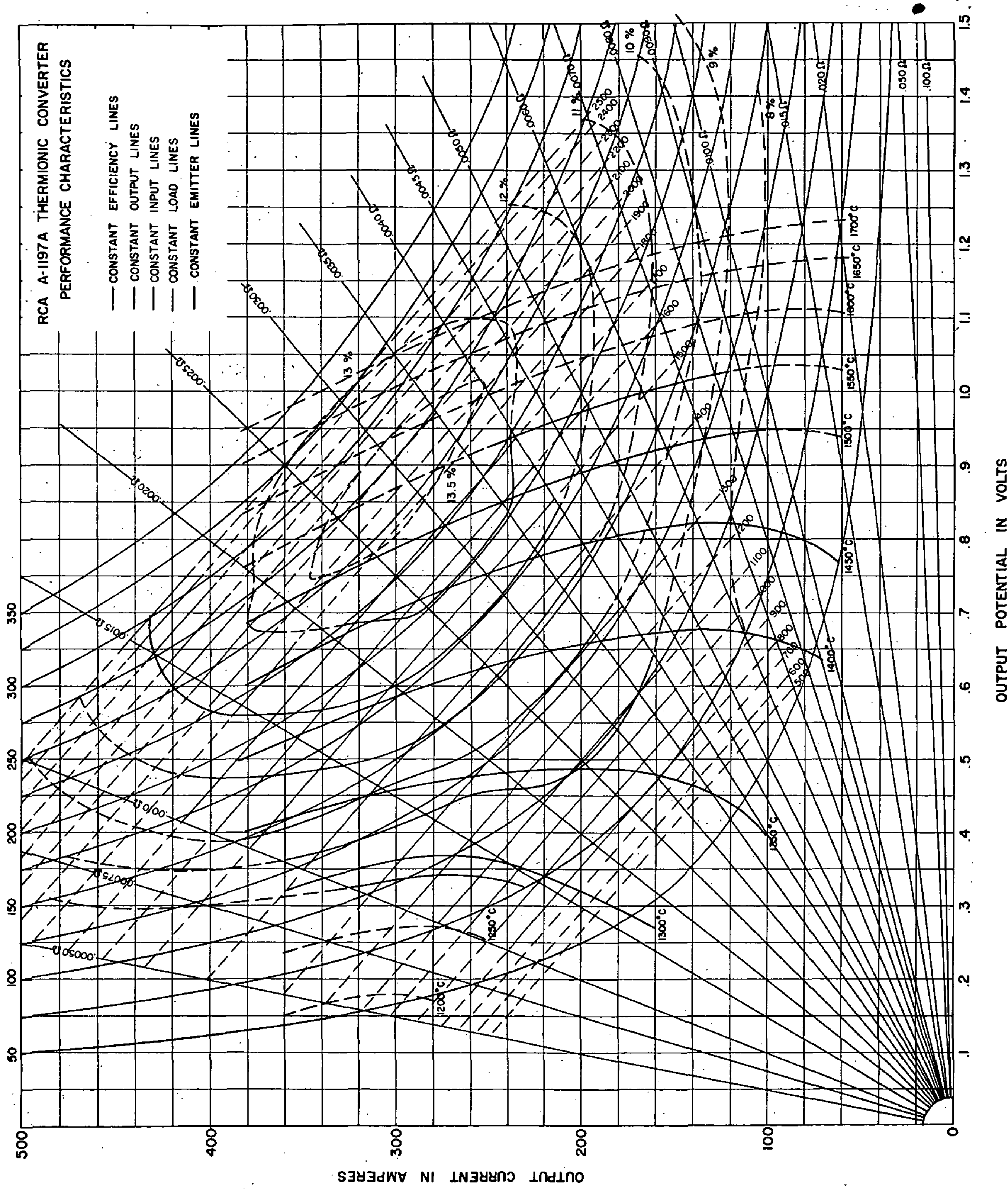

Figure 2-15 - RCA A-1197A Thermionic Converter Performance Characteristics

TABLE 2-6

GENERAL ELECTRIC DIODE ENDURANCE TESTS

Emitter Material	Emitter Temperature	Specific Power Out	Test Period
Molybdenum	1650°C	2.5 watts/cm^2	3200 hrs
Columbium	1760°C	2.6 watts/cm^2	8538 hrs
Tantalum	1760°C	4.6 watts/cm^2	5000 hrs

In-Pile Cessiated Diode Results

In contrast with the success reported on out of pile running, tests of diodes in-pile have been uniformly unsuccessful. The maximum operating time before failure reported (Reference 9) is 300 hours. A typical result is shown in Figure 2-16 Part of this may be because of limited test effort but Los Alamos Scientific Laboratories said they had run over 100 in-pile tests (Reference 9). The General Electric Company have run two in-pile tests, both tests lasting approximately 200 hours to failure. These tests are called IPOP (in-pile-out-of-pile) and were conducted under AEC contract AT (04-3)-189. All tests failed. According to report, these were mechanical failures not connected with the basic operation of a diode unit. The thermionic converters had a columbium emitter and a stainless steel collector. They were operated at an emitter temperature of 1700°C and a c ctor temperature of 630°C.

Conceptual Systems

No actual nuclear thermionic conversion system has as yet been developed, built, and operated. The conceptual systems differ as to the location of the thermionic converter in relation to the nuclear reactor. Figure 2-17 shows three different general arrangements with their operating temperature levels. A fourth scheme represented by General Electric's STAR-R system locates the thermionic converter between the nuclear pile and the radiator elements with solid state heat conduction from converter to radiator. Reactor core heat transfer requirements restrict this last configuration to relatively small systems. Present for-instance designs are based on 20 kw electrical output (Reference 12). Four π nuclear shielding is not possible without drastic modification of the present STAR-R concept.

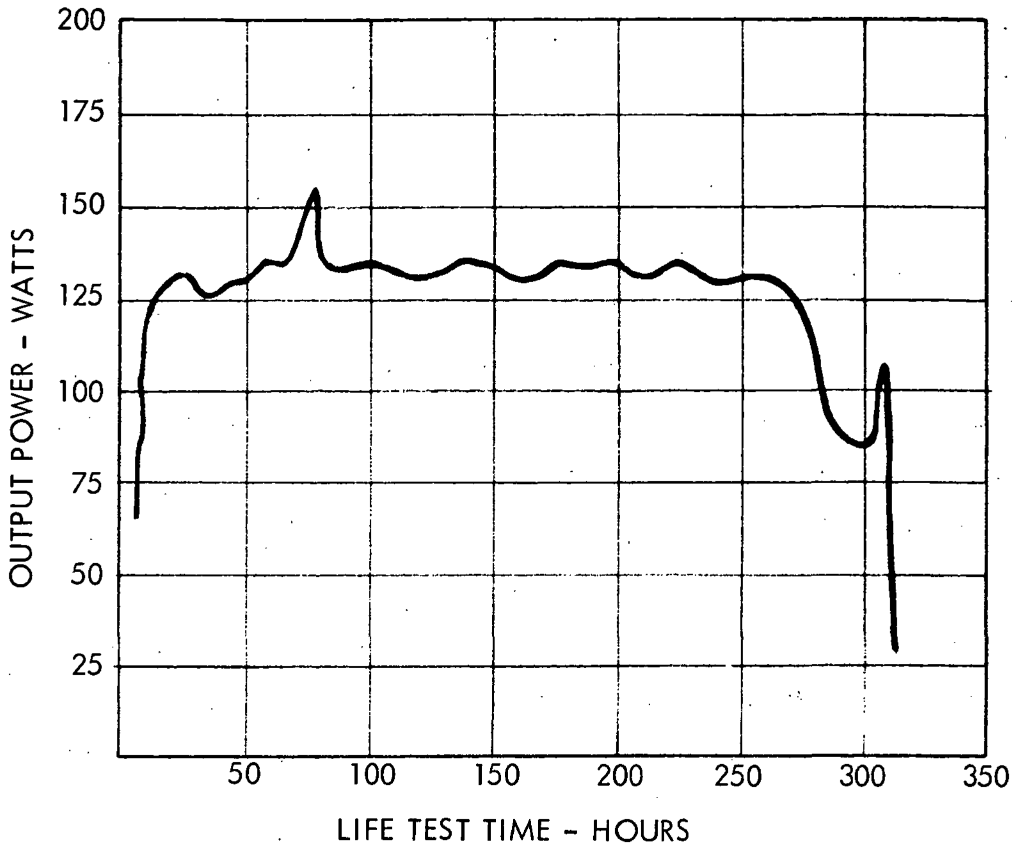

Figure 2-16 - RCA In Pile Test
Output Power Versus Time

Electrical Output	Max. liquid-metal temp.	Emitter temp.
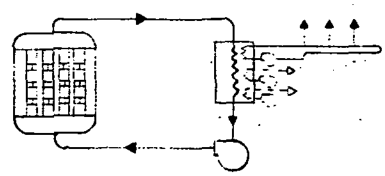 Converter in: fuel element	600°C-900°C	1200°C-1500°C
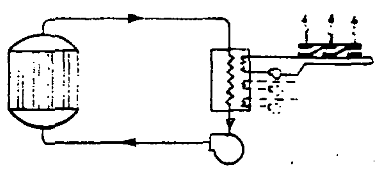 Converter on: radiator	1300°C-1600°C	1200°C-1500°C
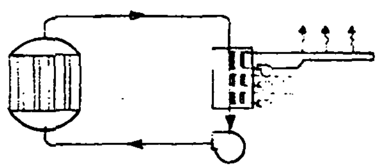 Converter in: heat exchanger	1300°C-1600°C	1200°C-1500°C

Figure 2-17 - Nuclear Thermionic Conversion Concepts

Three conceptual system designs from three different companies, which have projected electrical output capabilities in excess of 1 Mw are presented in brief hereafter. All of these systems involve the use of the thermionic elements in the nuclear fuel element (in-pile). Systems of this sort avoid the extremely high temperature liquid metal loop problems of the 'converter or radiator' and "' in heat exchanger"' types. For the latter two schemes, liquid metal loop temperatures required are at least a generation beyond even present advanced development work as represented by the upper temperature levels being considered for SNAP 50/SPUR.

Using the thermionic converters in-pile quite obviously results in compromises in reactor and converter technology. One of the more prominent results is to give a "bare" reactor core of substantially larger dimensions than is necessary using a straight fluid cooled reactor. Where four π nuclear shielding is required the weights of such shielding will be substantially higher than for the straight fluid cooled reactor.

Figure 2-18 shows schematically the arrangement of General Electric's STAR-C (Reference 12) system with the thermionic converters in-pile. A primary coolant loop of liquid Na transfers heat from the collector surface to an external heat exchanger shared by a secondary liquid Na loop which completes the ultimate heat rejection to space through its radiator. The intermediate heat exchanger restricts the radioactive fluid to the general vicinity of the reactor core. One disadvantage inherent in the design is the ΔT between the collector surface and the surrounding liquid Na coolant. For a specified liquid Na coolant temperature, the required collector temperature will be several hundred degrees higher. Sensible conversion efficiencies require an emitter temperature nearly double that of the collector temperature, therefore a high coolant temperature requirement is reflected throughout the entire system in higher temperature levels.

General Electric proposes UO_2 as fuel because of the large amount of experience which has been accumulated in in-pile loop operation. However, this experience has been with pressurized water and boiling water reactors where water was a moderator as well as a heat transfer fluid. The direct extrapolation of this experience to nuclear thermionic conversion system

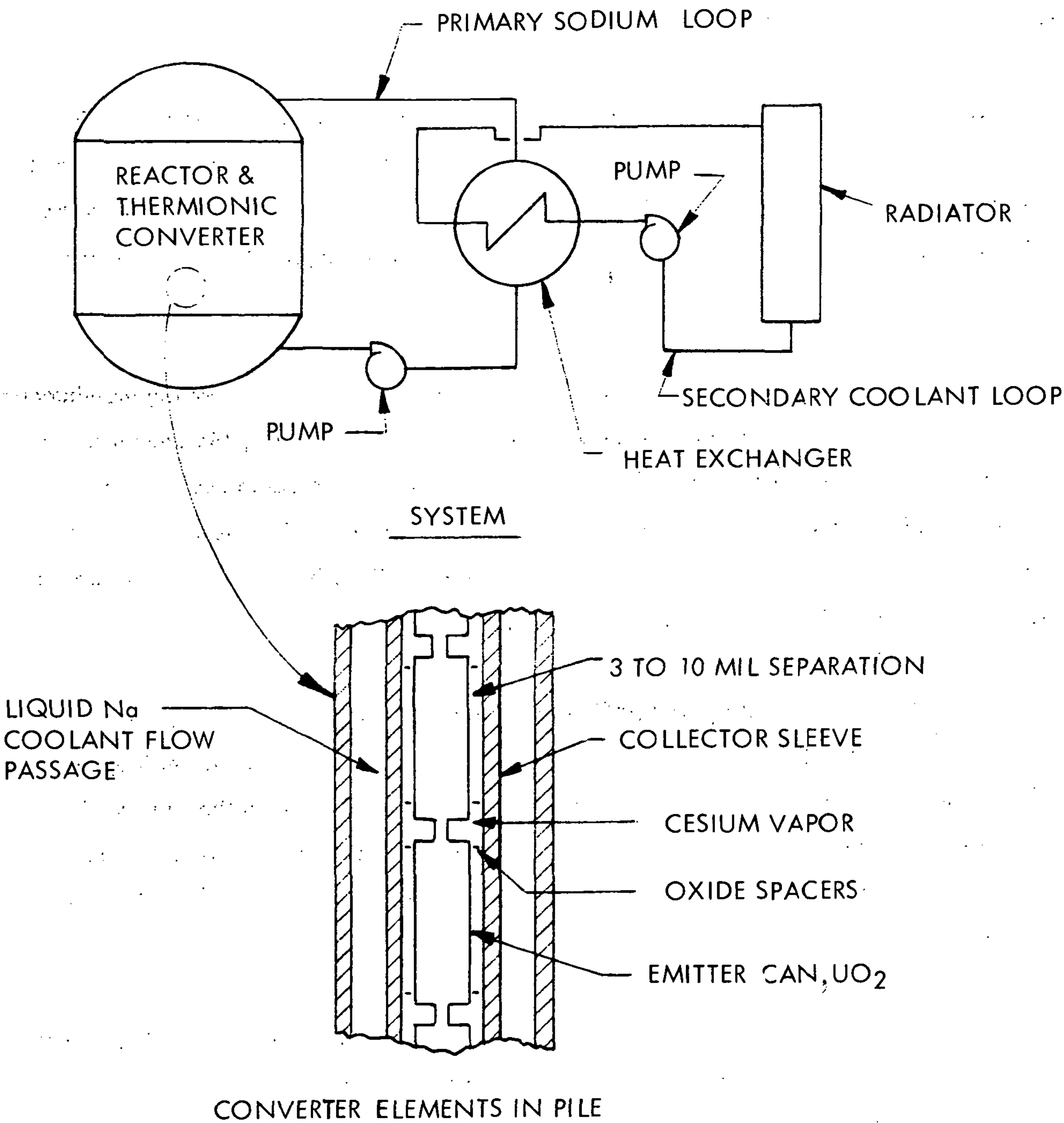

Figure 2-18 - Schematic of General Electric Co. STAR-C Concept could encounter difficulties. The specific weight level of General Electric's present STAR-C designs is on the order of 150 lb/kw.

The Martin Company (Reference 10) design concept is shown schematically in Figure 2-19. This design is one which is specifically being examined by the Martin Company under contract to NASA, for lunar use. Its design is predicated on installation in a lunar crater to avoid the prohibitive weight of nuclear shielding the design would otherwise require for lunar surface use.

The concept comprises the nuclear reactor with in-pile thermionic converters having molybdenum emitters, cesium vapor gaps, columbium collectors. The fuel pellets of UO_2-Mo cermet are in the form of thin walled hollow cylinders, clad with molybdenum, the cladding serving as the emitter surface and also forming a pressure vessel for containment of fission product gas. In operation, the surface temperature of the emitters is held to 1530°C,"below the temperature at which large quantities of fission products are released."

The system coolant is NaK operating at 1300°F outlet, 1100°F inlet—the temperature range already covered by SNAP-8 technology. The coolant is pumped through the system loop removing decay heat from the nuclear fission reaction, transferring the heat to the radiator for rejection to space. During possible lunar surface storage the pump is powered by a thermoelectric, radioisotope, power source of 500w thermal, 25w electrical capacity. The thermal energy serves to keep the coolant liquid.

The radiator is cylindrical, as shown, thermal radiation reflectors would be employed to direct the radiation upward from the crater or depression in which the system would be located. Control of the nuclear reactor is achieved by a movable nuclear reflector mounted outside of the reflector element integral with the reactor. The design operating point results in a thermionic diode power density of only 1.5 watts/cm^2, with increase to 4 watts/cm^2 a growth possibility.

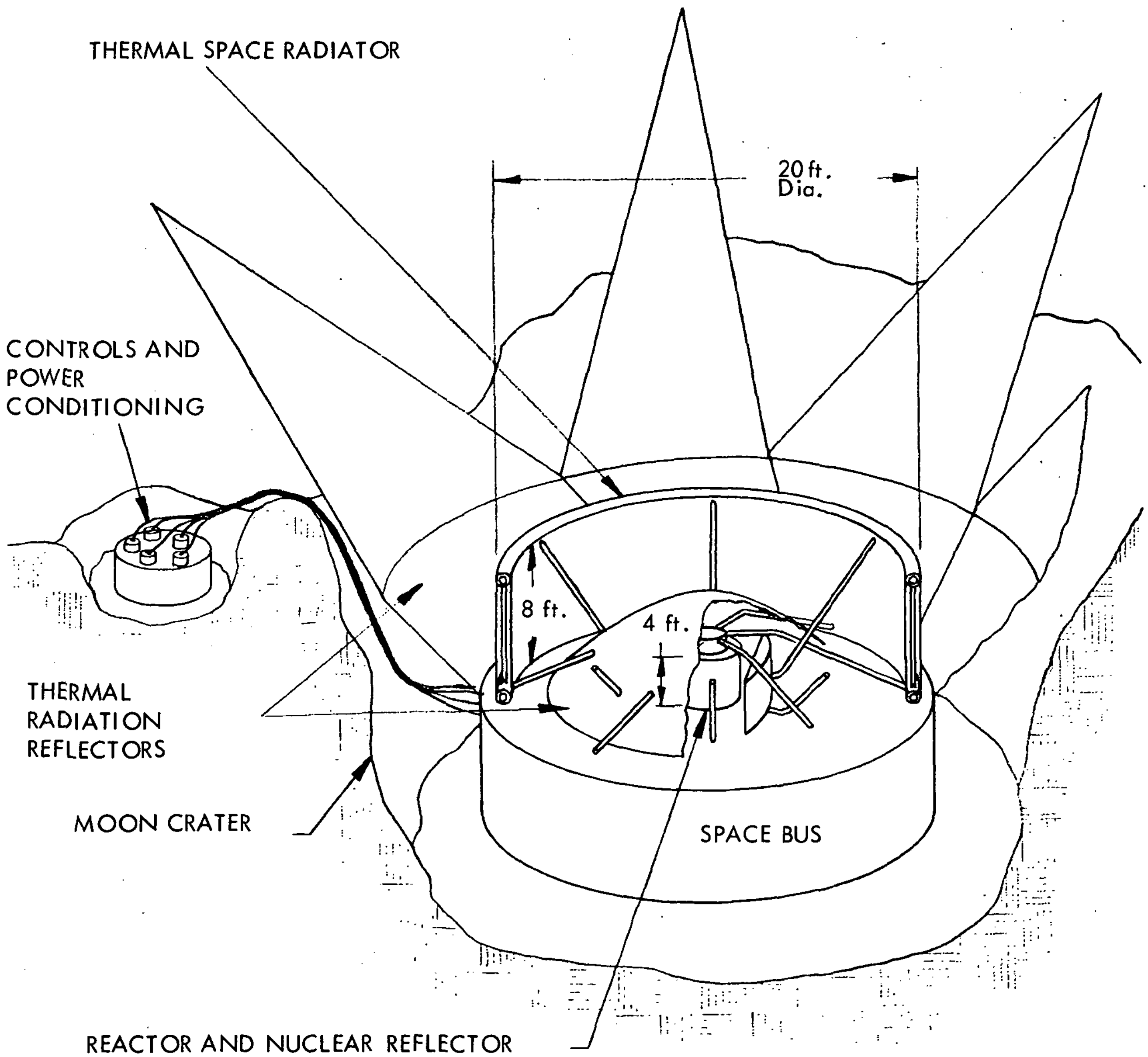

Figure 2-19 - 100 kw Lunar Nuclear Thermionic Plant Concept (Martin-Marietta Co.)

The Martin design is aimed at 100 kw(e) at 90 lbs/kw unshielded. They feel that they have taken a position of extreme conservatism in operation and down-rating of all components. However, none of the diodes have yet been operated in-pile.

The Pratt & Whitney (Reference 13) in-pile thermionic converter design concept is shown diagrammatically in Figure 2-20 and a schematic of a fuel element in Figure 2-21. As shown, the thermionic converters are integral with the reactor. A primary liquid lithium coolant loop transfers the reaction heat through a heat exchanger to the secondary loop and the radiator. Auxiliary loops and radiators maintain proper temperature levels in the reactor shield, at the cesium reservoir, and at the electrical power conditioning and control zone.

The combined thermionic converter-nuclear fuel element consists of a cylindrical UC-ZrC fuel element, tungsten clad, surrounded by a concentric cylinder of columbium, spaced off 0.020 inch to form the cesium vapor gap. Fission gases are separated from the cesium vapor by a tantalum shield and are ducted through hollow electrical leads to a point where they are vented to space. The calculated emitter temperature is 1760°C, the collector 740°C, the thermionic diode power density, 5 watts/cm^2, the system weight—direct shielding only—from 10.5 lbs/kw(e) to 15.8 lbs/kw(e) depending upon choices of coolants and radiator materials. The system design power level is of the order of 1 Mw.

CONCLUSIONS

As evidenced by the reported results of General Electric, Radio Corporation of America, Martin-Marietta Company, and others, the problems of construction and operation of cessiated diodes in series strings, without reference to a power generation system as a whole, is well in hand. Long life at potentially useful (in power systems) levels of efficiency and electrical output are being achieved. This is a major step forward.

It would appear that if nuclear reactor-heat transfer loop combinations were available to supply heat energy at 1700-1800°C to out-of-pile thermionic systems, very rapid development of thermionic conversion systems would be possible. Unfortunately, such a reactor-loop combination is a generation beyond even the present advanced development program of SPUR/SNAP 50.

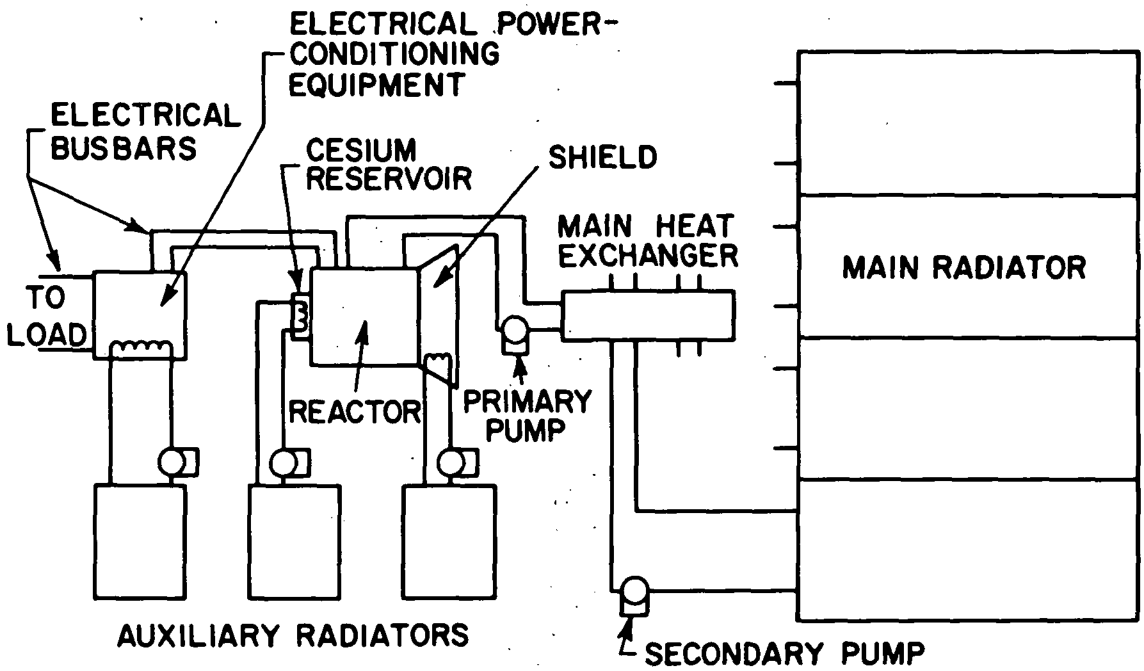

Figure 2-20 - Thermionic Reactor Space Electric Powerplant Schematic

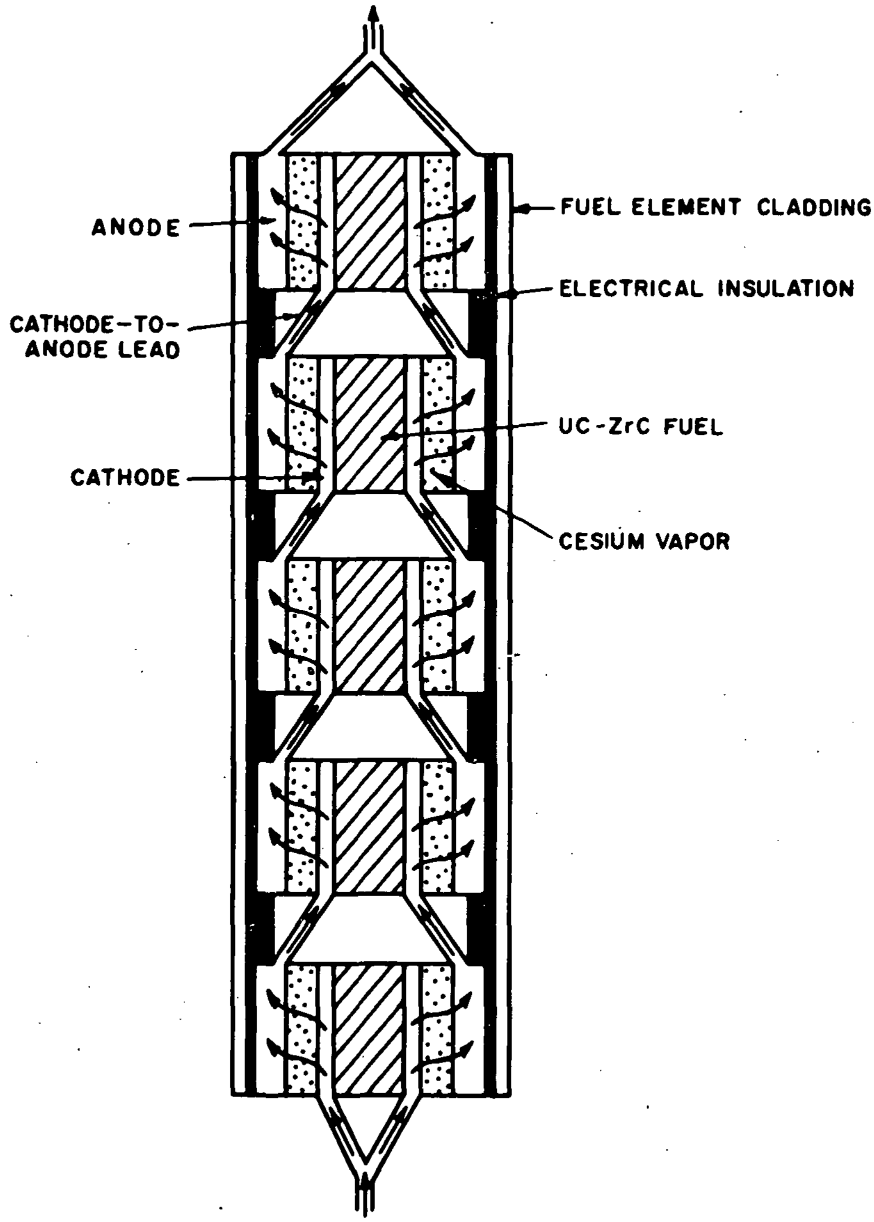

Figure 2-21 - Electron Flow Through Fuel Element

A way to avoid the high temperature loop is to place the thermionic converter in the nuclear reactor with the emitter next to the nuclear fuel. However, efforts to use the same technology (which has resulted in thousands of hours of useful life out-of-pile) has uniformly, to date, given failure in less than 300 hours when used in-pile. It would appear on the surface, at least, that a better understanding of the problems of making this transition is needed.

Conceptual designs based on the assumption of a successful transition from out-of-pile to in-pile thermionic converters give specific power output levels which vary by a factor of 10. The system value is strongly dependent on the assumed specific power output level of thermionic converters, which in turn is a strong function of the assumed emitter temperatures and in the end of the fuel element clad temperature. Assuming values of emitter temperature around 1780°C gives specific weights of about 15 lb/kw. Dropping the assumed temperature to 1530°C raises estimates to 90 lb/kw and even lower temperatures increase the specific weight estimate still more. However, even a 150 lb/kw plant would be useful in the context of this lunar base power plant study. All of the foregoing specific weights are for plants of minimum nuclear shielding. Only enough shielding is included to protect plant components.

Placing the thermionic converters in the nuclear pile increases the size of the basic reactor core over that required for a straight fluid cooled reactor (by a factor of roughly two in diameter). As a result, shielding of such a core, for protection of the external environment and personnel, requires an unusually large amount of material. Use of lunar materials or lunar topography as the shield will be necessary to stay within the 25,000 lb payload limit of this study.

Estimates of the time to develop a flight type nuclear thermionic conversion system vary from 8 (Reference 12) to 15 (Reference 3) years. Because of the major unresolved problems of using thermionic converters in actual nuclear power conversion systems, all development time estimates must be treated as "best guesses."

THERMIONIC REFERENCES AND LIST OF GOVERNMENT CONTRACTS ON THERMIONICS

Thermionic References

1. Hall, W. B.; Hernqwist, K. G.; The plasma triode - A low Temperature Thermionic Converter; Proceedings 15th Annual Power Sources Conference of U. S. Army Signal Corp. 9-11 May 1961.

2. Ulrich, A. J., Thermionic Energy Conversion Diode Using a Film Boiling Liquid Metal Electron Collector - Advanced Energy Conversion Vol. 3, pp. 397-405, Pergamon Press 1963.

3. Brosens, P. and Hatsopordos, G. N., Thermionic Energy Converter with A Liquid Collector - Advanced Energy Conversion Digest, Vol. 3 pp. 387-396, Pergamon Press 1963.

4. Kennedy, A. J ; Research and Development on Barium Vapor-Filled Thermionic Plasma Energy Converters, Martin Nuclear Div.,Report MND-2812-4 (Classified) May 1, 1963.

5. Knechtli, R. C., Fox, Marvin; Theory and Performance of Auxiliary Discharge Thermionic Energy Converters, Advanced Energy Conversion Vol. 3, pp. 333-349, Pergamon Press 1963.

6. Theory and Experiment of a Capillary Emitter INA Thermionic Converter, Dresser, D. L., Laurita, W. G., Dunlop, J. D., and Huber, H. LeBihan, M., AIAA, June 1963.

7. Weinberg, A. F.; Yang, L; Interdiffusion between Uranium Bearing Reactor Fuels and Refractory-Metal Thermionic Emitters, Advanced Energy Conversion, Vol. 3 pp. 101-111, Pergamon Press 1963.

8. Sinclair, C. E. Et. al Visit to NASA-Lewis - Engineering Study of Nuclear Power Plant for Manned Lunar Bases, Westinghouse Electric Corporation, Report WANL-TR-2271, October 14, 1963.

9. Pouchot, W. D.; Mayer, M.; Discussion of Thermionic Conversion with LASL, Group N-5, Westinghouse Electric Corporation,Report WANL-TR-2311, October 21, 1963.

10. Mayer, M.; Pouchot, W. D.; Lance, J. R.; Discussion of Thermionic Conversion with Martin Co. Nuclear Division, Westinghouse Electric Corp.,Report WANL-TR-2467, November 14, 1963.

11. Lance, J. R.; Pouchot, W. D.; Discussion of Thermionic and Thermoelectric Converters with RCA Direct Energy Conversion Department, Westinghouse Electric Corporation, Report WANL-TR-2469, November 14, 1963.

12. Ott, D. G.; Pouchot, W. D.; Discussion of the Status of the STAR-R and STAR-C Thermionic Power Plants with GE SPNSO, Westinghouse Electric Corporation, Report WANL-TR-2313, October 23, 1963.

13. Advanced Nuclear Electrical Power Generator - Quarterly Progress Report, Report No. PWA 2157, Vol. II (October 1 through December 31, 1962).

14. Quarterly Status Report on Lampre Program, Los Alamos Scientific Laboratory, Report No. LAMS 2875, for period ending February 20, 1963.

15. PWA - 2107 - Vol. II. "Thermionic Nuclear Space Power Plant", July-Sept. 1962.

16. ANS Transactions, June 1963, p 93, Summary of GA design.

17. Preprint - Thermionic Space Power Systems, Herman Miller, Third Symposium on Advanced Propulsion Concepts, USAF Office of Scientific Research and General Electric Company, Flight Propulsion Division.

18. "Thermionic Conversion Systems May be Operational by 1970," Nucleonics, December 1962.

19. Thermionic Development Program, Quarterly Progress Report No. 6 Martin Company, MND-P-2890-3, Jan. 1st through March 31, 1963.

20. Thermionic Generator, Martin Company, MND-P-2901, Final Report June 1963.

21. Thermionic Development Program, Quarterly Report No. 5, Martin Company, MND-P-2890-2, October 1 through December 31, 1962.

22. Thermionic Development Program, Quarterly Report No. 4, Martin Company, MND-P-2890-1, July 2 through September 28, 1962.

23. SNAP 9A Radioisotope-Fueled Generator, Martin Company, MND-P-2775-1, August 1962.

24. Thermionic Development Program, Quarterly Report No. 3, Martin Company, MND-P-3019 II, April 1st through June 30, 1962.

25. Energy Conversion Techniques, Hernquist, K. G., Proceedings IRE, May 1962.

26. Plasma Synthesis and Its' Application to Thermionic Power Conversion, Hernqwist, K. G., RCA Review, Vol. 22, March 1961. pp 7-20.

27. Conversion of Heat to Electricity by Thermionic Emission, Wilson, V. C., J. Appl. Phys. Vol. 30, April 1956.

28. Conversion of Thermal Energy into Electrical Energy by Means of Thermionic Emission, Margulis, N. D., and Marcheck, D. M., Ukranian Phys. J. Vol. 2, April 1957, pp 370-380.

29. Studies of Externally Heated Hot Cathode Arcs, Walter, L., and Johnson, E. D., RCA Review, Vol. 12, (September 1951, pp 415-435).

30. Plasma Thermionic Converters, Salmi, E. W., Proceedings, 14th Annual Power Sources Conference, U. S. Army Signal Research & Development Laboratory.

31. Some Critical Materials Problems of Thermionic Cathode Systems for Fission-Heat Conversion, Yang, L., Carpenter, F. D., and Weinberg, A. F., Advanced Energy Conversion, Vol. 3, January-March 1963.

32. Optimization of a Radiation-Cooled Thermionic Converter, Blue, E., and Ingold, J. H., AIAA Journal Vol. 1, No. 5, (May 1963).

33. Thermionic Nuclear Space Power Plant, Quarterly Progress Report, PWA-2107, Vol. II.

34. Development of a Nuclear Thermionic Fuel Element, Quarterly Progress Report, G. E. AEC Contract No. AT(04-3)-189, December 1st, 1962 - February 28, 1963.

35. Development of a Nuclear Thermionic Fuel Element, Quarterly Progress Report, G. E. AEC Contract No. AT(04-3) - 189, September 1, 1962 - November 30, 1962.

36. Thermionic Converters - Design Status and Forecast, Baum, E. A., and Jensen, A. D., Proceedings, 15th Annual Power Sources Conference, U. S. Army Signal Research and Development Laboratory.

37. The Design, Development, and In-Pile Testing of a Nuclear-Fueled Thermionic Energy Converter, Block, F. G., Eastman, G. Y., and Harbaugh, W. E., RCA Direct Energy Conversion Department.

38. Thermionic Converter Operation in Multiple Connection, Eastman, G. Y., Basiulis, A., and Harbaugh, W. E., RCA Direct Energy Conversion Department.

39. Feasibility Study of Water-Cooled Thermionic Nuclear Power Plant, MND-2903, Vol. I, November 1962, The Martin Company.

40. Thermionic Nuclear Space Power Plant, Quarterly Progress Report, PWA-2157, Vol. II, October 1 - December 21, 1962.

41. Thermionic Emission, Hatsopoulos, G. N., Proceedings, 12th Annual Battery Research and Development Conference, U. S. Army Signal Research & Development Laboratory, May 1958.

42. Thermionic Emission, Wilson, V. C., Proceedings, 13th Annual Power Sources Conference, U. S. Army Signal Research & Development Laboratory, April 1959.

43. Commercial Aspects of Thermionic Power, Coltman, J. A., Westinghouse Research Laboratories Internal Report, August 28, 1959.

44. Experimental Determination of Work Function Distributions of Emitter Surfaces, Kitrilakis, S., Miskolczy, G., and Lieb, D., AIAA, June 1963.

45. Thermionic Conversion of Heat to Electricity, Nottingham, W. B., Hatsopoulos, and Carabateas, E. N., IAS Paper No. 61-73, January 1961.

46. Experimental Research on the Cesium Thermionic Converter, Rasor, N. S., IAS Paper No. 61-72, January 1961.

47. An Evaluation of the In-Radiator Approach to Nuclear-Thermionic Space Power Systems, Bell, D. W., AIAA No. 63-219, June 1963.

48. Performance of Low Temperature Thermionic Converters. Silverberg, M., AIAA No. 63-159, June 1963.

49. Generalized Theoretical Study of Vapor Filled Thermionic Converters, Psarouthakis, J., AIAA No. 63-157, June 1963.

50. Feasibility Study of Water-Cooled Thermionic Nuclear Power Plant, Martin Company, MND-2903, Vol. II, November 1962.

51. Thermionic Conversion Study Utilizing Diodes Practical for a Large Scale Power Plant. Proposal to U. S. Air Force Aeronautical Systems Division, Westinghouse Central Laboratories, April 1961.

52. A Preliminary Evaluation of Nuclear Thermoelectric and Thermionic Power Plants for Space Use, Martin Company, MND-1666.

PIC - Power Information Center

53. Conversion of Nuclear Fission Heat in Plasma Diode. PIC 297, December 1960.

54. Development of a Thermionic Converter for Use With Nuclear Materials, PIC 641, August 1961.

55. Investigation of Carbides as Cathodes for Thermionic Space Reactors, PIC 700 C, May 1961.

56. Uranium Bearing Emitters, PIC 727, July 1962.

57. Compatible Emitter - Collector Pairs for Thermionics, PIC 805, December 1962.

58. Investigation of High Temperature Refractory Metals and Alloys for Thermionic Converters, PIC 831, January 1963.

LIST OF GOVERNMENT CONTRACTS ON THERMIONICS

PIC	Corporation	Contract No.	Amount	Agency	Contract Awarded	Predicted Completion	Subject
110	AGN	AF 33(616)-8110	100 K	WP AFB	3-61	4-62	Determine Feasibility of TC mounted on radiator tubing of liquid metal fast reactor (300 kw)
611	RCA	AF 19(604)-6175		AF Cambridge Research Labs	-	-	Fundamental research on TC for space; Semi-annual reports issued 6-60, 12-60, 6-61
	RCA	NAS - 3-2531	96 K	NASA Lewis	-	-	Research on vapor filled TC's (Dec. 1, Dec. 15, 1962)
839	GE(VA)		65 K	Weapons Lab AF Systems Command	8-63	-	STAR-R Define potential of 1-100 kwe thermionic reactor-cooled by radiation to space. STAR-C is earlier design which is liquid metal cooled. GE(VA) is currently building a 200 K facility for engineering development of nuclear thermionic device.
661	GE(VA)	Nobs 86289	153 K	BuShips	9-61	9-62	Thermionic Cathode Material Properties

LIST OF GOVERNMENT CONTRACTS ON THERMIONICS (Cont)

PIC	Corporation	Contract No.	Amount	Agency	Contract Awarded	Predicted Completion	Subject
661	GE(VA)		475 K	AEC	1962	-	Thermionic research on high-temp. materials and fuel element design (Nucleonics Dec. 1962)
	GA		400 K	AEC	Spring 1962	-	Test in-pile converters fast reactors (Nucleonics Dec. 1962)
700	GA	NAS 5-1253	185 K	NASA Lewis	6-61	9-62	Carbide cathodes for TC; Status (4-62) Vaporization & diffusion measurements made - progress reports available.
	P & W	NASW-360	-	-	-	-	Parametric analysis of 1 Mwe power plant completed (Details available in PWA-2107 Vol. II. PWA-2157 Vol. II which we have)
516	AI	AT(11-1)-GEN-8	198 K	AEC	FY 1962	Continuing	SNAP Supporting Technology - TC Research
142	AI	AT(11-1)-GEN 8	1280 K	AEC	FY 1961	Continuing	SNAP Supporting Technology - TC Research. (Some fraction of money will be spent on TC basic research and design of TC reactor

LIST OF GOVERNMENT CONTRACTS ON THERMIONICS (Cont)

PIC	Corporation	Contract No.	Amount	Agency	Contract Awarded	Predicted Completion	Subject
688	Martin	AT(30-1)-2490	70 K	AEC (Army Reactors)	-	-	In core TC-water cooled reactor (We have many of Martin's classified research reports)
786	Martin	AF 33(657)-10077	100 K	WP AFB	12-62	12-63	UO_2 fueled TC's

LIST OF CONTRACTS

Corporation	Contract No.	Amount	Subject
GA	NAS 3-2532	840 K	UC/ZrC Fuel and Emitter
GE	NAS 3-2544	312 K	Combinations Oxides-Endurance testing seals and ceramics
EOS	NAS 3-2529	--	Emission Data
GE	NAS 3-2533	146 K	Spacecraft Integration
Martin	NASW-667	90 K	Inpile lower power (100 K)
P & W	NASW-763 Applications	85 K	5 mw Thermionics
AI	NAS 3-2530	95 K	SNAPS/Lunar Application
GE	NAS 3-4160	85 K	SNAPS/Space Study (Houston)
Martin	NAS 3-4161	40 K	Isotope Systems - Langley-Small Space Station
Thermo Electric Engineering	NASA-Lewis	93 K	Thermionic Diodes
AI with Thermo Electric & Battelle Institute	AF Systems Command	--	Design, build, test TC with simulated operations
RCA	BuShips NOBS 84823	--	Inpile Converter for Naval Use

LIST OF CONTRACTS (Cont)

Corporation	Contract No.	Amount	Subject
RCA	BuShips, ARPA NOBS 88622	--	Life Test of Converters for Naval Reactors
RCA	Wright Field AF 33(657-8005)	--	Out of Pile TC for use with liquid metal
RCA	Naval Research Labs NONR 4012	--	Low work function collectors
RCA	USA Signal Corp	--	Fossil Fuel Heated Converters
	AF 33(016)-8262	--	Thermionics R & D Fundamental Measurement and theoretical calculations

D. STIRLING CYCLE ENGINES

The heat-to-power process embodied by the obsolete STIRLING HOT AIR engine has attracted renewed interest in recent years. Advances in the state-of-the-art of engine design, materials fabrication, and system analysis make the Stirling cycle again an attractive possibility for certain power system applications. Within the frame of reference of space and lunar power plants it offers opportunity for the use of a reciprocating engine in an inert gas closed cycle with externally supplied heat from the sun or some nuclear energy source.

Inherently, the Stirling cycle carries with it the advantages and disadvantages of a reciprocating prime mover. Its chief advantage (relative to a rotating prime mover such as a turbine) is high mechanical and hence high thermal efficiency in small sizes with high torque at low rpm. The chief disadvantage is a relatively short operating life between overhauls—a problem, associated with the wear and sealing problems of reciprocating piston motion. The recently reported experiences of the Allison Division of the General Motors Corporation (Reference 6) when accumulating 1000 hours total running time on a Stirling cycle engine strongly indicate that, in spite of modern technology, those problems causing short operating lifetime between overhauls are not solved. Because of this the Stirling cycle engine is not suitable for use as a major part of a central station type electrical power generation plant where longtime continuous running without outage for repair or maintenance is required.

INTRODUCTION

The Stirling engine was invented in 1816 (Reference 1) and is a heat engine which operates with its working fluid always in the gaseous state. The working fluid (air in Stirling's case) is compressed in a low-temperature cylinder while being held at constant temperature by the heat sink of the cycle. It then passes through a regenerator and a heater where its temperature is raised tothe maximum temperature of the cycle; and then expands isothermally in a high-temperature cylinder which is receiving heat from the cycle heat source. The working fluid then passes reversibly through the regenerator, re-entering the low-temperature cylinder where the cycle is repeated. The heat source in this cycle is external and the working fluid is in a closed cycle.

The working medium within the engine must be heated; must be cooled; must store and recover heat energy from a regenerator; and must be compressed and expanded at the proper times. These requirements prescribe the five major components of the Stirling thermal engine: (1) the engine heater and heat input source, (2) the regenerator, (3) the engine cooler and heat sink, (4) a displacer piston to control the movement of the working fluid through the heater, regenerator and cooler, and (5) the power piston to compress and expand the gas. The primary function of the power piston is to compress and expand the working fluid, and the primary function of the displacer piston is to move the working fluid to where it may be heated and cooled—in phased relationship with the compression and expansion portions of the total cycle.

The relative motion of the power piston and the displacing piston is the result of the rhombic (pantographic) drive. Figure 2-22illustrates graphically 4 stages within the cycle. In stage 1, most of the working fluid is in the cool region of the cylinder. The power cylinder is at BDC, and the displacer cylinder is at TDC. As the cycle progresses to stage 2 (where the power cylinder reaches TDC) the working fluid is compressed, and heat is rejected through the cooler to the heat sink, in order to maintain the working fluid at the low temperature portion of the cycle. Proceeding to stage 3, the displacer piston has moved downward toward the power piston, and without change of volume, has moved the working fluid through the regenerator and heater and into the hot region of the cylinder. From stage 3 to stage 4 the working fluid expands, the heat input through the walls of the hot space keeping the temperature nearly constant as the power piston and displacer piston move toward BDC. From stage 4 back to stage 1, the displacer piston moves the working fluid back from the hot space, through the heater, regenerator, and cooler into the cool region of the cylinder (without change of volume)

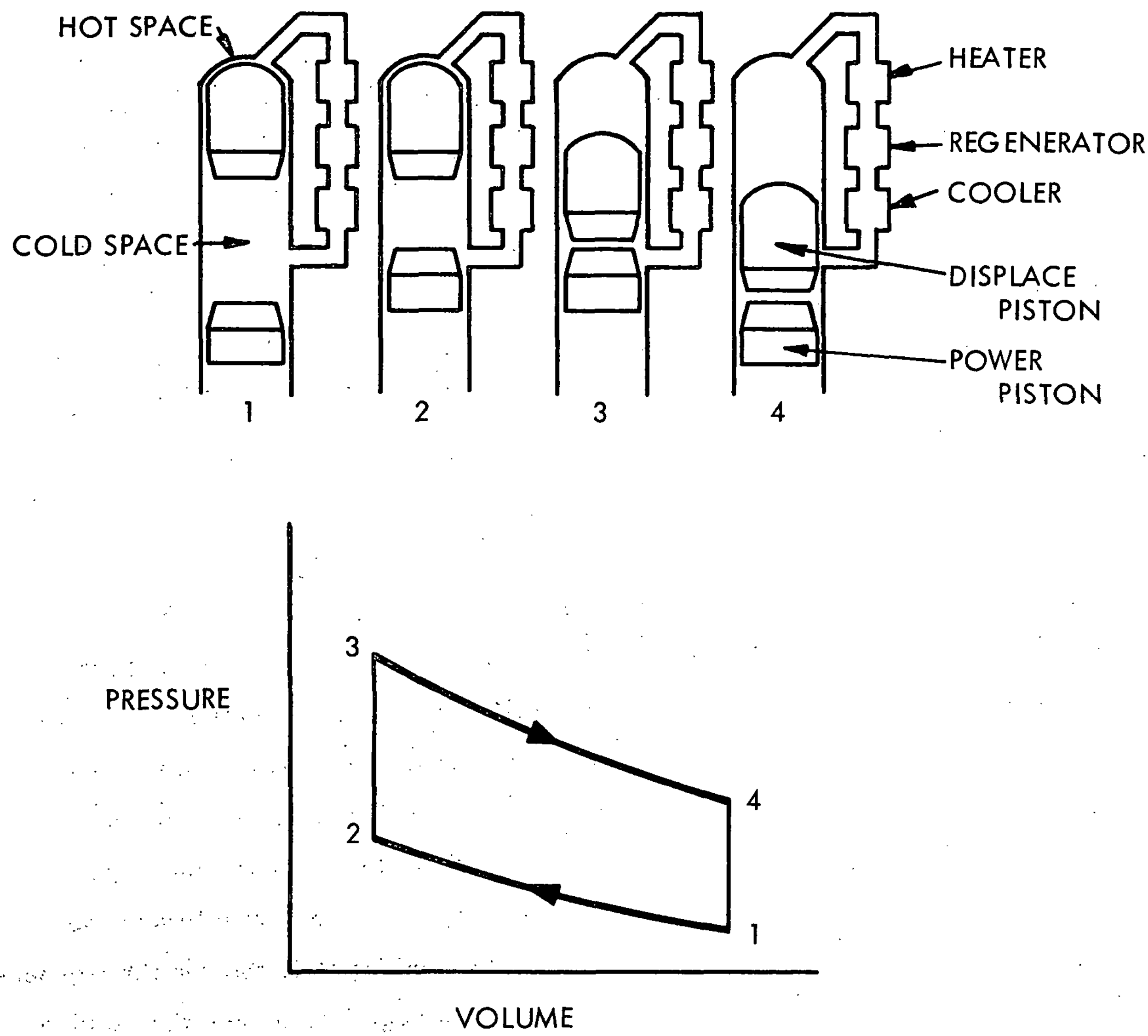

Figure 2-22 - Stirling Engine Cycle Passes and Cylinder Operating Cycle as it approaches TDC. The stages are then repeated. The P-V diagram is of course idealized for discussion as are the events of the stages. The actual engine cycle, however, approximates this description.

Stirling's original engine is the basic configuration used in the most modern engines. In the 140 odd years since it was invented, there have been many less attractive configurations invented and built. During the third quarter of the nineteenth century, the "hot air" engine was very popular and many thousands were built. In general these engines all had low efficiency and developed very low power per unit of displacement. In the early 1940's the Philips Industries in Eindhoven, Netherlands, initiated an R & D program on the Stirling engine (Reference 2). In 1958, General Motors entered into an agreement with Philips relative to this engine.

STATE OF THE ART

There is no generalized, reliable body of records on operating performance of Stirling engines in the nineteenth century—such as would be available if the modern design versions of the Stirling engine had been widely applied. Nonetheless, development work and operational running have been reported by Philips Industries of Holland (as stated previously) and the General Motors Corp. (Reference 6) in the USA. In addition the Stirling engine has been factored into comparative studies of power plants for space and lunar use by Allison Division of GMC (References 3 and 7), Martin-Marietta Corp, (Reference 4) and Westinghouse Electric Corp. (Reference 5). The latter two studies lean heavily on the Allison Div. of GMC work.

Modern Development Work

Philips Industries

Philips has been much more successful in developing Stirling engines with high efficiency than were earlier developers of these engine systems. The specific reasons for this are numerous; but, as would be expected, they are mostly associated with a much more advanced state of the art compared to the earlier period when effort on the Stirling engine was at a maximum. Philips (Reference 8) has built Stirling cycle engines showing 40 percent efficiency at a heater temperature of 750°C (1382°F). See Figure 2-23. However, so far as is known, Philips' work on power generation engines has not led to successful commercial use.

Philips' development work did lead to successful commercial refrigeration units and gas liquifaction systems. Stirling cycle refrigeration engines and heat pumps of the same mechanical configuration as the power generating test engines have a vastly more favorable environment in the low-temperature region of these processes.

Allison Division, General Motors Corporation

Allison has run a Stirling Cycle Engine for 1000 hours of overall operating time. The engine was repaired a number of times during this run.

The problems revealed during the 1000 hours of operation of the Allison engine were as follows:

1. Performance dropped 20 percent in first 400 hours, inspection revealed the cause as bore creep and cylinder wall distortion.
2. After an additional 400 hours of operation a braze joint failed—between dome and displacer piston.
3. Seal ring troubles.

Performance values given for the engine at the start of running are listed in Table 2-7.

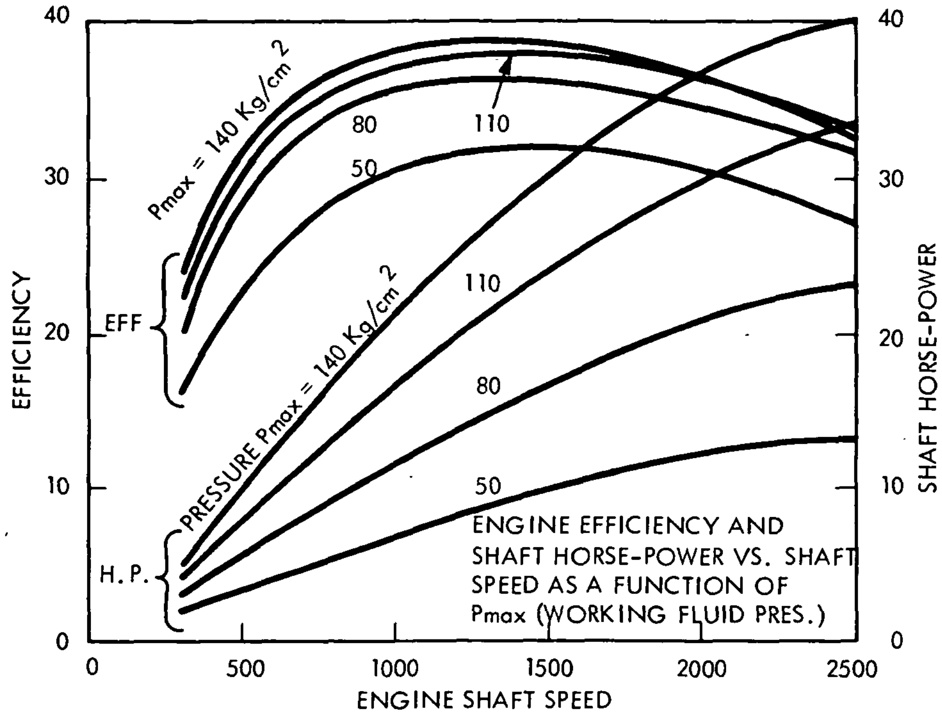

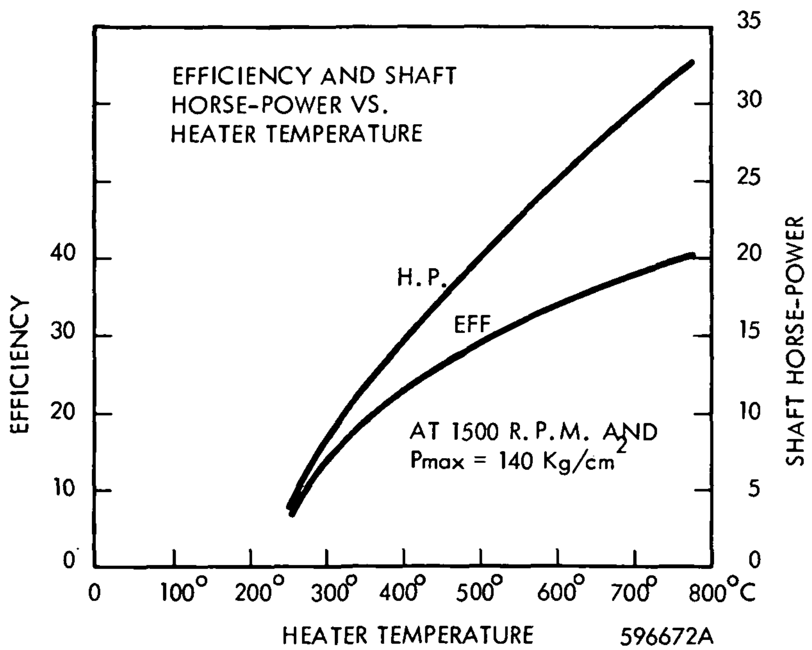

NOTE: Data for curves taken from Philips Technical Review test data on a 40 H.P. Philips Hot Gas Engine (Stirling Engine)

Figure 2-23 - Philips' Engine Operating Characteristics

TABLE 2-7 - ALLISON HOT AIR ENGINE

Engine Speed	1500 rpm	2500 rpm
Top Temperature	1300°F	—
Gross Power From Engine*	3.0 kw	4.5 kw
Gross Engine Thermal Efficiency*	30%	28%

* Brake shaft power output with circulating heat exchanger loop power externally supplied and no electric generator attached.

Values of internal losses for the engine given by Allison were (1) mechanical friction - 1100 watts, (2) windage - 400 watts, and (3) seal leakage - 500-600 watts.

Allison says the most serious Stirling engine problems are seals, windage, and dead space in compression.

Space Application Studies

Studies of the possible use of the Stirling cycle engine in space or on the moon have centered about the 3-5 kw power level with a solar or isotope heat input. Information from two of these studies, with reference to Stirling cycle engines only, will be presented. The first is a study by the Martin-Marietta Company in connection with a manned orbital space station (Reference 4). The second is by the Westinghouse Electric Corporation (Reference 5) in connection with a lunar base shelter. Both studies depend heavily on information originating with the Allison Division of GMC (Reference 3).

Martin-Marietta Company Study

The Martin study involves the use of a Stirling cycle engine with a nuclear isotope heat source to produce 4 kw net electrical power.

In brief, the isotope space power plant concept includes two heat exchanger loops:

1. A NaK hot loop, for transfer of heat from the isotope source to the engines, and
2. An ethylene glycol coolant loop for transfer of the engines rejected heat to the space radiator.

Two engines are employed in the system, with a single isotope heat source, in order to increase system reliability. Either engine is capable of providing the required net power. Because of the inflexible nature of the isotope heat source, the engines and systems are started up before launch into space.

Martin bases their Stirling cycle estimates on Allison's 29 percent engine efficiency with an engine operating between a hot temperature of 1200°F and a cold temperature of 150°F. A 29 percent engine efficiency combined with other component values (electrical generator - 85 percent; heat exchanger loops - 95 percent, loop circulating power - 600 watts) results in an overall efficiency of 20 percent for a 4 kw net electrical power output.

The weight of the plant was estimated as 1200-1500 lb, without nuclear shield, depending upon the isotope chosen. Nuclear shield weights varied from 300 lb for the isotope polonium-210 to 6000 lb for the isotope strontium-90. The two engines and generators weigh 685 lb. The space radiator weighs 226 lbs and has 390 square feet of area.

Of particular interest here is the weight of the power conversion unit (engines, generators, and space radiator) which is 911 lbs. This gives a specific weight for the power conversion system of 228 lb/kw.

For a non-redundant system Martin gave a value of 410 lb for the engine generator. If this value is used the specific weight of the power conversion system would be 159 lb/kw.

Information from the Martin study is not directly applicable to the most demanding lunar situation because of the higher rejection temperature required at mid-day on the moon as compared to orbital heat rejection conditions. A minimum heat rejection temperature of around 300°F is necessary during lunar day environments of 200°F to 250°F. The change of engine efficiency which would result requires knowledge of the true cycle of the engine. It is different from the ideal Stirling cycle in that the efficiency realized is only 50 percent of that given by the ideal Stirling cycle. Using a simple $\Delta T/T$ ratio as a basis, the overall cycle efficiency would probably be reduced from 20 percent to 13-14 percent for a given power output, and the weight would increase inversely—about in proportion to the decrease in engine efficiency.

Westinghouse Electric Corporation Study

The Westinghouse study involves a Stirling cycle engine coupled to a reflector for use with a solar heat source. The system is evaluated in a lunar environment with an effective ambient temperature for heat rejection of 100°F.

The top temperature of the engine cycle was taken as 1250°F. The bottom temperature (minimum radiator temperature) for minimum total system weight was found to be 500°F by a parametric analysis involving components of the system. Allison engine information taken from Reference 3 was used to estimate engine parameters. The radiator for the system was designed around kw segments to have 0.99 probability of no penetration in 3 years.

Of particular interest here are results giving power conversion system weight as a function of power output. The system evaluated was not redundant. Only weights for a single engine, generator, etc., are included. Values converted to specific weight are given in Table 2-8. Weights of the solar mirror and collector assembly are not included in the values given.

TABLE 2-8 - STIRLING CYCLE POWER CONVERSION SYSTEM SPECIFIC WEIGHTS

Power Level	Specific Weight
5 kw	112 lb/kw
10 kw	96 lb/kw
15 kw	81 lb/kw
25 kw	67 lb/kw

If all the components of the power conversion system except the radiator were doubled up to increase reliability, the specific weight of the 25 kw output system would increase to 112 lb/kw.

CONCLUSIONS

The Stirling engine, cycle-wise, is a complicated one and requires extensive analytical work to achieve good results. The availability of better high temperature materials have permitted more recently designed Stirling engines to operate with a very much larger difference between the maximum and minimum cycle temperature—thereby benefiting the Carnot efficiency.

The power per unit mass of working fluid in the Stirling engine is much lower than in the internal combustion engine and approaches more nearly that of the gas turbine. However, the use of high pressure levels in the closed cycle engine as well as the use of good heat transfer working fluids (such as helium) permits the achievement of power per unit volume of the same order as the internal combustion engine. It appears at present that Stirling engines can be designed with approximately the same efficiency as internal combustion engines and, if a pressurized system is used, without a very much greater weight or size per unit power.

Inherently, the Stirling cycle engine has both the advantages and the problems associated with piston engine equipment. The design problems would seem to be in the reduction of dead space (compression ratio) and the reduction of windage effects. The mechanical problems would seem to be metallurgical — creep, distortion, wear, fatigue, and seal leakage. The thermal problems would seem to be possible degradation of heat exchanger efficiency in the cooler, regenerator, and heater, such as might occur through diffusion and deposition of lubricant. Based on the troubles reported by Allison during their 1000-hour run on a Stirling engine those problems — causing short operating lifetime between overhauls — for reciprocating prime movers have not been solved in spite of modern technology. For this reason the Stirling cycle engine is not well suited for use as a major part of a central station type electrical generating plant, where long-time continuous running without outage for maintenance or repair is required. In the event the operating life problems of the Stirling engine are solved, it would appear that a redundant Stirling power conversion system (but with a single main space radiator) might produce 100 kw net electrical power within a 10,000 lb weight limit. To this weight, however, would be added the weight of a reactor and shield system to provide a heat source for the plant. In total for large power systems, the Stirling engine does not appear to have any potential specific weight advantage over other systems which are at more advanced stages of development and have greater potential for low specific weights and/or longer life before failure or maintenance.

REFERENCES AND CONTRACTS

References

1. Flynn, Gregory Jr; Percival, Worth H; Heffner, F. Earl, Revival of 1816 Stirling, SAE Journal, April 1960.
2. Redding, A. H., Stirling Engine Discussions at Battelle Memorial Institute, Westinghouse Electric Corporation Internal Correspondence, Oct. 19, 1961.

,. Investigation of a 3 kw Stirling Cycle Solar Power System, System Evaluation, Allison Div. GMC, Report No. WADD-TR-61-122, Vol. II, March 1962, U.S. Government Contract AF33(616)-6771.

4. Mitchell, P. V.; Pouchot, W. D.; Martin Company Isotope Space Power Plant Briefing, Westinghouse Electric Corp. Report No. WANL-TNR-136, Sept. 24, 1963.

5. Engineering Study of Multipurpose Engine and Fuel System for Manned Lunar Base, Westinghouse Electric Corp. Report No. WANL-PR(s) 003-B, Nov. 30, 1963, U.S. Govt. Contract DA-49-129-ENG(NASA)-1.

6. Monson, Don; Allison Hot Air Engine (Stirling Cycle) paper given at Solar Dynamics Systems Symposium of Interagency Advanced Projects Group, Sept. 24 & 25, 1963.

7. Abstract of SAE Technical Paper No. 594C., Design News, June 12, 1963.

8. Geyer, M. A.; Mintz, R. A.; Stirling Engine D-C Electric Power System, Aerospace Electrical Division, Westinghouse Electric Corp. Report D-709534-DI, May 10, 1962.

Contracts

AF33(616)-8332 - Allison Div. General Motor Corp. - completed.

AF33(616)-6771 - Allison Div. General Motor Corp. - completed.

NAS3-4161 - Martin-Marietta Corp. - in progress.

E. MAGNETOHYDRODYNAMIC POWER GENERATION

INTRODUCTION

Within the past five years considerable interest and a progressively greater amount of work has been evidenced in the field of magnetohydrodynamics (MHD) for electrical power generation. In MHD power generation, the heat energy of a gas or vapor thermodynamic working fluid is transformed directly into electrical energy by electromagnetic induction—thus providing a direct conversion of heat energy to electrical energy.

Basically, the conversion to electrical energy is accomplished as in an ordinary rotating generator, by forcing a conductor to pass through a magnetic field—thus, inducing a voltage which causes a current to flow through an appropriate load. In the case of the MHD system, the conductor is an electrically conducting fluid which is accelerated to a substantial velocity in a nozzle and then passed through the magnetic field. Functionally then the MHD generator is the combination of a turbine-generator in a single machine—except that it generates direct rather than alternating current. This device has the advantage that it has no high speed rotating parts operating at high temperature. It is, therefore, theoretically possible to go to higher temperatures in the converter—thus obtaining higher system efficiencies and/or high radiator heat rejection temperatures. In space systems using a nuclear heat source, this tends to shift temperature limitations from the turbine, if such is the case, to the heat source or reactor.

A second theoretical advantage of the MHD generator is that the power output is a volume dependent process whereas the predominant losses (friction, heat transfer, etc.) are area dependent. By comparison, in a turbine both the transmitted power and the losses are area dependent. Therefore, as the power output becomes larger, the efficiency of an MHD generator increases more rapidly than that of a turbine (Reference 1).

From a practical standpoint, however, there are many basic problems to be solved before the MHD generator can be considered at a state of development from which to embark on the design of a useful power system. These problems range from the necessity for a better understanding of plasma physics and a more thorough knowledge of the various processes present in the MHD generator, to the more practical engineering problems of developing high temperature materials and developing superconducting magnets with adequate flux concentration. Problems such as these that must be solved in the laboratory before serious consideration can be given to power system development based on the MHD principle (Reference 15).

STATE-OF-THE-ART

The major problem in the MHD power plant is to make the working fluid electrically conducting. Two basic approaches to providing an electrically conductive working fluid have been considered for MHD power generating systems.

Thermal Ionization

The first approach is to rely on thermally induced ionization to produce the necessary working fluid conductivity. In this case, the working fluid is seeded with an alkali metal such as cesium or potassium (unless one of these materials is used as the working fluid). In general, the ionization is a strong function of temperature, and it is generally agreed that it is impossible to achieve sufficient conductivity for an attractive MHD duct with inlet temperatures below 3000°F.

Figure 2-24 illustrates a conceptual design of a 1000 kw MHD space nuclear electric generating plant with a thermally ionized metal vapor Rankine cycle that was the result of an internal Westinghouse study.

Ionization is not in itself an immediate problem when either electrically heated gases or combustion gases can be used since high temperatures are achievable, and by seeding these

Page Intentionally Left Blank

~~CONFIDENTIAL~~

A FLASH EVAPORATOR - SEPARATOR
B MHD DUCT
C LEAD VAPOR CONDENSERS
D LEAD LIQUID - LEAD: CESIUM VAPOR SEPARAT
E LEAD FEED PUMP
F SHIELD
G REACTOR REFLECTOR
H REACTOR CORE

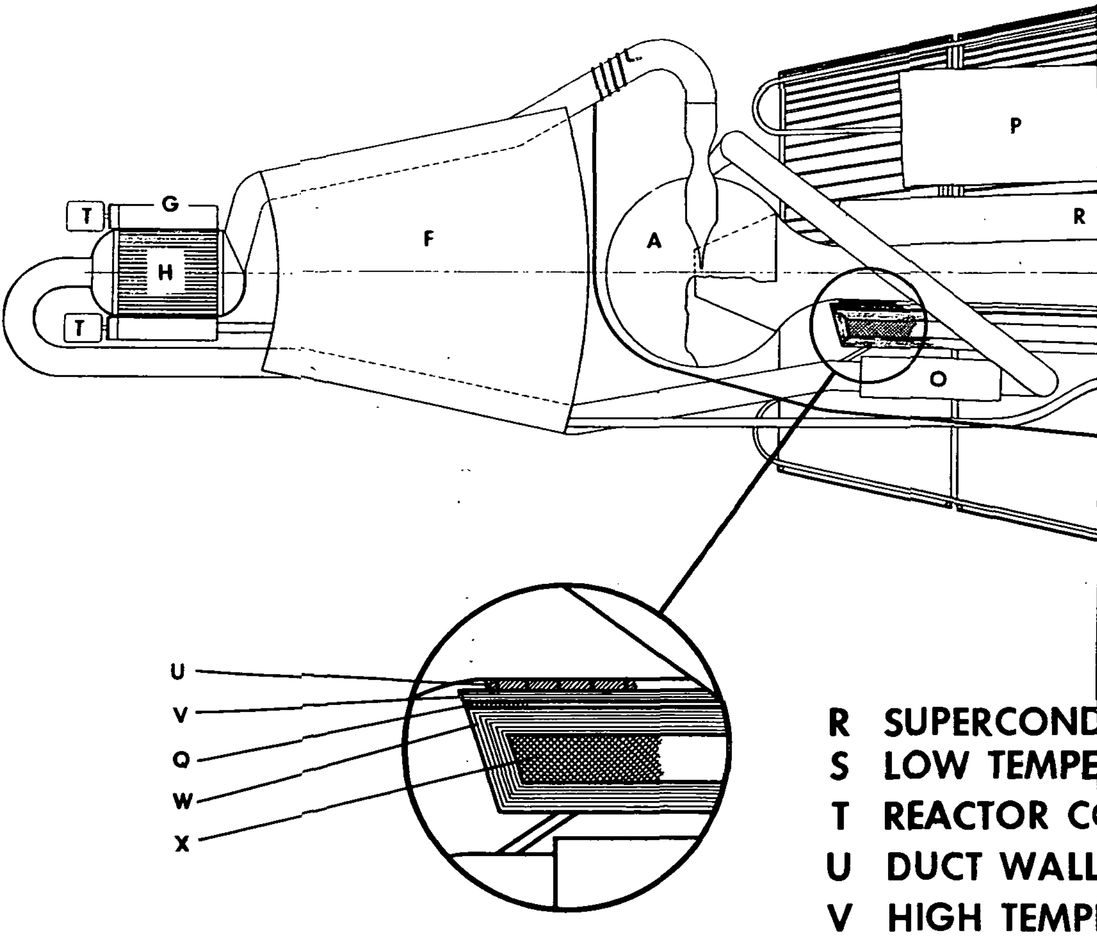

R SUPERCOND
S LOW TEMPE
T REACTOR C
U DUCT WALL
V HIGH TEMP
W LOW TEMPE
X SUPERCOND

~~CONFIDENTIAL~~

I HIGH TEMPERATURE RADIATOR
J HIGH TEMPERATURE RADIATOR LITHIUM CIRCULATOR
)R K CESIUM: LEAD VAPOR CONDENSER
L INTERMEDIATE TEMPERATURE RADIATOR
M I. T. RADIATOR LITHIUM CIRCULATOR

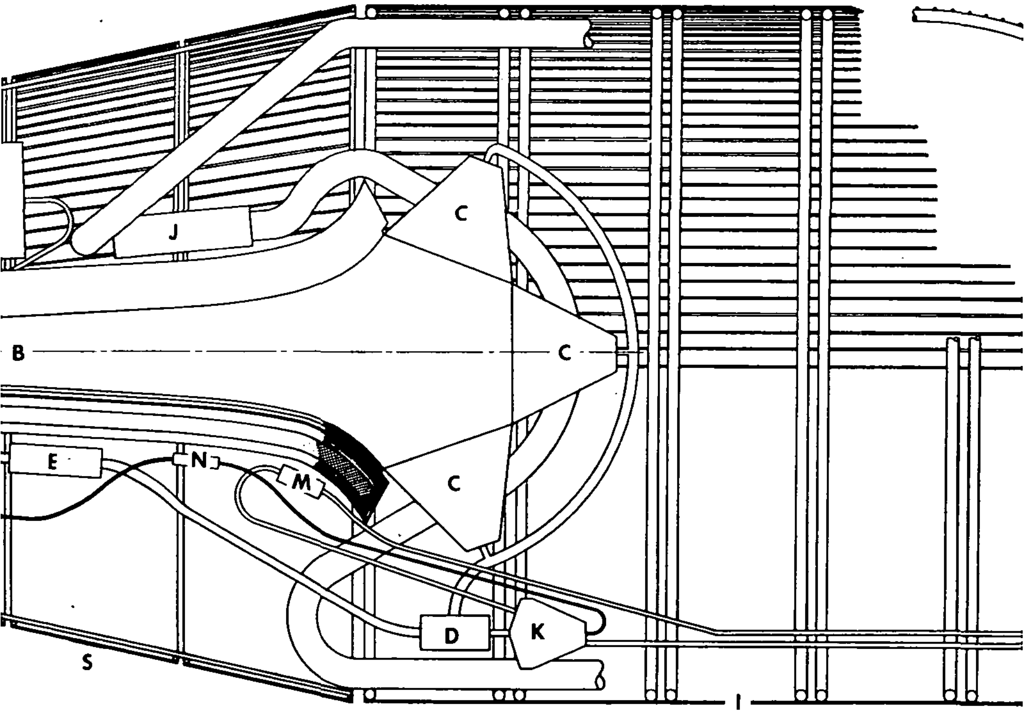

JCTING (CRYOGENIC) MAGNET
ATURE RADIATOR
NTROL DRUMS
(ELECTRODES & ELECTRICAL INSULATORS)
RATURE DUCT THERMAL INSULATION
RATURE MAGNET INSULATION
JCTORS

CESIUM LIQUID FEED PUMP
REACTOR LEAD COOLANT
CIRCULATING PUMP
CRYOGENIC REFRIGRATION PLANT
DUCT LOW TD TEMPERATURE
COOLING PASSAGES

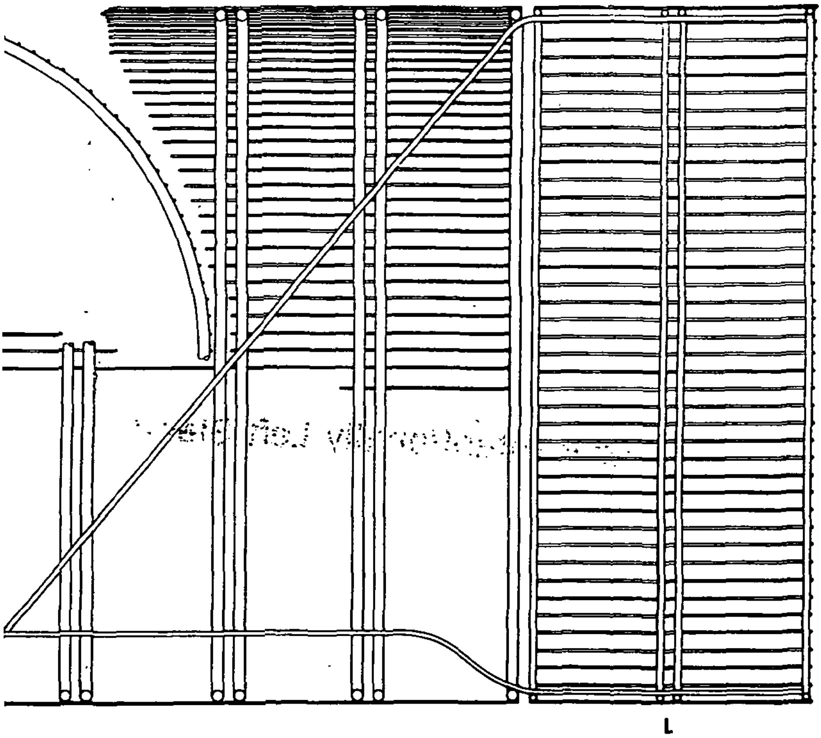

560830

Figure 2-24 Over-all MHD Plant

Page Intentionally Left Blank

gases with cesium or potassium sufficient ionization can be accomplished. At the present time MHD generators are, in general, operated in open cycles for short periods of time (and at low efficiency) using these techniques. The most practical present-day MHD application is, therefore, for use as large power-short lifetime power supplies using an open cycle combustion system.

For closed systems using nuclear reactors as heat sources to provide power over an extended period of time, material development problems obviously preclude the use of a system in which duct temperatures must exceed 3000°F. Such temperatures are obviously well in excess of the present day state-of-the-art in nuclear reactor heat source technology.

Non-Thermal Ionization

The second approach to providing a conductive working fluid is to rely on non-thermal ionization or techniques which are only weakly temperature dependent. There are a number of different techniques being investigated for accomplishing this objective, and most of these are being explored by various laboratories throughout the country. In general, these techniques are theoretically sound, but none have been demonstrated to be physically feasible in real machines.

Recently the most attention has been given to magnetically induced ionization. In this method an attempt is made to have the electron temperatures in the fluid elevated above the gas temperature by using the induced voltages present in the MHD generator. Since the degree of ionization is in equilibrium with the electron temperature, the ionization is increased in some proportion to the electric field present. The general theory has been demonstrated many times by the use of applied electric fields in non-magnetic surroundings; however, only a small measure of success has been obtained when magnetic fields are present as is the case in MHD generators. This method was originally suggested for application to MHD generators by Kerrebrock (Reference 2). In this paper a factor-of-three improvement in conductivity was obtained for a potassium seeded argon plasma without a magnetic field.

Since that time a number of tests have been run in MHD generators with a magnetic field present. Robben (Reference 3) reported no increase of conductivity in a potassium seeded argon plasma with a magnetic field present. More recently at the Westinghouse Research Laboratory (Reference 4), conductivities between 1×10^{-2} and 3×10^{-2} mho/m were measured in cesium seeded helium for conditions where 1.9×10^{-3} mho/m was expected for thermal equilibrium. Tests at General Electric indicate measurements of 3.6×10^{-3} mho/m at 650°C, 18.1 psia, 260 m/sec and 20,000 gauss in argon seeded with cesium (Reference 5). Similar results have also been obtained at Martin-Marietta (Reference 6) where an electron temperature of 1427°C was obtained in a plasma at 870°C.

Most of these tests indicate that magnetically induced ionization is present. However, none of the results show sufficient ionization for large power densities. It, therefore, remains for proper accounting of the loss mechanisms to be established in order to correlate test results with theoretical predictions. Beyond this, testing of magnetically induced ionization under higher magnetic fields and at higher conductivities must be accomplished.

Other internal methods of ionization being investigated include; metastable effects as in a Penning discharge, the ionization due to internally emitted photons, or thermionic emission from droplets (Reference 8). These methods, as yet, are relatively undeveloped and require extensive investigation to determine the magnitude of conductivity obtained and thus, the applicability of these techniques to MHD generators.

External means of ionization include photoionization by means of a high intensity light source, electron beam ionization by use of an electron gun and ionization by use of R.F. Theoretically all three of these methods can be utilized in systems for space application (Reference 9).

Photoionization has been examined experimentally using plasma-jet light sources of high radiation efficiency. Conductivities in cesium vapors of up to 0.2 mho/m have been obtained in preliminary experiments at the Westinghouse Research Laboratories. Quantitative theoretical information is discussed in Reference 10 in which 10 mho/m may be attainable with the proper light source.

Electron beam injection is a method in which high energy electrons are injected into the system through a suitable window or slit, ionizing the gas atoms upon collision. This method is also very well known and has been discussed in Reference 11 as well as other documents. By its nature it requires complex equipment (as does photoionization) and the development of windows which can maintain their integrity when in contact with the hot working fluid—at the same time absorbing only small amounts of power from the electron beam. The availability of suitable windows is as yet not apparent.

R. F. studies have been confined mostly to extremely low pressures which are not adequate for large power generation systems. Gourdine and Hollister report a conductivity of 2,640 mho/m in argon at a pressure of 3 mm Hg seeded with 6 microns of mercury.

The preceding references indicate in summary fashion the many approaches being taken in an effort to obtain a workable system utilizing non-thermal ionization. At this point in time it is difficult to predict which of the methods will yield a workable system and, therefore, what type of system should be developed.

RELATED WORK

A large number of experiments are being performed on both open noble gas systems and closed loop noble gas and metal vapor systems. The closed loop system (Reference 4) which is being tested at the Westinghouse Research Laboratories uses a cesium seeded helium gas in which the gas is heated with an arc jet. Current tests at General Electric (Reference 7) are underway on an argon blowdown facility. Preliminary results of this work are presented earlier in this report. They currently have a potassium blowdown facility and potassium closed loop. All General Electric systems are designed to operate utilizing magnetically induced ionization.

C.A. Parsons & Co., Ltd (Reference 12) has a helium-cesium closed loop under study in which they are considering thermal ionization and various methods of non-equilibrium ionization such as photoionization and surface ionized cesium.

Martin-Marietta Corporation (Reference 13) is operating a closed loop (results presented earlier) in which they are investigating various methods of non-equilibrium ionization also using a seeded noble gas. Many similar MHD devices are under study or construction at such laboratories as at Allison Division of General Motors, AVCO, etc. The important point is that all of these loops are preliminary laboratory test loops—aimed not only at developing working power systems, but also at exploring fundamental physical principles.

Superconducting magnets offer the only possibility of low weight to power ratios for MHD conversion systems under approximately 10 megawatts electrical output. Research and development work is proceeding on superconducting magnets at various laboratories. Sizes suitable for application are being developed primarily at AVCO and the Westinghouse Research Laboratories. Reference 14 is probably the latest and most comprehensive study of the design requirements and state-of-the-art of these magnets.

CONCLUSIONS

From the various MHD approaches mentioned and their current state-of-development, it is apparent that a technically established basis on which to design a power system does not exist. It will, in all likelihood, be at least 5 to 10 years before a feasible concept on which to base an MHD power conversion system can be defined, and it will be several years after this before a prototype power system from which useful power can be extracted will be developed. Consideration of MHD power generation for the early phases of lunar exploration is, therefore, out of the question. However, if the problems associated with MHD power generation can be solved satisfactorily, MHD power generation offers a very attractive system applicable to a space environment.

REFERENCES

1. T. C. Tsu. Effect of Size on Performance of MHD Machines. Westinghouse Research Memorandum 62-118-266-M5; August 7, 1962.
2. J. L. Kerrebrock. Conduction in Gases with Elevated Election Temperature. Second Symposium on the Engineering Aspects of MHD, Philadelphia, Pa.; March 9-10, 1961.
3. F. Robben. Non-equilibrium Ionization in an MHD Generator. Amer. Phys. Soc. Bull., Vol. 7, pp. 371-372; April 23, 1962.
4. Westinghouse Electric Corporation. Final Report, Long Life Closed Loop MHD Research and Development Unit-Phase I. Contract AF33(657)-8311, AF Aero-Propulsion Laboratory, AFSC, Wright-Patterson Air Force Base, Dayton, Ohio.
5. Private Communication, W. S. Emmerich.
6. The New York Times, December 20, 1963.
7. General Electric Company, Investigation of Non-Thermal Ionization for MHD Energy Conversion. AF 33(657)-8298, AF Aero-Propulsion Laboratory, AFSC, Wright-Patterson Air Force Base, Dayton, Ohio.
8. A. W. Rowe and J. L. Kerrebrock. Quarterly Progress Report, Number 70. Research Laboratory of Electronics, Massachusetts Institute of Technology, Cambridge, Mass., July 15, 1963, pp. 192-195.
9. W. S. Emmerich and R. E. Voshall to be presented at International Conference on Aerospace Electro-Technology, April 19-25, 1964.

10. L.S. Frost. Photoionization in MHD Ducts. Research Memo 63-128-511-MI, Westinghouse Research Laboratories, Pittsburgh 35, Pa.

11. E.J. Sternglass, T.C. Tsu, et.al. MHD Power Generation by Non-Thermal Ionization and Its Application to Nuclear Energy Conversion. Third Symposium on the Engineering Aspects of Magnetohydrodynamics, University of Rochester, Rochester, New York, March 28-30, 1962.

12. C.A. Parsons & Co. Ltd. MHD Power Generation Using Seeded Noble Gases. Contract N 62558-3127, Materials Sciences Office, ARPA, Washington 25, D.C.

13. Martin-Marietta Corp. Magnetohydrodynamic Power Generator. Contract NOnv 3866(00), Office of Naval Research, Washington 25, D.C.

14. Westinghouse Electric Corporation. Superconducting Magnet Research and Application to MHD Power Generators. RTD-TDR-63-4170, Contract AF 33(657)-10567, AF Aero-Propulsion Laboratory, AF SC, Wright-Patterson Air Force Base, Ohio, December 31, 1963.

15. T. C. Tsu and L. S. Frost. Current Status of MHD Power Generation: Its Processes and Problems. Proceedings of Third Symposium on Advanced Propulsion Concepts. Vol. I, Gordon and Breach, Science Publishers Inc., 1963.

F. BRAYTON CYCLE POWER SYSTEMS

INTRODUCTION

There has recently been a resurgence of interest in the use of the closed Brayton cycle as a power conversion system for space power units. Most of the recent development effort has been centered on systems in the low power range (less than 10 kw). The major effort is focused on the NASA Lewis Laboratory program to develop a small solar powered-Brayton cycle system. The AiResearch Company of Phoenix, Arizona is participating in this program with the Lewis Laboratory.

A number of organizations (both in government and industry) have also made preliminary or conceptual design studies of a range of nuclear powered Brayton cycle plants for space applications. These plants are in the larger sizes of 50 kw and above. One of the major problems with large Brayton cycle systems for space is the need for very large heat rejection radiators as compared with Rankine cycle power systems of equal power output. Typically, radiator requirements for a Rankine cycle plant range from 2 to 10 square feet per kw while Brayton cycle plant requirements are in the range of 30 to 40 square feet per kw. This characteristic of Brayton cycle systems (the result of the low temperature heat rejection requirement for such systems) seriously limits the potential of the Brayotn cycle for space power applications, where large blocks of power are required. This is particularly true of space vehicle applications where specific weight is all-important and the radiator is the major contributor to total plant weight.

For first generation lunar power plants, however, the Brayton cycle with a nuclear heat source must be considered a contender. In this application, the penalty associated with radiator weight is a less significant factor and growth potential to large plant sizes (above

300 kwe) does not offer a requirement until well beyond the mid 1970's. Of first order importance for this application is developability of an acceptable plant initially in the 100 kw to 200 kw range.

In considering closed Brayton cycle systems for the lunar application two basic types of power systems can be considered:

1. A direct cycle system using a gas cooled reactor as a heat source.
2. An indirect cycle using a liquid metal cooled reactor as a heat source.

With either system one limitation imposed on design is that inlet temperature to the turbine must be in the range of 1700°F. This is in order to obtain radiators of a size that are acceptable even for the lunar application.

STATE-OF-THE-ART

The Brayton cycle is a well-known thermodynamic cycle—the most common application of this cycle being in the open-cycle jet engine. As a consequence, there is a great deal of experience with Brayton cycle systems of various types. In the area of electrical power generation systems using a nuclear heat source, two major programs have been undertaken in recent years, the ML-1 program and the MCR program—both under the direction of the Army Reactor Program. The ML-1 is a closed cycle system using a gas cooled reactor as a heat source and so experience is of direct interest to the lunar program. Here a closed cycle is an obvious requirement. This system is also now in operation so that real experience is available on design characteristics of the Brayton cycle plant. In the case of the MCR program, the power conversion system is open cycle and is at this time primarily a paper system. Therefore, the primary interest in this program is in the approach taken to reactor development. Each of these programs will be discussed in detail later in this section. First, however, some general comments on the closed Brayton cycle are necessary.

The Basic System

In the typical Brayton cycle (See Figure 2-1) a high Pressure gas (Neon, Helium-Xenon or some other appropriate inert gas or mixture of inert gases) leaving either a reactor or heat exchanger enters a turbine (or turbines). In the case of the two turbine system, the first unit would be used to drive the compressor, and the second unit to drive the generator. The gas leaving the second turbine enters a recuperator, transferring its heat to the gases leaving the compressor for return to the heat source in order to reduce the energy input required in the heat source. The gases leaving the recuperator then enter a heat exchanger or space radiator, where the energy representing the cycle inefficiency is rejected to space. The cooled inert gas then enters the compressor where its pressure is increased and then passes through the recuperator and on to the heat source. Single, double and triple loop versions of such plants are illustrated in line diagram form in Figure 2-1, and similar plant concepts are described by members of the NASA's Lewis Laboratory staff and the AiResearch Company in References 1 through 6.

In summary, the plant we are interested in consists of a gas cooled reactor (or a gas cooled heat exchanger with a liquid cooled reactor), a high-temperature inert gas turbine (which may be split into two separate parts), a high-temperature, highly effective low-pressure-drop recuperator, a heat exchanger-radiator combination (or a radiator directly rejecting the heat from the inert gas to space), and a compressor.

In these reactor power plants two conflicting desires must be satisfied and a compromise reached. In general, a small size heat transfer apparatus, to perform its task effectively with low pressure drop, needs a very high pressure, low molecular weight gas. For instance, helium would be ideal, and neon is to be preferred to argon or zenon. However, the turbomachinery for these applications tends to be extremely small in size, run at very high speeds and have a large number of stages. All these characteristics are improved by employing higher molecular

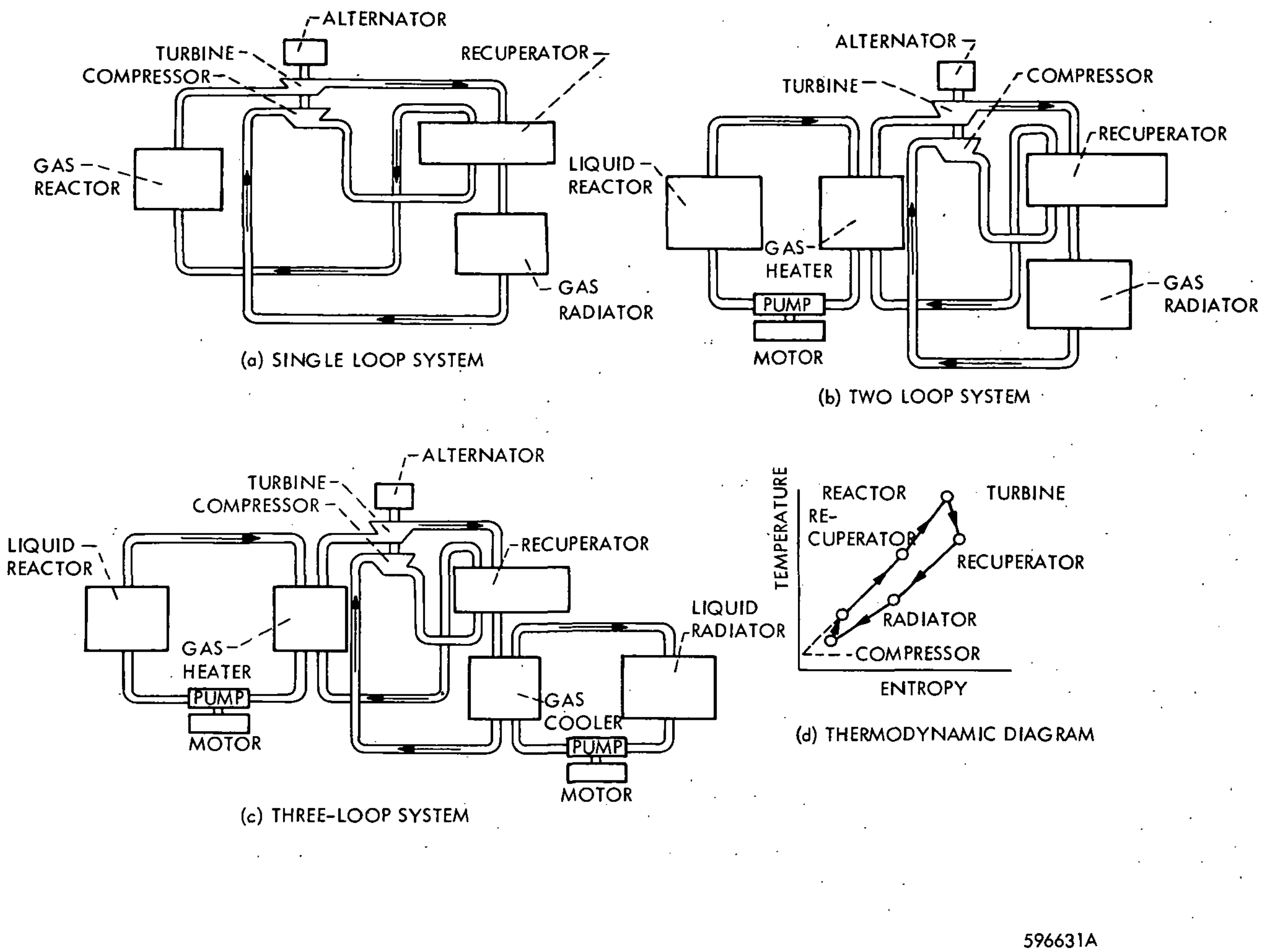

Figure 2-25. Brayton Gas Turbine Power Cycle

weight gases at lower pressures. The higher molecular weights are a very effective means of reducing the number of stages. In general, these compromises in pressure and molecular weight lead to either neon or argon as the working fluid, with pressure levels appreciably above atmospheric and with very small turbomachinery. Improvement in working fluid characteristics can be achieved by using mixtures of inert gas which result in characteristics superior to either of the constituents of the mixture. He-Xe is perhaps the best of these inert gas mixtures and is the mixture used in most recent plant conceptual designs.

Small Size Gas Turbines

In the past 20 years, a tremendous amount of money has been invested in the development of the Brayton cycle gas turbine engine. This effort can be considered as being divided into three groups of apparatus—aircraft propulsion systems, industrial gas turbines, and small portable gas turbines. The major portion of the development effort, as much as 90 percent, has been invested in the development of aviation propulsion gas turbine. These aviation gas turbines normally consist of a compressor, a hydrocarbon fuel burning combustion chamber, and a turbine supported on a bearing system. The bearing system consists of hydrocarbon lubricated antifriction bearings and in a turboprop engine, a reduction gear connecting to the propeller.

Of these elements, the primary interest from the standpoint of the state-of-the-art is the compressor and turbine. However, these compressors and turbines are designed for extremely high flow, the compressor element generally has capability at design of from 50,000 to several hundred thousand cubic feet per minute. The compressors and turbines have received many hundreds of millions of dollars worth of development effort and can be considered to be at the pinnacle of their state-of-the-art. Basic principals acquired from this development can obviously be applied to space Brayton cycle gas turbines. However, it must be recognized that in the lunar base Brayton cycle the primary concern is with flows smaller by a factor of approximately 100.

Industrial Gas Turbines

The second category of Brayton cycle gas turbines which has been under development in the past two decades is industrial gas turbines. To a great extent, these have followed the state-of-the-art of the aviation gas turbine, and have also incorporated structural and life-time features more nearly associated with steam turbine practice. Those gas turbine plants that have been developed and used in the United States are almost entirely open cycle. In other words, they have the same basic components as the aviation gas turbines, except that the plants are geared or directly connected to an electric generator rather than to a propeller. These plants have not had sufficient efficiency to compete economically with steam plants where the cost of fuel in the generation of electricity is a prime consideration. They have found substantial application in areas of low fuel cost and in applications where a supply of high pressure products of combustion are desirable; that is, as a hot gas generator.

Gas turbine power plants are receiving increasing acceptance for electric utility peak load due to the fact that gas turbine plant costs less than a steam power plant of similar capacity, and for peak operation the lower efficiency has not been a serious handicap.

Portable Gas Turbines

A third area of gas turbine Brayton plant application has been in small portable plants. Many of these have been designed and built for applications such as truck propulsion, fire fighting pump drives, portable electric generation, etc. Here their usefulness is characterized by the fact that an air breathing gas turbine burning a hydrocarbon fuel is by far the lightest mechanical drive prime mover that has so far been devised.

Heat Transfer Apparatus

It has been recognized that a gas turbine would be a more effective and efficient power plant if a suitable regenerator or recuperator were developed to utilize some of the waste heat from the turbine to heat the compressed gas leaving the compressor—thus reducing the heat required in the combustion chamber or heat addition regions. It appears that some advantages could accrue from indirect firing. A principal advantage, based on a Escher Wyss patent, would be that by varying the density of working fluid in the plant, the power level could be varied and operate within the most efficient operating modes. In support of these concepts, a program of heat transfer apparatus development has been carried out in parallel to the gas turbine development, and information for certain applications has been obtained. For instance, the work that has been done on small gas turbine power plants for motor cars, in general, is based on the use of a recuperator. Chrysler, Ford and others associated with this industry have completed considerable development work in this area. All designs employ the open cycle, i. e., fresh air is brought into the compressor and the products of combustion are discharged after leaving either the turbine or the recuperator.

Experience with the closed cycle has been limited in this country—probably to just one plant, the ML-1 Portable Nuclear Reactor Generating Plant, which has been developed by the U. S. Army. Appreciable work has been completed in Germany and Switzerland on closed cycle plants.

Due to the advantages of having the heat transfer apparatus operate at elevated pressure, the physical size of the turbomachinery tends to be smaller than in open cycle plants. This has led in the past to reductions in efficiency which may not have been anticipated, and which have severely impaired the attainment of design objectives.

<u>Brayton Cycle Lunar Power Generation</u>

The Brayton cycle as applied to space power generation and particularly to the lunar environment has, from a conversion equipment standpoint, three principal problem areas. The first is with performance. In the applicable Brayton cycle, upwards of 70 percent of the power generated in the turbine does not reach the generator. This amount of power is absorbed in driving the compressor and indirectly in forcing the working fluid through the three principal heat exchangers—the heat source, the recuperator and the heat sink (or radiator). Because of this, a small change in the efficiency of any or all of these components can result in a marked change in the performance of the overall plant. This has resulted in a great effort aimed at performance development in the gas turbine Brayton cycle. However, much of this effort has been in sizes appreciably larger than we are considering. Of equal importance in the case of Brayton cycle components is that no large step-changes or breakthroughs in component efficiencies are likely over what appears reasonable at the present time. As stated earlier the substantial work done in this area indicates that there are upper limits in achievable efficiency which are very nearly being approached. Each percentage point gain in component performance will be hard to come by.

The NASA-Lewis program within the next several years will extend the size of this machinery to an area appreciably below that in which we are interested and, therefore, will permit much more realistic evaluation of performance potential.

The performance degradation in small size Brayton cycle turbomachinery is due to two factors. The first factor is associated with the reduced Reynolds number as the sizes decrease. The second factor is associated with the failure in these very small sizes to maintain good geometric similarity to the larger size prototype. Although these two effects have not been adequately evaluated, there is sufficient overall Reynolds number information to inform us that the effects in the size of interest to us are real but tolerable. Reference 7 gives one of many analyses of Reynolds number effects which might be expected. This particular analysis deals with a family of small centrifugal compressors which are of particular interest in this work. The effect of failure to scale properly, with inherent manufacturing difficulties as we go to smaller sizes is not completely understood.

As analysis of a method for predicting closed cycle turbomachinery performance is discussed in Closed Brayton Cycle Turbomachinery Performance Analysis, and correlated to the ML-1 turbomachinery performance, indicates a substantial dropping off which can only be explained by failure to scale geometrically as the physical size of power turbomachinery components decreases.

In gas turbine plants of the same output, the Reynolds number (with consistent geometry, working fluid, etc.) will vary directly as the square root of the pressure. From Reynolds number criteria alone, one would, therefore, expect better performance from the turbomachinery at the same rating from a closed cycle (high pressure) plant than from an open cycle plant. A possible explanation is contained in the following logic.

As you reduce power output and physical size of a power plant, the cost must reduce with it for most normal applications. Basically this means many shortcuts are taken in scaling to small sizes of turbomachinery. If it is truly important to achieve high component efficiencies (and in an application such as ours this is the case), it appears that much better results should be expected in the small sizes than have been achieved so far. Even with the lack of directly applicable data it would not appear unreasonable to tentatively assume for a 100 kw plant level a compressor efficiency of about 80 percent and a turbine efficiency of about 85 percent, these estimates agree with those postulated in Reference 2.

The second major problem has to do with structural material integrity and particularly with the problem of excessive creep in the turbine. This creep would result in rubbing if sufficiently large clearance were not allowed to start with. Because of the necessity for radiating waste heat rather than using a simple heat sink (such as the water available on earth), and particularly because of the high ambient temperatures in the lunar day, it is necessary for any reasonable efficiency to operate a space lunar Brayton cycle gas turbine at high turbine inlet temperatures. In fact, it is desirable to operate for periods of tens of thousands of hours at the same turbine inlet temperature used in current aviation engine practice for takeoff in the most modern gas turbine engines. On the surface, this is obviously impossible without a major breakthrough in the state-of-the-art.

In fact, however, this operation is not nearly as difficult as it seems because of the following factor. The aviation gas turbine is an air-breathing machine which has an oxygen-rich combustion chamber so that the products of combustion entering the turbine at high temperature have a considerable excess of oxygen. This means that materials used in the turbine must be highly corrosion-resistant and particularly highly oxidation-resistant. The refractory metals, which show far greater high temperature strength properties than the super alloys currently used in aviation gas turbines, are extremely susceptible to oxidation and cannot be used at high temperature in the presence of even a very small part of oxygen.

However, the lunar Brayton cycle plants would operate with an inert gas as working fluid. If the concentration of oxygen in this inert gas can be held to a low enough value (and this is believed possible), then refractory metals with their extremely high strength properties can be used in these gas turbines and turbine inlet temperatures in the order of 1800°F are not on the surface impractical. However, it must be remembered that there is little creep data for these materials for periods of operation above 1000 hours.

The third principal problem area has to do with the bearing and seal system. There are two possible approaches to this problem. The first is to use hydrocarbon lubricated bearings, either anti-friction or oil film (either of which is a well known technology), along with a seal system (based on an unknown technology) which must keep the leakage both of the inert gas and the lubricant to a minimum. Otherwise, the inert gas and lubricant must be allowed to mix and then be separated, probably by refrigeration (which appears impractical), before they can be returned to their respective reservoirs.

The second approach would be to use gas bearings, using the working fluid as a lubricant in dynamic or hydrostatic bearings. These bearings require extremely small clearances, and although they have been used very successfully for light loads at ambient temperatures, it is believed that the development effort required to permit their use under the conditions of thermal distortion that exist in the high transient temperature field of a Brayton cycle gas turbine would require a substantial improvement in the state-of-the-art. It is questionable whether these problems can be solved in time for a lunar base reactor plant.

Another problem inferred by earlier discussions which must be faced in construction of closed cycle Brayton systems is matching of the system—a task which can only be done ultimately by the cut and try process during integrated system testing. This task postpones a major potential problem until the late stages in plant development—an undesirable feature when a very tight schedule is to be met.

CONCLUSION

In conclusion, it can be said that a huge expenditure of development effort has been made in the development of the gas turbine Brayton cycle. However, it appears that only a small amount of this effort is applicable to the problems which will appear in the application of the Brayton cycle to the lunar base reactor plant and a large engineering development effort will be required to achieve a satisfactory plant. To embark on this development the Brayton systems must clearly show advantages in performance and growth potential as required by the lunar application in order to be selected as the reference plant design.

THE ML-1 PLANT

Objectives of the Program

The main objective of the Army Gas-Cooled Reactor Systems Program is to develop plans, specifications and a prototype unit for a mobile nuclear power plant suitable for military field use. The significant projects under the AGCRSP program included the design, development and test of a gas cooled reactor heat source and the operation of the reactor in a test facility; the parallel development of a Brayton Cycle (closed) secondary system; and finally the operation and test of an integrated prototype power plant. The ML-1 reactor achieved initial criticality in March 1961 at NRTS. Operation of the power plant was achieved in September 1962. The ML-1 reactor and power conversion equipment are transportable on standard army trailers, railroad flatcars, barge, ship, or large transport aircraft. For such transport the complete plant is divided into separate packages holding: the reactor, the power conversion equipment, and the auxiliary equipment.

CONCEPT DESCRIPTION

The ML-1 reactor power plant is a closed loop Brayton cycle power conversion system using a gas-cooled, water-moderated reactor as a heat source. The working fluid, nitrogen or air, passes through the reactor where it is heated from 800°F to approximately 1200°F. From the reactor, the working fluid passes directly to the turbine (direct cycle) which provides power for both a 60 cycle generator and the compressor unit of the system. The turbine and compressor are on a common shaft. From the turbine the fluid enters a gas-to-gas recuperator and then goes to a gas-to-air heat exchanger where the cycle waste heat is dissipated to the atmosphere. From the precooler, the working fluid then goes to the compressor and ultimately back to the reactor through the secondary side of the recuperator. Table 2-9 lists a summary of general system design characteristics.

Reactor and Shield

The reactor design selection was governed by tight requirements for shutdown radiation dose rate and overall package weight. A water-moderated, gas-cooled reactor concept in conjunction with a direct cycle Brayton power conversion system was selected as best meeting requirements to minimize plant weight.

TABLE 2-9 - GENERAL SYSTEM DESIGN CHARACTERISTICS

Design performance at 100° F		
Gross electrical output	400 kw	
Net electrical output	330 kw	
Reactor thermal power	2.9 Mw to gas; 3.3 Mw total	
Cycle efficiency	13.3%	
Plant thermal efficiency	10%	
Coolant flow	92,000 lb/hr	
Dose rate at control cab at 500-ft during full power operation	5 mr/hr (with expedient shielding as needed)	
Dose rate at 25 ft, 24 hr after shutdown (direction of transport vehicle driver with P-C skid in place)	15 mr/hr	
Overall plant dimensions	279 x 113 x 93 in. high	
Overall plant weight and dimensions	Weight, lb	Dimensions (in.)
Reactor package	30,000	111 x 110 x 93 high (plus ion exchange column on end)
Power conversion package	30,000	168 x 113 x 93 high
Control cab	6,500	145 x 82 x 81 high
Auxiliary equipment	15,000	----------------------
Operating supplies (startup and 90 day operation):		
Demineralized water	2900 gal	
Nitrogen (with 0.5 vol% oxygen)	2400 scf	
Oxygen	200 scf	
Anhydrous boric acid (B_2O_3)	1200 lb	
Mixed bed ion exchange resin	900 lb max.	
Lubricating oil	60 gal	
Filter elements	7	
Plant startup time	12 hr	
Auxiliary power requirements		
Pre-startup	30 kw max.	
Normal startup	75 kw max.	
Normal shutdown	45 kw max., 3 kw ave	
Emergency shutdown	None	
Reactor drying	36 kw max.	

The reactor core consists of 61 fuel elements through which the nitrogen or air coolant flows at a pressure of approximately 300 psig. The coolant is heated to 1200°F from the 800°F at which it enters the core. The fuel elements are contained in pressure tubes that are surrounded by slightly pressurized, demineralized water and are enclosed in a heavy metal reflector shield. Each fuel element contains 19 pins, 18 of which are fueled. Fueled elements have 22-inch long sections fueled with ceramic pellets. In six of the pins, the pellets are highly enriched UO_2; in the other twelve, UO_2 diluted with BeO. The pins are clad with Hastalloy X tubing and contained within an insulated, stainless steel jacket. The 61 stainless steel pressure tubes that separate the nitrogen coolant from the moderator water are arranged in a triangular lattice between the 55 tube-sheets. The reactor is controlled by six pairs of semaphore type tapered, neutron-absorbing blades that are inserted in the water passages between fuel elements. The core assembly is surrounded by a gamma shield and is submerged in an aluminum task which is filled during operation with a boric acid solution to provide neutron shielding. Tables 2-10 through 2-19 summarize reactor system parameters.

Power Conversion System

The power conversion equipment in the primary circulatory system includes a 60 cycle generator driven by a turbine, a compressor driven directly by the same turbine, a regenerative gas-to-gas heat exchanger (recuperator) to improve the thermodynamic cycle efficiency, and a gas-to-air heat exchanger (precooler) to dissipate the cycle waste heat to the atmosphere. A starting motor, coupled through the alternator to the T-C set provides the capability for startup and controlled shutdown of the power plant. Decay heat generation following reactor scram is accommodated by the coastdown of the T-C set and the heat removal capacity of the water moderator in the system. During operation, the only radioactive waste product released from the plant is gaseous coolant leaking through imperfect seals and piping joints. This gaseous release, monitored by standard instruments will be maintained at a minimum level by curtailing plant operations, if necessary, to prevent undue radiological hazards in the area. Table 2-20 through 2-24 summarizes the design parameters of the power conversion system.

TABLE 2-10 - REACTOR THERMAL CHARACTERISTICS

Power density	700 kw/ft^3
Maximum heat flux	140,500 Btu/hr/ft^2
Average heat flux	78,200 Btu/hr/ft^2
Heat transfer surface	126.5 ft^2
Maximum to average heat flux ratio	
Axial	1.5
Radial	1.2
Maximum fuel center temperature (including hot spot factors)	2160° F (BeO-UO_2) 2650° F (UO_2)
Maximum moderator temperature	190° F
Maximum surface temperature of fuel cladding (nominal, average)	1520° F
Maximum surface temperature of fuel cladding (including hot spot factors), reference	1750° F

TABLE 2-11 - REACTOR NUCLEAR CHARACTERISTICS

Average thermal neutron flux (fuel)	1.9×10^{12} neut/cm^2-sec
Average fast neutron flux (fuel)	1.7×10^{13} neut/cm^2-sec
Maximum: average thermal flux ratio	3.9
Hydrogen to U-235 atom ratio	40
Core buckling	0.0059 cm^{-2}
Fermi age	60 cm^2
Square of thermal diffusion length, L^2	2.05 cm^2
Thermal utilization, f	0.75
Infinite multiplication factor, k	1.54
Neutron lifetime	1.9×10^{-5} sec
k_{eff}, cold, clean core; no shims or burnable poison	1.067
Operating k_{eff}, cold, clean core, with shims and burnable poison	1.014
Core life, full power	3000 hr min; 10,000 hr design
Burnup (U-235), average	3.6% in 10,000 hr
Maximum	6.5%
Prompt temperature coefficient, $\Delta k/k$-°C	
at 0°C	$+0.3 \times 10^{-6}$
at 90°C	-0.5×10^{-6}

TABLE 2-12 - REACTOR VESSEL

Materials	
Tube sheet	Stainless steel, Type 304, 2.94 in. thick
Pressure tubes	Stainless steel, Type 321
Source tube	Stainless steel, Type 321
Gas ducts and plenums	Stainless steels, Types 304-L, 321, and 347
Baffle	Stainless steel, Type 321, tungsten and Inconel X (springs)
Outside diameter	30.960 in. max. (exclusive of upper flanged connection)
Overall height	79.5 in.
Pressure tube length	24 in. between inside surfaces of tube sheets
Design pressure	345 psia (gas)
Design temperature	525° F (max.)
Wall thicknesses	Tubes 0.020 in. Plenum 2.12 in. min
Source tube	0.020 in. wall thickness; 0.500 in. OD

TABLE 2-13 - REFLECTOR

Composition, top	2 in. H_2O; 4.5 - 5.0 in. stainless steel; 1.5 in. W
Bottom	3-4 in. stainless steel; 3 in. W
Radial	1.8 in. Pb; 2 in. W; 180° segment 4 in. Pb; 180° segment
Total heat generation	6×10^5 Btu/hr
Maximum power density	360 Btu/hr-in.^{3}

TABLE 2-14 - BIOLOGICAL SHIELDING

Composition	3-1/2 to 4 in. lead and tungsten, plus 30 in. of borated water (10% boric acid)

TABLE 2-15 - CORE (EXCLUDING REFLECTOR)

Diameter	22 in. equivalent
Height	22 in.
Number of fuel elements	61
Number of coolant passages	61
Number of coolant passes	1
Type of geometry of fuel elements	Clusters of 19 pins (18 fueled)
Cold, clean critical mass, U-235, no shims, no burnable poison	37 kg
U-235 loading	49 kg
Enrichment, inner 6 pins	93% U-235 as UO_2
Outer 12 pins	31 vol% UO_2, 93% enriched U-235 69 vol% BeO

Core composition

Materials	Volume %
UO_2	4.3
BeO	3.3
Stainless steel	3.6
Hastelloy X	7.0
H_2O	58.6
Insulation	7.0
Gas void	16.2
Total	100.0

TABLE 2-16 - FUEL ELEMENT

Dimensions	1.72 in. OD x 32 in.
Fuel material	BeO-UO_2 (outer pins); UO_2 (inner pins)
Number of pins per element	19 (12 w/BeO-UO_2; 6 w/UO_2; 1 empty)
Pin outside diameter	0.241 in.
Pin cladding material	Hastelloy X
Pin cladding wall thickness	0.030 in.
Pin spacer	0.040 in. OD Hastelloy wire
Heat transfer material (pin internal)	He
Pellet diameter	0.176 in. (nominal)
Type burnable poison	Cadmium
Reactivity worth of burnable poison	0.6% at startup

TABLE 2-17 - CONTROL ELEMENTS

Type	Tapered blades
Location	Moderator
Number: Shim blades	3 pairs (3 actuators)
Safety blades	2 pairs (2 actuators)
Regulating blades	1 pair (1 actuator)
Absorber material: Safety and shim blades	5 wt% Cadmium- 15 wt% Indium- 80 wt% Silver
Dimensions (each blade)	4 x 10.5 x 0.25 to 0.62 in.
Regulating blades	Stainless steel
Dimensions (each blade)	4 x 9 x 0.25 to 0.62 in.
Cladding material	None
Reactivity worth of control elements:	
Safety and shim blades	0.058 Δk/k
Regulating blades	0.004 Δk/k
Total	0.062 Δk/k
Actuating time for regulating blade:	
Drive	13.3 sec for full insertion or withdrawal
Scram	0.35 sec (max.) for full insertion from signal
Safety and shim actuator:	
Drive	4.0 min for full insertion or withdrawal
Scram	0.35 sec (max.) for full insertion from scram signal

TABLE 2-18 - MODERATOR

Type	Water
Reactor inlet temperature	180° F
Reactor outlet temperature	190° F
Pressure	30 psi max.
Flow rate	300 gpm
Type of flow circulation	Forced
Purity:	
Total solids	1 ppm
Resistivity	10^5 to 10^6 ohm-cm
Total heat removal rate	1.5×10^6 Btu/hr

TABLE 2-19 - REACTOR WORKING FLUID FLOW

Working fluid	99.5 vol% N_2 + 0.5 vol% O_2 (nominal)
Reactor inlet temperature	800° F nominal
Reactor mixed-mean outlet temperature	1200° F max.
Average velocity in core	160 ft/sec
Maximum velocity	180 ft/sec
Inlet pressure	315 psia (max.)
Core ΔP	15 psi
Reactor ΔP	22 psi

TABLE 2-20 - POWER CYCLE

Type	Brayton cycle with regeneration		
Total volume of working fluid system	120 ft^3		
Total system working fluid inventory full load at 100° F	52 lb		
Working fluid transit time	2.0 sec		
Cycle characteristics:			
Ambient temperature	100° F	0° F	-65° F
Net power, kw	330	330	330
Reactor inlet, ° F	791	597	597
Turbine inlet, ° F	1200	990	990
Compressor inlet, ° F	132	24	24
Compressor inlet, psia	117	93	93
Compressor outlet, psia	320	294	294
Reactor inlet, psia	313	288	288

TABLE 2-21 - TURBINE-COMPRESSOR SET

	Stratos t-c Set	Clark t-c Set
Speed, rpm	18,338	22,000
Turbine stages	2	2
Turbine rotor material	Incoloy 901	Incoloy 901
Turbine blade material	Inco 713	N 155
Turbine stator blade material	Inconel	N 155 or 19-9DL
Expansion ratio	2.38	2.38
Compressor stages	2	11
Compressor material	Al 355 T71	403 stainless steel
Rotor shaft	SAE 4340	SAE 4340
Compressor ratio	2.72	2.72
Case material	304 stainless steel	304 stainless steel
Seals		
At journals	Buffered labyrinth	Buffered labyrinth
Interstage	Plain labyrinth	Plain labyrinth
Shaft	Buffered labyrinth	Double "L" ring seal oil buffered
Bearings		
Journal	Tilting pad	Plain babbitt
Thrust	Kingsbury type	Kingsbury type (in low pressure area)
Support	Overhung turbine	Turbine and compressor supported between bearings

TABLE 2-22 - ALTERNATOR

Output	60 Cycle Operation	50 Cycle Operation
Rating	500 KVA 3 ϕ	417 KVA 3 ϕ
Voltage	2400/4160 V	2000/3467 V
Rotor shaft speed	3600 rpm	3000 rpm
Case		
Diameter, maximum	40.25 in.	
Length, without starting motor	30 in.	
Length, with starting motor	35.5 in.	
Weight, alternator only	5900 lb	
Weight, starting motor	400 lb	
Temperature, operating (hot spot)	300° F internal max.	

TABLE 2-23 - RECUPERATOR

Length (including insulation)	81 in.
Outside diameter (including insulation)	49.25 in.
Headers	
High pressure inlet	8 in.
High pressure outlet	8 in.
Low pressure inlet	20 in.
Low pressure outlet	14 in.
Effectiveness	79%
Pressure loss	
High pressure $\Delta p/p$	2.5%
Low pressure $\Delta p/p$	0.85%
Type	Shell and tube regenerator
Tubes	4 passes x 840 tubes
Shell	1 pass
Surface	External fins
Materials	300 series stainless steel

TABLE 2-24 - PRECOOLER, MODERATOR COOLER AND OIL COOLER ASSEMBLY

Dimensions:	
Length, overall	166 15/16 in.
Precooler	122 5/16 in.
Moderator cooler	32 1/8 in.
Oil cooler	11 5/16 in.
Width	113 in.
Thickness, overall	32 in.
Core	15 in.
Fans and plenums	17 in.
Materials	
Tubes and fins	Series 1100 aluminum
Headers	Series 2219 aluminum
Weight	6500 lb
Precooler:	
Header, inlet	One, 14 in.
Header, outlet	One, 10 in.
Effectiveness	90%
Total $\Delta p/p$	3.25%
Air flow	247,500 lb/hr
Type	Fin fan air-to-gas exchanger
Tubes	1105 tubes, single pass
Surface	Internal and external fins
Moderator cooler:	
Headers, inlet and outlet	4 in.
Total Δp	2.77 psi
Water temperature	
In	190°F
Out	180°F
Air flow	73,250 lb/hr
Type	Fin fan air-to-water exchanger
Tubes	88 tubes per pass, three passes
Surface	External fins

TABLE 2-24 - (continued)

Oil cooler:	
Connections, inlet and outlet	1 1/2 in.
Total Δp	9.38 psi
Oil temperature	
In	180° F
Out	150° F
Oil flow	18, 900 lb/hr
Air flow	27, 500 lb/hr
Type	Fin fan air-to-oil exchanger
Tubes	45 tubes, 2 passes
Surface	Internal and external fins

Summary

The system is now in operation, but, due to difficulties with the power conversion system, the plant has not yet generated design output of 330 KWe. The maximum plant output to date has been approximately 250 KWe at heat rejection temperatures considerably below the design heat rejection temperature of 100°F.

THE MCR PLANT

Objective of the Program

The objective of the MCR (Military Compact Reactor) Project is to develop the technology for and produce the prototype of a transportable electric generating plant utilizing a fission heat source. This plant is intended for field use to supply electricity as required for a variety of military missions; hopefully, the plant can be adapted to furnish propulsion power for vehicles of the overland-train type, although this application has low priority. The immediate and definite objective is to develop a plant to deliver 3 megawatts of electrical power (with the ambient temperature 60°F) to a load with a 0.8 power factor. The complete plant weight is not more than 120,000 pounds with individual package weights not to exceed 30,000 pounds and 8 ft 9 in. high, 8 ft 9 in. wide maximum, with a maximum of 25 ft long. These limitations are derived from the Berne clearance limits for rail shipment, the capability of the M-172 A trailer for highway shipment, and the requirements of the C-130 A cargo plane for air equipment.

CONCEPT DESCRIPTION

General Description

The Military Compact Reactor system is an indirect cycle plant. The heat source is a nuclear reactor from which heat is removed by a closed forced circulation loop in which liquid potassium is used as the heat transfer medium. Heat is removed from this loop in a heat exchanger and transferred to air, which is the working fluid of the power conversion unit. The prime mover is an air turbine driving a compressor (and the electrical generator) arranged with the heat exchanger in a Brayton process (or "open Brayton cycle"). Because this process discards and replaces its working fluid continuously, no heat sink is required; for the same reason, the plant as a whole is not suitable for use on the lunar surface. The technology of the reactor and primary system is, however, adaptable to the design of equivalent components of a lunar surface reactor power plant. Consequently, detailed information presented here is limited to the reactor core, shield, vessel and primary coolant loop, and the auxiliaries of these subsystems. For orientation purposes, however, a brief summary of overall power plant characteristics is included in Table 2-25; the reactor characteristics are summarized in Table 2-26.

Reactor Core

This fast spectrum reactor is UO_2-fueled BeO-reflected, and its core is made of individually clad fuel rods arranged in a right circular cylinder 15 inches in diameter and 15 inches high; unfueled portions of the fuel rods make them approximately 20 inches long. Two basic core designs are being considered, one being based on UO_2 ceramic fuel and the other being based on UO_2-Cb (or UO_2-Mo) cermet fuel. In both designs the fuel is highly enriched UO_2, the fuel cladding is Cb-1Zr alloy, and the core structural components are type 316 stainless steel. Table 2-2 summarizes the important design parameters of the two alternatives being considered.

At the MCR power level, core size is established by nuclear considerations rather than heat transfer to the coolant so the diameter of the fuel pins is determined by their internal design and temperature limitations. The UO_2 ceramic fuel pins are only 0.264 in. in diameter; in these heat is transferred through a filling gas (helium) from the ceramic pellets to the cladding, which is 0.015 in. wall tube. The UO_2 cermet fuel pins are 0.497 in. in diameter; in these heat is transferred by conduction through a metallurgical bond between the cermet and the cladding. Both types of fuel rods contain BeO segments at each end to serve as axial reflectors for the core. Other than diameter, an additional difference is that the UO_2 ceramic fuel elements contain a void space for the accumulation of fission product gases, while the UO_2 cermet elements do not have such a reservoir.

Additional information about the core design is summarized in Table 2-27.

Control System

The core is surrounded by a radial reflector 5 inches thick made of massive BeO sections

TABLE 2-25 - PRINCIPAL PERFORMANCE AND DESIGN DATA

(60° F day is the design point of the plant)

OVERALL POWERPLANT

1. Plant Life

Core	5,000 equivalent full power hours
Other components	25,000 hours of operation

2. Power and Heat Balance

	Units			
Ambient Temperature		-65° F	50° F	100° F
Net Power Output	kw_e	3000	3000	2270
Generator Losses	kw_e	160	160	135
Shaft Power to Main Generators	kw_e	3160	3160	2405
Shaft Power to Auxiliary Alternators	kw_e	170	170	170
Reduction Gear Losses	kw_e	35	35	25
Gross Engine Output	kw_e	3365	3365	2600
Engine Thermal Efficiency		0.218	0.228	0.204
Heat Transferred in Primary HX	kw_{th}	15,440	14,760	12,740
Heat Lost in Afterheat HX	kw_{th}	40	40	40
Heat Lost Through Primary Loop Insulation	kw_{th}	60	60	60
Heat Added by Primary Pumps	kw_{th}	-100	-100	-100
Reactor Heat Transferred to Primary Coolant	kw_{th}	15,440	14,760	12,740
Gamma and Neutron Heating in Shield	kw_{th}	260	240	210
Total Reactor Power	mw_{th}	15.70	15.00	12.95

3. Principal Temperatures

Reactor Exit (average)	°F	1277	1500	1500
Reactor Inlet	°F	963	1200	1241
Turbine Inlet	°F	1160	1400	1400
Compressor Exit	°F	432	595	635
Compressor Inlet	°F	-65	60	100

TABLE 2-25 - (continued)

	Units	
4. Size and Weight		
Width and Height (all packages)	in.	96 x 92
Overall Length (assembled end to end)	ft	65 ft 0 in.
Estimate Gross Weight (all packages)	lb	116, 700
5. Plant Control Mode		
Engine-Generator Speed		Held constant by HX bypass valve
Reactor Power		Matched to engine power by control drums, holding constant flow

TABLE 2-26 - REACTOR CHARACTERISTICS AND DESIGN DATA

REACTOR

	Units	Recommended Concepts: Ceramic	Recommended Concepts: Cermet
1. Type of Core			
Power	mw_{th}	15.0	15.0
Heat Removed by Primary Coolant	mw_{th}	14.76	14.76
Core Lifetime	mwd	3600	3600
Coolant Exit Temperature	°F	1500	1500
Coolant Entry Temperature	°F	1200	1200
Coolant Flow	lb/sec	250	250
Coolant Pressure (maximum)	psig	110	110
Coolant		K-39*	K-39*
Core Diameter and Active Length	in.	15.0	15.0
Reflector Thickness (radial and axial)	in.	5.5	5.5
2. Materials			
Fuel		UO_2	UO_2-Cb (or Mo) Cermet
Clad		Cb-1% Zr	Cb-1% Zr or Mo
Moderator (core)		None	None
(reflector)		5.5-in. BeO	2-in. BeO
Core Internal Structure		Type 316 SS	Type 316 SS
3. Fuel Pins			
Number (approximately)		2520	750
Diameter	in.	0.264	0.497
Average Heat Flux	BTU/hr-ft^2	230,000	412,000
Temperature (maximum center)	°F	2700	2350

CONFIDENTIAL
RESTRICTED DATA
[redacted]

TABLE 2-26 - (continued)

	Units	Recommended Concepts: Ceramic	Recommended Concepts: Cermet
Temperature (maximum clad)	°F	1610	1645
Prompt Negative Reactivity Coefficient		Yes	Yes
(means)		Combined factors	Expansion
4. Control Drums			
Number		10	10
Diameter	in.	5	5
Poison		B_4C in SS	B_4C in SS
5. Reactor Vessel			
Inside Diameter	in.	26	26
Wall Thickness (cylinder)	in.	0.44	0.44
Material		Type 316 SS	Type 316 SS
Height (approximately)	in.	40	37.75

	Units	Recommended Concepts
SHIELD		
Fixed Shield		
Coolant		Organic
Material (inside to out)		SS-Pb
Outside Diameter (average)	in.	39
Removable Shield		
Coolant		Organic
Material (inside to out)		LiH-Pb-LiH
Outside Diameter (average)	in.	101
Dose Rate at Control Cab (full power, end of life at 450 ft)	mr/hr	10

Astronuclear

TABLE 2-26 - (continued)

	Units	Recommended Concepts
PRIMARY SYSTEM		
Number of Loops in Series		1
Number of Loops in Parallel (each with pump and HX)		2
Flow (total)	lb/sec	250
Pressure (pump inlet)	psig	50
Loop (pressure drop)	psi	60

*Natural K with K-41 content reduced to 0.07%

~~CONFIDENTIAL~~
~~RESTRICTED DATA~~
~~Atomic Energy Act 1954~~

TABLE 2-27 - SUMMARY OF REACTOR DESIGN DATA

	Units	Recommended Concepts: Ceramic	Recommended Concepts: Cermet
1. General			
Nominal	kw_{th}	15,000	15,000
Heat Transferred to Primary Coolant	kw	14,760	14,760
Heat Transferred to Shield	kw	240	240
2. Core			
Lifetime	mwd	3125	3125
Diameter	in.	15	15
Length (fueled)	in.	15	15
Length (overall)	in.	21.2	19
Composition, Volume Fraction			
Fuel		0.615	0.754
Moderator		None	None
Coolant		0.217	0.163
Clad and Structure		0.168	0.083
Maximum-to-Average Power Ratio		1.3**	1.3
3. Fuel			
Material		UO_2	70% UO_2-30% Cb or Mo
Initial Loading (U)	kg	235	206
Enrichment (U-235)	%	47	75
Rod OD	in.	0.264	0.497
Number of Fuel Pins		2520	750
Cladding Material		Cb-1 Zr	Cb-1 Zr or Mo
Cladding Thickness	in.	0.015	0.010
Fuel-Clad Bond	in.	Helium	Metallurgical Bond
Maximum Fuel Irradiation	mwd/tonne	13,300	15,170
Maximum Central Temperature	°F	2700	2350
Maximum Clad Temperature	°F	1610	1645
Heat Transfer Surface Area	ft^2	218	122

TABLE 2-27 - (continued)

	Units	Recommended Concepts Ceramic	Cermet
Spacing Between Pins	in.	0.020	0.021
Average Heat Flux	BTU/hr-ft^2	230,000	412,000
Maximum Heat Flux	BTU/hr-ft^2	300,000	536,000
4. Moderator			
Material		Thick BeO in Reflector, none in Core	Thin BeO in Reflector, none in Core
5. Coolant			
Material		K-39†	K-39†
Inlet Temperature	°F	1200	1200
Outlet Temperature	°F	1500	1500
Velocity in Core	ft/sec	22.5	30
Nominal Pressure	psia	100	100
Flow Area	ft^2	0.27	0.20
Heat Transfer Coefficient	BTU/hr-ft^2-°F	16,000	14,500
Pressure Drop Across Vessel ††	psi	39	40
6. Control Drums			
Number		10	10
Diameter	in.	5	5
Height	in.	19.5	19.5
Poison Material		B_4C	B_4C
Coolant (K) Volume Fraction		0.10	0.10
7. Reflector			
Inner Layer			
Materials	v/o	BeO(80); K(10); SS(10)	BeO(80); K(10); SS(10)
Thickness	in.	2	2
Outer Layer			
Materials	v/o	BeO(75); K(10);SS(10); $B_4^{10}C$(5)	SS(85); K(10); $B_4^{10}C$(5)
Thickness	in.	3.5	3.5

TABLE 2-27 - (continued)

	Units	Recommended Concepts: Ceramic	Recommended Concepts: Cermet
8. Nuclear Data			
Initial Loading of Fuel	kg	271	324
Initial Loading of U	kg	235	206
Initial Loading of U-235	kg	110	154
Fuel Enrichment	%	47	75
NH	atoms of H/cm^3 of YH	None	None
H/U-235 Atomic Ratio		None	None
Prompt Reactivity Coefficient	$\Delta k/k/°C \times 10^{-6}$	-3 to -6	-3 to -4
Control Drums Worth (K)	%	10	9.6
Initial Excess Reactivity Requirements (K)	%	5	2.5
9. Pressure Vessel			
Outside Diameter	in.	26.88	26.88
Height (overall)	in.	40.0	37.75
Wall Thickness	in.	0.44	0.44
Neck Height	in.	--	--
Material		Stainless Steel	Stainless Steel
Nozzles			
Inlet	in.	1-8	1-8
Outlet	in.	1-8	1-8

*At 3.0 mw_e plant output on 60°F day

**Requires variable fuel enrichment loading

†K-39 + 0.07% K-41

†† Including shield plugs in nozzles

canned in stainless steel. Within this reflector annulus are 10 control drums, rotatable about axes parallel to that of the core. Approximately 40 percent of the volume of each drum consists of B_4C in the form of stainless steel-clad pins; the remaining volume of the drums is BeO. The drums are rotated by individual drives so that the neutron absorbers, the B_4C pins, are removed from the periphery of the core and are replaced by reflector material.

Reactor Vessel and Coolant Loop

The entire reactor is enclosed in a pressure vessel of type 316 stainless steel. The pressure vessel lengths are slightly different from the two core designs, but otherwise the vessels are the same. The vessel is somewhat protected from neutron irradiation by the reflector annulus and absorbers always present between it and the core, and is cooled by the incoming stream of potassium. The vessel design, and that of the entire primary coolant loop, is based on the creep properties of the material, type 316 stainless steel.

Additional information concerning the coolant system and auxiliaries is summarized in Table 2-28.

Shield

The shield included in the MCR plant is designed specifically for the MCR conditions and is not directly applicable to a lunar surface power plant. It is designed for the MCR reactor power level, it protects the environment from air-scattered radiation, and it is divided quite arbitrarily into a removable operating shield and a fixed shut-down shield to meet the package weight limitations.

Additional information concerning the shield design is summarized in Table 2-29.

SUMMARY

The MCR program has achieved a conceptual reactor design and is in the process of selecting a reference design. Development testing has been started on some power conversion system components. This is consistent with the objective of testing the prototype plant in 1968.

TABLE 2-28 - SUMMARY OF PRIMARY COOLANT LOOP DESIGN DATA

	Units	Recommended Concepts
1. General		
Rating	kw_{th}	14,760
Coolant		K-39*
Flow Rate	lb/sec	250
Maximum Temperature	°F	1500
Differential Temperature	°F	300
Maximum Pressure	psig	115
Loop Pressure Drop	psi	60
Coolant Velocity in Piping	fps	25-35
Coolant Inventory (including reactor)	ft^3	15
2. Piping		
Material		316 SS
Number Required		2 Pipe Loops in Parallel
Size (ID and wall thickness)		6-in. Sch. 40
3. Valves		
Type		Check
Location		Dump Inlet
4. Pumps		
Type		Centrifugal
Number Required		2
Seal		Labyrinth
Drive		400-cycle Electric Motor
Power Per Pump	Fluid hp	46
Flow Per Pump	gpm	1310
Pump Head	psi	60
Efficiency	%	75
5. Surge Tank		
Expansion Volume (1/2 tank volume)	ft^3	3.5

*K-39 + 0.07% K-41

TABLE 2-29 - SUMMARY OF SHIELD DESIGN DATA

	Units	Recommended Concept Radial Midplane	Axial Down	Axial Up
1. Assembled Configuration				
Core Radius	in.	7.5	7.5	7.5
Reflector				
Inner Layer				
Materials		BeO	BeO	BeO
Thickness	in.	2	3	1.5
Outer Layer				
Materials		BeO	SS	SS
Thickness	in.	3.5	1.5	6
Plenum Thickness	in.	--	1.5	1.5
Pressure Vessel				
Material		Stainless Steel		
Thickness	in.	0.44	0.44	0.44
Insulation				
Material		Min-K (Johns-Manville)		
Thickness	in.	0.5	0.5	0.5
Inner Gamma Shield (including liners)				
Material		Pb with Al Canning		
Thickness	in.	*7.9 to 6.1 **6.8 to 4.9	6.1 4.9	-- --
Inner Neutron Shield (including liners)				
Material		LiH with Al Canning		
Thickness	in.	N/A		
Gamma Shield (including liners)				
Material		Pb with Al Canning		
Thickness	in.	N/A		
Outer Neutron Shield (including liners)				
Material		LiH with Al Canning		
Thickness	in.	N/A		

TABLE 2-29 - (continued)

	Units	Recommended Concept: Radial Midplane	Axial Down	Axial Up
2. Shield Coolant System				
Rating	kw	240		
Coolant		Monoisopropyldiphenyl		
Flow Rate	lb/sec	20		
Pressure Drop	psi	40		
Pressure	psig	0		
Temperature (inlet)	°F	256		
Temperature (outlet)	°F	280		
Inventory	lb	600		
Makeup Requirements for 5000-fph Operation	lb	Included in Inventory		
Expansion Volume (-65 to 250°F)	ft^3	0.8		
Operating "HBR" Equilibrium	w/o	25 maximum		
3. Shield Performance †				
Operating Dose Rate at 450 ft from Core Center Line on Reactor	mr/hr			
Horizontal Midplane				
In Forward Direction		10		
In Rearward Direction		10		
Shutdown Dose Rate 12-hr after Shutdown (removable shield in place)	mr/hr			
Forward Direction 10 ft from Core Center Line		N/A		
Rearward Direction 10 ft from Coolant System		N/A		
Shutdown Dose Rate 12 hr after Shutdown (removable shield separated)	mr/hr			

TABLE 2-29 - (continued)

	Units	Recommended Concept Radial Midplane	Axial Down	Axial Up
Forward Direction 10 ft from Core Center Line		170		
Rearward Direction 10 ft from Coolant System		590		

N/A - Not Available

*Ceramic Core

**Cermet Core

†At 15.00 mw_{th}, 60° F day

CLOSED BRAYTON CYCLE TURBO MACHINERY

Performance Analysis

Since very little data exists on closed Brayton cycle power conversion equipment, open cycle equipment must serve as an initial basis of analysis. Figures 2-26 and 2-27 are linear plots of various open cycle turbine and compressor efficiencies as a function of power level of the combined turbo machinery units. These plots indicate the drastic effect of power level on efficiency as power level decreases.

While Figures 2-26 and 2-27 are instructive, they are hard to read. Figures 2-28 and 2-29 are semi log plots of the same data. These Figures clearly demonstrate present state-of-the-art and the progress made in the last 10 years. It is obvious from the test units available in 1952 that much of the performance gains were made in the early 1950's. All of the impetus of the commercial aircraft, military aircraft, and auxiliary power units has not provided a really significant increase in component efficiency since the early 1950's. Further increases can be expected to be even more difficult, costly, and time consuming to obtain. Systems which propose component efficiencies appreciably greater than the envelopes of Figures 2A and 2B should be viewed with skepticism.

A direct extrapolation of open cycle data for comparison to closed cycle systems does not tell the entire story. It does not explain, why ML-1 turbomachinery does not appear to meet design predictions, since if one examines the expected turbine and compressor efficiencies at 450 (the gross design shaft power of the ML-1) one would predict a compressor and turbine efficiency of 84.5 percent and 87.5 percent respectively. The design values were 83.9 percent and 86 percent respectively. The explanation must lie in the difference between closed cycle turbomachinery and open cycle turbomachinery.

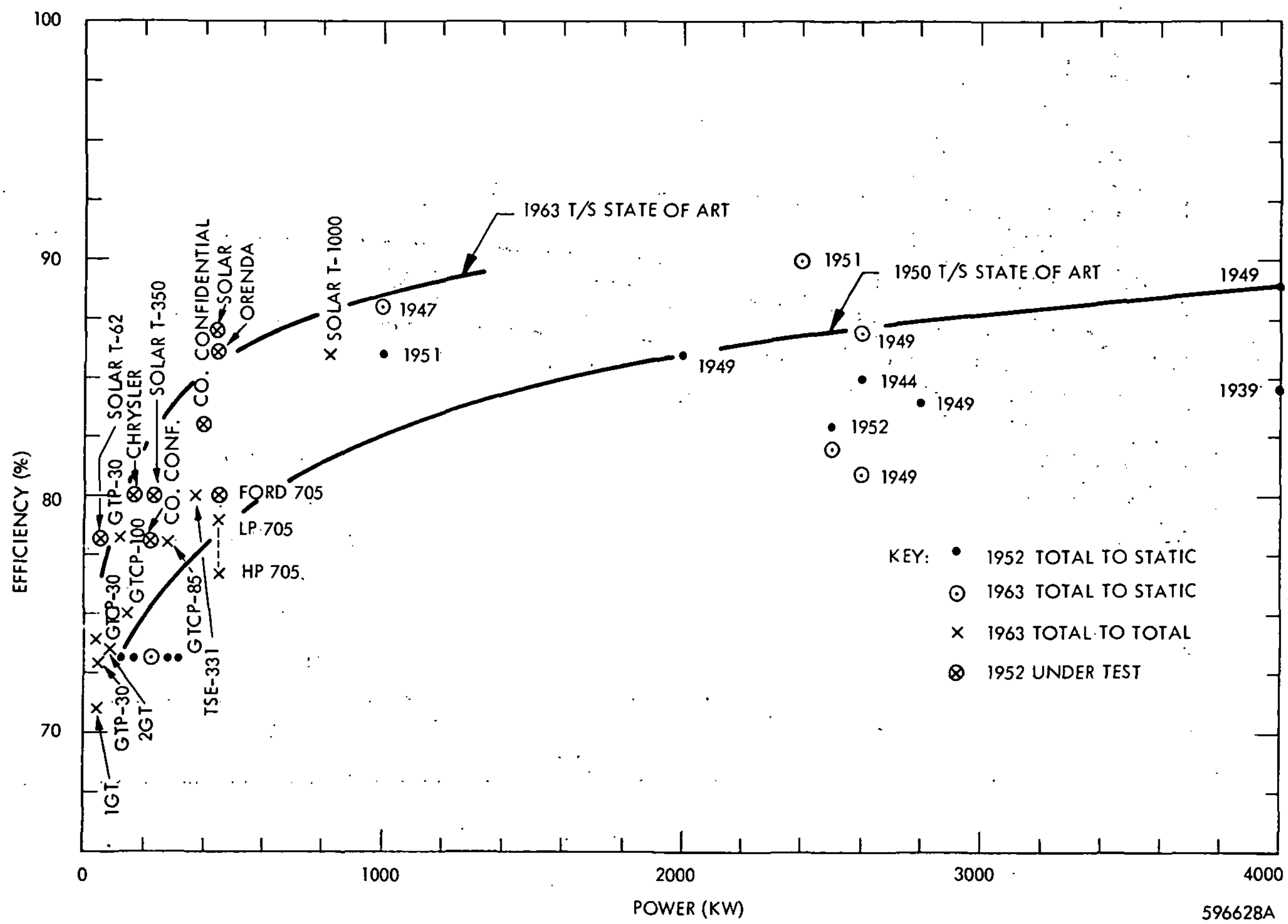

Figure 2-26. Open-Cycle Comprssor Efficiency vs. Power

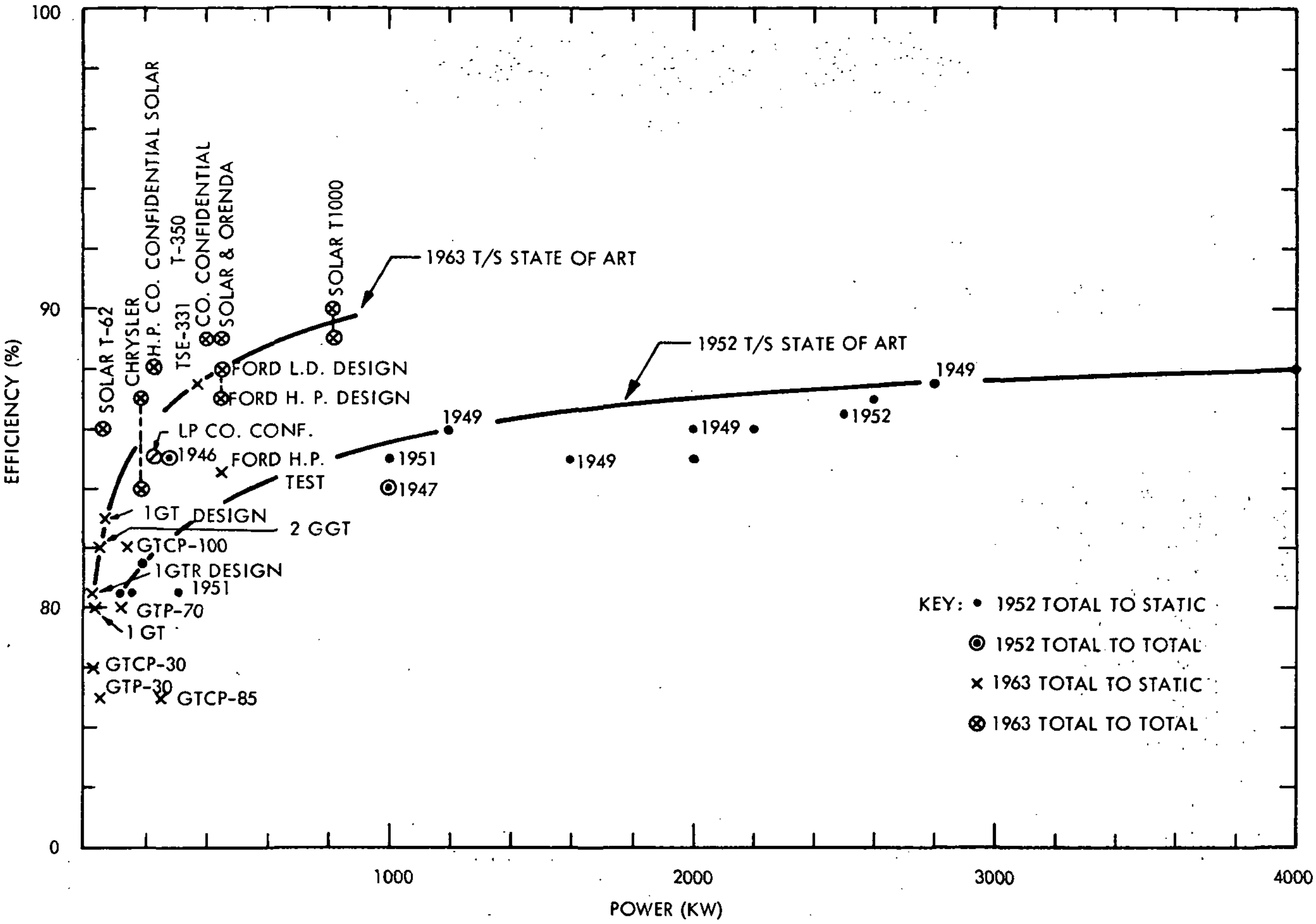

Figure 2-27. Open-Cycle Turbine Efficiency vs. Power

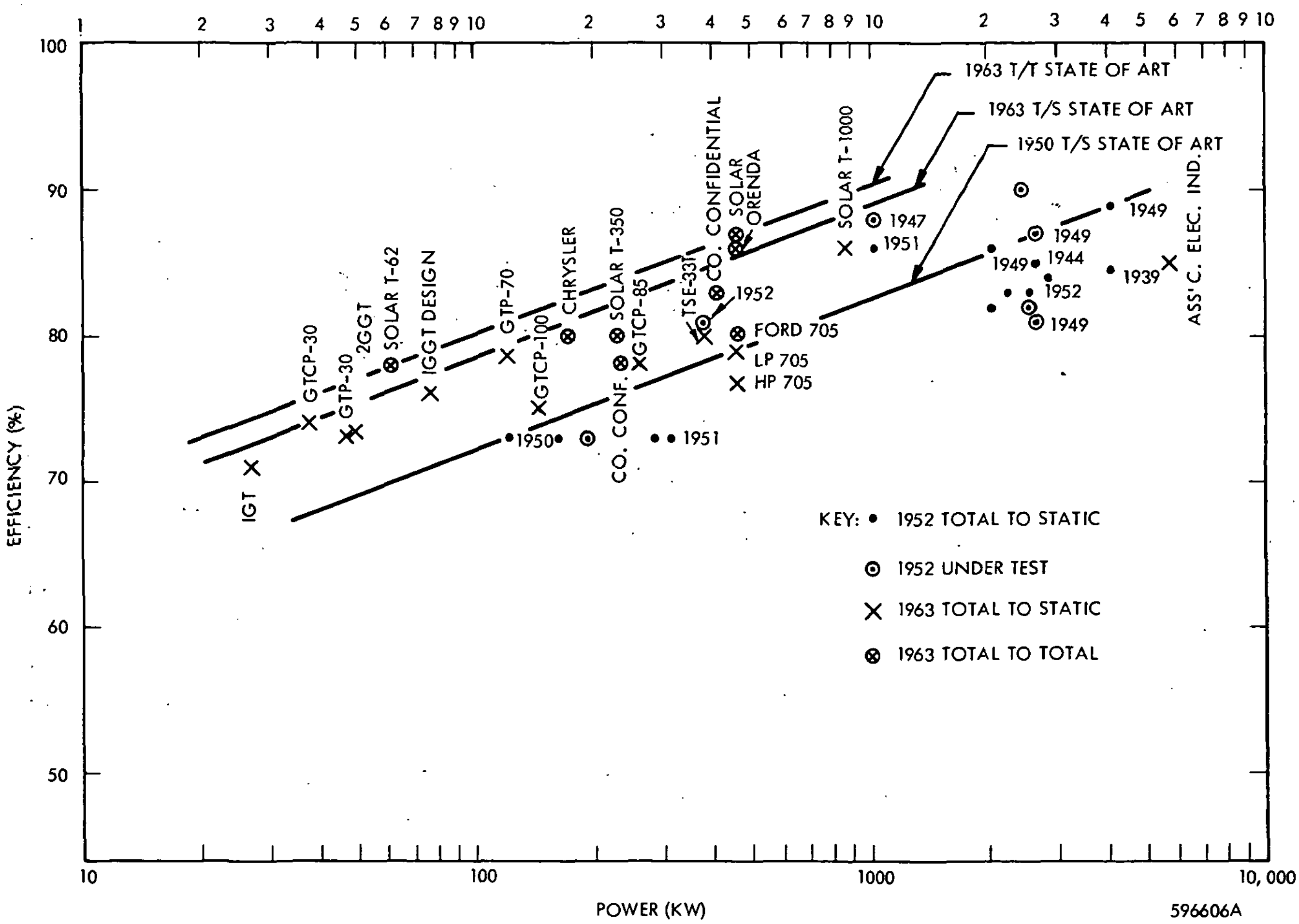

Figure 2-28. Open-Cycle Compresor Efficiency vs. Power

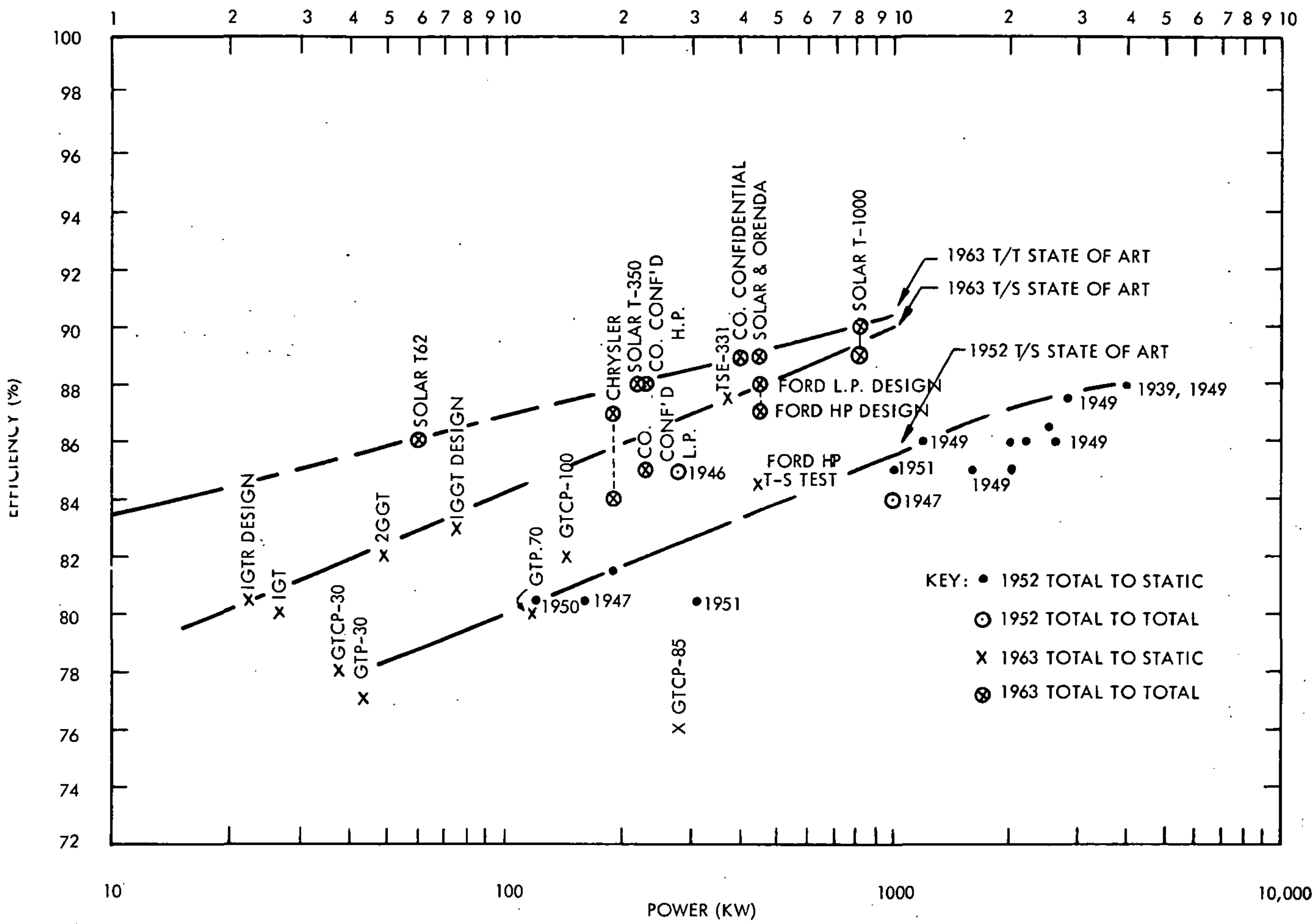

Figure 2-29. Open-Cycle Turbine Efficiency vs. Power

The difference between the closed-cycle ML-1 turbomachinery and the open-cycle turbomachinery available as a basis of comparison is one of size. Figures 2-26 and 2-27 indicate a significant size effect, in that reduced power level is uniquely tied to a reduction in turbomachinery size. When one considers that, because of an eight-fold pressure level increase, ML-1 is eight times smaller than an equivalent open-cycle machine of the same power, it can be seen that considerable size effects can be encountered. The remainder of this analysis is an attempt to evaluate these size effects and determine their influence on turbomachinery development.

Exclusive of Reynolds number, which is taken as a secondary influence, and considering only a single gas (thus omitting the gas constant R), the three dimensionless performance parameters which fall out of a dimensional analysis of turbomachinery are:

$$\frac{P_2}{P_1}, \quad \frac{W \quad T}{D^2 \, P_1}, \quad \frac{ND}{T_1}$$

P = pressure
w = mass flow
T = temperature
N = rotational speed
D = characteristic dimension

For a given machine, D is not needed as a performance parameter and the subgroups become:

$$\frac{P_2}{P_1}, \quad \frac{W \quad T_1}{P_1}, \quad \frac{N}{T_1}$$

As explained in Shepherd's "Principles of Turbonachinery," (p 43) Reynolds number effects, as a first order approximation, may be neglected as a minor effect. For purposes of simplicity, Reynold's number effects will be neglected during initial phases of this analysis. While Reynolds number is often a secondary factor in comparison with other considerations, when these have been satisfied it becomes of consequence in its effect of gaining the final few points of efficiency. These Reynolds number effects will be treated later.

Utilizing the performance parameters developed above, a typical compressor map has been displayed in Figure 2-30. The performance parameters establish the operating map by showing the complete interactions among the performance parameters for a given machine. The efficiency, however, is not described and can only be determined from the aerodynamic design and superimposed upon the map. This map demonstrates no effect of density in the operating performance map and indicates that mass flow is proportional to pressure. If this is not completely obvious from the consideration of the map and the performance parameters, a more detailed presentation of the same conclusions may be found in "Principles of Turbomachinery" (pp 42-43).

If all other parameters except pressure are held fixed, the fact that mass flow is proportional to pressure or the power developed or consumed in the turbine or compressor, yields a method to scale closed-cycle performance from open-cycle performance. This is well known from plots similar to 2-28 or 2-29. The technique is as follows: If a given open-cycle compressor or turbine is constructed to withstand increases in pressure and is operated in open cycle, the efficiency of either unit may be determined from relatively well known performance maps similar to Figure 2-30. One may also determine this power either developed or consumed in the turbine or compressor. (Henceforth, when pressure changes are considered, all other parameters are held fixed unless otherwise specified.) As pressure (mass flow) is increased, the power developed or consumed in either unit increases in proportion to the pressure, but the efficiency (neglecting Reynolds number effects) remains constant. Thus a closed cycle

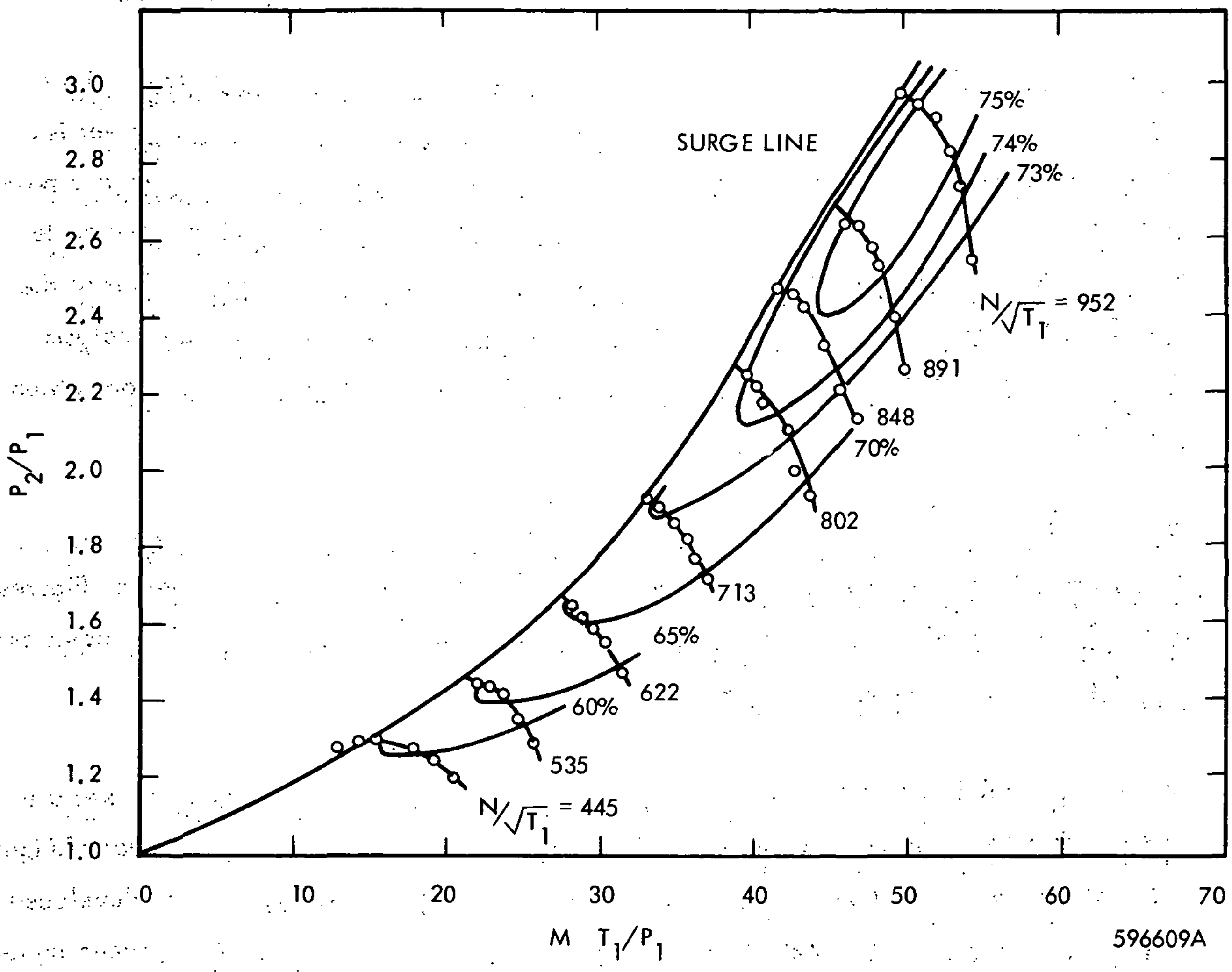

Figure 2-30. Typical Compressor Performance Map

compressor can be expected to have the efficiency of an open-cycle compressor which produces or consumes the fraction $\frac{14.7}{P_1}$ of the closed-cycle power (where P_1 is closed cycle compressor inlet pressure). A similar relationship exists for a closed cycle turbine.

In theory this technique is fine, but in practice complications arise. Obtaining turbine and compressor efficiencies as a function of gross shaft power or net electrical power is a *major undertaking. To obtain efficiencies as a function of component thermodynamic power* is impossible within any reasonable amount of time or effort. An attempt has been made to utilize the turbine and compressor efficiencies as a function of gross shaft power of the combined turbine-compressor units. One approximation is needed to facilitate analysis. It can be shown that this approximation has a negligible effect upon the predictions which can be made.

An approximation is made that parasitic power losses in bearings, seals, windage, etc., is 15 percent of the gross shaft power, and Figures 2-28 and 2-29 are reconstructed on Figures 2-31 and 2-32 respectively with the required shift in power level scale to obtain efficiencies as a function of gross thermodynamic power.

It should be noted that scaling the power developed or consumed as a function of pressure in the turbine or compressor is equivalent to scaling the gross thermodynamic power of Figures 2 or 3 since these powers are obviously proportional. For example, if a turbine developed 500 kw of thermodynamic power and a compressor consumed 400 kw of thermodynamic power in the open cycle configuration, the gross thermodynamic power would be 100 kw. If the pressure level were increased by a factor of eight, the turbine thermodynamic power would be 4000 kw, the compressor thermodynamic power would be 3200 kw and the gross thermodynamic power would be 800 kw. Thus, scaling either is equivalent.

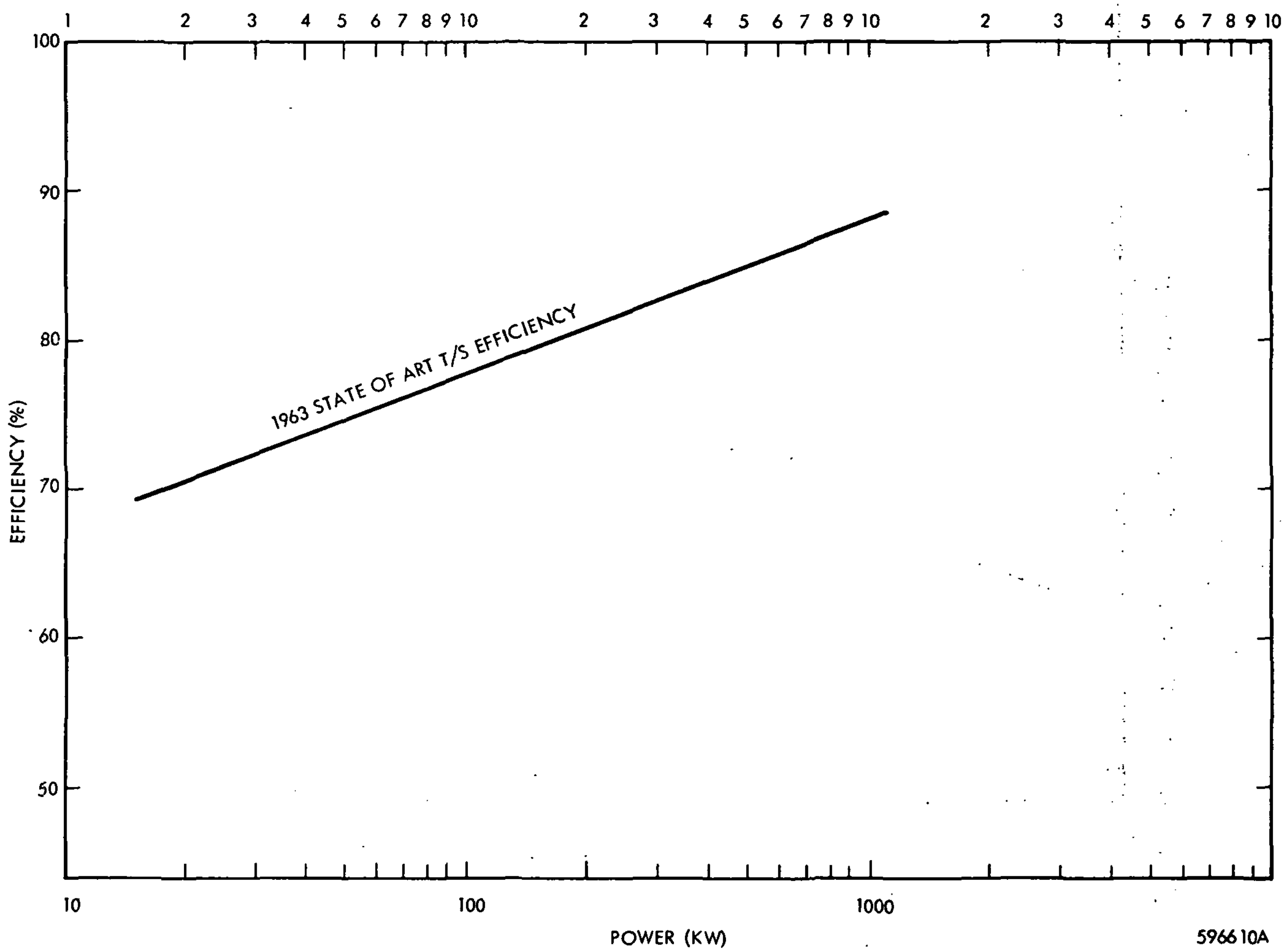

Figure 2-31. Open-Cycle Compressor Efficiency vs. Power

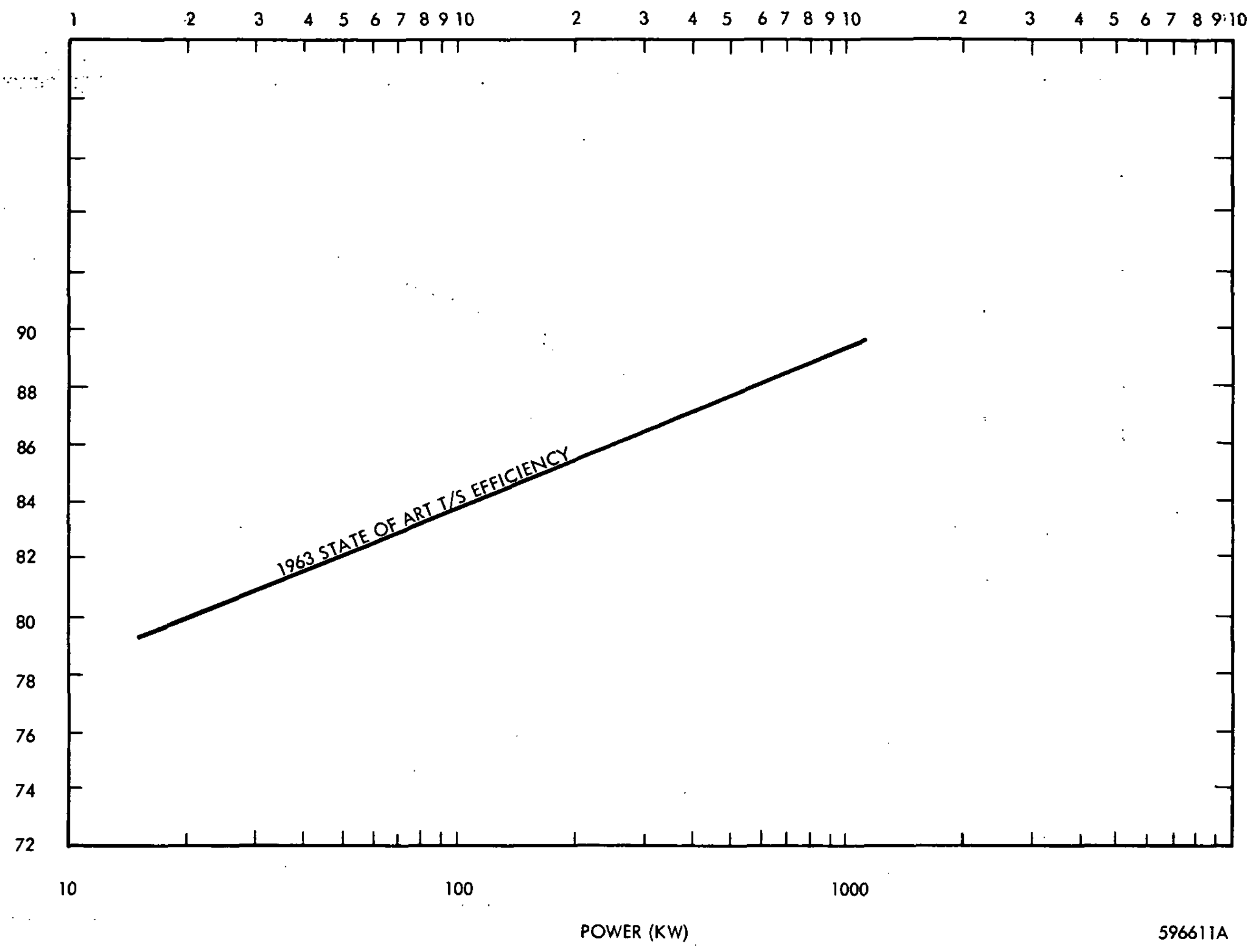

Figure 2-32. Open-Cycle Turbine Efficiency vs. Power

The following is an anology of the previous scaling technique: The closed cycle efficiency of a turbine or compressor is equal to the efficiency of an open cycle turbine or compressor which produces a gross thermodynamic power equal to the fraction $\frac{14.7}{P_1}$ of the closed cycle gross thermodynamic power.

The above technique provides a first order approximation which neglects Reynolds number effects. The Reynolds number effects have been handled separately for axial flow turbines, axial flow compressors and centrifugal compressors in Annexes C, D, and E respectively. The difficulty of evaluating Reynolds number effects is obvious from a review of the literature. The statements of AGN's turbomachinery consultant, AGN-VA 17, (p 2), are incorporated here as typical of statements which may be found in Clark design reports, "Principle of Turbomachinery" and elsewhere in the literature.

To evaluate the effect of Reynolds number on the performance of the turbomachines it is necessary to carry out tests at different pressure levels in the system. Information obtained from such tests will make it possible to evaluate the design performance of TC sets from low-pressure acceptance tests undertaken in an open cycle. Clark Bros., Report TS-149 shows that the problem of correlating performance data with Reynolds number is not fully understood and that available methods cannot be applied with a sufficiently high degree of accuracy.

Vavra's statements are of interest because they point out the need to determine the density effects and not really the Reynolds number effect as such. It is apparent from the terms which make up Reynolds number, that Reynolds number effects evaluate size effects D, velocity effects V, and viscosity effects μ, as well as density effects ρ. It is also obvious that size effects are more influential factors on turbomachinery efficiency because of the associated leakage and bypass flow losses as well as flow and energy transfer matching problems. Thus generalized Reynolds number correlations can only be utilized as gross approximations. These correlations include in the most part size effects and would predict a larger Reynolds number effect than is encountered in the expected density changes.

Only one useful reference has been found which mainly evaluates the density effects in turbomachinery. Davis, Kottas, and Moody, "The Influence of Reynolds Number on the Performance of Turbomachinery," ASME Transactions Vol 73 (1951). This reference has been used with other information available in the literature to evaluate the change in efficiency expected from open- to closed-cycle operation.

The maximum predicted efficiency increased utilizing this data are:

Axial Flow Turbine (Ref. Annex C)	1%
Axial Flow Compressor (Ref. Annex D)	5%
Centrifugal Compressor (Ref. Annex E)	1%

Table 2-30 summarizes the predictions of this analysis and the available test results.

While this confirmation of test results gives some confidence in the validity of the analysis it is not conclusive and further confirmation would be desirable. Three other checks are possible and are discussed in the following paragraphs.

This analysis is based upon the premise that size or volumetric flow rate is the single most important parameter for turbine and compressor efficiencies in this power range. Based upon this premise one can conclude from the slope of either Figure 2-28 or 2-29 that, since a turbine has in the order of twice the volumetric flow of the compressor due to increased temperature

TABLE 2-30 - MAXIMUM PREDICTED EFFICIENCY INCREASE

Component	Predicted Open Cycle Efficiency	Predicted Reynolds Number Effect	Predicted Closed Cycle Efficiency	Tested Open Cycle Efficiency	Tested Reynolds Number Effect	Tested Closed Cycle Efficiency
Axial Flow Turbine	82.5%	+ ~1%	83.5%	82.0%	--	--
Axial Flow Compressor	75.5%	+ ~5%	80.5%	75.0%	+ 4.6%	79.6%
Centrifugal Compressor	75.5%	+ ~1%	--	--	--	--

level in the turbine, the turbine efficiency should always be better than the compressor efficiency at a given power level. It can also be noted that the axial compressor curve slope is steeper than the turbine slope. This is attributed to the more influential Reynolds number effect in the compressor.

One can also compare the volumetric flow rate of another recently developed closed cycle turbine and compressor and predict the efficiencies which were obtained. The turbomachinery in question is the Helium turbomachinery developed by La Fleur Enterprises. The following pertinent data is compared to the Nitrogen ML-1 turbomachinery:

	La Fleur (He)		ML-1 (N_2)	
Parameter	Turbine	Compressor	Turbine	Compressor
lb/sec	10	16	26.4	26.4
RPM	19,500		22,000	
T inlet (^oF)	1200	70	1200	134
T outlet (^oF)	1039	176	908	368
P inlet (psia)	258	181	291	118
P outlet (psia)	190	268	122	323

As can be seen these compressors and turbines are fairly similar except for volumetric flow rates. Compressor and turbine volumetric flow rates are compared below at average temperatures and pressures.

compressor: $\frac{\text{Vol Flow}_{He}}{\text{Vol Flow}_{N_2}} = \frac{W_{He}/\rho_{He}}{W_{N_2}/\rho_{N_2}} = 3.45$

turbine: $\frac{\text{Vol Flow}_{He}}{\text{Vol Flow}_{N_2}} = 2.55$

From the curves of Figure 2-27 or 2-28, a factor of 3.45 in volumetric flow rate is worth five compressor efficiency points and a factor of 2.55 is worth two turbine efficiency points. The La Fleur compressor and turbine efficiencies are 83 and 85 percent respectively. This would predict ML-1 compressor and turbine efficiencies of 78 and 83 percent respectively. It is known than a very conservative design appraoch was taken on the La Fleur turbo machinery and this probably accounts for the relatively low compressor efficiency.

An independent evaluation can be made with the use of the Ford Motor Company 705 development program. This engine consists of a low-pressure and high-pressure spool providing an over-all pressure ratio of 16:1. Thus, the low-pressure spool acts as an open cycle 4:1 pressure ratio unit, while the high-pressure spool has the characteristics of a 4:1 pressure ratio closed cycle unit. One can use the low-pressure and high-pressure spools to evaluate the size effects caused by increased pressure levels. For the compressor:

High pressure is 76.7%
Low pressure is 79.0%

Thus indicating a loss of 2.3 efficiency points for a factor of four in pressure level. The prediction of ML-1 compressor efficiency is then:

$$= 84.5\% - \frac{8}{4}(2.3\%) = 84.5\% - 4.6\% = 79.9\%$$

where: $\frac{P_1}{14.7}$ for the ML-1 = 8

For the turbine, insufficient data exists at this time to make accurate predictions, but an obvious decrease in efficiency with pressure level is observed in the Ford 705 data.

All of these analyses indicate not only a qualitative but also a quantitative effect of volumetric flow rate on turbine and compressor efficiency. The ease with which existing closed cycle test results may be predicted lends confidence to the accuracy and usefulness of the analysis in determining preliminary estimates of closed-cycle turbomachinery performance.

Tables 2-31 through 2-34 summarize current state-of-the-art in compressers and turbines.

Astronuclear

TABLE 2-31 - COMPRESSORS

No.	Power (KW)	Efficiency (%)	No. of Units	Status or Date of Initial Operation	Location	Builder	Pressure Ratio	Shaft Speed 1000 RPM	No. of Stages	Type
1	120	73.0	1	1950	A	A	3.0	36.0	1	Centf.
2	160	73.0	20	1947	A	A	3.0	36.0	1	Centf.
3	160	73.0	8	1951	A	A	3.0	36.0	1	Centf.
4	160	73.0	8	1951	A	A	3.0	36.0	3	Centf.
5	160	73.0	3	1952	A	A	3.0	36.0	1	Centf.
6	190	73.0	2	Under Test	A	A	4.2	36.0	1	Centf.
7	280	73.0	4	1946	A	A	3.0	36.0	1	Centf.
8	310	73.0	8	1951	A	A	3.0	36.0	1	Centf.
9	370	81.0	1	Test	B	B	4.0	6.0	25	Axial
10	1000	88.0	1	Shop Test 1947	C	C	4.0	4.5	3	Centf.
11	1000	86.0	1	1951	D	E	4.25	8.0	13	Axial
12	2000	86.0	1	1949	F	F	3.2	7.3	11	Axial
13	2000	82.0	1	--	G	G	4.9	5.0	16	Axial
14	2200	83.0	1	Under Const.	H	H	5.0	6.3	24	Axial
15	2400	90.0	1	Under Test	I	I	3.9	5.65	14	Axial
16	2500	82.0	1	Under Test	J	F	5.4	7.0	14	Axial
17	2500	83.0	2	1952	K	L	4.6	3.5	4	Centf.
18	2600	85.0	1	1944	M	N	4.1	5.18	20	Axial
19	2600	87/81	1	Shop Test 1949	O	O	2.63/2.05	4.5	17/11	Axial
20	2800	84.0	1	1949	P	N	5.2	5.7	20	Axial
21	4000	84.6	1	1939	Q	R	4.4	3.0	23	Axial
22	4000	89.0	1	1949	S	R	4.6	3.6	--	Axial

TABLE 2-31 - (continued)

Key to Compressor Survey

A - Boeing Airplane Co, USA

B - C A Parsons & Co, Ltd, England

C - Maschinenfabrik Oerlikon, Switz.

D - British Admirality, Pyestoch, England

E - W H Allen Sons & Co, Ltd, England

F - Metropolitan-Vickers Elec Co, England

G - Brush Electrical Engrg Co, Ltd, England

H - Elsinore Shipbldg & Engrg Co, Ltd, Den.

I - Swenska Turbinsfabrik Aktiebolaget, Ljungstrom, Sweden

J - Metropolitan Water Board, Ashford, England

K - East African Power & Lighting Co, Ltd, Nairobi, Kenya

L - British Thomson-Houston Co, Ltd, England

M - U.S. Naval Engrg Exp Station, Annapolis, Maryland

N - Allis-Chalmers Mfg Co, USA

O - Pametrada (Parsons and Marine Engrg Turbine Research and Development Association), England

P - Locomotive Propulsion Committee, Dunkirk, New York

Q - Municipal Elect. Supply, Neuchatil, Switz.

R - Brown, Boveri & Co, Ltd, Switz.

S - Corp. Peruano del Santo, Chembotie, Peru

T - Laboratories Turbines a Gas, St. Denis, France

TABLE 2-32 - COMPRESSORS 1963 SURVEY

No.	Power (KW)	Efficiency (%)	Reference, Designation, Builder	Pressure Ratio	Shaft Speed (RPM x 10^3)	No. of Stages	Type
1	26.6	71.0	Co. Rep. IGT Aero Industries	2.0	32.0	1	C
2	37.3	74.0	Local Rep. GTCP-30 Airesearch	2.56	52.8	1	C
3	43.4	73.0	Local Rep. GTP-30 Airesearch	2.53	52.8	1	C
4	48.5	73.5	Co. Rep. 2 CGT Aero Industries	2.6	39.0	1	C
5	60	78*	Local Rep. T-62 Solar	3.2	--	1	C
6	74.5	Design Target 76.0	Co. Rep. IGGT Aero Industries	3.0	42.0	1	C
7	119	78.5	Local Rep. GTP-70 Airesearch	3.23	40.8	2	C
8	142	75.0	Local Rep GTCP-100 Airesearch	6.30	35.0	2	C
9	170	80.0*	Gas Turb. Prog. Mt'g (P.18), Automotive, Chrysler	4.1	--	--	C
10	224	80*	Local Rep. T-350 Solar	4-4.5	35.1	1	C
11	230	78.0*	Co. Confidential	5.7	33.15	6 1	A C
12	258	78.0	Local Rep GTCP-85 Airesearch	4.02	40.8	2	C
13	373	80.0	Local Rep TSE-331 Airesearch	6.40	40.95	2	C

TABLE 2-32 - (continued)

No.	Power (KW)	Efficiency (%)	Reference, Designation, Builder	Pressure Ratio	Shaft Speed (RPM x 10^3)	No. of Stages	Type
14	400	83.0* Velocity Head = 6.5%	Co. Confidential	6.1	30-40	3 1	A C
15	H.P. 450	Test Data 76.7	705 Quarterly Prog. Rpt, (P. 52), Ford	4.0	75	2	C
15	L.P. 450	Test Data 79.0	705 Quarterly Prog. Rpt. (P. 38), Ford	4.0	36.6	2	C
16	450	80.0*	"Gas Turbine", March 62 (P. 31), 705 Ford Motor Co.	16.0	75	2	C
17	450	87.0*	"Gas Turbine", March 62 (P. 31), Solar	3.8	21.5	6	A
18	450	86.0*	"Gas Turbine" March 62, (P. 31), Orenda	4.0	26.8	6	A
19	820	86.0*	Gas Turb. Prog. Mt'g (P. 191), Saturn T-1000 Solar	6.5	22.3	8	A
20	5600	85.0	"Gas Turb." May 61, Yarrow Admiralty Research Dept., Ass'c Elec. Ind.	6.3	--	13	A

* Total to Total Efficiencies   A Axial   C Centrifugal

CONFIDENTIAL
RESTRICTED DATA
Atomic Energy Act 1954

TABLE 2-33 - TURBINES 1952 SURVEY

No.	Power (KW)	Efficiency (%)	No. of Units	Status or Date of Initial Operation	Location	Builder	Turbine Inlet Temp.	Pressure Ratio	Shaft Speed (1000 RPM)	No. of Stages	Type
1	120	80.5	1	1950	A	A	1600	3.0	36.0/7.5	1/1	Axial
2	160	80.5	20	1947	A	A	1550	3.0	36.0/2.9	1/1	Axial
3	160	80.5	8	1951	A	A	1550	3.0	36.0/2.7	1/1	Axial
4	160	80.5	8	1951	A	A	1550	3.0	36.0/25.5	1/1	Axial
5	160	80.5	3	1952	A	A	1550	3.0	36.0/2.3	1/1	Axial
6	190	81.5	2	Under Test	A	A	1550	4.2	36.0/2.3	1/1	Axial
7	280	85.0*	4	1946	A	A	1550	3.0	36.0	1	Axial
8	310	80.5	8	1951	A	A	1550	3.0	36.0/2.7	1/1	Axial
9	1000	84.0	1	Shop Test 1947	C	C	1022	4.0	4.5/3.0	5/5	Axial
10	1000	85.0	1	1951	D	E	1200	4.25	8.0/6.75	2/1	Axial
11	1200	86.0	1	1949	T	U	1300	--	--	2	Axial
12	1600	85.0	1	1949	V	V	967	4.35	9.0	3	Axial
13	2000	86.0	1	1949	F	F	1240	3.2	7.3/5.0	1/4	Axial
14	2000	85.0	1	--	G	G	1160	4.9	5.0/3.0	2	Axial
15	2200	86.0	1	Under Construction	H	H	1200	5.0	6.3/5.4	8	Axial
16	2500	86.5	2	1952	K	L	1200	4.6	3.5	9	Axial
17	2600	86.0	1	1949	O	O	1250	5.4	4.5/3.1	13/8	Axial
18	2800	87.5	1	1949	P	N	1300	5.2	5.7	6	Axial
19	4000	88.0	1	1939	Q	R	1020	4.0	3.0	--	Axial
20	4000	88.0	1	1949	S	R	1100	4.6	3.6	--	Axial

* Total to Total

TABLE 2-33 - (continued)

Key to Turbine Survey

A - Boeing Airplane Co, USA

B - C A Parsons & Co, Ltd, England

C - Maschinenfabrik Oerlikon, Switz.

D - British Admirality, Pyestoch, England

E - W H Allen Sons & Co, Ltd, England

F - Metropolitan-Vickers Elec Co, England

G - Brush Electrical Engrg Co, Ltd, England

H - Elsinore Shipbldg & Engrg Co, Ltd Den.

I - Swenska Turbinsfabrik Aktiebolaget,
Ljungstrom, Sweden

J - Metropolitan Water Board, Ashford, England

K - East African Power & Lighting Co, Ltd,
Nairobi, Kenya

L - British Thomson-Houston Co, Ltd, England

M - U.S. Naval Engrg Exp Station, Annapolis, Maryland

N - Allis-Chambers Mfg Co, USA

O - Pametrada (Parsons and Marine Engrg Turbine
Research and Development Association), England

P - Locomotive Propulsion Committee, Dunkirk, New York

Q - Municipal Elect. Supply, Neuchatil, Switz.

R - Brown, Boveri & Co, Ltd, England

S - Corp. Peruano del Santo, Chembotie, Peru

T - Laboratories Turbines a Gas, St. Denis, France

TABLE 2-33a - TURBINES 1963 SURVEY

No.	Power (KW)	Efficiency (%)	Reference, Designation, Builder	Turbine Inlet Temp. (^{o}F)	Pressure Ratio	Shaft Speed (RPM x 10^3)	No. of Stages	Type
1	26.6	80.0	Co. Rep. 1GT Aero Industries	1200	2.0	32.0	1	R
2	37.3	78.0	Local Rep. GTCP-30 Airesearch	1650	2.49	52.8	1	R
3	43.4	77.0	Local Rep. GTP-30 Airesearch	1650	2.47	52.8	1	R
4	48.5	82.0	Co. Rep. 2GGT Aero Industries	1340	2.6	39.0	1	R
5	60	86*	Local Rep. T-62, Solar	1450	3.2	--	1	R
6	74.5	Design Target 83.0	Co. Rep. 1GGT Aero Industries	1620	3.0	42.0	1	R
7	119	80.0	Local Rep. GTP-70 Airesearch	1650	3.10	40.8	1	R
8	142	82.0	Local Rep. GTCP-100 Airesearch	1100	6.10	35.0	1	R A
9	190	87/84*	Gas Turb. Prog. Mt'g, (P. 18) Automotive Chrysler	1600	4.1	--	2	A
10	224	88*	Local Rep. T-350, Solar	1450	4-4.5	35.1	1	R
11	H.P. 230	88*	Co. Confidential	1725	3.4	50.953	2	A
11	L.P. --	85*	Co. Confidential	--	2.4	33.150	2	A

TABLE 2-33a - (continued)

No.	Power (KW)	Efficiency (%)	Reference, Designation, Builder	Turbine Inlet Temp. (°F)	Pressure Ratio	Shaft Speed (RPM x 10^3)	No. of Stages	Type
12	258	77.0	Local Rep. GTCP-85 Airesearch	1600	3.90	40.8	1	R
13	373	87.5	Local Rep. TSE-331 Airesearch Co.	1735	6.18	40.95	3	A
14	400	89.0* Velocity Head = 10%	Confidential	1750-1800	6.0	30-40 / 22 or 6	-	-
15	H.P. 450	Test Data 84.5 (expected: 1-1-1/2 more) T/T at Diffuser exit	705 Quarterly Prog. Rpt., 31 Oct. 62, Fig.6.3, Ford Motor Co.	--	2.6	75.7	1	R
15	L.P. 450	88.0*	"Gas Turb." Mar. 62(P.31), 705 - Ford Motor Co.	--	6.15	--	1	A
	H.P.							R
	-	87-88*		1750	2.6	75	1	A
16	450	89.0*	"Gas Turb," Mar. 62 (P.31) Solar	1600	3.8	21.5	1	A
17	450	89.0*	"Gas Turb," Mar. 62(P. 31) Orenda	1735	4.0	26.8	1	A
18	820	Just Under 90.0*	Gas Turb. Prog. Mt'g(p.191) Saturn T-1000 Solar	1500	6.5	22.3	8	A
19	820	89.0*	Gas Turb. Sept. 60 Design Point	1500	6.6	22.3	8	A

* - Total to Total Efficiencies   A - Axial   R - Radial Inflow

CONFIDENTIAL
RESTRICTED DATA
Atomic Energy Act 1954

In "Principles of Turbomachinery" (p 335), Shepherd indicates that for axial flow turbines there is a critical Reynolds number of about 1×10^5 above which the loss coefficient is approximately constant, but below which it increases rather rapidly. The existence of a critical Reynolds number is evident from theoretical considerations. The actual value of Reynolds number has been confirmed by test results. The ML-1 turbines have a Reynolds number of approximately 1×10^5 in the open-cycle configuration.

$$\frac{\rho VD}{\mu} = \frac{1}{8} \quad \frac{13\,(1100)\,(^{\circ}5/12)}{27.8 \quad \times 10-6} = 1.0 \times 10^5$$

One would, therefore, expect no significant change in turbine efficiency between open- and closed-cycle operation.

This conclusion is further substantiated by the work of Davis, Kottas and Moody "The Influence of Reynolds Number on the Performance of Turbomachinery." ASME transactions Vol 73 (1951). An extract from this article is presented as Figure 2-33. Here, Kinematic Viscosity (υ), machine speed (U), or machine diameter (D) is varied to alter machine Reynolds number (U^{D}/D). Since most of this data is for a variation of ρ it is directly applicable to the question at hand. How does a variation of density effect the efficiency of a given turbine?

The machine Reynolds number of the ML-1 turbines is approximately 2×10^6 and 1.6×10^7 for open- and closed cycle operation respectively. It is apparent that even before the critical open-cycle Reynolds number of 1×10^5 is reached (equivalent to about 2×10^6 Machine Reynolds number in Figure 2-33), the effect of Reynolds number (density) has diminished to rather minor proportions, especially for the higher performance - higher efficiency turbines, shown on Figure 2-33. It is felt that the high-efficiency turbines are more representative of ML-1 turbomachinery than the lower performance units.

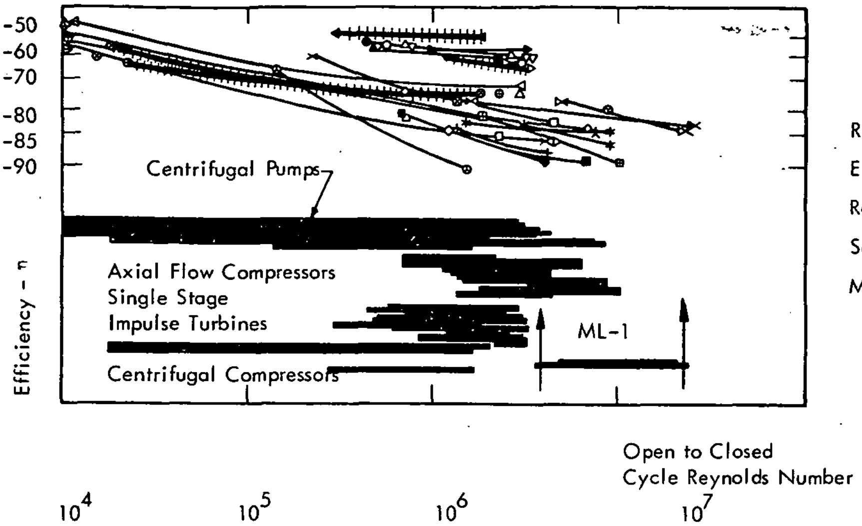

Relation Between Machine Efficiency and Machine Reynolds Number For Several Types of Turbo-Machinery

SYMBOL	MACHINE TYPE	VARIABLE	BIBLIOGRAPHY REFERENCE
○	SINGLE STAGE IMPULSE TURBINE	ν	3
○	SINGLE STAGE IMPULSE TURBINE	ν	3
△	SINGLE STAGE IMPULSE TURBINE	ν	3
△	SINGLE STAGE IMPULSE TURBINE	ν	4
◁	SINGLE STAGE IMPULSE TURBINE	ν	4
◁	SINGLE STAGE IMPULSE TURBINE	ν	4
▽	SINGLE STAGE IMPULSE TURBINE	ν	8
▽	SINGLE STAGE IMPULSE TURBINE	ν	8
▷	SINGLE STAGE IMPULSE TURBINE	ν	8
▷	SINGLE STAGE IMPULSE TURBINE	ν	8
□	AXIAL FLOW COMPRESSOR	ν	5
□	AXIAL FLOW COMPRESSOR	ν	6
◇	AXIAL FLOW COMPRESSOR	ν	6
◇	AXIAL FLOW COMPRESSOR	ν	7
+	AXIAL FLOW COMPRESSOR	ν	7
×	AXIAL FLOW COMPRESSOR	ν	7
⊕	SINGLE STAGE IMPULSE TURBINE	ν	PRIVATE COMMUNI- CATION
⊕	SINGLE STAGE IMPULSE TURBINE	ν	
⊞	AXIAL FLOW COMPRESSOR	ν	
⊠	AXIAL FLOW COMPRESSOR	ν	7
△	CENTRIFUGAL PUMP	ν	2
◁	CENTRIFUGAL PUMP	ν	2
▽	CENTRIFUGAL PUMP	ν	2
▷	CENTRIFUGAL PUMP	ν	2
Y	CENTRIFUGAL PUMP	ν	9
⅄	CENTRIFUGAL PUMP	ν	10
⊗	CENTRIFUGAL PUMP	ν	10
⊗	CENTRIFUGAL PUMP	ν	11
✳	AXIAL FLOW COMPRESSOR	ν	7
✳	AXIAL FLOW COMPRESSOR	ν	7
⋉	CENTRIFUGAL COMPRESSOR	ν	ELLIOTT CO. TEST DATA
⧗	CENTRIFUGAL COMPRESSOR	ν	
⋊	CENTRIFUGAL COMPRESSOR	ν	

Figure 2-33. Relation Between Machine Efficiency and Machine Reynolds Number for Several Types of Turbo-Machinery

While the single-stage impulse turbine data presented is not entirely representative of ML-1, 2 stage turbines, Shepherd in "Principl es of Turbomachinery" (p 335), indicates that single-stage (cascade) test results show a stronger influential effect of Reynolds number on efficiency than do multistage turbine tests. Therefore, it can be stated that the influence of Reynolds number on ML-1 turbine efficiency will be less than or equal to the data presented here.

Utilizing the maximum turbine exponent from Figure 3C in equation (6), a maximum expected efficiency increase can be predicted from this data of Davis, Kottas, and Moody. Assuming that this exponent is applicable up to the critical Reynolds number for single-stage (cascade) data 2×10^5, equivalent to a machine Reynolds number of 4×10^6 in Figure 2-33 and assuming no further gains in efficiency with further increases in Reynolds number, a maximum possible increase of 1.5-2 efficiency points may be predicted. The actual increase for multistage turbines must be considerably less than this since single-stage (cascade) data has been assumed applicable.

The conclusion is that no significant change in turbine efficiency can be expected due to Reynolds number effects in changing from open- to closed-cycle operation. The best estimate in view of the data presented is less than one efficiency point.

The following comments by Shepherd on page 408 of "Principles of Turbomachinery", are indicative of the difficulty of correlating Reynolds number effects in axial flow compressors:

> The existence of a critical value of Reynolds number has been discussed in Chap.5, this value being of the order of 2×10^5 based on blade chord. It is difficult to formulate any very definite rules for compressors, since the turbulance level exerts an effect and variousworkers report rather different values of critical Reynolds number and of the rate of increase of loss for still lower values. However, whatever the turbulence level, a Reynolds number below 1×10^5 is almost certain to lead to a higher C_D, and the value should preferably be above 3×10^5. Once above the critical value, the improvement with larger values is small. The effect of increased turbulence is toprevent separation of a laminar boundry before a turbulent boundary layer is re-established by causing a much earlier transition to the turbulent condition."

The Reynolds number of the ML-1 axial flow compressor is about 1×10^5 in open-cycle operation. Thus, no conclusions can be drawn from Shepherd's generalized comments.

Once again the work of Davis, Jottas and Moody (Ref Annex C) is usefulin determining the effects to be expected when the density of the working fluid is varied in the compressor. Figure 2-34 shows the effect of an increase in density on efficiency in the range of the Machine Reynolds number in question (2.3×10^6 to 1.8×10^7 open cycle to closed cycle respectively). One can deduce from this data (on the basis of direct applicability of a factor of eight increase in Reynolds number) that the improvement in efficiency from open- to closed-cycle operation could be approximately two to eight efficiency points. We believe the prediction of an increase approximately eight efficiency points at higher Reynolds number (from the slope of the curve at lower Reynolds number) to be unrealistic

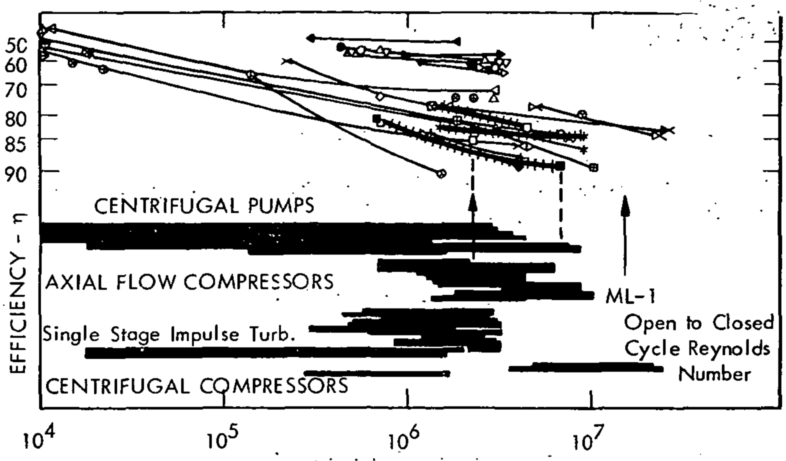

RELATION BETWEEN MACHINE EFFICIENCY AND MACHINE REYNOLDS NUMBER FOR SEVERAL TYPES OF TURBO-MACHINERY

SYMBOL	MACHINE TYPE	VARIABLE	BIBLIOGRAPHY REFERENCE
O	SINGLE STAGE IMPULSE TURBINE	ν	3
O	SINGLE STAGE IMPULSE TURBINE	ν	3
Δ	SINGLE STAGE IMPULSE TURBINE	ν	3
Δ	SINGLE STAGE IMPULSE TURBINE	ν	4
◁	SINGLE STAGE IMPULSE TURBINE	ν	4
◁	SINGLE STAGE IMPULSE TURBINE	ν	4
▽	SINGLE STAGE IMPULSE TURBINE	ν	8
▽	SINGLE STAGE IMPULSE TURBINE	ν	8
▷	SINGLE STAGE IMPULSE TURBINE	ν	8
▷	SINGLE STAGE IMPULSE TURBINE	ν	8
□	AXIAL FLOW COMPRESSOR	ν	5
□	AXIAL FLOW COMPRESSOR	ν	6
◇	AXIAL FLOW COMPRESSOR	ν	6
◇	AXIAL FLOW COMPRESSOR	ν	7
+	AXIAL FLOW COMPRESSOR	ν	7
×	AXIAL FLOW COMPRESSOR	ν	7
⊕	SINGLE STAGE IMPULSE TURBINE	ν	PRIVATE
⊗	SINGLE STAGE IMPULSE TURBINE	ν	COMMUNI-
⊞	AXIAL FLOW COMPRESSOR	ν	CATION
⊠	AXIAL FLOW COMPRESSOR	ν	7
⟁	CENTRIFUGAL PUMP	ν	2
◁	CENTRIFUGAL PUMP	ν	2
▽	CENTRIFUGAL PUMP	ν	2
▷	CENTRIFUGAL PUMP	ν	2
Y	CENTRIFUGAL PUMP	ν	9
λ	CENTRIFUGAL PUMP	ν	10
⊗	CENTRIFUGAL PUMP	ν	10
⊗	CENTRIFUGAL PUMP	ν	11
*	AXIAL FLOW COMPRESSOR	ν	7
*	AXIAL FLOW COMPRESSOR	ν	7
⋉	CENTRIFUGAL COMPRESSOR	ν	ELLIOTT CO.
⧗	CENTRIFUGAL COMPRESSOR	ν	TEST DATA
⋊	CENTRIFUGAL COMPRESSOR	ν	

Figure 2-34. Relation Between Machine Efficiency and Machine Reynolds Number for Several Types of Turbo-Machinery

for the axial-flow compressor in question since it indicates a constant continuing increase in efficiency even after the maximum value discussed by Shepherd is reached and passed.

We believe the most realistic approach to predicting a maximum expected efficiency increase to be as follows:

Utilizing the steepest slope in Figure 2-34, find the increase in efficiency expected from an increase in Reynolds number from 1×10^5 to 3×10^5 (equivalent to Machine Reynolds number of 2.3×10^6 to 6.9×10^8 in Figure 1D). According to the previous discussion by Shepherd, this is about the maximum range for which an effect should be expected. This steepest curve can be found to give approximately five efficiency points. Since the efficiency cannot be expected to be improved substantially for further increases in Machine Reynolds number above 3×10^5, a five efficiency points is a good approximation of the maximum expected increase in efficiency in changing from open- to closed-cycleoperation.

Shepherd, discusses the effect of Reynolds number on the efficiency of radial compressors on page 262 of "Principles of Turbomachinery." The Reynolds number of the ML-1 centrifugal compressor is 4.5×10^6 and 3.6×10^7 in the open and closed cycles respectively. Figure 6.31 on page 262 would predict an efficiency increase of three percentage points. As discussed in the body this of analysis, this is a maximum increase since it is primarily a measure of size (as opposed to density) effects and size effects are much more influential than density effects on the efficiency of turbomachinery.

Figure 2-35, showing the work of Davis, Kottas, and Moody, would appear to be of small benefit since for centrifugal compressors only tip speed (U) and machine diameter (D) are varied and we would like to find the effect of density. However, one thing is immediately obvious, size effects (D) are more influential than tip speed (U) on centrifugal compressors in the range of the Reynolds number under consideration. It is known from leakage loss

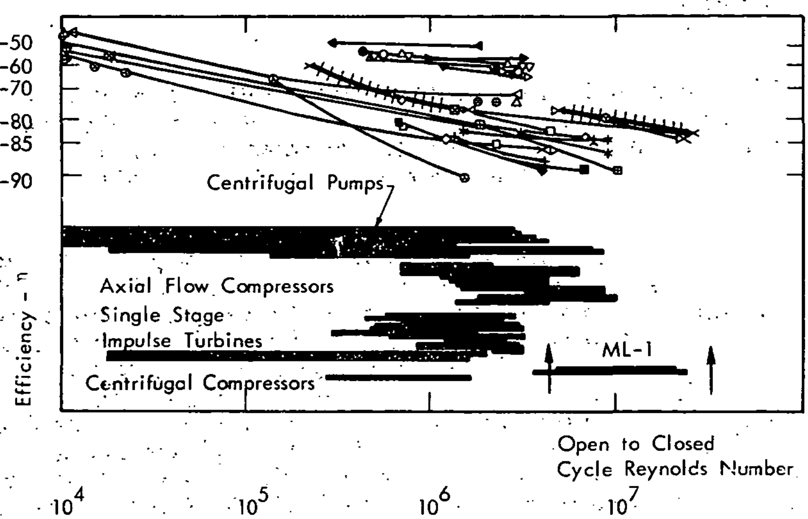

Relation Between Machine Efficiency and Machine Reynolds Number For Several Types of Turbo-Machinery

SYMBOL	MACHINE TYPE	VARIABLE	BIBLIOGRAPHY REFERENCE
○	SINGLE STAGE IMPULSE TURBINE	ν	3
○	SINGLE STAGE IMPULSE TURBINE	ν	3
△	SINGLE STAGE IMPULSE TURBINE	ν	3
△	SINGLE STAGE IMPULSE TURBINE	ν	4
◁	SINGLE STAGE IMPULSE TURBINE	ν	4
◁	SINGLE STAGE IMPULSE TURBINE	ν	4
▽	SINGLE STAGE IMPULSE TURBINE	ν	8
▽	SINGLE STAGE IMPULSE TURBINE	ν	8
▷	SINGLE STAGE IMPULSE TURBINE	ν	8
▷	SINGLE STAGE IMPULSE TURBINE	ν	8
□	AXIAL FLOW COMPRESSOR	ν	5
□	AXIAL FLOW COMPRESSOR	ν	6
◇	AXIAL FLOW COMPRESSOR	ν	6
◇	AXIAL FLOW COMPRESSOR	ν	7
+	AXIAL FLOW COMPRESSOR	ν	7
×	AXIAL FLOW COMPRESSOR	ν	7
⊕	SINGLE STAGE IMPULSE TURBINE	ν	PRIVATE COMMUNI-CATION
⊗	SINGLE STAGE IMPULSE TURBINE	ν	PRIVATE COMMUNI-CATION
⊞	AXIAL FLOW COMPRESSOR	ν	PRIVATE COMMUNI-CATION
⊠	AXIAL FLOW COMPRESSOR	ν	7
△	CENTRIFUGAL PUMP	ν	2
◁	CENTRIFUGAL PUMP	ν	2
▽	CENTRIFUGAL PUMP	ν	2
▷	CENTRIFUGAL PUMP	ν	2
Y	CENTRIFUGAL PUMP	ν	9
⅄	CENTRIFUGAL PUMP	ν	10
⊗	CENTRIFUGAL PUMP	ν	10
⊗	CENTRIFUGAL PUMP	ν	11
✳	AXIAL FLOW COMPRESSOR	ν	7
✳	AXIAL FLOW COMPRESSOR	ν	7
⋉	CENTRIFUGAL COMPRESSOR	ν	ELLIOTT CO. TEST DATA
⧗	CENTRIFUGAL COMPRESSOR	ν	ELLIOTT CO. TEST DATA
⋈	CENTRIFUGAL COMPRESSOR	ν	ELLIOTT CO. TEST DATA

Figure 2-35. Relation Between Machine Efficiency and Machine Reynolds Number for Several Types of Turbo-Machinery

and flow matching considerations that size effects are more influential than density effects, but how much cannot be determined from the centrifugal compressor data.

The centrifugal pump data provides a means to determine the magnitude of the difference between size and density effects. Centrifugal pumps are really only centrifugal compressors which pressurize less compressible fluids. Figure 2-36 shows the differences between the variation of efficiency with size and kinematic viscosity (density) and curve B-BB shows the effect of size. The relative slope of the two curves indicate that the size effect is about four times more influential than the kinematic viscosity (density) effect. Thus, from either Figure 6.31 in "Principles of Turbomachinery" or Figure 2-35, the effect of the increased density in going from open- to closed-cycle operation with ML-1 centrifugal compressor can be expected to be less than one efficiency point.

REFERENCES

1. Warner L. Stewart, Arthur J. Glassman, and Richard P. Krebs, "The Brayton Cycle for Space Power," 741A Society of Automotive Engineers, Sept. 23-27, 1963.
2. Arthur J. Glassman and Warner L. Stewart, "A Look at the Thermodynamic Characteristics of Brayton Cycles for Space Power," 63-218, AIAA Summer Meeting, June 17-20, 1963.
3. A. J. Glassman, R. P. Krebs, and T. A. Fox, "Brayton Cycle Nuclear Space Power System and Their Heat-Transfer Components," No. 57, American Institute of Chemical Engineers, August 11-14, 1963.
4. L. W. Norman, "The Application of the Recuperated Brayton Cycle to Space Power Conversion Systems," No. 63-220, AIAA Summer Meeting, June 17-20, 1963.
5. W. G. Harrach, R. T. Caldwell, "System Optimization of Brayton-Cycle Space Power Plants," No. 63-WA-87, The American Society of Mechanical Engineers, July 29, 1963.

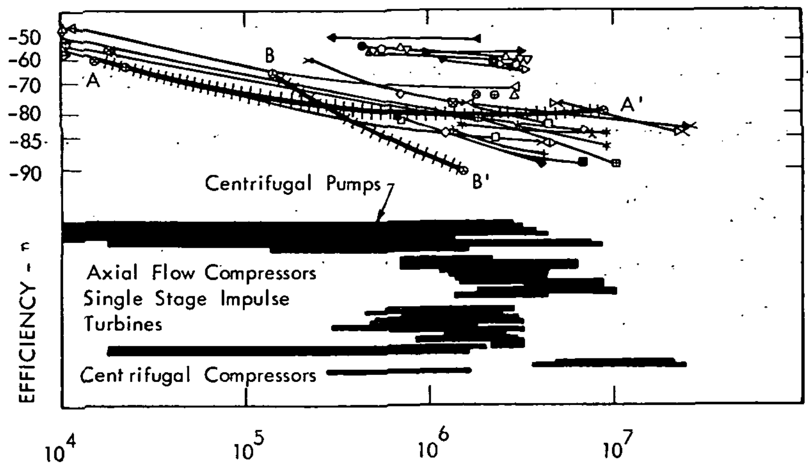

Relation Between Machine Efficiency and Machine Reynolds Number of Turbo-Machinery

SYMBOL	MACHINE TYPE	VARIABLE	BIBLIOGRAPHY REFERENCE
○	SINGLE STAGE IMPULSE TURBINE	ν	3
○	SINGLE STAGE IMPULSE TURBINE	ν	3
△	SINGLE STAGE IMPULSE TURBINE	ν	3
△	SINGLE STAGE IMPULSE TURBINE	ν	4
◁	SINGLE STAGE IMPULSE TURBINE	ν	4
◁	SINGLE STAGE IMPULSE TURBINE	ν	4
▽	SINGLE STAGE IMPULSE TURBINE	ν	8
▽	SINGLE STAGE IMPULSE TURBINE	ν	8
▷	SINGLE STAGE IMPULSE TURBINE	ν	8
▷	SINGLE STAGE IMPULSE TURBINE	ν	8
□	AXIAL FLOW COMPRESSOR	ν	5
□	AXIAL FLOW COMPRESSOR	ν	6
◇	AXIAL FLOW COMPRESSOR	ν	6
◇	AXIAL FLOW COMPRESSOR	ν	7
+	AXIAL FLOW COMPRESSOR	ν	7
×	AXIAL FLOW COMPRESSOR	ν	7
⊕	SINGLE STAGE IMPULSE TURBINE	ν	PRIVATE COMMUNICATION
⊗	SINGLE STAGE IMPULSE TURBINE	ν	PRIVATE COMMUNICATION
⊞	AXIAL FLOW COMPRESSOR	ν	PRIVATE COMMUNICATION
⊠	AXIAL FLOW COMPRESSOR	ν	7
△	CENTRIFUGAL PUMP	ν	2
◁	CENTRIFUGAL PUMP	ν	2
▽	CENTRIFUGAL PUMP	ν	2
▷	CENTRIFUGAL PUMP	ν	2
Y	CENTRIFUGAL PUMP	ν	9
⅄	CENTRIFUGAL PUMP	ν	10
⊛	CENTRIFUGAL PUMP	ν	10
⊛	CENTRIFUGAL PUMP	ν	11
✳	AXIAL FLOW COMPRESSOR	ν	7
✳	AXIAL FLOW COMPRESSOR	ν	7
⋉	CENTRIFUGAL COMPRESSOR	ν	ELLIOTT CO. TEST DATA
⧗	CENTRIFUGAL COMPRESSOR	ν	ELLIOTT CO. TEST DATA
⋊	CENTRIFUGAL COMPRESSOR	ν	ELLIOTT CO. TEST DATA

Figure 2-36. Relation Between Machine Efficiency and Machine Reynolds Number for Several Types of Turbo-Machinery

6. Yasutoshi Senoo, "Gas Medium Selection and Turbomachinery Matching for Closed-Brayton-Cycle Space Power System," No. 63-WA-86, The American Society of Mechanical Engineers, July 29, 1963.

7. John Warner, John Misoda, "Correlation of Reynolds-Number Effect for a Family of Small Centrifugal Compressors.

G. RANKINE CYCLE POWER SYSTEMS

INTRODUCTION

Such a vast amount of work has been and is being done in the design and development of Rankine cycle power conversion systems that even a cursory review of the development of the technology and the state-of-the-art would fill countless volumes. It is perhaps sufficient to say that the Rankine cycle power conversion system utilizing a nuclear reactor as a heat source must be considered at the present time the primary competitor for providing a space power supply of reasonable specific weight, where sizeable quantities of power must be generated continuously over a long period of time. This does not imply that at some future date other power conversion schemes such as thermionic systems or MHD systems may not be better suited to these requirements. However, within the state-of-the-art today, the Rankine cycle is by far the furthest developed and offers the greatest near-term potential for achieving power plant specific weights that make large scale power production possible in a space environment.

Conversely, there are also many problems still to be solved in the development of nuclear powered-Rankine cycle space power systems. However, these problems are, for the most part, well defined, and programs are underway in most cases to solve them. This is perhaps the greatest single argument for the Rankine cycle system for near-term application.

Within the general area of Rankine cycle plants, it is obvious that liquid metal systems have basic characteristics well suited to space requirements. Because the only method of heat rejection for space or lunar power systems is by radiation, it is obviously desirable to have heat rejection temperatures as high as possible—thus minimizing radiator size and weight. Liquid metal Rankine cycle systems are very attractive in this respect and, thus, such systems offer the potential of a much more compact, lightweight, over-all plant as compared to a water Rankine cycle system or a Brayton cycle plant. However, just as Brayton systems cannot be automatically dismissed in considering a specific application, neither can water systems be summarily dismissed without examination—particularly in view of their advanced state of development in the lower temperature ranges (below 600°F). Initially, therefore, both water and liquid metal systems were considered as potential competitors.

In the following pages, design characteristics are summarized for various Rankine cycle plants (and where applicable, their associated reactors) whose technologies are pertinent to the lunar base application. Mercury, potassium and water systems are discussed in that order. Brief summaries of related technological development work now in progress are also included where this is of significance. No attempt is made at detailed evaluation of development problems associated with each design, since the technologies are discussed and evaluated in detail in Volume II - Part 2.

STATE-OF-THE-ART

The Mercury Rankine Cycle - mercury vapor turbine systems offer the best possible argument for the use of liquid metals in the special conditions posed by space and lunar base environments. There are several decades of Central Station operating experience with mercury turbines developed by General Electric, the SNAP 2 and Sunflower mercury system turbine alternators have been operated and the SNAP 8 power conversion system has been designed, although not yet operated. It has been shown by these programs, however, that the change from water to a liquid metal can be successfully accomplished and is not an impractical or insoluble problem. The further change which is now being undertaken, from one liquid metal to another (mercury to potassium), is an extension of the state of the art instead of the immensely burdensome creation of a new art.

The expansion problems involved in operating turbines with "wet" vapors are the usual ones—supersaturation, loss of efficiency due to liquid drag, and blade erosion if the threshold values of blade tip speed and moisture content are exceeded. These problems are not predominant in the small SNAP turbines developed so far. SNAP 2 and Sunflower experience has shown that the mechanical problems of the machine and the seal leakage losses are the major causes of difficulty and reduced efficiency. Table 2-34 compares the major characteristics of SNAP 2, SNAP 8, and Sunflower.

Increased efficiency in any proposed machine, as compared to the SNAP 2, 8 and Sunflower machines, should be secured by design improvement aimed at lowering the leakage losses, and obtaining better basic efficiency through the use of two reaction stages for the last two stages of the turbine.

Turbine design is perhaps the most critical design area in liquid metal Rankine system, but is by no means the only problem. The individual reviews that follow discuss each power generation system within the context of its own design requirements, and show the degree of development and problem areas remaining for each system.

SNAP 8

Objectives of the Program

The broad program objective is the development of a nuclear powered auxiliary power unit emphasizing a zirconium hydride moderated reactor as a heat source and a mercury vapor Rankine cycle power conversion unit.

Current development effort is focused fundamentally on a system from which basic operational test data can be obtained, through operation in terrestrial test facilities which simulate the

TABLE 2-34 - PLANT CHARACTERISTICS

	SNAP 2	Sunflower	SNAP 8
Inlet Conditions			
Temp. (°F)	1198	1250	1250
Pressure (psia)	115	240	265
Exhaust Cond.			
Temp. (°F)	625	605	680
Pressure (psia)	8.7	7.0	16.5
Shaft Power Produced kw	~5	~4	5.7
Expected Aero Efficiency (%)	53	51	63.5
Speed (rpm)	36000	40000	12000
Max. Tip Speed (ft/sec)	~400		302
Number of Stages	2	3	4

space environment. The net electrical output of the reference plant will be 35 kwe, and the system will be designed for 10,000 hours of continuous operation. Beyond this initial objective, various items of "hardware" within the over-all plant have their own individual development objectives looking toward a higher performance system. For example, core design is aimed at achieving a thermal output of 600 kwt corresponding to an ultimate plant output of perhaps 60 kwe for the space APD application.

Concept Description

The SNAP 8 power plant is comprised essentially of four closed loops, as follows:

1. The primary or reactor coolant loop containing a uranium zirconium hydride (U-Zr Hi) fueled thermal reactor utilizing NaK as a coolant and heat transfer fluid.
2. The Rankine cycle power conversion loop utilizing mercury (Hg) as a working fluid.
3. The heat rejection or radiator loop also utilizing NaK as a heat transfer fluid.
4. An auxiliary system containing ET-378 which provides bearing lubrication for rotating machinery and is also utilized for auxiliary cooling where a low temperature coolant is required.

A flow schematic showing the SNAP 8 system and its major components is shown in Figure 2-37. The over-all requirements of the reference plant design are summarized in Table 2-35, while Tables 2-36 and 2-37 respectively summarize basic system design parameters and the current weight estimates for the plant.

Reactor Design

The reactor core design for SNAP 8 is essentially an upgraded SNAP 2, the specific power having been increased from 0.18 Mw/ft^3 for the SNAP 2 to 0.94 Mw/ft^3 for the SNAP 8, which corresponds to an increase in thermal output from 50 kwt to 600 kwt. The reactor exit temperature has been increased 100°F to 1300°F. The basic design characteristics for the reactor system— core, shielding, control, vessel—are listed in Table 2-38.

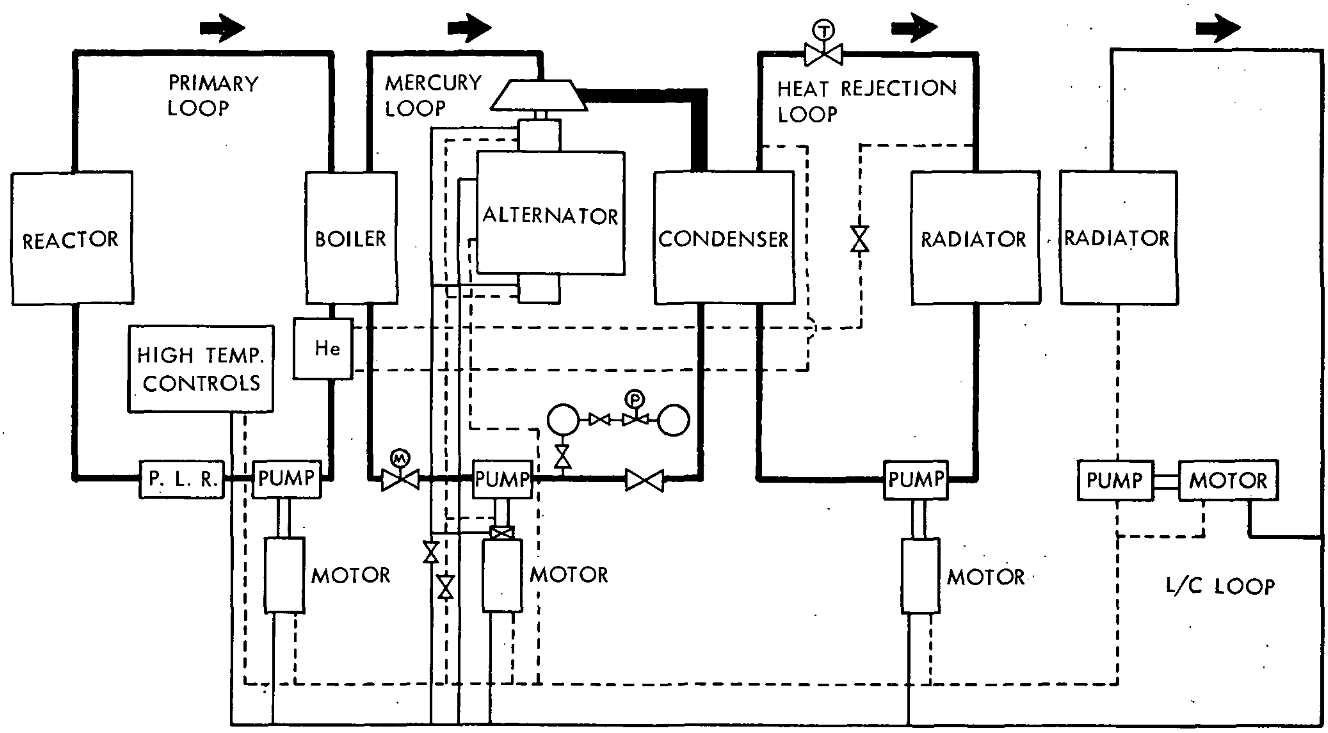

Figure 2-37 - SNAP 8 Flow Schematic

TABLE 2-35 - SNAP 8 OVERALL PLANT DESIGN REQUIREMENTS

Power	
Output Power	35 Kw (min) at .75 P.F. lag
Frequency	400 cps ±1%
Voltage	120 v, line-to-neutral 208 v, line-to line
Voltage Regulation	±5%
Harmonic Content	8% RMS line-to-line with full balanced linear load at P.F. 1.0
Operating Lifetime	10,000 hours
Envelope Size	Truncated cone 20"D x 96"D x 264" Long
Reliability Objective	80% Overall survival probability for 10,000 hours (including meteoroid prot.)
Operating Environment	Space vacumn 0g and 1g for 10,000 hours 3.5g for 5 minutes (in flight thrust) ±4.5g lateral for 5 minutes
Startup - Shutdown	Single start-up in space - restart capability for ground tests only. Shutdown in space.
Shielding	Shadow Shield - unmanned pay loads. Neutrons 10" nvt Gammas 10^6 rods.

TABLE 2-36 - SNAP 8 GENERAL SYSTEM DESIGN CONDITIONS WORKING FLUID

	Temperature (°F)	Flow lb/hr	Pressure (psia)
Primary Loop			
Reactor Outlet	1300		37
Boiler Inlet	1297		36
Boiler Outlet	1099		31
Reactor Inlet	1100		40
Secondary Loop			
Boiler Outlet	1263	9800	270
Turbine Inlet	1250	9800	265
Turbine Outlet	680	9800	16.5
Condenser Inlet	680	9800	16.4
Condenser Outlet	505	9800	11.5
Boiler Inlet	513	9800	340
Heat Rejection Loop			
Condenser Outlet	665	34,700	36
Radiator Inlet	665	34,700	33
Radiator Outlet	495	34,700	47
Condenser Inlet	496	34,700	42
Cooling and Lubricating Loop			
Radiator Inlet	245.8	5860	54
Radiator Outlet	210	5860	38

TABLE 2-37 - SNAP 8 SYSTEM WEIGHT ESTIMATES

	Lb
Nuclear System	
Reactor and Control (without shielding)	600
Radiator System Including Structure	
To be government furnished	
No current detailed design work being done in this area	3800
Power Conversion System	
Primary Loop (except reactor, control and shield)	250
Boiler	530
Secondary Loop (Mercury)	140
Condenser	70
Turbine - Alternator	295
Heat rejection loop (excluding radiator)	230
Start-up System	380
Electrical assembly	500
Structure	175
Total (Estimated weight unshielded)	7060

TABLE 2-38 - SNAP 8 REACTOR DESIGN CHARACTERISTICS

General	
Thermal Power	600 Kwt
Reactor Inlet T.	1100°F
Reactor Outlet T.	1300°F
Coolant	NaK-78
Coolant Flow Rate	13.6 lb/sec at 600 Kwt
Life objective	10,000 hrs.
Reliability objective	N 93%
Total Weight (Core, Reflection, vessel, control)	600
Core Design	
Active Core Diameter	8.6 in.
Active Core Length	16.5 in.
L/D Ratio	1.92
Specific Power	94 Mw/ft^3
Fuel	Zirconium - Hydride 10.5% Uranium 6×10^{22} H_2 $atoms/cm^3$
H_2 to Zr Atomic Ratio	1.7
Rod O.D.	0.560 in.
No. of fuel Rods	211
Cladding Mat.	Hastalloy N (glass lined ID)
Cladding Thickness	0.010 in.
Fuel-Clad Gap (Initial)	0.0075 in.
Design Burn-up	4 a/o
Maximum Clad Surface T. (Peak)	1480°F
Fuel center line T. (Peak)	1580°F
Rod Spacing and Pitch	0.570 in. triangular pitch
Heat flux (average)	55,000 Btu/hr. H^2
Kg Uranium 235	7.0
Axial Reflection Thickness	None
Reflection Material	

TABLE 2-38 - SNAP 8 REACTOR DESIGN CHARACTERISTICS (Continued)

Shielding	
Type	Shadow Shield - Two No. 1 LiH with enriched Li-7
Material	Region No. 2 LiH
Control	
Type	Drum Reflector
No. of Drums	6
Material	Beryllium
Thickness	
Axial	None
Radial	3 in.
Vessel	
Core and Vessel Material (Structural)	SS
Vessel ID	9.214
Wall Thickness	0.105
Length	22.4

Power Plant Design

The power conversion system is a mercury Rankine cycle consisting of a boiler, turbine-alternator, condenser, condensate pump, valves, seals and a mercury injection 11.5 psia system. Mercury enters the turbine at 1263°F and 270 psia, and leaves at 508°F and 11.5 psia. The heat rejection loop uses NaK-78 as the working fluid, entering the radiator at 665°F and leaving at 495°F. Detailed system design conditions are presented in Table 2-39.

CURRENT DEVELOPMENT PROGRAM

Major Problems

Major areas of development with the SNAP 8 system are as follows:

1. Containment of H_2 in the core at a reactor outlet temperature of 1300°F is still not completely solved; the schedule shows a developed confinement system for 10,000 hours of operation by 1967-68. However, lifetimes beyond this time are questionable.
2. The feasibility of space condensers must be proven. Extensive design information is needed in the areas of freeze-up, flow distribution, two phase flow pressure drop, and condensing heat transfer. Only extensive operation in space will fully determine extended condenser performance, although this is a problem common to all Rankine cycle dynamic systems.
3. Extensive radiator design information must be developed. Improvements in fabrication techniques—joining and machining—and quality control must be developed.
4. Additional information is needed in the area of mercury boiling and stability (chugging), boiler effects on system stability, and flow distribution in parallel paths where boiling occur.
5. Manufacturing and reliability problems in the turbine, bearing, seal area must be overcome as well as turbine cavitation and blade erosion.

TABLE 2-39 - SNAP 8 POWER PLANT

	Boiler	Condenser
No.	1	1
Type	Counterflow once thru	Straight-once thru counterflow
Length	42 in.	39 in.
Diameter		10 in. (max)
Materials		
Tubes	9 Cr- 1 Mo Steel	9 Cr- 1 Mo Steel
Shell	316 SS	9 Cr- 1 Mo Steel
Tube Configuration	Helically wound with sprial ribbon turbulators	
No. of Tubes	4	73 tapered
Tube OD	3/8"	1/4" Dia. at outlet
Tube Wall Thickness	0.028	0.028 in.
Tube Length	60 ft.	
Tube Spacing		
ΔP Primary	5 psia	4.9 psia
ΔP Secondary	70 psia	6 psia
Weight	530 lb.	70 lb.
Capacity (Thermal)	400 Kwt	370 Kwt
Inlet Fluid State		Hg Vapor
Inlet Fluid Velocity		150 ft/sec.
Outlet Fluid State		Hg liquid
Outlet Fluid Velocity		Few ft/sec
Primary Fluid Material	NAK-78	Hg

Pump Motors	Hg	NaK
Type	Centrifugal	Centrifugal
Pressure Rise		13 psi ΔP

TABLE 2-39 - SNAP 8 POWER PLANT (Continued)

Turbine	
No.	1
Type	Overhung-four stage impulse type
Inlet T.	1250°F
Inlet P.	265 Psia
Outlet T.	680°F
Outlet P.	16.5 Psia
Materials	
Rotor	Stellite 6B
Blades	Stellite 6B
Casing	9 Mo- 1Cr Steel
RPM.	12,000
Weight (Turbine-alternator)	295 lb.
Generator	
No.	1
Type	Homo-polar-inductor radial gap, 400 cps, Aircraft type
RPM.	12,000
Weight (turbine and alternator)	295
Bearings (Type)	Ball Bearings
Lubrication	ET-378
Cooling Fluid	ET-378
Heat Rejection Loop	
Radiator	
Area	1600 ft^2
Type	Flatpanel or cylindrical
Materials	
Tubes	9 Mo- 1Cr Steel
Fins	Beryllium or Cu or SS.

TABLE 2-39 - SNAP 8 POWER PLANT (Continued)

Weight (including armor)	1790
Inlet Temp.	665°F
Inlet Press.	33 psia
Outlet Temp.	495°F
Outlet Press.	12 psia
Heat rejection Capability	364 Kwt
Cooling and Lubrication Loop	
Radiator	
Inlet T.	245.8°F
Inlet P.	54 Psia
Outlet T.	210°F
Outlet P.	38 Psia
Fluid	ET378

6. Several materials technology problems remain, examples of which are crud formation, corrosion and mass transfer in the Hg loop. With 9M material, a 10,000 hour power conversion system life is expected to be near the maximum achievable limit.

Schedule and Funding

The S8ER is currently operating and will continue to operate through early FY 1965 to obtain data on the operation of the nuclear system. A development system (S8DS) will begin operation in FY 1965 and, though not fully flight rated, is designed to demonstrate 10,000 hour capability. The first fully flight rated system (S8FS) is scheduled for FY 1968; it will also be designed for 10,000-hour life. Two systems are scheduled for delivery to NASA in FY 1968.

Under the old contract approximately $14.5 million of NASA funds was spent for power plant development. The total value of the new NASA contract has been set at less than $50 million. AEC funding was $8.8 million for FY 1963.

Facilities

The GPTF (Ground Prototype Test Facility) in which S8DS will be operated is a modification of an existing facility. These modifications are underway. The testing of S8FS will require a new facility sized to accommodate a complete SNAP 8 power plant under space environmental simulation. This facility is in final design. Both of the above facilities will be located at the Santa Susana facility. Additional complete flight prototype test facilities will be available at the NASA Plum Brook site.

SNAP 2

Objectives of the Program

The SNAP 2 program, the first program directed toward the application of nuclear reactor power in space, is basically oriented toward the development of the necessary technology and systems to provide small quantities of power for use in military and scientific satellites. The specific objective of the SNAP 2 program is to develop, test and qualify a 3-4 kw nuclear auxiliary power unit (NAPU). The development effort is directed toward the following objectives.

1. Unattended, automatic, maintenance-free operation for 10,000 or more hours.
2. Maximum reliability and ruggedness.
3. Maximum safety—remote startup.
4. Maximum ease of handling and production.
5. Minimum size and weight.
6. Maximum economy.

General Description

The SNAP 2 power plant is a two loop system which includes in the primary (NaK) loop, the reactor, a thermoelectrically driven electro-magnetic pump, the shell side of a boiler, an off line expansion compensator, and parasitic load heaters.

The reactor consists of the core, a beryllium radial reflector which is movable for reactivity control, the control drum motors, and a lithium hydride shield. The NaK transfers heat to a mercury Rankine cycle system which includes the tube side of the boiler, the turbine-generator, a condenser-radiator, the condensate pump, regulator tank, flow regulator and flowmeter.

This system was not designed for high performance, but aims for compactness and minimum weight in proving the general concept. Table 2-40 shows the over-all plant design requirements, Table 2-41 shows system weight estimate, and Figure 2-38 gives general system design conditions. Figure 2-39 shows an expanded view of the SNAP 2 system as it will appear in the flight vehicle.

TABLE 2-40 - SNAP 2 OVERALL PLANT DESIGN REQUIREMENTS

Power	
Output Power	50 kw and 4 dw(e)
Frequency	1000 cps
Voltage	210 L-M volts
Operating Lifetime	10,000 hours
Startup and Shutdown	single startup in space. shutdown by ejection of reflector.
Shielding	300 lb LiH 50 lb structure neutron - 1.8×10^2 nvt 10^7 r gamma

TABLE 2-41 - SNAP 2 FLIGHT SYSTEM WEIGHT ESTIMATE

Component	Weight (lb)	
REACTOR SUBSYSTEM		289.7
Reactor Structure	48.3	
Reflector Assembly	118.2	
Core Fuel	123.2	
RADIATION SHIELD		355.0
Shielding Material	300.0	
Container (Shell)	55.0	
PRIMARY SUBSYSTEM		62.8
Piping Assembly	21.8	
Parasitic Load Heaters	2.0	
Expansion Compensator	16.0	
Flow Trimmer	2.0	
Startup Pump	4.3	
Ground Test Heaters (Flight Weight Only)	10.0	
NaK Inventory	6.7	
POWER CONVERSION SUBSYSTEM		336.3
CRU Module	82.1	
Boiler Assembly	52.1	
PCS Structure	11.9	
Regulator Tank	21.6	
Mercury Start Components	123.6	
Mercury Inventory (Steady State)	45.0	
STRUCTURAL HEAT - REJECTION SUBSYSTEM		269.6
Radiator-Condenser (RC-11)	256.9	
Nose-Cone Ejection Structure	1.8	
Mercury Vapor Riser Piping	10.9	
ELECTRICAL STARTUP AND CONTROL SUBSYSTEM		132.7
Reactor Control Equipment	9.5	
Parasitic Load Control	26.5	
Electrical Power Distribution Equipment	56.2	
Startup Circuitry	35.7	
Safety Circuitry	4.8	
FLIGHT INSTRUMENTATION SUBSYSTEM		102.7
Temperature Instrumentation	30.9	
Pressure and Flow Instrumentation	17.8	
Position Indication Instrumentation	11.2	
Structural Instrumentation	11.3	
Event Markers (Limit Switch and Relay Contact)	6.5	
Radiation Monitoring	10.0	
Thermal Barrier	15.0	
DESTRUCT CHARGE SUBSYSTEM		15.0
Destruct Assembly	15.0	
MISCELLANEOUS		54.2
	Total	1618

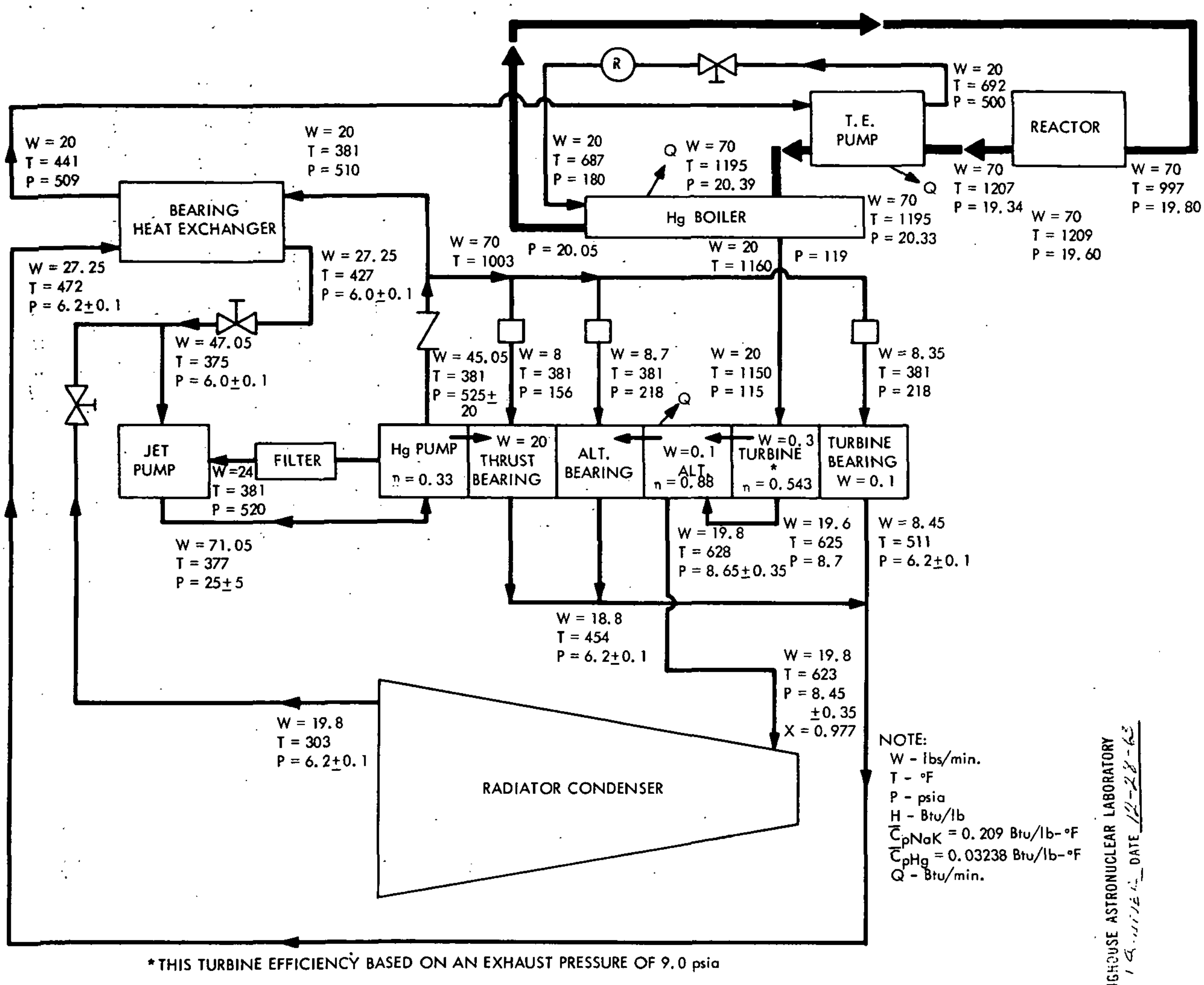

Figure 2-38 - SNAP 2 System Flow and Energy Schematic

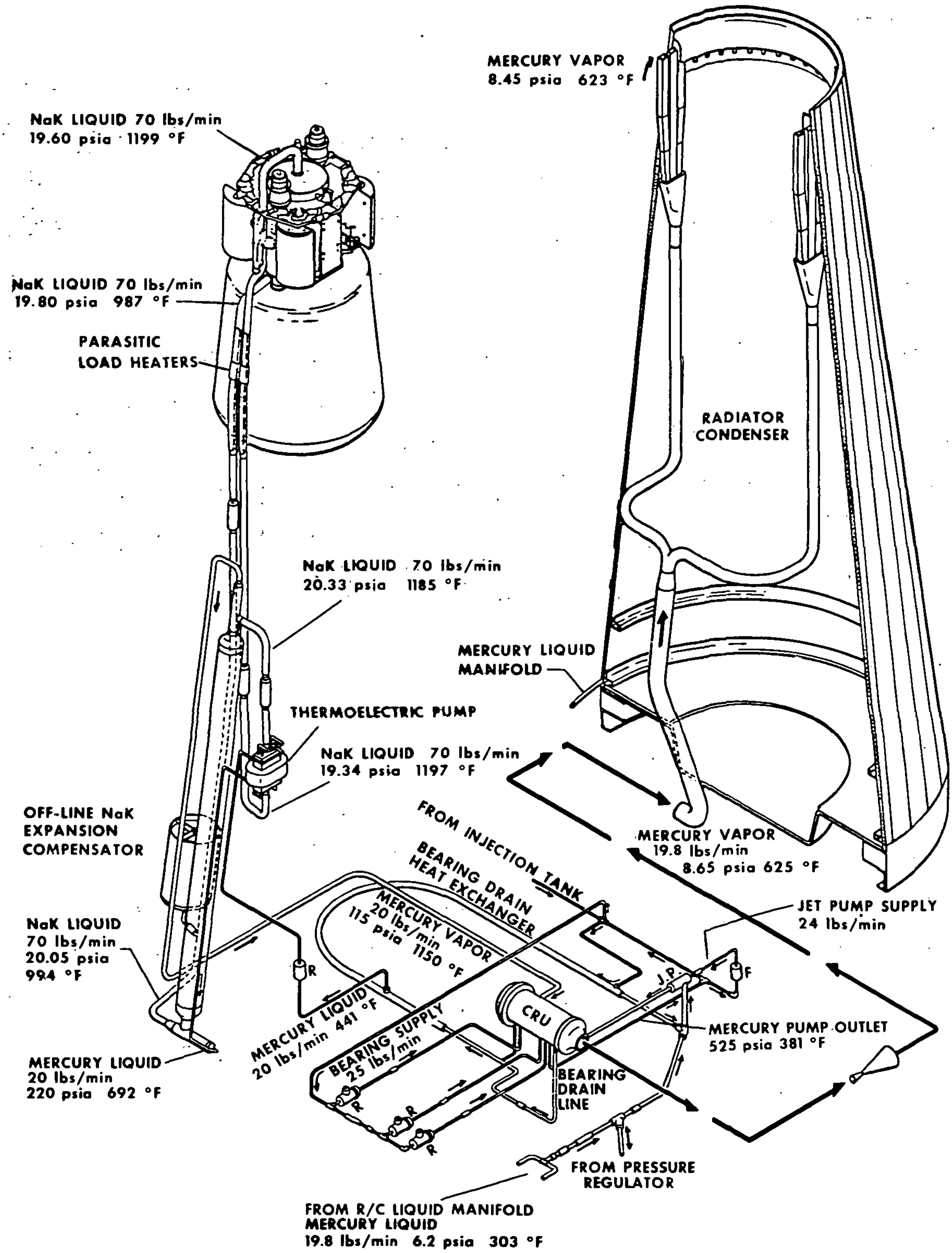

Figure 2-39 - SNAP 2 Flight System

Reactor and Shield

General Description

SNAP 2 is the first of the zirconium-hydride moderated reactors whose development was undertaken by Atomics International. The objective is to provide a reactor having the control characteristics of a water-moderated reactor, but operating at higher temperatures than a water system could achieve and without the heavy containment associated with water systems.

The fuel is a hydrided uranium-zirconium alloy, $(Zr-10U)H_{1.7}$, clad in Hastelloy N with an internal glass coating to reduce hydrogen loss. The core consists of 37 fuel rods each about 10 in. long and 1.25 in. in diameter. The reactor coolant, NaK, enters the reactor at 1000°F and leaves at about 1200°F. Types 316 and 304 stainless steel are the structural materials. The reactor thermal power is about 50 kw and the net electrical output is estimated at 4 kw.

Reactor design characteristics are listed in Table 2-42.

POWER CONVERSION SYSTEM

The power conversion system uses mercury as the working fluid. The turbine, the generator and the boiler feed pump are all mounted on a single shaft and make up a hermetically sealed combined rotating unit (CRU). The turbine is a two stage, partial admission impulse machine whose shaft output is about 4 kw. The boiler feed pump is an open-faced centrifugal pump relying upon a jet pump to raise the NPSH to an acceptable level. The generator is a permanent magnet machine. Design values of the power conversion loop equipment are shown in Table 2-43.

TABLE 2-42 - SNAP 2 REACTOR DESIGN CHARACTERISTICS

General	
Thermal power	50 kwt
Reactor inlet temperature	1000° F
Reactor outlet temperature	1200° F
Coolant	NaK
Coolant flow rate	70 lb/min
Life objective	1 year
Reliability objective	
Total weight (core, reflector, vessel, control)	299.2 lb
Core Design	
Core diameter	8 in. across flats
Core length	10 in. long
L/D ratio	1.25
Specific power	0.156 Mw/ft^3
Fuel	10% uranium in zirconium hydrided to 6.5 x 10^{22} H/cm^3
Fuel length	10 in.
Fuel rod OD	1.25
No. of fuel rods	37
Cladding mat	Hastelloy N
Cladding thickness	0.010 in.
Maximum clad surface temperature	1220° F
Maximum fuel center line temperature	1250° F
Heat flux (average)	17,000 Btu/hr-ft^2
Nuclear flux	3.1 x 10'' n/cm^2-sec
Kg Uranium 235	4.3
Radial reflector thickness	2.3
Reflector material	Be

TABLE 2-42 (continued)

<u>Shielding</u>	
Type	Shadow
Material	LiH
Design Dose Criteria	
<u>Control</u>	
Type	Pivoting reflector segments
Number	4
Material	Be
Thickness	2-3 in.

TABLE 2-43 - SNAP 2 POWER PLANT DESIGN CHARACTERISTICS

Boiler	
Number	1
Type	counter flow - once thru
Tube material	Haynes 25
Tube configuration	4 parallel helically wound
No. of Tubes	4
Tube OD	3/8 in.
Tube wall thickness	0.020 in.
ΔP Primary	0.28 psia
ΔP Secondary	10 psia
Weight	30-40 lb
Capacity (thermal)	50 kw
Primary fluid	NaK
Secondary fluid	Hg
Turbine	
Number	1
Type	2 stage impulse type
Inlet temperature	1150° F
Inlet pressure	115 psia
Outlet temperature	628° F
Outlet pressure	9 psia
Materials	
Rotor	Haynes 25
Blade	15-7 Mo
Casing	Nivco 10
RPM	36,000
Weight (turbine and gen.)	30
Eff.	50%

TABLE 2-43 (continued)

<u>Generator</u>	
Number	1
Type	permanent magnet
Materials Conductors	silver
RPM	36,000
Eff.	85%
Weight (turbine and generator)	30 lb
Bearings (type)	sleeve
Cooling Fluid	Hg
Control	parasitic load
<u>Heat Rejection Loop</u>	
<u>Radiator</u> - Condenser	
Area	< 110 ft^2
Type	truncated cone tube and fin
Materials	
Tubes	stainless steel
Fins	Al, Cu, or Be
Weight	269.6 lb.
Inlet temperature	623° F
Inlet pressure	8.45 ± 0.35 psia
Outlet temperature	297° F
Outlet pressure	6.20 ± 0.1 psia
Flow	19.8 lb/min

Current Development Program

A. Major Problems

Since the SNAP 2 reactor is used in the SNAP 10A system, most components are under construction and/or test. The general problems with this system are the same as those discussed for SNAP 8 except that they are less severe because of the smaller sizes of components of the system and the lower temperatures of the plant.

B. Schedule and Funding

The SNAP 2 reactor is currently scheduled for flight testing in the SNAP 10A system early in 1965, and the integrated SNAP 2 system is due for flight test in mid 1966. The funding level for SNAP 2 was $17.4 million in FY 1963.

~~CONFIDENTIAL~~
~~RESTRICTED DATA~~
~~Atomic Energy Act 1954~~

SUNFLOWER

Objectives of the Program

The Sunflower program is directed to the development of the technology for employing solar heat energy in generating of electrical power and the use of the technology in systems capable of sustained operation in space. The principal specific objectives center on development of an energy collector system light enough for space flight yet capable of packaging for launch and deployment in orbit. Additional objectives, not unique to the program, are the development of mercury-lubricated bearings, alternators which can be sealed against the mercury environment, turbine blade erosion resistance, and control of boiling and condensing under zero gravity. Because heat must be stored for use during the dark cycle if continuous power is to be generated, a further objective is development of LiH as a heat storage device.

General Description

Sunflower is the designation for a 3 kw electrical space power system utilizing solar energy and a mercury Rankine cycle power conversion system. The Sunflower system includes a solar collector, boiler, heat storage unit, combined rotating unit and primary and secondary condenser radiator. Original specifications required that an orbital altitude flexibility from 300 to 20,000 nautical miles be included in the design. A weight penalty of 100 pounds is imposed for this multiple orbit capability. Table 2-44 shows overall plant design requirements for the present concept and an advanced system. Table 2-45 shows flight system weight estimates for both the present and advanced system.

Solar Collector

The solar collector must be capable of stowing within a boost vehicle for launch and also must be deployed to full size for short operation. The specific function of the collector is to intercept solar energy and reflect and concentrate it into the cavity of the boiler. Specific

TABLE 2-44 - SUNFLOWER OVERALL PLANT DESIGN REQUIREMENTS

Power	
Output Power	3 kwe
Frequency	200 cps ± 1%
Voltage	110 v/ton ac
Operating Lifetime	1 year
Operating Environment	Space
	Shade time 35 min. up to 72 min. Orbital period 90 min. up to 24 hrs. Operating in Og or during acceleration of lg in any direction.
Heat Storage	Heat of fusion of LiH

	Present System	Advanced
Collector OD (ft)	32.2	30
Collector ID (ft)	0.6	5
Collector Orientation Accuracy (°)	3/4	1/8
Collector Surface Error (°)	1/2	1/8
Sun Heat Input to Boiler Kw/hr	62.8	74.0
Net Boiler Heat Input Kw/hr	34.3	43.2
Boiling Temperature (° F)	1050	1050
Boiling Pressure (psia)	240	240
Superheat Temperature (° F)	1250	1250
Turbine eff. (%)	51	60
Turbine Exhaust Pressure (psia)	7	2
Condensing Temperature	605	505
Cycle Flow Rate	13.7	16.8
Turbine Output Power (kw)	5.0	9.6
Shaft Losses (kw)	0.88	0.88
Alternator Output (kw)	3.5	7.85
Control Power (kw)	0.5	0.2
Net Electrical Output (Kw)	3.0	7.65

TABLE 2-45 - SUNFLOWER SYSTEM WEIGHT COMPARISON

	Present System (300 NM)	Advanced System
Collector	186	343
Boiler Heat Storage	200	245
Turboalternator	30	45
Radiator Condenser	62	109
Mercury Inventory	15	30
Speed Control	15	25
Start Auxiliaries	65	100
Structure & Misc.	67	120
Total	640	1017
Specific Power lb/kw	213	131

weight of the collector has an initial design value of 0.25 lb/ft^2. Surface deviation of the collector has a design objective value of $1/2^o$ over 90 percent of the surface area. Total reflectivity objective is 91 percent. Table 2-46 shows collector parameters, design objectives and status to date.

Power Plant

The power plant for the Sunflower system consists of a turbo-alternator assembly with a three stage axial impulse turbine, a permanent magnet alternator and a mercury pump on a single shaft. CRU components use the liquid mercury working fluid for cooling and lubricating the journal and thrust bearings. The boiler-heat storage unit is constructed of 316 stainless stell and uses LiH as the storage material. This plant is now well into the final stages of development, and the major components have had extensive operational test, i.e., mercury turbines have had over 4000 hours of continuous running without any major problems or indication of erosion or corrosion.

POTASSIUM WORKING FLUID SYSTEMS

Many of the liquid metal Rankine cycle systems which have been studied are based upon the use of potassium as the working fluid. At this point in time there is no potassium vapor turbine experience—since to date there have been no alkali metal vapor turbines run. However, government sponsored programs are now underway at General Electric Corporation, AiResearch Corporation and other locations aimed specifically at obtaining data on potassium vapor turbines, and many government laboratories and industrial concerns are working on other phases of high temperature potassium power conversion systems. The justification for this work is threefold:

1. If higher temperatures than 1300^oF are to be considered for power conversion systems, mercury becomes undesirable as a working fluid because of the increased system pressure required.

TABLE 2-46 - SUNFLOWER SOLAR COLLECTOR DESIGN PARAMETERS

Outer Diameter	32.2 ft.
Inner Diameter	9.6 ft.
Focal length	17.0 ft.
Operative angle	53°
Cavity Aperature	12. ft.
Concentration Ratio	600
Weight (Based on minimum percentage sun time 62.5% at 300 MN)	186 lb.

Status Review

	Design	Achieved
Weight	186 lb (0.25 lb/ft^2)	195 lb (0.26 lb/ft^2)
Surface Deviation	0.5° over 90% of area	Approx. 1.0°
Total Reflectivity	91%	90.7% small scale 84% full panel
Efficiency	90% C 0°	72%
	74% at 0.75°	Not evaluated
Environmental	0.8 g's at 5 cps	Confirmed
	7.5 g's at 2000 cps	Stowed and deployed

2. Potassium has characteristics that make it potentially better from a corrosion, erosion standpoint than mercury.
3. From an engineering standpoint, it is the technical judgement of most personnel close to liquid metal systems that the potential problems involved with potassium differ only in degree, not in kind, from those encountered and being solved in steam systems and mercury vapor systems.

The major problem with potassium systems at the moment is lack of data on which to base the design of high performance systems designed for long unattended operation. As will be seen in the brief discussion of various programs now underway, such information is being developed and will begin to be available in sizeable quantity during calendar year 1964.

SPUR/SNAP 50 PROGRAM

Objectives of the Program

The SPUR/SNAP 50 program proposes to extend the technology of space nuclear reactor power plants into the higher temperature ranges that may make feasible plant specific weights in the 10-20 lb/kw range—thus making high capacity power plants feasible for space use. This requires the use of refractory metal alloys as reactor system construction materials, requires development of high temperature reactor fuel materials (such as the uranium carbides, UO_2-BeO and the uranium nitrides) and makes desirable (and even necessary in some cases) the use of lithium as the reactor coolant.

The higher operating temperatures in the power generation system also require the use of refractory metal alloys for structures. Another effect of the higher temperatures is either to require a change of working fluids from mercury to a fluid with a lower vapor pressure or else to build a high pressure system. The latter alternative is undesirable because of the excessive weight of structural material that would be required for containment; hence potassium is the design coolant material.

Concept Description

The raising of operating temperatures and lowering of specific weights are not ends in themselves, but are means for achieving higher power levels. Thus the SNAP 50 development is aimed at producing a system capable of generating approximately 1 Mwe. A plant of this capability could feasibly power a large space station, a large lunar base or an electric propulsion system for a space vehicle. Although no specific application for this system has been chosen, design objectives in terms of power levels, temperatures and specific power have been selected and the SNAP 50 is designed to meet these objectives.

The tables of characteristics are given here for a 300 kwe system. However, the complete SNAP 50 system (4 loops) is intended to have an output of 1.2 Mwe. The initial test vehicle will include a reactor capable of the full design power output but with only one of the four power generation loops installed. This lower power level plant is included here because in capacity it is a more appropriate size for the lunar base application.

Figure 2-40 is a flow schematic of a 300 kwe version of the SNAP 50 concept. The reactor core for this concept consists of UC rods clad with Cb-1Zr. The reactor coolant is Li^7. The Rankine cycle working fluid is potassium. The radiator loop fluid is also potassium.

As presently conceived, a 300 kwe test unit will weigh approximately 20,000 lbs. with only a shadow shield for electronic components, and no shielding for man. Of this total weight, 5100 lbs. is allotted to the reactor loop, 2400 lbs. to the power conversion loop, 2700 lbs. for shielding and approximately 9000 lbs. for auxiliary power equipment (of which 4000 lbs. is chemical fuel).

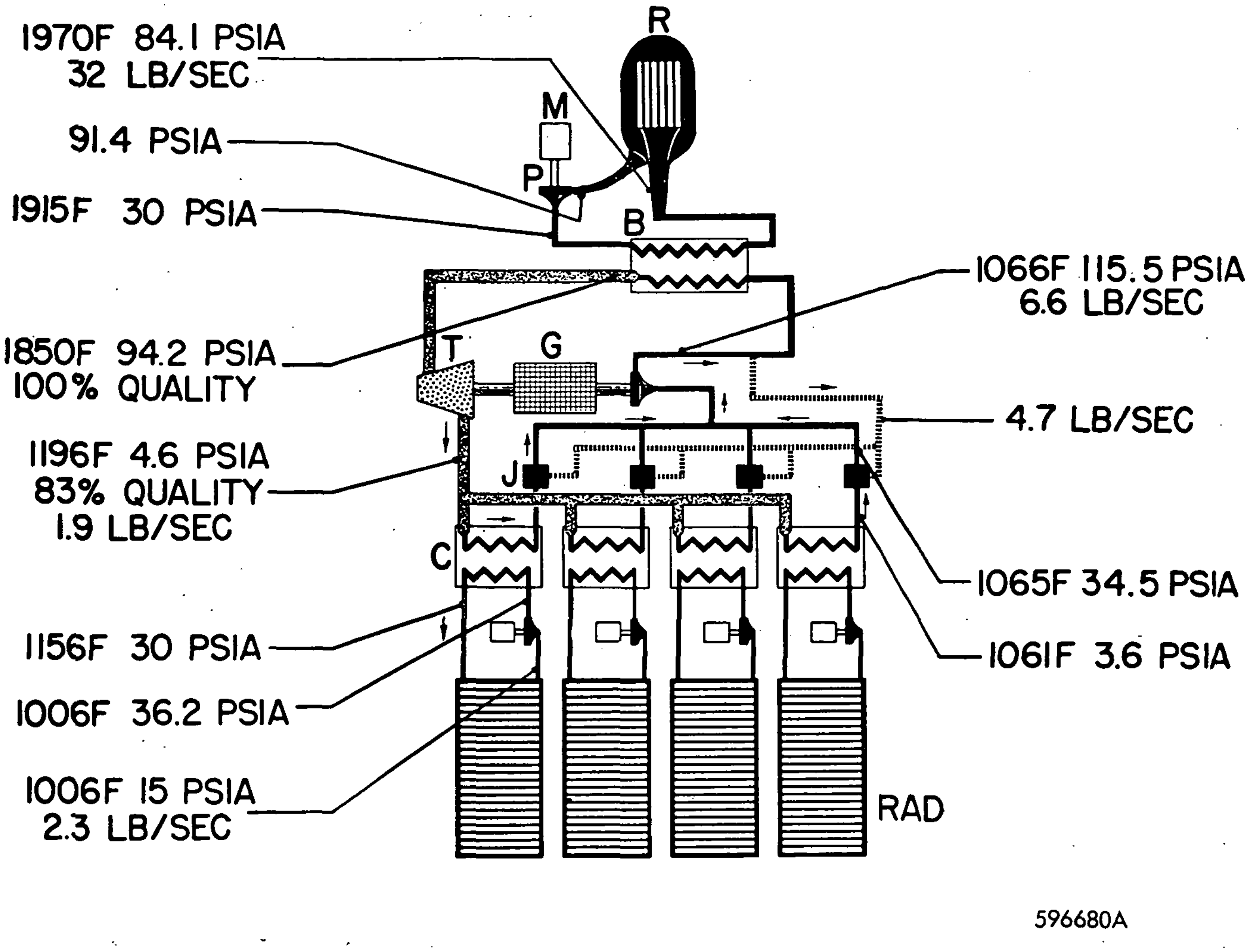

Figure 2-40 - 300 KW SNAP 50 Flow Schematic

Reactor Design

The reactor is designed for a thermal power of 8 Mw but will be operated at only 2 Mw for 300 kwe output. It is a small, fast spectrum reactor nominally fueled with $UC_{1.08}$ although other fuels are being considered. The general characteristics of the reactor system are given in Table 2-47.

Power Plant Design

The full scale SNAP 50 plant has four completely separate power generation systems which use the reactor system as a common heat source. Thus the single unit test plant will differ from the 1.2 Mwe plant only in plant layout. Table 2-48 shows the design characteristics of the plant components for the 300 kwe plant. The components themselves were previously show schematically in Figure 2-40.

Current Development Program

Major Problems

The recent definition of SNAP 50 as a technology development program rather than a plant design project points up the degree to which this is a pioneering effort. Among the problems to be solved are:

1. Fuel swelling with a 2200°F cladding hot spot and the development of a satisfactory fuel-cladding barrier. These problems are discussed in detail in Part 3, Section I of this volume.
2. Liquid superheating in the boiler. The "chugging" action at the initiation of boiling is observed in this and other liquid metal systems. The cause of this phenomenon must be determined before corrective measures can be taken.
3. Condensing heat transfer and pressure drop. The use of an all-liquid radiator eliminates some of the problems of a combined condenser-radiator but other

TABLE 2-47 - SNAP 50 REACTOR DESIGN CHARACTERISTICS

General	
Thermal Power	2 Mwt
Reactor Inlet Temperature	1915° F
Reactor Outlet Temperature	1970° F
Coolant	Li^7
Coolant Flow Rate	32 lb/sec
Life Objective	10,000 hrs.
Reliability Objective	
Core Design	
Active Core Diameter	10.48 in.
Active Core Length	10.48 in.
L/D Ratio	1.0
Specific Power	3.88 lb/ft^3
Fuel	$UC_{1.08}$
Fuel Rod OD	0.432 in.
Number of Fuel Rods	434
Cladding Material	Cb-1 % Zr
Cladding Thickness	0.010 in.
Rod Spacing and Pitch	0.449 in. triangular pitch
Heat Flux (average)	162,000 $Btu/hr\text{-}ft^2$
Fuel Loading	84 kg U^{235}
Reflector and Control	
Control Type	Reflector movement - mechanism not yet selected
Material	BeO
Thickness	1.6 in.

TABLE 2-48 - SNAP 50 POWER GENERATION SYSTEM CHARACTERISTICS

	Boiler	Condenser
No	1	4
Type	counterflow, once through	counterflow, tube and shell
Length		
Materials	Cb-1Zr	
Tube Configuration	curved	
No. of Tubes	about 200	
Tube OD	0.25 in.	0.5 in.
Tube Wall Thickness	0.025 in.	0.050 in.
Tube Spacing		0.600 in.
Δp Primary	54.1 psi	2 psi
Δp Secondary	21.3 psi	--
Weight	240 lb	57 lb
Capacity (Thermal)	2.12 kw	430 kw
Inlet Fluid State	liquid	84% quality vapor
Outlet Fluid State	saturated vapor	liquid
Outlet Fluid Velocity		

Turbine	
Number	1
Type	free vortex
Inlet T.	1850°F
Inlet P.	94.2 psia
Outlet T.	4.6 psia
Outlet P.	1196°F
Materials	
Rotor	TZM, Mo-1/2 T_i or Kennametal
Blade	integral with rotor
Casing	Cb-1% Zr
RPM	24,000

TABLE 2-48 (continued)

	Boiler	Condenser
Generator		
Number		1
Type		Inductor
Materials		Ni clad copper windings
RPM		24,000
Effi.		88% at 0.75 PF
Bearings (Type)		Pivoted shoe, visco seal, molecular pump
Lubrication		Potassium
Cooling Fluid		Potassium
Heat Rejection Loop		
Radiator		
Area		625 ft^2
Type		tube and fin
Materials		
Tubes		SS
Fins		Copper
Weight		1816 lb
Inlet Temp.		1227°F
Inlet Press.		28 psia
Outlet Temp.		1077°F
Outlet Press.		19 psia

problems remain. Condensing coefficients and pressure drop are still not reliably calculable, so that further testing is required.

4. Radiator design. For the 300 kwe version the use of a fixed radiator is feasible, thus avoiding the difficulties of designing a reliable deployable radiator. Even so, other problems remain, such as the selection of a good fin and meteoroid armor material. Copper is currently proposed for use on SNAP 50 but little development work has been done. Beryllium alloys seem more promising, but alloys must be developed which will withstand impact.
5. Turbine design. No one has yet built a turbine of the type required. Its small physical size causes problems in maintaining high efficiency, but even with small rotor diameters the blade tip speed may become limiting. Blade erosion by liquid droplets are also a concern. Bearing development is still in an early stage.
6. Generator design. High temperature generators are required to avoid excessive heat losses and weight penalties associated with existing low temperature generators. Exposure to liquid metal vapors remains a problem, with work proceeding on bore seals and sealed rotors.

Schedule and Funding

The SNAP 50 development schedule is at present not well established since the recent cancellation of LCRE; however, discussions indicate the early 1970's for a working prototype plant if development proceeds satisfactorily with high temperature fuels materials. It must be recognized that this is on the basis of a high temperature plant objective above 2000°F.

Facilities

Complete plant testing facilities are still in the planning stage.

ORNL BOILING POTASSIUM REACTOR—MPRE

Objectives of the Program

The MPRE is a direct cycle boiling potassium reactor concept, and as such, the major objective of the work being done at Oak Ridge is to develop basic information on the characteristics of such a system. Primary concern is with the reactor itself rather than the power conversion chain and planned test work is largely in this area.

Concept Description

The MPRE is intermediate in power level and temperature between the SNAP 8 and SNAP 50 concepts—with selection of parameters based to a large extent on the groundrule of using existing or relatively uncomplex materials technologies. The reactor is a UO_2-fueled, stainless steel clad, rod-type core. Potassium vapor formed in the core passes through a vapor separator that is structurally integral with the core and then goes directly to the turbine. The system is shown schematically in Figure 2-41.

Since the peak cycle temperature is about 1500°F, the complete structure is based on the use of 316 SS. Assuming that the long term creep strength is satisfactory, the theoretically more difficult fabrication properties of refractory metal alloys are avoided.

The general reactor characteristics are shown in Table 2-49. No data are given for the other loop components since, with the exception of jet pump and bearing tests, there have been insufficient funds available to prepare significant designs for the power conversion equipment.

One of the main advantages of the system is the potential simplicity of the direct cycle system as compared to indirect cycle plants, in addition to the thermodynamic advantage of eliminating the temperature drop associated with the heat exchanger in an indirect cycle system.

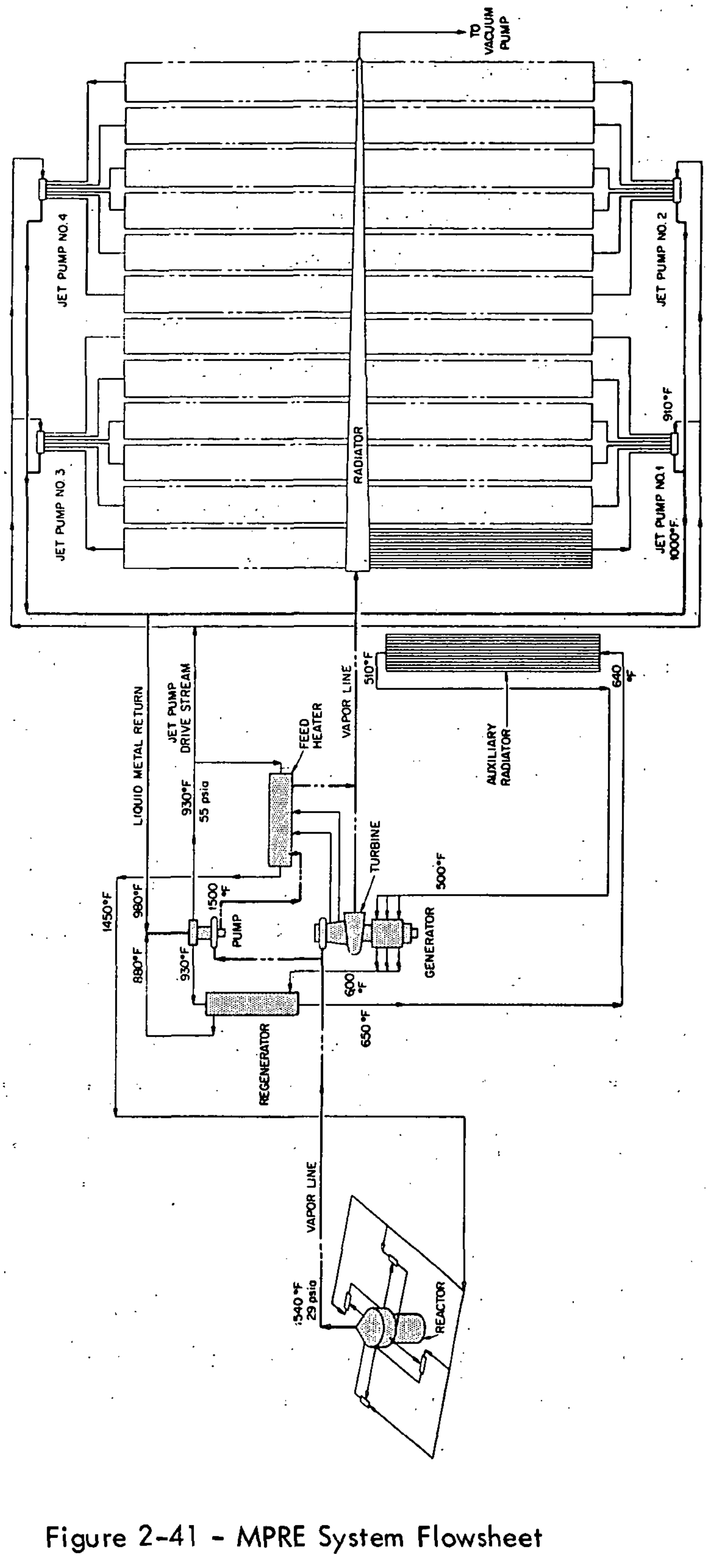

Figure 2-41 - MPRE System Flowsheet

TABLE 2-49 - MPRE DESIGN CHARACTERISTICS

General

Thermal Power	1000 kw
Reactor Outlet Temperature	1540°F
Coolant	K^{39}
Coolant Flow Rate (total)	4.33 lb/sec
Vapor Flow Rate	1.08 lb/sec
Weight of Reactor Assembly	750 lbs

Core Design

Core Diameter	9.56 in.
Core Length	12 in.
L/D Ratio	1.26
Specific Power	2.0 Mw/ft^3 (70.6 w/cm^3)
Fuel	UO_2
Fuel Rod Diameter	0.50 in.
Spacing and Pitch	0.5625 in. triangular pitch
Number of Rods	241
Cladding Material	SS 316
Cladding Thickness	0.020 in.
Average Heat Flux	108,300 Btu/hr ft^2
Core Pressure Drop	1.0 psi
Vapor Quality at Core Exit	25%

Development Program

Among the major development problems are:

1. Hydraulic "bumping" due to unstable boiling. Some ORNL experiments have demonstrated several hundred degrees of superheat before the onset of boiling, with periodic "bumping" continuing to occur. Means proposed thus far to overcome the superheat do not appear desirable in a reactor system.
2. The direct cycle requires complete integrity of all fuel elements to avoid making the whole plant a radiation source. The use of K^{141} eliminates significant activation of the coolant itself, but any contaminant could become activated and ruin the effectiveness of the system.
3. The vapor separator must be very effective or else the turbine blading may become seriously damaged. Since no superheat is used, the vapor quality depends entirely on the vapor separator.
4. The use of UO_2 fuel under the MPRE operating conditions appears to be similar to ML-1 experience. Under these conditions there may be a large amount of fission gas release and fuel swelling even though the centerline temperature is held below 2900°F.

Scheduling and Funding

This effort is being carried at the relatively low funding level of about $2.2 million per year for both FY 1963 and FY 1964. The main development effort thus far has been in running thermal and hydraulic tests and critical experiments. Plans are being made for an experimental reactor system test but the funding of this effort is as yet uncertain.

Facilities

All development work to date has made use of existing ORNL facilities. A proposed MPRE test facility would be based on modifying an existing facility at Oak Ridge.

GENERAL ELECTRIC COMPANY TURBINE DEVELOPMENT

One of the most significant potassium system component development programs other than those associated with SPUR/SNAP 50 work primarily (work of Pratt & Whitney and AiResearch) is the work at the General Electrical Company, Evandale, Ohio, plant where a two stage potassium test turbine is being designed and fabricated under NASA contract NAS 5-1143.

The objectives of this program are to study the effects of vapor wetness on performance, demonstrate condensate extraction, study blade erosion with different blade materials, study super-saturation and droplet formation, improve the accuracy of General Electric's calculated Mollier diagrams and to establish accurate fluid flow design methods for potassium turbines operating in the design region.

Work began on this program in May 1961, and performance tests are scheduled to begin in early January 1964 on a two-stage test trubine representing the third and fourth stages of a hypothetical five-stage 500 kw turbine. This turbine will accept 2. 8 lb/sec of variable quality 1600°F potassium vapor.

As an integral part of this program, nozzle tests are being conducted to find the variation of the polytropic exponent with temperature and quality and the variation of the degree of supersaturation with inlet temperature and quality.

This program as well as the AiResearch turbine program being conducted as part of the SPUR/SNAP 50 effort will begin to yield specific results during calendar 1964.

WESTINGHOUSE ELECTRIC CORPORATION ELECTRICAL COMPONENT DEVELOPMENT

The Westinghouse Aerospace Electrical Division at Lima, Ohio, has contracts with the

Air Force and NASA for the analysis and development of electrical components for potassium vapor power conversion system. The Air Force contracts are for the development of 50 kva potassium-cooled inductor generator. An experimental air-cooled version of this generator has been tested and a potassium-cooled machine will soon be in operation. This unit is designed to operate at 24,000 rpm with an average coolant temperature of 600°F and winding temperatures as high as 1000°F.

Under the NASA contract, components have been designed for a 1 mwe system. The components involved in this study are generators, circuit breakers, transformers, rectifiers and exciter-regulators.

Astronuclear

WATER SYSTEMS

Introduction

There is at present no coordinated program underway to develop a nuclear power plant for space or lunar sufrace operation with water-substance as either the reactor coolant or the working fluid. However, it is relevant to examine such systems as they might be applied to such applications in the light of current terrestrial technology.

State-of-the-Art

Development programs are going on in the fields of naval reactor propulsion plants, utility system power reactors, and to a more limited extent, in supercritical steam power plants, but these are not compatible with the requirements of the space or lunar environments. Almost by definition, naval reactor plants have access to an excellent heat sink, the sea, which has no counterpart on the moon. Utility system power stations are located where an adequate heat sink is available. Only in the field of supercritical steam power systems do temperatures approach those necessary for lunar surface operation. This development is guided by economic constraints far different from those that apply to lunar or space operations.

As a preliminary step in looking into a water technology and its potential, consideration was given to a steam turbine plant utilizing a typical low-temperature pressurized water reactor as the heat source. Obviously, technology in this area is in a high state of development compared to other reactor plant technologies. The results of consideration of such a plant making use of a steam cycle were as follows.

It was quickly apparent that for a steam cycle the volumetric flow of the steam would be so small for plants of interest that a system turbine would have extremely low efficiencies. The study was, therefore, based on the use of a uniflow steam engine. Using initial conditions of 1250 lbs at 572.4°F, it appeared that for a vertical radiator with the sun at the zenith using a radiator emissivity of 0.8, a lunar emissivity of unity, and a lunar absorbtivity of 0.875, that a radiator temperature of about 363°F would be optimum. With a steam engine efficiency of 64 percent with a factor of 0.7 to take care of generator inefficiencies and pumping power, a plant efficiency of 8.2 percent results. This gives a radiator area of approximately 87 sq. ft/KW which is more than a factor of 2 higher than might be required for a Brayton plant and an order of magnitude higher than might be required for a liquid metal Rankine cycle plant. On the basis of the very large areas which would be required even for reasonable power (i.e., 17,400 sq ft for 22 KW) in the steam plant and the potential of other systems, the steam plant with a low temperature pressurized water reactor is obviously out of the question.

To achieve reasonable radiator sizes, high radiator temperatures are necessary and the working fluid must be above the critical temperature for water. This leads essentially to a new area of technology. To minimize the size of plant components, high pressures must be used to obtain reasonable fluid density. Therefore, the stress and temperature problems encountered in terrestrial supercritical water systems will also be encountered in the lunar systems. Not to be underestimated is also the fact that an entirely new approach to water plants must be taken—one of designing a completely sealed and maintenance free system, something that there is little or no incentive for in earth applications.

Extension of present power plant technologies to encompass lunar surface operation could result in two classes of plants—all-water and liquid metal-water. If the power generating system is topped by a liquid metal cooled reactor rather than a water cooled reactor, the problems of insuring isolation of the metal and water streams, never solved completely at lower temperatures, will be found more difficult at the higher temperature.

Astronuclear

A group of new problems result from the chemical activity of water-substance at high temperature. Increased rates of corrosion, erosion, mass transfer, dissociation, and gas absorption may produce effects that cannot be extrapolated from presently available data obtained at lower temperatures and pressures. These effects must be investigated by experimental programs which presently are not being undertaken.

The only programs on supercritical reactors for terrestrial use are in a paper stage with some very limited work on heat transfer. Estimates are that it will be 8 to 10 years before a prototype system is in operation, and 4 to 5 years before adequate design data is available. Again the problem is that a program must be gotten underway to define the problems even before they can be solved. Equally important, for such a plant to be utilized, it would inevitabley be heavier than a comparable liquid metal plant, and would have less growth potential. Therefore, if it appears reasonable to say that liquid metals are feasible, this is the direction in which to go. In the case of liquid metals, data are still missing, but programs are well underway to obtain the data that is needed.

~~SECRET~~
~~RESTRICTED DATA~~
~~Atomic Energy Act - 1954~~

CLASS. MSG. NO.
A 9 6 3 5 1

~~SECRET~~
~~RESTRICTED DATA~~
~~Atomic Energy Act - 1954~~

INFORMATION CATEGORY	
~~Secret Restricted Data~~	
C E Sinclair	1/4/64
Authorized Classifier	Date

THIS IS COPY NO. 53 . . . . OF 125 COPIES.

THIS DOCUMENT CONTAINS 267 PAGES.

[redacted]